

Soluble Copper(I)-Chalcogenones: Synthesis, Characterization and Catalytic Applications

Mr. Katam Srinivas

R. No: CY13P0004

A Dissertation Submitted to
Indian Institute of Technology Hyderabad
In Partial Fulfillment of the Requirements for
The Degree of Doctor of Philosophy



भारतीय प्रौद्योगिकी संस्थान हैदराबाद
Indian Institute of Technology Hyderabad

Department of Chemistry

January, 2018

Declaration

I declare that this written submission represents my ideas in my own words, and where others ideas or words have not been included, I have adequately cited and referenced the original sources. I also declare that I have adhered to all principles of academic honesty and integrity and have not misrepresented or fabricated or falsified any idea/data/fact/source in my submission. I understand that any violation of the above will be a cause for disciplinary action by the Institute and can also evoke penal action from the sources that have thus not been properly cited, or from whom proper permission has not been taken when needed.



(Signature)

Mr. Katam Srinivas

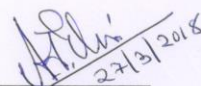
(– Student Name –)

CY13P0004

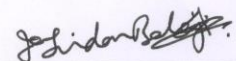
(Roll No)

Approval Sheet


This thesis entitled “**Soluble Copper(I)-Chalcogenones: Synthesis, Characterization and Catalytic Applications**” by **Mr. Katam Srinivas (CY13P0004)** is approved for the degree of Doctor of Philosophy from IIT Hyderabad.


27/3/2018

Prof. Anil J Elias
Professor, Department of Chemistry, IIT Delhi
Examiner



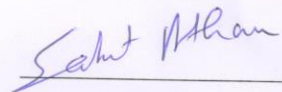
Prof. Balaji R Jagirdar
Professor, Department of Inorganic and Physical Chemistry,
IISc, Bangalore
Examiner



Prof. Tarun K Panda
Associate Professor, Department of Chemistry, IIT Hyderabad
Internal Examiner



Prof. Ganesan Prabusankar
Associate Professor, Department of Chemistry, IIT Hyderabad
Adviser/Guide



Prof. Saket Asthana
Associate Professor, Department of Physics, IIT Hyderabad
Chairman

Acknowledgements

This thesis is the end of my journey in obtaining my Ph.D. However, undertaking this PhD has been a life-changing experience for me, upon which many people have contributed and given their support.

First and foremost, I would like to express my deepest gratitude to my thesis advisor Dr. Ganesan Prabusankar, for giving me the opportunity to work in his group. I would like to thank him for encouraging my research and for allowing me to grow as a research scientist. His advice on both research as well as on my career have been invaluable. I was blessed in the five years, with his guidance, encouragement, unreserved help, hospitality, motivation, enthusiasm, immense knowledge, invaluable technique, and editorial advice, which really supported me through my whole PhD studies. Dr. G. Prabusankar is dynamic, enthusiastic and very energetic and I hope that I could be like him one day.

Besides my advisor, I would like to thank the rest of my thesis committee: Dr. M. Deepa and Dr. Tarun Kanti Panda for being part of my thesis committee and their encouragement, insightful comments, and hard questions. I am very thankful to Dr. Osamu Tsutsumi, Dept. of Applied Chemistry, Ritsumeikan University, for accepting me as an intern student to work in his laboratory. And also Dr. Anjana Devi, Chair II of Inorganic Chemistry, Ruhr University Bochum, for accepting me as an intern student in her laboratory.

I take this opportunity to sincerely acknowledge the UGC for the JRF & SRF fellowship, DST-SERB (Project No: SB/S1/IC-07/2014) for the financial support and Department of Chemistry, Indian Institute of Technology Hyderabad for providing sophisticated facilities.

A good support system is important for surviving and staying sane in PhD. I was lucky to have lab colleagues. Lab mates formed the core of my research time in the institute. I couldn't have survived without them. We've all been there for one another and have taught ourselves and each other many techniques and issues of reaction schemes. I know that I could always ask them for advice and opinions on lab related issues. Furthermore, I must also express my deepest gratitude and sincere thanks to all my group members; P. Suresh, A. Sathyanarayana, Ch. Nagababu, M. Bhanu Prakasa Rao, G. Raju, V. Moulali, K. Ramesh, M. Maruthupandi, M. Adi Narayana and Dr. M. Nirmla for their fruitful discussion on the research. Finally, I am grateful to my parents, my siblings, my wife Srilatha and my son Abhinav for their love, encouragement and understanding over the years. It is difficult for me to recall all the names here but I really appreciate all of my friends very much who have supported me during this journey.

Dedicated to

My family members

Abstract

The focus on copper chalcogenide chemistry is experiencing continuous growth and interest over last few decades owing to their novel properties and significant applications in materials chemistry. The property of copper chalcogenides is mainly controlled by chalcogen sources. For example, the recent works have also witnessed the active role of decade old ligand system imidazolin-2-chalcogenones for this endeavor. Notably, imidazolin-2-chalcogenone ligands have potential to serve as a ligand with copper in medicine. Some other potential applications of these imidazolin-2-chalcogenone ligand supported copper included their use as precursor for nanomaterial synthesis and co-ligand in catalysis. However, these recent efforts have not answered the critical questions such as, do “homoleptic two coordinated” key intermediates exist in the catalytic process? How essential is “more π accepting imidazoline-2-selone” to isolate the homoleptic two coordinated coinage metal derivatives? In order to address these challenges, this thesis deals with the three main aspects of Imidazolin-2-chalcogenones (ImC), such as (1) synthesis of soluble copper(I) chalcogenone, (2) catalytic efficiencies of ImC–Cu complexes, and comparison of catalytic activity of ImC–Cu with NHC–Cu (Chart A). Indeed, twenty one new structurally interesting copper(I) chalcogenones have been isolated and characterized by CHN analysis, FT-IR, multinuclear NMR, TGA, UV-vis, and single crystal X-ray diffraction techniques. These new molecules are found to be very active catalysts in ‘carbon-boron’, ‘carbon-nitrogen’ and ‘carbon-silicon’ bond formation reactions.

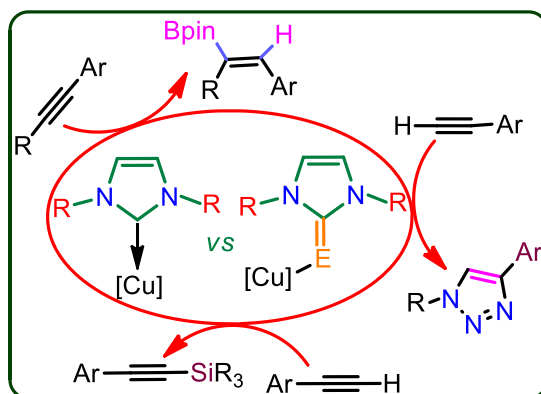


Chart A. Represents the ImC–Cu complexes established in this thesis

Preface

This thesis embodies the synthesis, characterization and catalytic applications of copper(I) chalcogenones. These new compounds have been characterized by CHN analysis, FT-IR, and multinuclear (^1H and ^{13}C) NMR spectroscopic studies, TGA, UV-vis and single crystal X-ray diffraction techniques.

Chapter 1 (Introduction) reviews the complete literature on Imidazolin-2-chalcogenones (ImC) supported Cu(I) complexes. Synthesis and structure of Cu(I)-chalcogenone derivatives are reported along with applications of metal–ImC derivatives.

Chapter 2 describes the linear Cu(I) chalcogenones: synthesis and application in borylation of unsymmetrical alkynes

Chapter 3 depicts the synthesis and application of large Cu^{I}_8 cages, in [3+2] cyclo addition and hydroamination alkynes.

Chapter 4 discourses the synthesis and applications of copper(I) complexes of C, S, Se and P donor ligands in C–N and C–Si bond formation reactions.

Chapter 5 (Summary and conclusion) summarizes the results described in the chapters 2-4, making important correlations between the compounds.

Abbreviations

Å	Angstrom
aq.	Aqueous
Ar	Aryl
Bp	Boiling point
ⁿ Bu	<i>n</i> -butyl
Cat.	Catalyst
dipp	2,6-diisopropylphenyl
d	Doublet
DCM	Dichloromethane
DEPT	Distortionless Enhancement by Polarization Transfer
DFT	Density functional theory
DMF	Dimethyl formamide
DMSO	Dimethyl sulfoxide
Et	Ethyl
EtOAc	Ethyl acetate
EI-MS	Electron ionization mass spectrometry
ESI	Electrospray ionization
Eq	Equivalence
EWG	Electron Withdrawing Group
EDG	Electron Donating Group
FT-IR	Fourier transform – infrared
GC-MS	Gas chromatography - mass spectrometry
GOF	Goodness of fit
HOMO	Highest occupied molecular orbital
H	Hour
HMBC	Heteronuclear multiple-bond correlation spectroscopy
HSQC	Heteronuclear Single Quantum Coherence or Heteronuclear Single Quantum Correlation
HRMS	High resolution mass spectra
Hz	Hertz
IAD	(1,3-bis(adamantyl)imidazol-2-ylidene)
Im	Imidazole
<i>J</i>	Coupling constant (NMR)

KO ^t Bu	Potassium tertiary butoxide
Kcal	Kilocalories
LUMO	Lowest occupied molecular orbital
M	Multiplet (NMR), medium (IR)
Me	Methyl
MeOH	Methanol
MeCN	Acetonitrile
Mes	2,4,6-trimethyl phenyl
M.P	Melting point
Mol wt	Molecular weight
mL	Milliliter
MHz	Mega hertz
Mmol	Millimole
NMR	Nuclear magnetic resonance
NHC	N-heterocyclic carbene
Nm	Nanometer
-OAc	O-Acetyl
Pet-ether	Petroleum ether
Ppm	Parts per million
ⁱ Pr	Isopropyl
Ph	Phenyl
Py	Pyridyl
Q	Quartet
R	Alkyl or aryl group
RT	Room temperature
s	Singlet (NMR), strong (IR)
t	Triplet
THF	Tetrahydrofuran
TMS	Tetra methyl silane
TLC	Tin layer chromatography
TM	Transition metal
UV	Ultra violet
w	Weak

List of Figures

Figure		Page No
Chapter 1		
1.1	The three types of carbenes	04
1.2	Commercially available NHC-Cu complexes by Sigma Aldrich	06
1.3	Antithyroid drugs and their biological significance	09
1.4	Structural comparison between NHC and ImC	13
1.5	π -electron distribution in ImC's	15
1.6	Coordination modes of NHC vs ImC	15
1.7	π -accepting nature of various NHC's predicted using ImC's	16
1.8	Factors effecting the π -accepting nature of NHC	16-17
1.9	Molecular structure of Cu(I) complex, Cu₆₁	31
1.10	Mixed and thio ligands supported Rh complexes used in Hydro-formylation reaction	34
1.11	NHC supported Rh complexes used in Hydro-formylation reaction	35
1.12	Catalysts used for vinyl polymerization of norbornene	36
1.13	Catalysts used for the oxidative coupling of benzylamine	37
1.14	Heck coupling products isolated Pd(II) catalyst, Pd₈	39
1.15	Heck, Suzuki-Miyaura, and Sonogashira coupling products isolated by catalyst, Pd₉	40
1.16	ImC-metal complexes used as drugs for antibacterial activities	43

Chapter 2

2.1	Molecular structure of 1-2	60
2.2	Neat FT-IR spectrum of 3-4	61
2.3	Neat FT-IR spectrum of 4	63
2.4	¹ H NMR spectrum of 4	63
2.5	¹³ C NMR spectrum of 4	64
2.6	Molecular structure of 5-6	64
2.7	Molecular structure of 7-8	65
2.8	Neat FT-IR spectrum of 5	66
2.9	¹ H NMR spectrum of 5	66
2.10	¹³ C NMR spectrum of 5	67
2.11	¹¹ B NMR spectrum of 5	67
2.12	¹⁹ F NMR spectrum of 5	68
2.13	UV-vis spectra of molecules 1-8	72
2.14	TGA plots of molecules 1-8	73

Chapter 3

3.1	Neat FT-IR spectrum of 9	86
3.2	¹ H NMR spectrum of 9 in DMSO- <i>d</i> ₆ at room temperature	87
3.3	¹³ C NMR spectrum of 9 in DMSO- <i>d</i> ₆ at room temperature	87
3.4	³¹ P NMR spectrum of 9 in DMSO- <i>d</i> ₆ at room temperature	88
3.5	¹⁹ F NMR spectrum of 9 in DMSO- <i>d</i> ₆ at room temperature	88
3.6	Solid state structure of 9 and 10	89

3.7	Neat FT-IR spectrum of 10	90
3.8	¹ H NMR spectrum of 10 in DMSO- <i>d</i> ₆ at room temperature	91
3.9	¹³ C NMR spectrum of 10 in DMSO- <i>d</i> ₆ at room temperature	91
3.10	³¹ P NMR spectrum of 10 in DMSO- <i>d</i> ₆ at room temperature	92
3.11	¹⁹ F NMR spectrum of 10 in DMSO- <i>d</i> ₆ at room temperature	92
3.12	PXRD <i>vs</i> SCXRD patterns	95
3.13	TGA curves of 9 and 10	95
3.14	UV-vis spectra of 9 and 10 along with corresponding ligands	96
3.15	Trans-metallation progress during the reaction	97
3.16	¹ H NMR spectrum of trans-metallation reaction mixture in DMSO- <i>d</i> ₆ at room temperature	98
3.17	¹ H NMR spectrum of 9 @pyrene in DMSO- <i>d</i> ₆ at RT	99
3.18	9 @Perylene reaction progress by UV-visible spectroscopy	100
3.19	9 @Perylene reaction progress by FT-IR spectroscopy	100
3.20	¹ H NMR spectrum of 9 @pyrene in DMSO- <i>d</i> ₆ at RT	102
3.21	9 @Perylene reaction progress by UV-visible spectroscopy	102
3.22	9 @Perylene reaction progress by FT-IR spectroscopy	103
3.23	¹ H NMR spectrum of 9 @C ₆₀ in DMF- <i>d</i> ₇ at RT	104
3.24	Solid state structures of Ia , Ib , IIa and IIb	107
3.25	Recycling ability of catalyst 9	109
3.26	PXRD studies on reused catalyst 9	110

Chapter 4

4.1	Molecular structures of 11-15	128
4.2	Molecular packing diagrams of 11-13	130
4.3	Molecular packing diagrams of 14-15	131
4.4	¹ H NMR spectra displays the aryl region of 11-15	132
4.5	Molecular structures of 17, 19 and 21	136
4.6	¹ H NMR comparison between 11 and 17	137
4.7	HMBC spectrum of (IMes=S)CuCl (11) in DMSO- <i>d</i> ₆ at RT	138
4.8	HSQC spectrum of (IMes=S)CuCl (11) in DMSO- <i>d</i> ₆ at RT	138
4.9	HMBC spectrum of [(IMes=Se) ₂ Cu][CuCl ₂] (17) in DMSO- <i>d</i> ₆ at RT	139
4.10	HSQC spectrum of [(IMes=Se) ₂ Cu][CuCl ₂] (17) in DMSO- <i>d</i> ₆ at RT	139
4.11	Solid state structure of 22	143
4.12	Molecular structures of 23 and 24	144
4.13	Packing diagram of molecule 23	145
4.14	UV-vis analysis of 11-24	148
4.15	Catalysts 11-24 screening in click catalysis	150
4.16	Solvent screening in click catalysis	151
4.17	FT-IR analysis of click reaction crude	153

List of Schemes

Scheme		Page No
--------	--	---------

Chapter 1

1.1	Synthesis of first NHC-metal complex <i>by in situ</i> NHC generation	5
-----	---	---

1.2	Stable N-heterocyclic carbene (NHC) isolated by Arduengo in 1991 (White solid)	5
1.3	Possible zwitter ionic forms of imidazolin-2-chalcogenone (ImC)	8
1.4	General approach to access ImC from various starting materials	10
1.5	Known coordination properties of ImC with metals	11
1.6	Synthesis of Cu(II) complex, Cu₁	17
1.7	Synthesis of Cu(II) complexes, Cu₂₋₄	18
1.8	Regio-selective borylation of alkynes catalyzed by Cu₅	18
1.9	Synthesis of Cu(I) complexes, Cu₅₋₁₀	19
1.10	Synthesis of Cu(I) complexes, Cu₁₁₋₁₂	20
1.11	Synthesis of Cu(I) complexes, Cu₁₃₋₁₄	20
1.12	Synthesis of Cu(I) complexes, Cu₁₅₋₁₆	21
1.13	Synthesis of Cu(I) complexes, Cu₁₇₋₂₀	22
1.14	Synthesis of Cu(I) complexes, Cu₂₁₋₂₃	23
1.15	Synthesis of Cu(I) complexes, Cu₂₄	23
1.16	Synthesis of Cu(I) complexes, Cu₂₅₋₃₆	24
1.17	Synthesis of Cu(I) complexes, Cu₃₇₋₃₉	25
1.18	Synthesis of Cu(I) complexes, Cu₄₀₋₄₃	26
1.19	Synthesis of Cu(I) complexes, Cu₄₄	26
1.20	Synthesis of Cu(I) complexes, Cu₄₅₋₄₆	27
1.21	Synthesis of Cu(I) complexes, Cu₄₇₋₄₉	27

1.22	Synthesis of Cu(I) complexes, Cu ₅₀	28
1.23	Synthesis of Cu(I) complexes, Cu ₅₁₋₅₄	28
1.24	Synthesis of CO ^R from Cu ₅₁₋₅₄ by demetallation process	28
1.25	Synthesis of Cu(I) complexes, Cu ₅₅₋₆₀	29
1.26	Synthesis of Cu(I) complexes, Cu ₅₆₋₆₀ from mixed ligand based copper complexes, Cu ₅₁₋₅₄ by sulfur insertion method	30
1.27	Expected mononuclear complexes from binuclear Cu(I) complexes, Cu ₅₅₋₅₇	31
1.28	Synthesis of Cu(I) coordination polymer complex, Cu ₆₂	32
1.29	Synthesis of Cu(I) complex, Cu ₆₃	32
1.30	Synthesis of Pd(ImC) complex (Pd ₁) from Bi(ImC) (Bi ₁) by trans-metallation reaction	33
1.31	Synthesis of Cd(ImC) complex (Cd ₁) from Zn(ImC) complex (Zn ₁) by trans-metallation reaction	33
1.32	.Catalytic transfer hydrogenation of carbonyl compounds catalyzed by Ru ₁₋₄	34
1.33	Hydro-formylation reaction of 1-hexene catalyzed by Rh ₁₋₁₉	34
1.34	Vinyl polymerization of norbornene catalyzed by Ir ₁₋₄ , Ni ₁₋₆	35
1.35	Synthesis of 1,2-disubstituted benzimidazoles and aerobic oxidation of carbonyl compounds by Ir ₅₋₈	36
1.36	Oxidative coupling of benzylamine to imine by Ir ₉₋₁₄	37
1.37	Suzuki coupling catalyzed by <i>in situ</i> generated catalyst, Pd ₂	38

1.38	Suzuki coupling catalyzed by Pd(0) and Pd(II) catalysts, Pd ₃₋₄	38
1.39	Suzuki coupling reactions catalyzed by Pd(II) catalysts, Pd ₅₋₇	39
1.40	Reduction of nitroarenes to aromatic amines by Au ₁₋₆	40
1.41	Hydro-amination of alkynes catalyzed by catalysts, Au _{9,14}	41
1.42	Reduction of 4-nitro benzaldehyde catalyzed by Zn ₂₋₇	41
1.43	Barbier type reaction catalyzed by Zn _{8,9} and Cd ₂₋₅	42
Chapter 2		
2.1	Known linear/quasi-linear group-9 molecules	54
2.2	Synthesis of 2-8	59
2.3	Vital bond angles and bond lengths in molecules 1-8	61
2.4	Regioselective borylation of 1-phenyl-1-propyne using 1-8 .	74
2.5	Possible mechanism for hydroborylation reaction	75
Chapter 3		
3.1	Synthesis of 9 and 10	86
3.2	Synthesis of 9@perylene	99
3.3	Synthesis of 9@pyrene	101
3.4	Catalysts 9 and 10 mediated click catalysis	104
3.5	Catalysts 9 and 10 mediated one-pot click reaction	110
3.6	Hydroamination of alkynes by 9 and 10	111
Chapter 4		
4.1	Synthesis of 11-15	127

4.2	Synthesis of 17-20	134
4.3	Synthesis of 21	135
4.4	Expected structure for 17 in solution state	137
4.5	Synthesis of 22-23	141
4.6	Synthesis of 24	142
4.7	[3+2] cycloaddition of benzylazide with phenyl acetylene	149
4.8	[3+2] cycloaddition of benzylazide with terminal alkynes	152
4.9	Cross-dehydrogenative coupling of terminal alkynes	155

Chapter 5

5.1	Regio-selective borylation of alkynes by catalysts 1-8	162
5.2	Catalysts 9-10 mediated click reaction	164
5.3	[3+2] cyclo addition of azides with alkynes	166

List of Tables

Table		Page No
Chapter 2		
2.1	Selected bond lengths and bond angles in 1-8	68
2.2	Structural parameters of compounds 1-4	69
2.3	Structural parameters of compounds 5-8	71
2.4	Regioselective borylation of 1-phenyl-1-propyne using 1-8	75
2.5	Solvent screening in hydroborylation reaction	76
2.6	Regioselective borylation of unsymmetrical alkynes by 4	77
Chapter 3		
3.1	Selected bond lengths and angles in 9 and 10	90
3.2	Structural parameters in 9 and 10	93-94
3.3	Catalysts 9 and 10 optimization studies in click catalysis	105
3.4	Structural parameters of compounds Ia , Ib , IIa and IIb	108
3.5	Catalysts 9 and 10 optimization studies in hydroamination reaction	112
Chapter 4		
4.1	Structural parameters of compounds 11-14	133
4.2	Structural parameters of 15 , 17 , 19-20	140
4.3	Structural parameters of 22 , 23-24	146
4.4	Selected bond lengths and angles in 11-24	147
4.5	Cu(I) mediated cross-dehydrogenative coupling of alkynes with silanes	156

List of Charts

Chart		Page No
Chapter 1		
1.1	Early studies of the reactivity of N-heterocyclic carbenes (NHC)	4
1.2	Various catalytic reactions established with Cu–NHC until now	7
1.3	Selected NHC analogues of main group derivatives	7
1.4	Various classes of ImC's	9
1.5	Number of publications till January-2018)	11
1.6	ImC-metal catalysts mediated organic transformations	12
1.7	ImC-Metal complexes applications in various fields	13
Chapter 3		
3.1	Isolated click products by 9 and 10	106
3.2	Isolated one-pot click products by 9 and 10	111
3.3	Isolated hydroamination products by 9 and 10	113
Chapter 4		
4.1	σ -donor and π -accepting nature of phosphine, NHC and ImC	119
4.2	Known comparative catalysis reported between NMC-metal and ImC-metal complexes	120
4.3	H-bonding in the solid state structures of 11-15	129
4.4	Catalysts used for the substrate scope in click catalysis	151
4.5	1,2,3-triazoles isolated by click catalysis	152-153

4.6	Possible mechanistic pathway for click catalysis	154
4.7	Expected steric hindrance in click catalysis by catalysts 13 and 16	154
4.8	Catalysts used so far in cross-dehydrogenative coupling reaction	155

Chapter 5

5.1	Catalysts (1-8) isolated for region-selective borylation	162
5.2	NHC-metal <i>vs</i> ImC-metal efficiency in borylation of alkynes	163
5.3	Catalysts (9-10) isolated for click and hydroamination of alkynes	164
5.4	NHC-metal <i>vs</i> ImC-metal efficiency in click catalysis	165
5.5	Catalysts (11-24) isolated for click and cross-dehydrogenative coupling of alkynes	166
5.6	NHC-metal <i>vs</i> ImC-metal efficiency in click and dehydrogenative coupling of alkynes	167

Contents

		Page No
Chapter 1	Introduction	1-51
1.1	Timeline of N-heterocyclic carbene with organometallic chemistry	1
1.2	Nobel-prize winners related to OMC	2-3
1.3	Organometallic catalysis	3
1.4	N-heterocyclic carbene	3
1.5	NHC-Cu chemistry	6
1.6	Imidazolin-2-chalcogenon (ImC)	7
1.7	Types of ImC and their coordination modes	9
1.8	ImC-metal chemistry	11
1.9	Structural comparison between NHC and ImC	13
1.10	Structure, general properties and stability of ImC's	14-15
1.11	π -Acceptor Nature of ImC's and NHC's	16-17
1.12	ImC-Cu complexes	17-32
1.13	ImC-metal complexes and their applications	32
1.13.1	As trans-metallating agents	32
1.13.2	As catalysts in organic transformations	33-42
1.13.3	As an antibacterial agents	42-43
1.14	Scope of the work	44
1.15	Objectives	45

1.14	References	46-51
Chapter 2	Linear Cu(I) Chalcogenones: Synthesis and Application in Borylation of Unsymmetrical Alkynes	52-80
2.1	Introduction	53
2.2	Experimental Section	54
2.2.1	General remarks	54
2.2.2	Synthesis 1	55
2.2.3	Synthesis of 2	56
2.2.4	Synthesis of 3	56
2.2.5	Synthesis of 4	56
2.2.6	Synthesis of 5	57
2.2.7	Synthesis of 6	57
2.2.8	Synthesis of 7	57
2.2.9	Synthesis of 8	58
2.2.10	1-8 catalyzed regioselective boron addition to unsymmetrical alkynes	58
2.3	Result and discussion	58
2.3.1	Synthesis and characterization of 1-8	58
2.3.2	Single crystal X-ray structures of 1-8	60
2.4	UV-vis solid and solution state absorption study of 1-8	72
2.5	TGA analysis of 1-8	73
2.6	Copper(I) catalyzed borylation of unsymmetrical alkynes	73

2.7	Summary	77
2.8	References	78-80
Chapter 3	Large Cu^I8 Chalcogenone Cubic Cages with Non-interacting Counter Ion	81-117
3.1	Introduction	82
3.2	Experimental Section	82
3.2.1	General remarks	82
3.2.2	Synthesis of 9	83
3.2.3	Synthesis of 10	84
3.2.4	Synthesis of 9 @AuCl	84
3.2.5	Synthesis of 9 @Perylene	84
3.2.6	Synthesis of 9 @Pyrene	84
3.2.7	Cu(I) catalysts catalysed azide–alkyne cycloaddition reactions	85
3.2.8	Cu(I) catalysts mediated hydroamination of terminal alkynes	85
3.3	Result and discussion	85
3.3.1	Synthesis and characterization	85
3.4	PXRD and Thermogravimetric analysis	95
3.5	UV-visible absorption studies	96
3.6	Miscellaneous investigations	97
3.6.1	Trans-metallation reaction	97
3.6.2	Host-guest interactions on 9 with perylene	98
3.6.3	Host-guest interactions on 9 with pyrene	100

3.7	Catalytic investigations	104
3.8	Summary	113
3.9	References	113-117
Chapter 4	Copper(I) complexes of C, S, Se and P donor ligands for C-N and C-Si bond formation	118-160
4.1	Introduction	119
4.2	Experimental section	120
4.2.1	General remarks	120
4.2.2-4.3.14	Synthesis of 11-24	121-126
4.2.15	General procedure for the click catalysis	126
4.2.16	General procedure for C-Si bond formation reactions	127
4.3	Result and discussion	127
4.3.1	Synthesis and characterization of 11-15	127
4.3.2	Single crystal structures of 11-15	128
4.3.3	Molecular packing in 11-15	129
4.3.4	Synthesis and characterization of 17-21	133
4.3.5	Single crystal structures of 17-21	135
4.3.6	Synthesis of copper(I) coordination polymers 23-24	140
4.3.7	Single crystal structures of 22-24	142-147
4.4	UV-vis studies on 11-24	147-148
4.5	Cu(I) catalyzed click catalysis	149
4.6	Cu(I) mediated C-Si bond formation reactions	155

4.7	Summary	157
4.8	References	157-160
Chapter 5	Summary and Conclusions	161-167
	List of Publications	168-169
	List of Conferences Attended	170

Chapter 1

Introduction





The field of organometallic chemistry associates the aspects of traditional inorganic and organic chemistry. In particular, chemical compounds with at least one carbon–metal bond, including alkali, alkaline earth, transition metals, and sometimes broadened to include metalloids like boron, silicon, and tin, are considered as organometallic compounds (OMC's) [1-2]. Apart from the bonding to an organic fragments or molecules, bonding to 'inorganic' carbon, like carbon monoxide (metal carbonyls), cyanide, or carbide, are also considered to be organometallic compounds. Similarly, transition metal hydrides, metal nitrogen complexes and metal phosphine complexes are often included in discussions of organometallic compounds, though strictly speaking, they are not necessarily organometallic. In general, the related term "metalorganic compound" refers to metal-containing compounds lacking direct metal-carbon bonds but which contain organic ligands. Metal β -diketonates, alkoxides, dialkylamides, and metal phosphine complexes are representative members of this class [3].

1.1. Timeline of organometallic chemistry

- 1760 Louis Claude Cadet de Gassicourt discovered the fuming Cadet's liquid comprises of cacodyl oxide and tetramethyldiarsine.
- 1827 William Christopher Zeise discovered the first π -complex $K_2[PtCl_3(\eta^2-C_2H_4)]$ (Zeise's salt).
- Edward Frankland discovered several metal-alkyl complexes such as diethyl zinc (1848), diethyl mercury (1852), tetraethyl tin and trimethyl boron (1860).
- 1863 Charles Friedel and James Crafts prepared organochlorosilanes (R_nSiCl_{4-n}).
- 1868-1870 Schützenberger synthesized the first metal-carbonyl derivatives $[Pt(CO)_2Cl_2]$ and $[Pt(CO)Cl]_2$.
- 1890-1891 Ludwig Mond discovered the first binary metal-carbonyl complexes $\{[Ni(CO)_4]$ and $[Fe(CO)_5]\}$.
- 1899 Introduction of Grignard reaction by Victor Grignard.

- 1951 Ferrocene was discovered (Modern organometallic chemistry begins with this discovery).
- 1956 Dorothy Crowfoot Hodgkin discovered the first biomolecule found to contain a metal-carbon bond (Vitamin B12).
- 1960 Wanzlick proposed monomer dimer equilibrium of carbene.
- 1991 Arduengo (III) isolated and characterized the first N-Heterocyclic Carbene.

1.2. Nobel -prize winners related to OMC

Nobel -Prize Winners	Discovery
V. Grignard, P. Sabatier (1912)	Grignard reagent
	
K. Ziegler, G. Natta (1963)	Ziegler-Natta catalyst
	
E. O. Fisher, G. Wilkinson (1973)	Sandwich compounds
	
R. Hoffmann, K. Fukui (1981)	Woodward-Hoffman Rules
	

K. B. Sharpless, R.
Noyori, W. S.
Knowles (2001)



Hydrogenation and
oxidation

Y. Chauvin, R. H.
Grubbs, R. R.
Schrock (2005)



Metal-catalyzed alkene
metathesis

R. F. Heck, E.-i.
Negishi, A. Suzuki
(2010)



Palladium catalyzed cross
coupling reactions

1.3. Organometallic catalysis

Catalyst is a chemical substance, which increases the rate of a reaction by lowering the activation energy (threshold energy) so that more reactant molecules interact with enough energy to overcome the energy barrier. Catalysis plays a vital role in the production of fuels, commodity chemicals, fine chemicals and pharmaceuticals as well as providing the means for experimental safeguards all over the world. Most catalysts used in industrial and research laboratories are inorganic (often organometallic) compounds. It is worth mentioning that more than 60% of all chemical products and 90% of all chemical processes are based on catalysis. Catalysis can be of two types, Homogeneous [4-7] and Heterogeneous [8-11]. 1) Homogeneous: Catalyst and reactant in the same phase e.g.) Organometallic Compounds 2) Heterogeneous: Catalyst and reactant in different phases e.g.) Metal surface active process catalytic decomposition of formic acid on noble metals.

1.4. N-heterocyclic carbene

N-heterocyclic carbenes are neutral divalent carbons and are classified as Fischer, Schrock and persistent carbenes (Figure 1.1) [12]. In the Fischer (singlet) carbene compounds, a carbon center bears a lone pair of electrons in sp^2 hybridized orbital while a p orbital remains vacant. Schrock (triplet) carbenes are also known, where each of the two electrons occupy a degenerate p orbital. In addition, N-Heterocyclic carbenes (NHC's) are heterocyclic persistent

carbenes and cyclic molecules that contain one carbene and at least one nitrogen atom within the carbene-containing ring structure. While these species were initially not widely applied in chemistry, they have now been employed in a broad range of fields, including organo-catalysis [13] and organometallic chemistry [14-17]. Hundreds of different NHCs are known in the literature, and much has been learned about their properties and reactivity [18-20].

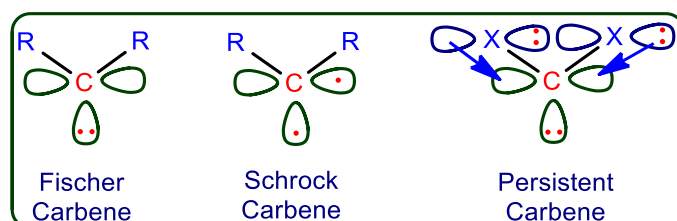


Figure 1.1: The three types of carbenes

Preceding to the isolation of stable NHCs, some information was known about the properties of these species (Chart 1.1). As early as the 1960s, researchers such as Wanzlick were active in probing the reactivity of NHC's generated in situ from, for example, the thermolysis of the corresponding dimers. In this way, the nucleophilic reactivity of these species with a number of reagents was characterized. Metal-carbene complexes were also prepared by Wanzlick and Schönherr, without isolation of the free carbene itself (Scheme 1.1) [21].

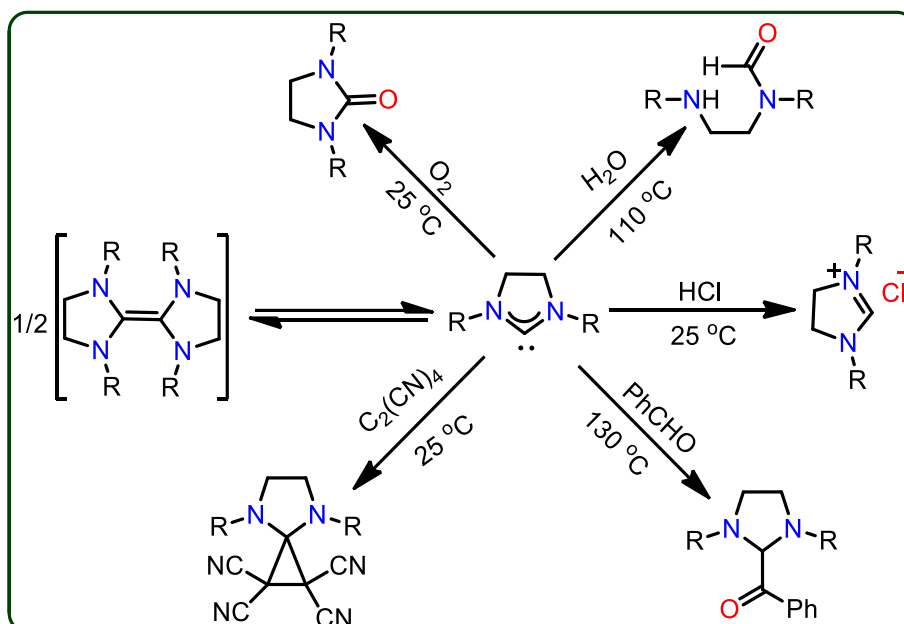
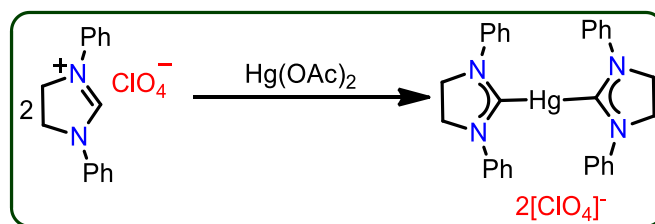
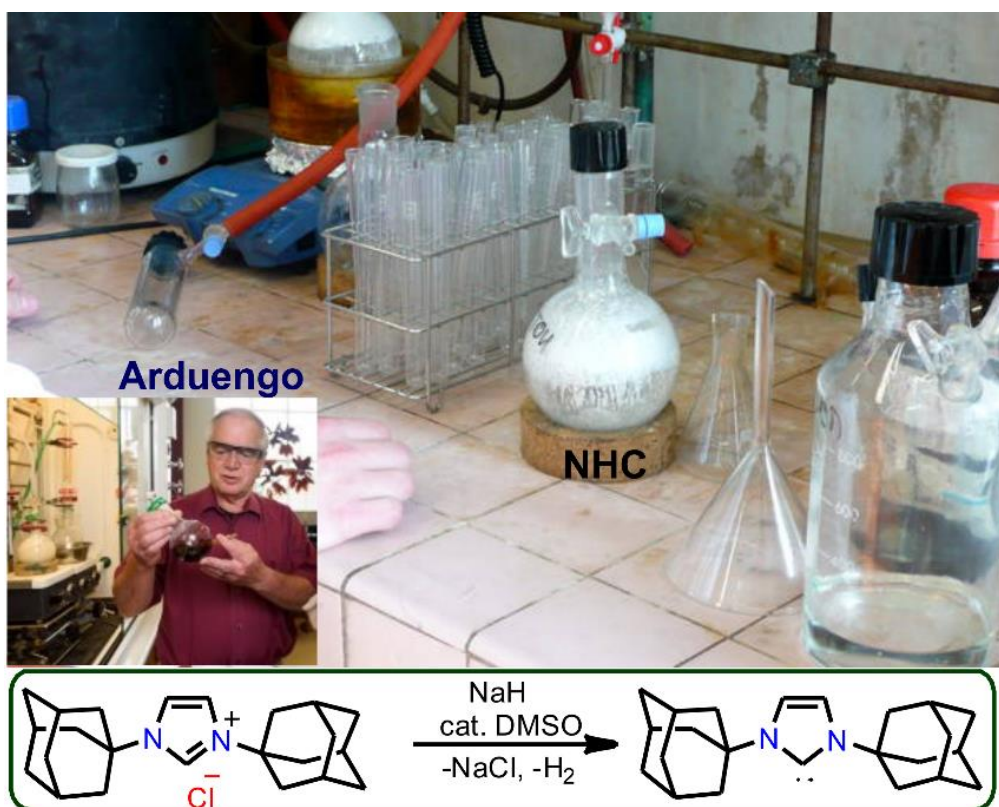


Chart 1.1: Early studies of the reactivity of N-heterocyclic carbenes (NHC)



Scheme 1.1: Synthesis of first NHC-metal complex *by in situ* NHC generation

The isolation of stable NHCs (Scheme 1.2, Arduengo, 1991) was a key event in the chemistry of this valuable class of compounds, as this allowed the preparation of material for detailed characterization [22]. In 1990s NHC's gained popularity as ligands, and then research continued towards isolable NHC's. Since then a large variety of NHCs have been synthesized. From the last 25 years, these NHC motifs have been modified by changing both the pendant groups and the skeletal ring structure [23].



Scheme 1.2: Stable N-heterocyclic carbene (NHC) isolated by Arduengo in 1991 (White solid)

1.5. NHC–Cu chemistry

Although, the chemistry of copper has a long history [24-25], the relatively contemporary discovery of N-heterocyclic carbene (NHC) as transition-metal supporting ligands has been legitimated novel outlooks to be discovered in copper reactivity and catalysis [22-26]. Soon after the inspirational discovery of Arduengo, Raubenheimer reported a neutral copper carbene complex [27]. However, the field remained dormant for almost ten years. In the early 2000s, new breakthroughs were achieved: first, the synthesis of NHC-copper using Cu_2O was reported by Danopoulos and followed by the first application in catalysis by Woodward [28-29].

The work by Buchwald and Sadighi appeared next, where the first catalysis using a well-defined complex was described [30]. The first reports in this field were based on systems used to mimic their phosphine relatives. NHCs have become ligands of significant interest due to their steric and electronic properties [31-33]. Combining the NHC ligand family and copper became, for some, an obvious and productive area [32-33]. Over the last decade alone, numerous systems have been developed. Copper-NHC complexes can be divided into two major classes: neutral mono-NHC and cationic bis-NHC derivatives: $[\text{Cu}(\text{X})(\text{NHC})]$ (X = halide, acetate, hydroxide, hydride, etc.) [34-36] and $[\text{Cu}(\text{NHC})(\text{L})][\text{Y}]$ (L = NHC or PR_3 ; Y = PF_6 , BF_4) [37-38]. Besides, few NHC-Cu catalysts available commercially have listed out in figure 1.2.

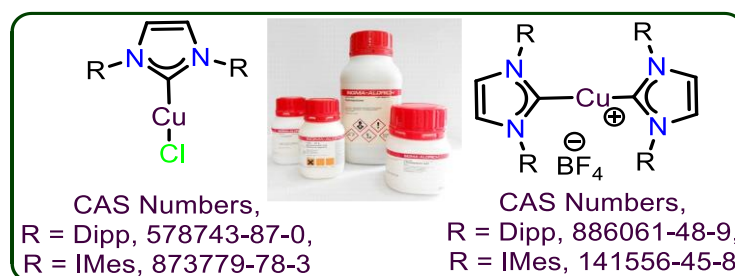


Figure 1.2: Commercially available NHC-Cu complexes by Sigma Aldrich

The neutral-halide-bearing complexes have been widely used in catalysis, mainly due to their ease of synthesis [31-33]. In addition to halide-bearing complexes, notable important related compounds have been reported: Nolan and co-workers disclosed the first hydroxide derivative $[\text{Cu}(\text{OH})(\text{IPr})]$ (IPr = *N,N'*-bis(2,6-diisopropylphenyl)imidazol-2-ylidene) and Sadighi published alkoxides, hydrides and borate species, which permitted novel reactivity to be explored [39-41]. With respect to

cationic derivatives, homoleptic and heteroleptic bis-NHC complexes have been reported and have been efficiently used in catalysis allowing important improvements (Chart 1.2) [37-38].

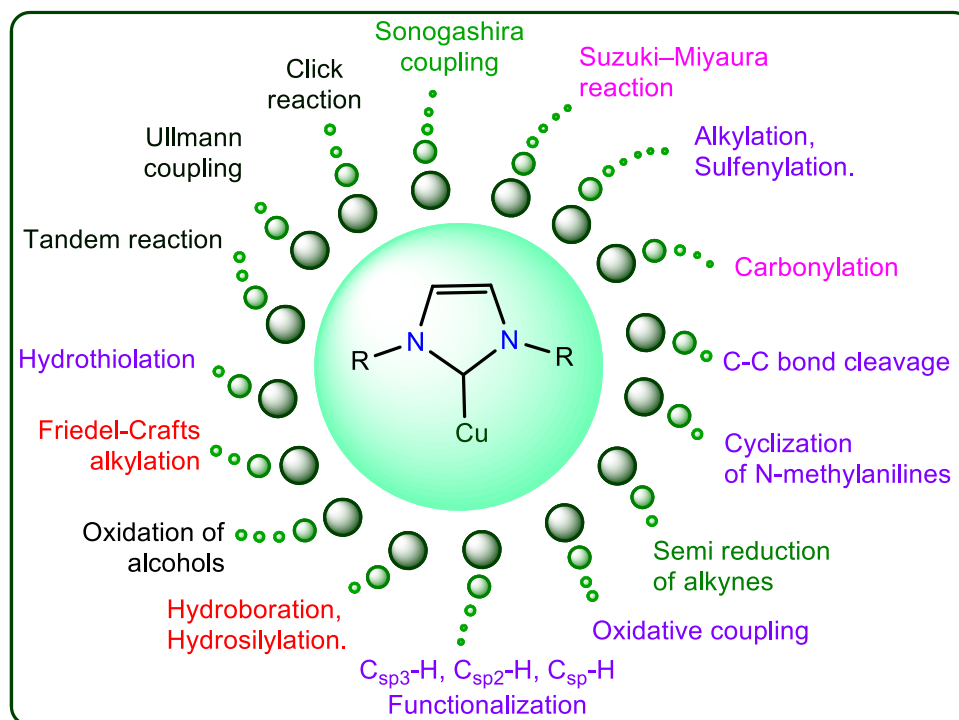


Chart 1.2: Various catalytic reactions established with Cu-NHC until now

1.6. Imidzolin-2-chalcogenone (ImC)

After the isolation of free carbene, NHC's gain high popularity as ligands and then research continued towards isolable NHC's (Chart 1.3) [42]. Among the analogues NHC's investigated, we have interested in studying the imidazolin-2-chalcogenones (ImC's) owing to their vast applications in medicinal, supramolecular, material fields and also due to the promising features in catalysis [43-45].

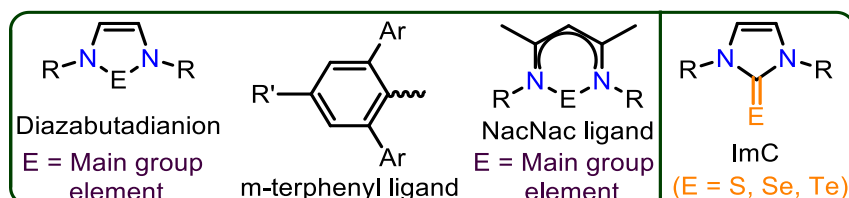
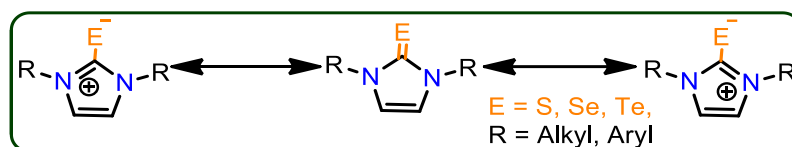


Chart 1.3: Selected NHC analogues of main group derivatives

Over the past few decades, organo chalcogenones have attracted an appreciable amount of research interest as a result of their unique reactivities and complexation properties. With an increase in the orbital size of the chalcogens (O; 2p, S; 3p, Se; 4p, and Te; 5p), the stability of the corresponding ketones gradually decreases owing to improper orbital overlap with carbon (C; 2p) [46]. Rationally, examples of chalcogenone monomers progressively decrease from O to Te. As a matter of fact, monomeric tellones are extremely rare [47-48], whereas similar oxones and thiones are quite common in nature. Selones, which are intermediate members of this family, often show interdisciplinary properties. As a result, they usually appear in partial zwitterionic forms ($C^{\delta+}=Se^{\delta-}$) in lieu of true $C=S$ or C^+-Te^- forms (Scheme 1.3), but still maintain substantial stability [49]. Such increased electron density on the Se center boosts its nucleophilic character [50-51].



Scheme 1.3: Possible zwitter ionic forms of imidazolin-2-chalcogenone (ImC)

Owing to this unique structural feature, ImC have been utilized as synthons in organic synthesis for an enduring period of time. Their use as ligating struts in complexation with transition metals has recently started to develop. Similar to tellones, monomeric thiones and selones also exhibit a tendency to dimerize unless placed in a sterically hindered alkyl or aryl environment or stabilized by electronic delocalization.

Moreover, such selenoketones have been used as inhibitors of lactoperoxidase-catalyzed oxidation and tyrosine nitration [52], as an analogue of the antithyroid drug methimazole (Figure 1.3) [53], in optoelectronics [54], as chemical sensors [55], and also as a chemical tool for Pd(II) extraction from water [56].

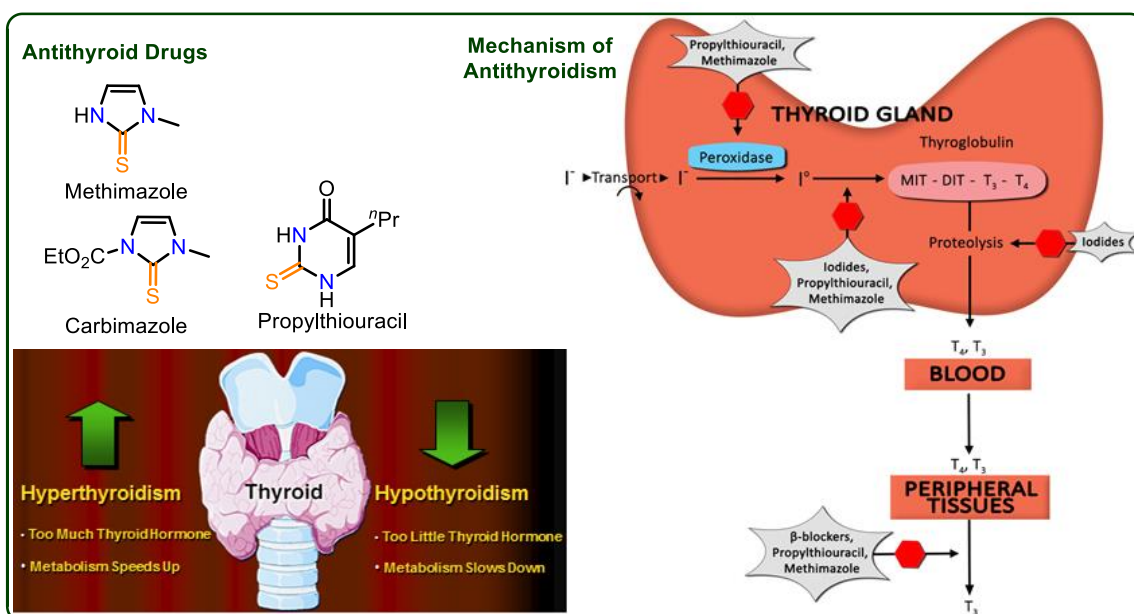


Figure 1.3: Antithyroid drugs and their biological significance

1.7. Types of ImC and their known coordination modes

ImC can be classified based on different types of existing molecules, which mainly based on the number of chalcogen donors in a single molecule. 1) Mono dentate ImC's, 2) bi dentate ImC's and 3) tri dentate ImC's as shown in chart 1.4.

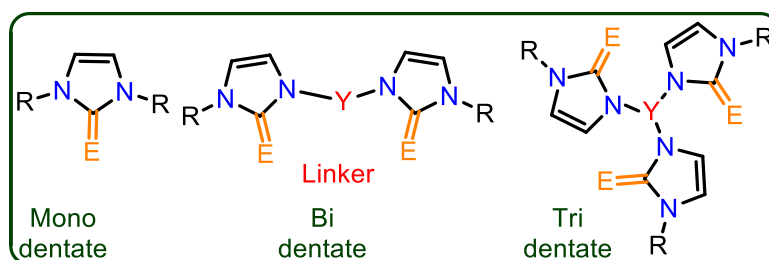
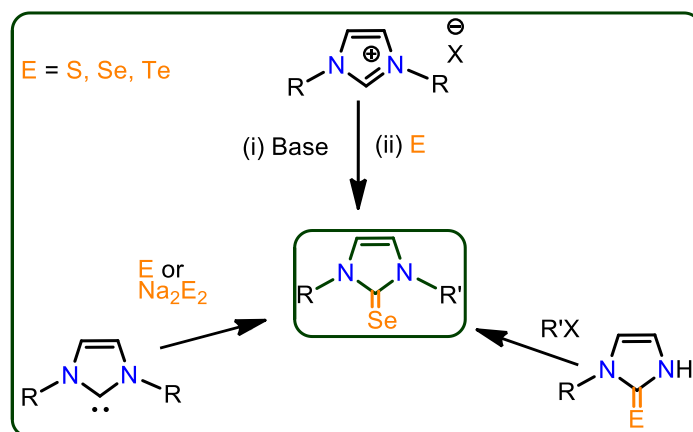


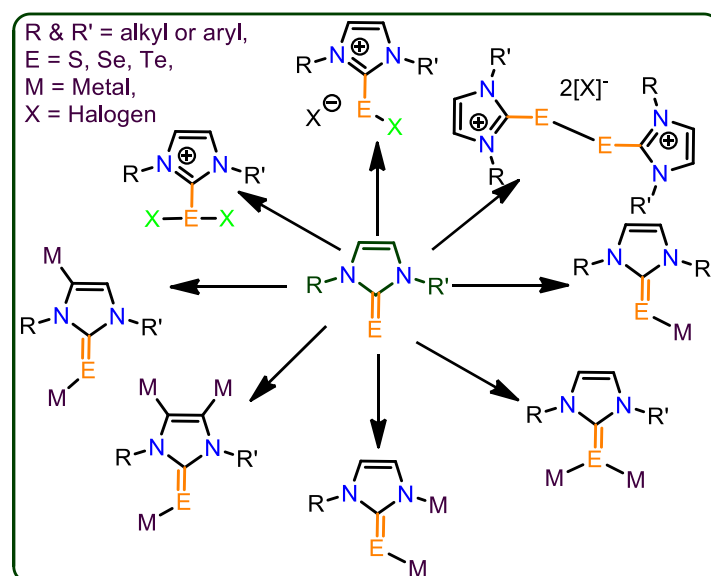
Chart 1.4: Various classes of ImC's

Since the first report of the one-pot synthesis of a selone starting from an imidazolium salt and elemental selenium by Jin *et al.* [57], a significant number of reports has been published following a similar synthetic protocol. A suitable synthesis of these imidazolin-2-chalcogenones starts with their imidazolin-2-ylidene or imidazolium salt or N-substituted ImC as precursors (Scheme 1.4) [57-59].



Scheme 1.4: General approach to access ImC from various starting materials

Imidazolin-2-chalcogenone forms one dative bond with most metal atoms, and two dative bonds by utilizing both the lone pair electrons. Interestingly, ImC can be a potential reducing agent to reduce metal salts. This reducing nature made them pivotal in biology to inhibit the lactoperoxidase-catalyzed oxidation, also in inhibition of peroxynitrite- and peroxidase-mediated protein tyrosine nitration [52]. Besides, the nitrogen coordination to metal along with C=E–M coordination could be possible by N-alkyl/aryl imidazolin-2-chalcogenones, while it is absent in N,N'-dialkyl/aryl imidazolin-2-chalcogenones. Similarly, imidazole backbone can also be activated by phosphorous, silicon, chalcogen and group IA/IIA metals [60-62]. Notably, two types of coordination of ImC has been detected with halogens (scheme 1.5).



Scheme 1.5: Known coordination properties of ImC with metals

1.8. ImC-metal chemistry

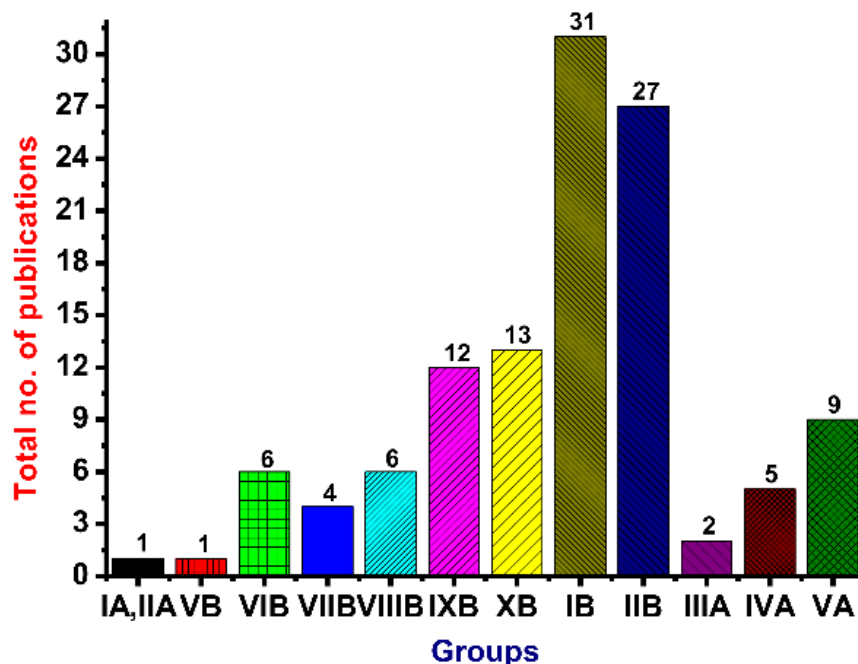


Chart 1.5: Number of publications till January-2018)

The preparation of ImC ligands with a variety of N-substituents is relatively easy, which allows tuning of the electronic properties and/or steric bulk of their complexes. However, metal-ImC chemistry is relatively new and not explored much compared to metal-NHC. 117 articles have been published up to date on imidazolin-2-chalcogenones (Chart 1.5). Although, over 1200 articles have been published on “NHC-copper” and utilized in various fields of chemistry, the ImC-Cu has merely 20 articles so far. The ImC can form different metal complexes by changing metal ligand ratio. Most of the complexes containing mono-ImC’s are mono nuclear and very few are multi nuclear complexes. Bis-ImC’s can also form mono nuclear complexes. But owing to the rotational freedom through linking groups between bis-ImC, complexes bridged by only one of these groups that tend to adopt a skewed arrangement, to minimize steric repulsions between the metal coordination spheres, therefore, the metals are quite widely placed in the complex. Generally the linker is either simple alkyl unit or aromatic unit, and sometimes linker consist donor atoms like C, N or S.

ImC, a special class of heteroketones, have gained increasing interest in recent years as efficient ligating agents in lieu of traditional N-heterocyclic carbenes. In fact, mono- and bis-imidazole selones have been extensively used to generate transition metal-based complexes [63-64] and have further been employed in versatile catalytic applications, such as

1.9. Structural comparison between NHC and ImC

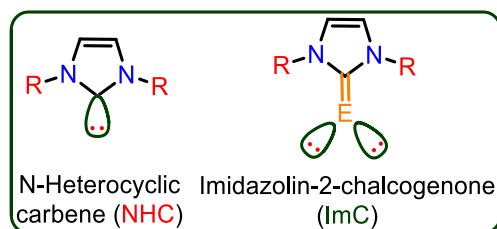


Figure 1.4: Structural comparison between NHC and ImC

NHC's are 2 σ -electron donors and have replaced all the classical 2 electron donors such as, phosphine, amine, ether, carbonyl etc. in organometallic chemistry. After which the modifications to NHC *via* substitution over nitrogen atom and substitution on backbone carbon atoms have been studied comprehensively so far. The modifications over carbene carbon or in place carbene carbon to generate carbene like moieties (analogues) have attracted considerable attention and have been a topic of interest after isolation of free carbene. In this context, a new area of NHC analogous such as, imidazolin-2-chalcogenones (ImC) have synthesized by introducing chalcogenone center at the carbene carbon and investigated to be perfectly analogues to NHC.

Property	ImC	NHC
Isolation	Easy	Inert atmosphere needed
σ -donating ability	Strong	Strong
π -accepting ability	Weak	Weak
Steric and electronic tunability	Tunable	Tunable
Electron density at the metal center	More electron rich	More electron rich
Stability in air	Stable	Unstable
Steric hindrance at the metal center	Relatively less	Relatively high

1.10. Structure, general properties and stability of ImC's

Compared to sulfur (2.58) or tellurium (2.10), the electronegativity of selenium (2.55) is much closer to carbon electronegativity (C = 2.55). As a result imidazolin-2-selone can be considered as a perfect analogue to NHC. The π -electron cloud between carbon and chalcogen atom in C=E bond is expected to be oriented in the middle of carbon and chalcogen atom. However, these imidazoline-2-chalcogenones mostly exist in the form of zwitter ionic form (66%). Signifying the stronger σ -donor abilities over NHC and the uneven distribution of electrons in C=E bond are displayed in figure 1.5.

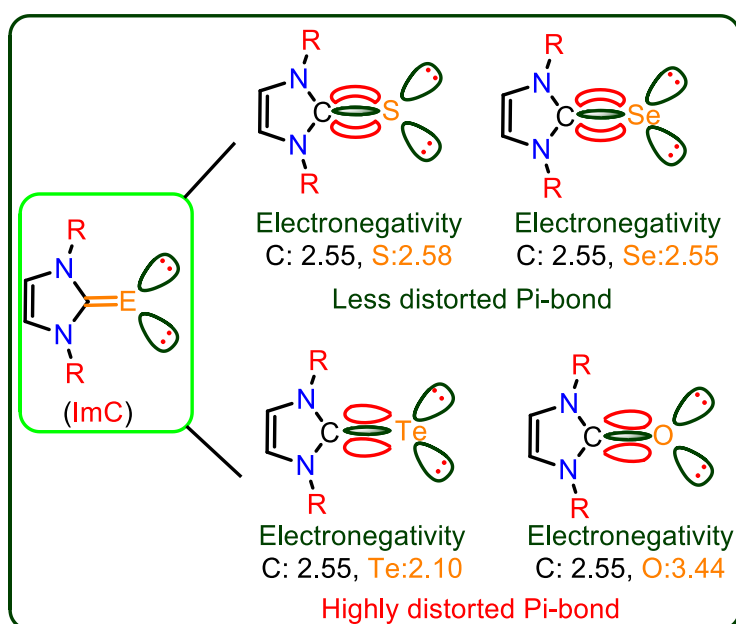


Figure 1.5: π -electron distribution in ImC's

As described the electronic and steric properties can be altered by modifying the substituents on nitrogen atoms and on carbon atoms of imidazole backbone. The steric hindrance is expected to be less in the complexes isolated with ImC compared to NHC-metal, since the metal stays away from carbene carbon through chalcogen center. Compared to NHC, ImC can coordinate to two metal centers in the molecule (Figure 1.6). And the recent investigations have confirmed the competitive efficiencies of ImC supported complexes in organic transformations.

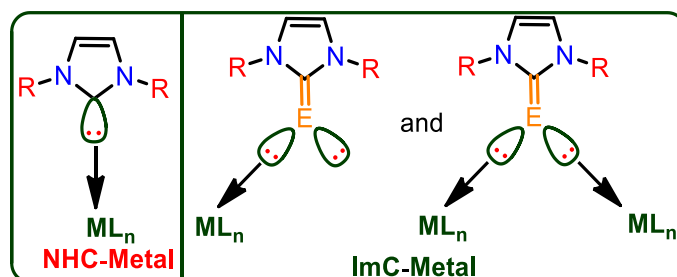


Figure 1.6: Coordination modes of NHC vs ImC

1.11. π -Acceptor Nature of ImC's and NHC's

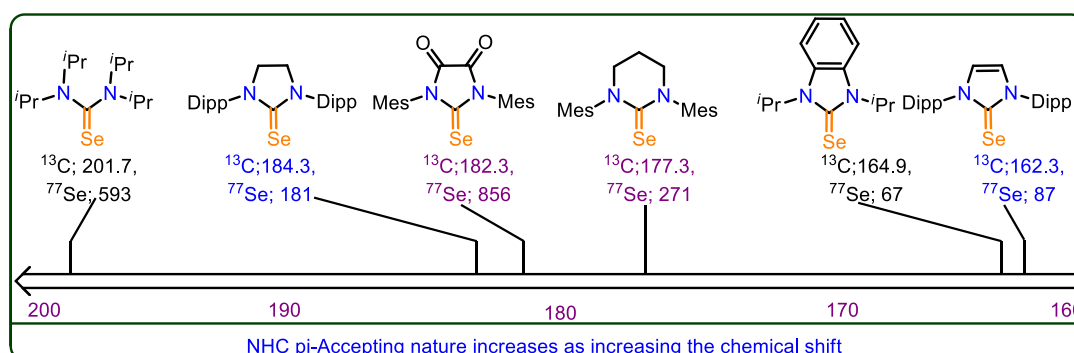
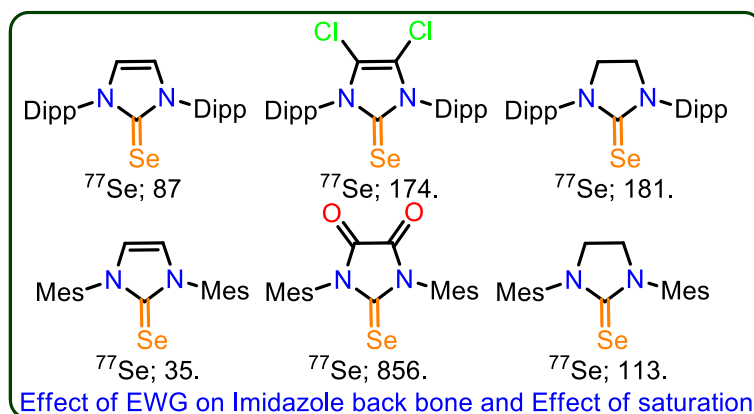


Figure 1.7: π -accepting nature of various NHC's predicted using ImC's

The important applications of ImC is to access the π -accepting nature of NHC. The π -accepting nature of NHC can be evaluated by measuring the ^{77}Se NMR of corresponding ImSe (Figure 1.7, 1.8). The major factors that alters the π -accepting nature are; (i) saturation of the backbone, (ii) introduction of electron withdrawing groups into the backbone, (iii) annulation of aromatic ring, (iv) an increase in NCN angle and (v) replacement of nitrogen by a weaker σ -donor such as sulfur etc.



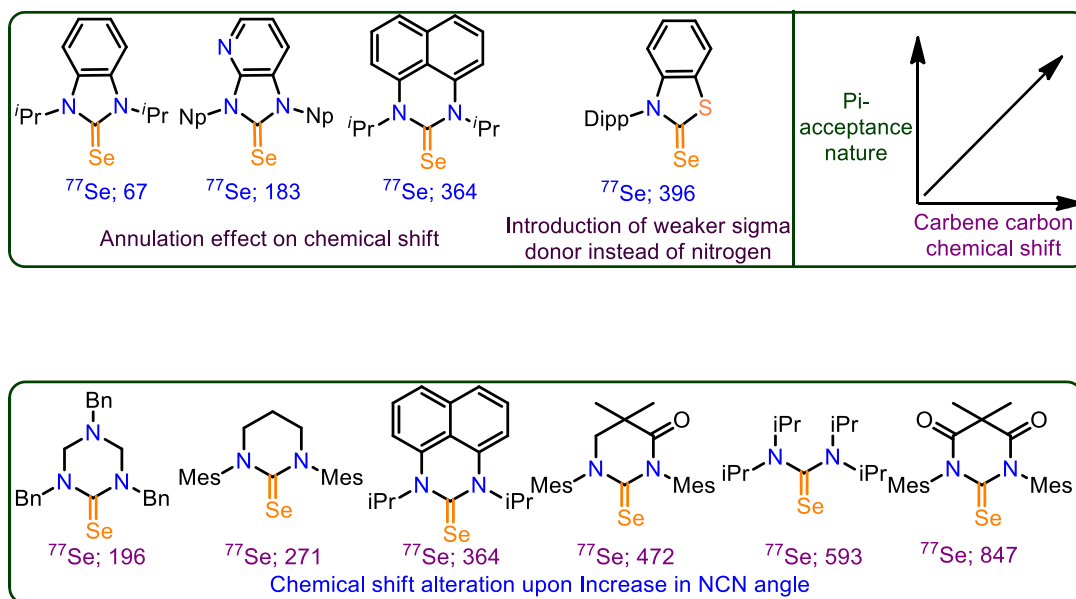
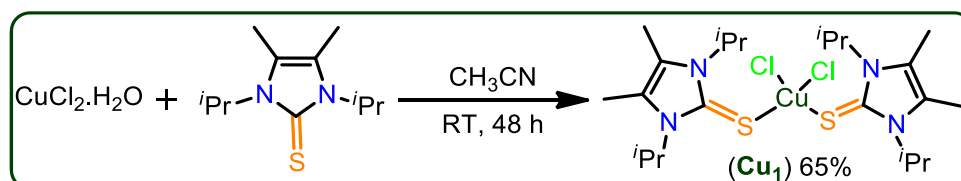


Figure 1.8: Factors effecting the π -accepting nature of NHC

The coordination entities isolated with the elements of periodic table (Except VIA and VIIA group) are presented herein by including their wide spread applications discovered so far.

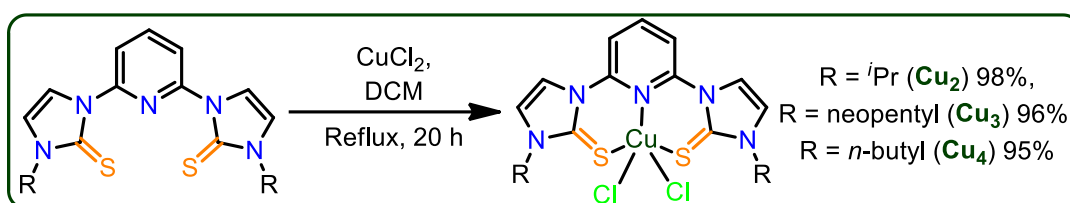
1.12. Copper–ImC complexes

Several ImC-Cu complexes have been synthesized and structurally characterized. In which, only four copper complexes have been isolated in its +II oxidation state. $[\text{CuCl}_2(\text{C}_{11}\text{H}_{20}\text{N}_2\text{S})_2]$ (**Cu₁**) has been synthesized at room temperature from an acetonitrile solution of 1,3-diisopropyl-4,5-dimethylimidazoline-2-thione and $\text{CuCl}_2 \cdot \text{H}_2\text{O}$ in 48 h. Blue crystals of **Cu₁** were obtained from the recrystallization of a saturated acetonitrile solution upon diethyl ether diffusion [71]. Cu(II) center in **Cu₁** display distorted tetrahedral geometry from two Cl atoms [$\text{Cu}-\text{Cl} = 2.2182(6) \text{ \AA}$] and two thione S atoms [$\text{Cu}-\text{S} = 2.3199(6) \text{ \AA}$]. The angles at the copper cation, which lies on a twofold rotation axis, are $\text{Cl}-\text{Cu}-\text{Cl} = 142.84(4)^\circ$, $\text{Cl}-\text{Cu}-\text{S} = 94.80(2)$ and $99.97(2)^\circ$, and $\text{S}-\text{Cu}-\text{S} = 132.46(4)^\circ$.



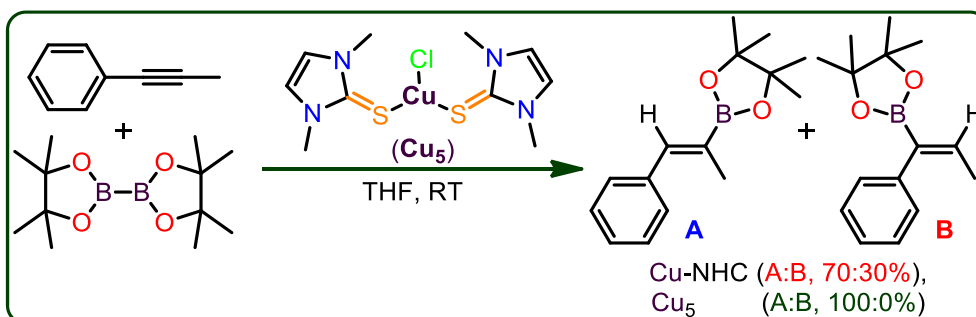
Scheme 1.6: Synthesis of Cu(II) complex, **Cu₁**

Similarly, a series of novel SNS pincer ligands were metallated with CuCl₂ in dichloromethane at reflux to produce tridentate SNS-coordinated copper(II) compounds (**Cu₂₋₄**) and were recrystallized from slow vapor diffusion of diethyl ether into a methanol solution containing the copper complex [72]. Cu(II) center in **Cu₂₋₄** display pseudo-square-pyramidal geometry. The Cu–N bond length is shorter in **Cu₃** (2.22 Å) than in **Cu₂** and **Cu₄** (2.29 and 2.33 Å, respectively). The Cu–S bond lengths are nearly identical for all of the complexes (ca. 2.31–2.32 Å). The Cu–Cl bond lengths are longest in **Cu₃** (2.36 and 2.31 Å) and shortest in **Cu₄** (2.27 and 2.30 Å). The Cu–Cl bond lengths in **Cu₂** (2.33 and 2.31 Å) are between those found in **Cu₃** and **Cu₄**.



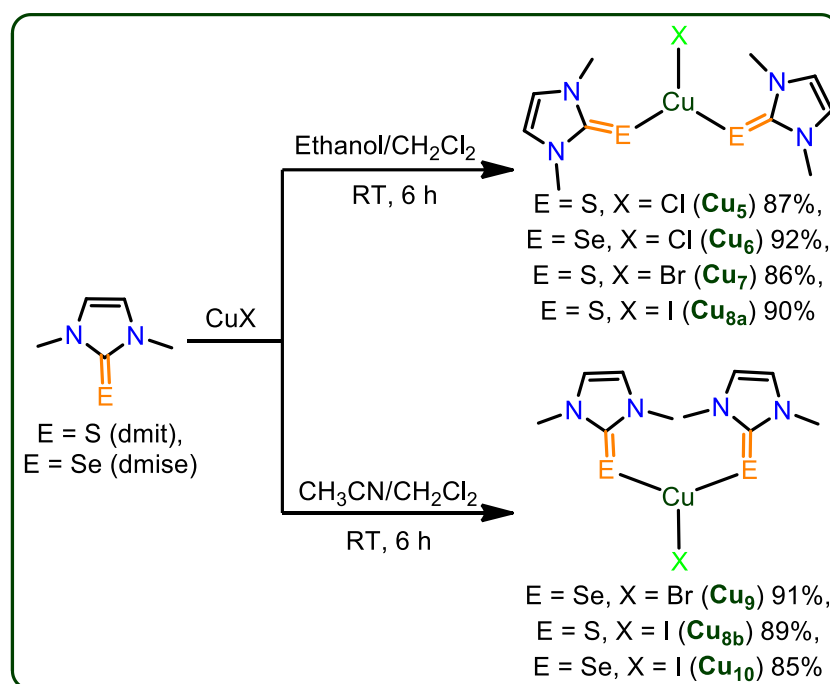
Scheme 1.7: Synthesis of Cu(II) complexes, **Cu₂₋₄**

The metal-ligand coordination in **Cu₅** was demonstrated by growing single crystals by slow vapor diffusion of pentane into a dichloromethane solution of mbit (mbit = 1,3-dimethyl-1*H*-imidazole-2(3*H*)-thione) and CuCl. Moreover, **Cu₅** produced better selectivity in hydroborylation of aromatic internal alkynes over NHC–Cu complexes [73]. The copper metal center in **Cu₅** adopts trigonal planar geometry. The C–S bond distance is elongated to 1.71 Å by coordination to copper and closer to a single bond (1.81 Å) than a double bond (1.56 Å).



Scheme 1.8: Regio-selective borylation of alkynes catalyzed by **Cu₅**

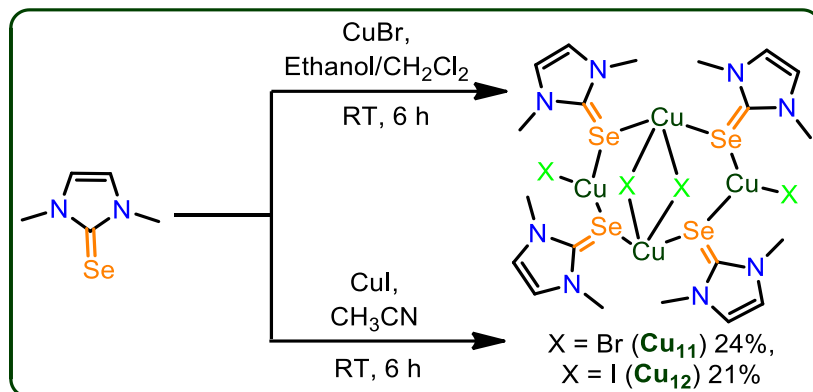
Cu₆₋₁₀ have been synthesized by an equimolar mixtures of ligand and copper halide in a mixed solvent system such as acetonitrile-dichloromethane (**Cu_{9,8b,10}**) or ethanol-dichloromethane (**Cu_{5,7,8a}**) solutions at room temperature for 6h. Interestingly, molecules **Cu_{8b,10}** show intramolecular π - π interactions (**Cu_{8b}**; 3.67 Å to 3.90 Å and **Cu₁₀**; 3.63 Å to 3.95 Å) between the two heterocyclic chalcogenone ligands in the complex. Coordination of the thione ligand to copper in complexes **Cu_{5,7,8a,8b}** results in almost identical S-C bond distances (1.71–1.72 Å), longer than the S-C bond distance in the free thione ligand (1.68 Å). Changes in the halide ligand have little effect on Cu-S bond distances, since the Cu-S bond lengths of 2.2345(10) Å for **Cu_{8a}**, 2.2401(11) Å for **Cu_{8b}**, 2.2376(6) Å for **Cu₅** and 2.2298(9) Å for **Cu₇** are similar. Similarly, the three-coordinate copper-selone complexes **Cu_{6,9,10}**, have identical Cu-Se bond distances of 2.34 Å [74].



Scheme 1.9: Synthesis of Cu(I) complexes, **Cu₅₋₁₀**

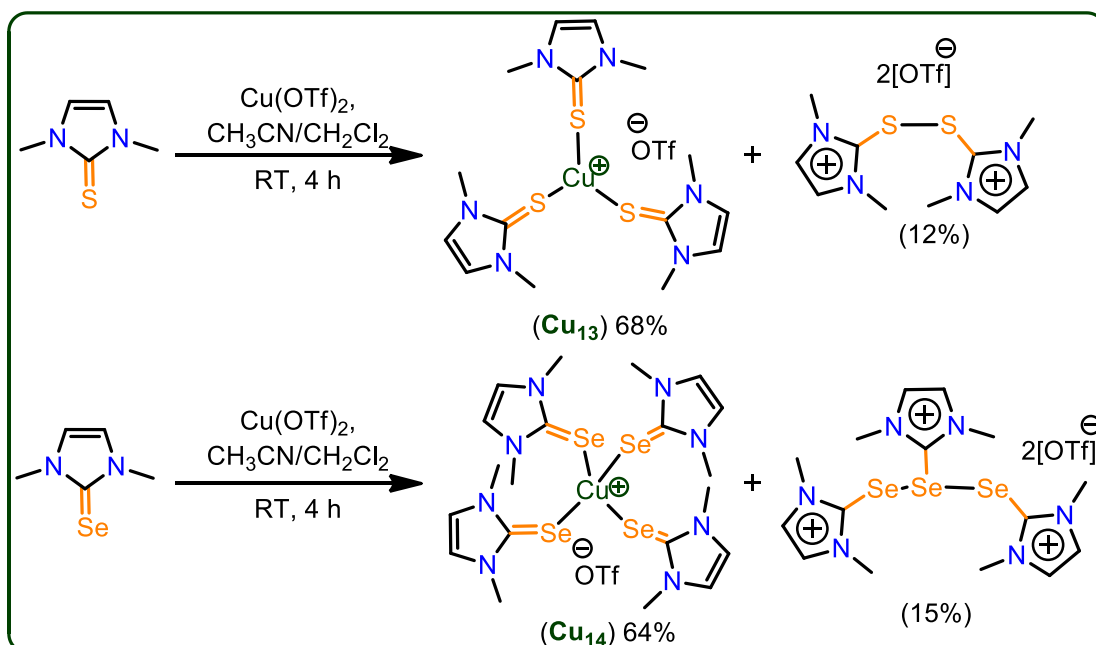
Cu₁₁₋₁₂ have been synthesized with an equimolar quantity of CuBr and CuI as a tetranuclear copper complexes with bridging selone ligands. **Cu₁₂** can also be synthesized *via* a two- step, one-pot reaction with molar equivalents of [Cu(CH₃CN)₄][BF₄] and dmise (1,3-dimethyl-1*H*-imidazole-2(3*H*)-selenone) in acetonitrile, resulting an insoluble precipitate, which can be re-dissolved by the addition of potassium iodide in methanol. The X-ray crystal structures of **Cu₁₁₋₁₂** display two different coordination geometries around copper metal centers, i.e., one of the copper adopts distorted trigonal planar geometry with two selenium

atoms (Cu–Se bond distances are 2.42 Å and 2.41 Å) and one halogen atom (Cu–I and Cu–Br bond distances are 2.58 Å and 2.43 Å), while the other copper exhibits distorted tetrahedral geometry with two selenium atoms and with two bridging halogens [74].



Scheme 1.10: Synthesis of Cu(I) complexes, **Cu₁₁₋₁₂**

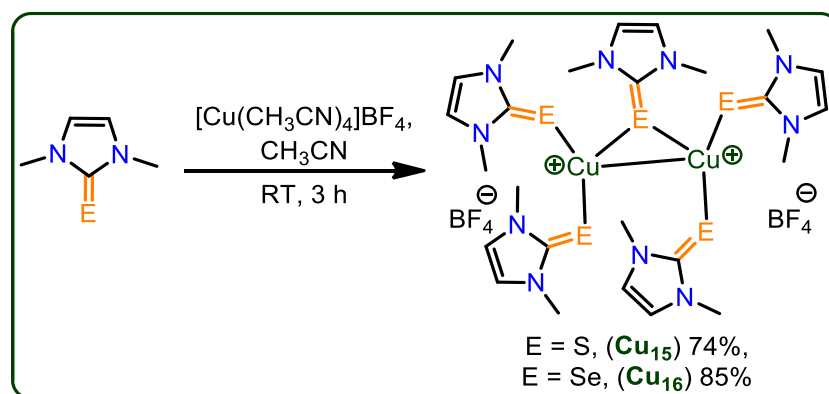
Cu₁₃₋₁₄ have been synthesized in moderate yields from a reaction of $\text{Cu}(\text{OTf})_2$ with an excess of ImC (dmit for **Cu₁₃** and dmis for **Cu₁₄**) in a mixture of acetonitrile and dichloromethane at room temperature for 4 h. Single-crystal X-ray analysis were grown by slow vapor diffusion of diethyl ether into a dichloromethane solution of **Cu₁₃** or into an acetonitrile solution of **Cu₁₄**.



Scheme 1.11: Synthesis of Cu(I) complexes, **Cu₁₃₋₁₄**

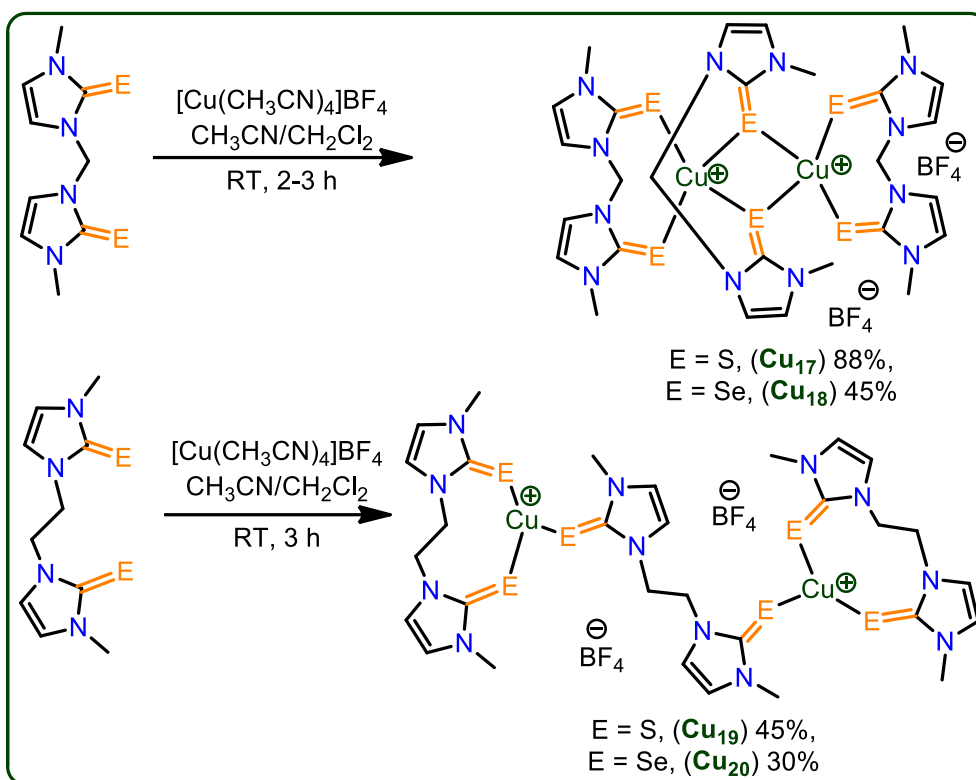
This crystal growth resulted in association with co-crystallized chalcogenone dications. The copper metal center in **Cu₁₃** adopts a distorted trigonal planar geometry, with an average Cu–S bond distance of 2.2454(10) Å, while in **Cu₁₄** copper metal exhibits tetrahedral geometry with Cu–Se bond distance of 2.4538(10) Å. Furthermore, the reduction potentials of ligands have been discovered using **Cu₁₃₋₁₄** i.e., the kinetic studies using UV-vis spectroscopy on **Cu₁₃₋₁₄** indicate that dmise reduces Cu²⁺ to Cu⁺ three times faster than dmit.

Cu₁₅₋₂₄ have been synthesized and structurally characterized. Dinuclear homoleptic copper(I) complexes (**Cu_{15,16}**) have been synthesized *via* the reaction of [Cu(CH₃CN)₄]BF₄ with the appropriate amount of dmit or dmise in acetonitrile at room temperature for 3 h. **Cu₁₅** has been characterized by various spectroscopic techniques while, **Cu₁₆** was additionally characterized by X-ray diffraction analysis. The X-ray quality crystals were obtained by slow diffusion of diethyl ether into an acetonitrile solution of the **Cu₁₆** complex. The structural unit of [(dmise)₂Cu(μ-dmise)Cu(dmise)₂](BF₄)₂ (**Cu₁₆**) is made up of two copper(I) centers, with the Se atom of the dimethylimidazole selone (dmise) ligands bridging the two copper atoms, forming a bent Cu–Se–Cu core. Each copper atom is further bonded to two dmise ligands and thus each copper adopts a distorted trigonal planar geometry. The average of four Cu–Se distances involving terminal dmise ligands (2.35 Å) is shorter than those involving the bridging dmise ligand (2.42 Å). The existing Cu(1)–Cu(2) bond distance is 2.6326(11).



Scheme 1.12: Synthesis of Cu(I) complexes, **Cu₁₅₋₁₆**

Cu_{17,18} are isostructural molecules with two terminal and one bridging bis-ligand to exhibit butterfly shape through Cu₂E₂ cores. Each copper metal adopts a distorted tetrahedral geometry, with Cu···Cu distances (2.96 and 2.97 Å for **Cu₁₇** and **Cu₁₈**, respectively). As expected, the terminal Cu–S and Cu–Se bond distances in **Cu₁₇** and **Cu₁₈** (averages 2.29 and 2.42 Å, respectively).

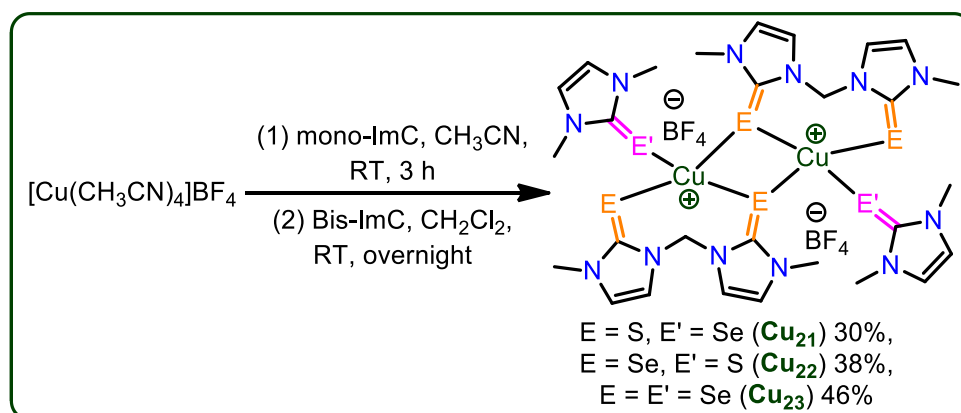


Scheme 1.13: Synthesis of Cu(I) complexes, **Cu₁₇₋₂₀**

The centrosymmetric complex **Cu₁₉** exhibits two copper(I) centers with distorted trigonal planar geometry arising from the coordination of a terminal bidentate ligand and one of the thione moiety from bridging bidentate ligand. The Cu-S distances are in the expected range (2.2871(16)-2.3030(16)). While, **Cu₂₀** has been structurally characterized by various spectroscopic techniques and the crystal structure investigations have not been derived.

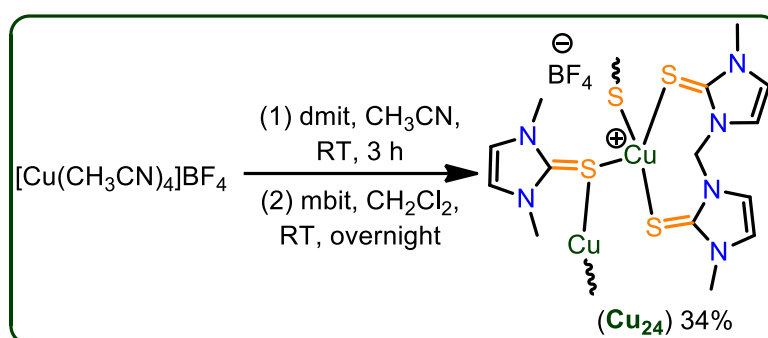
Cu₂₁₋₂₃ have been synthesized from mixed ligands in a mixture of acetonitrile and dichloromethane solvent and structurally characterized but the crystal structures were demonstrated only for **Cu_{21,23}**. The two dinuclear copper complexes (**Cu_{21,23}**) are centrosymmetric and exhibit rhombic Cu₂Se₂ cores, with all the bis(selenone) ligands exhibiting the unusual bridging monodentate:bidentate coordination mode. Each copper metal center is coordinated to a terminal dmit or dmise ligand and three selenone moieties from mbis (3,3'-methylenebis(1-methyl-1*H*-imidazole-2(3*H*)-selenone)) ligands (one terminal and two bridging), with an overall distorted tetrahedral geometry in each case. The weak Cu–Cu interactions were expected in molecules **Cu_{21,23}**, since the existing Cu···Cu distances (2.73 and 2.74 Å for **Cu₂₁** and **Cu₂₃**, respectively) are slightly shorter than the sum of the van der Waals radii of copper. The average lengths of the bridging Cu–Se bonds derived from mbis

ligands (2.52 and 2.51 Å for **Cu₂₁** and **Cu₂₃**, respectively) are longer than the average terminal Cu–Se bond lengths associated with the same ligands (2.42 Å for both complexes).



Scheme 1.14: Synthesis of Cu(I) complexes, **Cu₂₁₋₂₃**

The X-ray structure of **Cu₂₄**, reveals the formation of a coordination polymer in which an infinite chain of four-coordinate copper(I) centers are bound to two terminal sulfur atoms from a bidentate mbit (3,3'-methylenebis(1-methyl-1*H*-imidazole-2(3*H*)-thione)) ligand and two sulfur atoms from bridging dmit ligands. The geometry around Cu(I) is best described as distorted tetrahedral and the average Cu–S bond lengths of 2.36 Å [75].

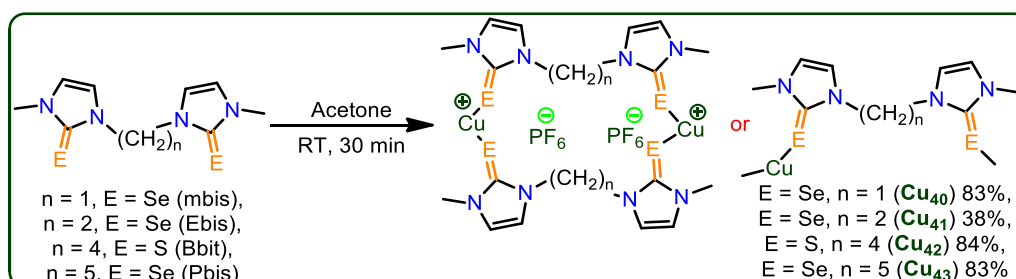
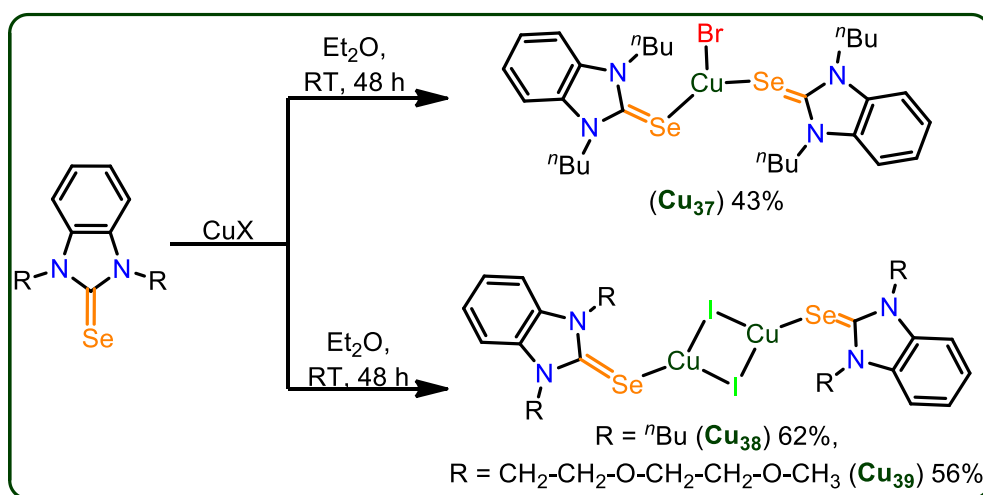


Scheme 1.15: Synthesis of Cu(I) complexes, **Cu₂₄**

All these complexes (**Cu₁₅₋₂₄**) were subjected to electrochemical studies to investigate their reduction potentials [64,76-77]. Upon examination of the reduction potentials for the copper complexes **Cu₁₅₋₂₄**, it is clear that the selenone containing complexes exhibit more negative Cu(II/I) reduction potentials relative to the analogous thione complexes irrespective of the bridging unit.

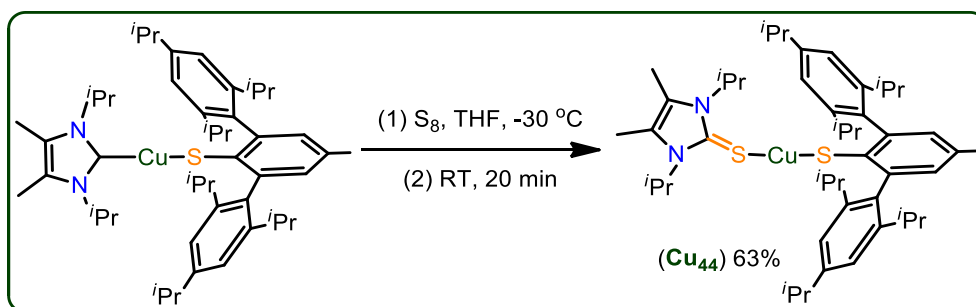
environment with comparable average Cu–Se (2.30 Å) and Cu–S (2.20 Å) bond distances. All the complexes were stable in their solid state for about 5–10 h, but are easily oxidized to Cu(II) in solution. The electrochemical studies on **Cu**_{25–36} revealed that the reduction potentials of the copper selenone complexes are more negative than the copper thione complexes [64,78].

The copper(I) complexes, **Cu**_{37–39} have been synthesized and structurally characterized. **Cu**_{37–39} synthesized by utilizing the appropriate selone ligand in diethyl ether followed by the addition of equimolar quantity of respective CuX (X = Br for **Cu**₃₇ and X = I for **Cu**_{38,39}). **Cu**_{37,38} obtained as precipitates from the reaction mixture which were recrystallized from dichloromethane, while **Cu**₃₉ was semisolid in nature. Therefore structural investigations have made only on molecule **Cu**₃₈ and was existing as a dimer in its solid state. The central (SeCuI)₂ unit is planar and the Cu–Se bond length is (2.331(1) Å) as expected. In this molecule, both the Cu–I distances differ from each other (2.537(1) Å and 2.640(1) Å) [79–80].



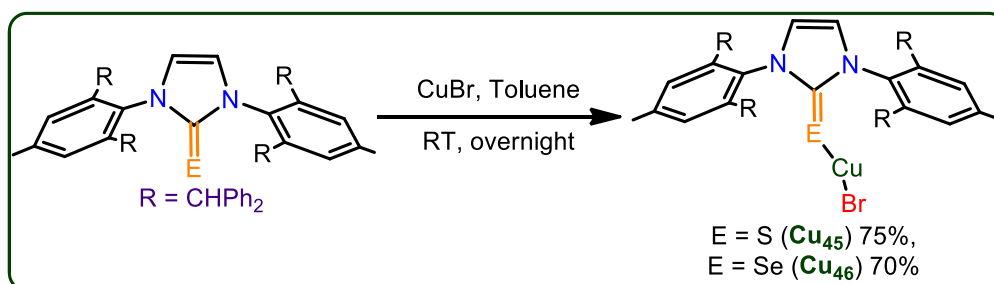
The Cu(I) complexes (**Cu**₄₀₋₄₃) have been synthesized by using equimolar quantities of [Cu(CH₃CN)₄]PF₆ and respective chalcogenone ligand in acetone at room temperature. X-ray structural information is not been evaluated while, spectroscopic techniques have been employed to characterize **Cu**₄₀₋₄₃ [81].

Cu₄₄ is a quasi-two-coordinate Cu(I) complex, which is structurally characterized. To a solution containing [Cu(SAr*)(ⁱPr₂NHCMe₂)] in of THF at -30 °C was treated with an equimolar solution of sulfur in of THF. The reaction was performed at room temperature for 20 minutes and the obtained yellow residue was extracted with *n*-hexane and recrystallized at -30 °C to yield colorless crystals. The Cu–S bond distance is 2.157(1) Å with aryl ring, while ImC S–Cu distance is 2.196(1) Å and the S–Cu–S angle deviated from linearity (152.98(4)°) [82].



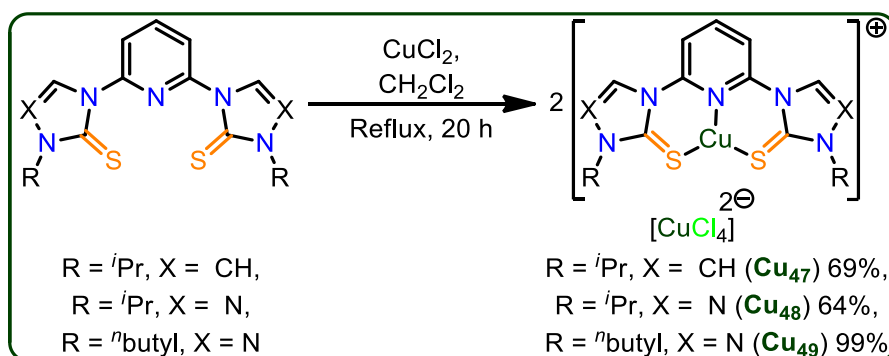
Scheme 1.19: Synthesis of Cu(I) complexes, **Cu**₄₄

The mononuclear copper complexes, **Cu**₄₅₋₄₆ have been isolated from the reaction between the corresponding ligand with equimolar quantity of CuBr in toluene at room temperature. Structurally characterized by various spectroscopic techniques while, crystallographic data refrained due to the poor quality data [83].



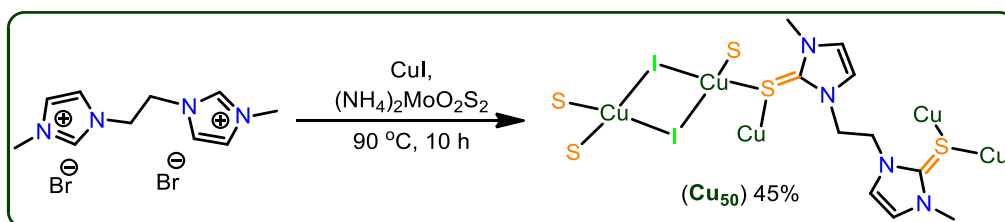
Scheme 1.20: Synthesis of Cu(I) complexes, **Cu**₄₅₋₄₆

A tridentate ligand with two sulfur and one nitrogen donor has been utilized to synthesize three-coordinate copper(I) complexes, **Cu**₄₇₋₄₉ by an equimolar quantities of ligand and CuCl₂ in dichloromethane at reflux for 20 h. X-ray quality crystals were grown by a slow vapor diffusion of diethyl ether into a methanol solution containing the copper complex (**Cu**_{48,49}). Copper metal center in **Cu**_{48,49} display pseudo-trigonal planar geometry, with C–S bond lengths ranging from 1.695 to 1.714 Å, which are between what is normally associated with a C–S single bond (1.83 Å) and a C=S double bond (1.61 Å). The Cu–N bond lengths in each system are approximately 2.0 Å and the Cu–S bonds are 2.2 Å [84].



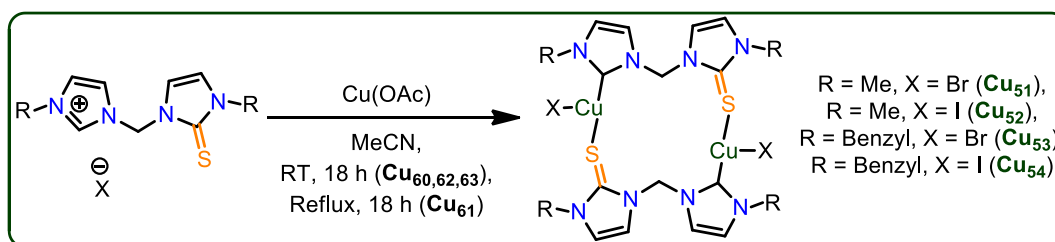
Scheme 1.21: Synthesis of Cu(I) complexes, **Cu**₄₇₋₄₉

The first poly-rotaxane complex (**Cu**₅₀) featuring the bi-imidazolium thiolate cation ligand is isolated by the formation of *in situ* C–S bonding *via* C–H bond activation. The synthesis includes the mixing of 1,1'-(ethane-1,2-diyl)bis(3-methyl-1*H*-imidazol-3-ium) bromide, CuI and (NH₄)₂MoO₂S₂ and grinding in an agate mortar followed by dissolution in DMF. The reaction mixture was transferred to a reaction flask followed by stirring at 90 °C for 10 h. The reaction mixture was then filtered and crystallized in the dark. 12-membered ring molecular box and related rotaxane structure exists in **Cu**₅₀. Two Cu ions coordinating with two μ₂-I [Cu–I, 2.650(1) Å] form a four-member ring. It is μ₂-S coordinating to copper [Cu–S, 2.415(3) or 2.434(3) Å] that bridge to connect above building blocks into the 12-member ring (–Cu–I–Cu–S–Cu–S–)₂, and extend into a 2-D network [85].

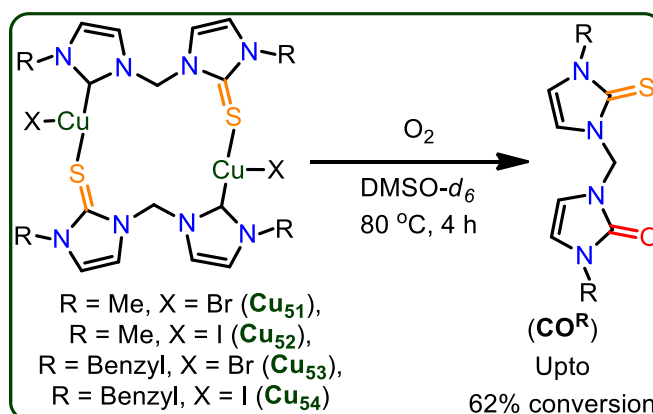


Scheme 1.22: Synthesis of Cu(I) complexes, **Cu**₅₀

Cu₅₁₋₅₄ are the Cu(I) complexes synthesized from mixed bidentate (CS-donor) ligands by treating with equimolar quantity of Cu(OAc) in acetonitrile at suitable temperature. X-ray quality crystals have been developed by slow vapor diffusion of saturated solutions of **Cu_{51,54}** in acetonitrile. Crystal structures revealed the dimeric structural arrangement of **Cu_{51,54}** in their solid state. Interestingly, **Cu₅₁** display a Cu–S–Cu–S ring resembling a parallelogram motif. The metal center in **Cu₅₁** adopts a distorted tetrahedral geometry and Cu–S distances are in the range of 2.4210(4) to 2.4458(4) Å, while **Cu₅₄** display distorted trigonal planar arrangement and Cu–S distances are in the range of 2.3557(6) to 2.8012(6) Å [86].



Scheme 1.23: Synthesis of Cu(I) complexes, **Cu₅₁₋₅₄**

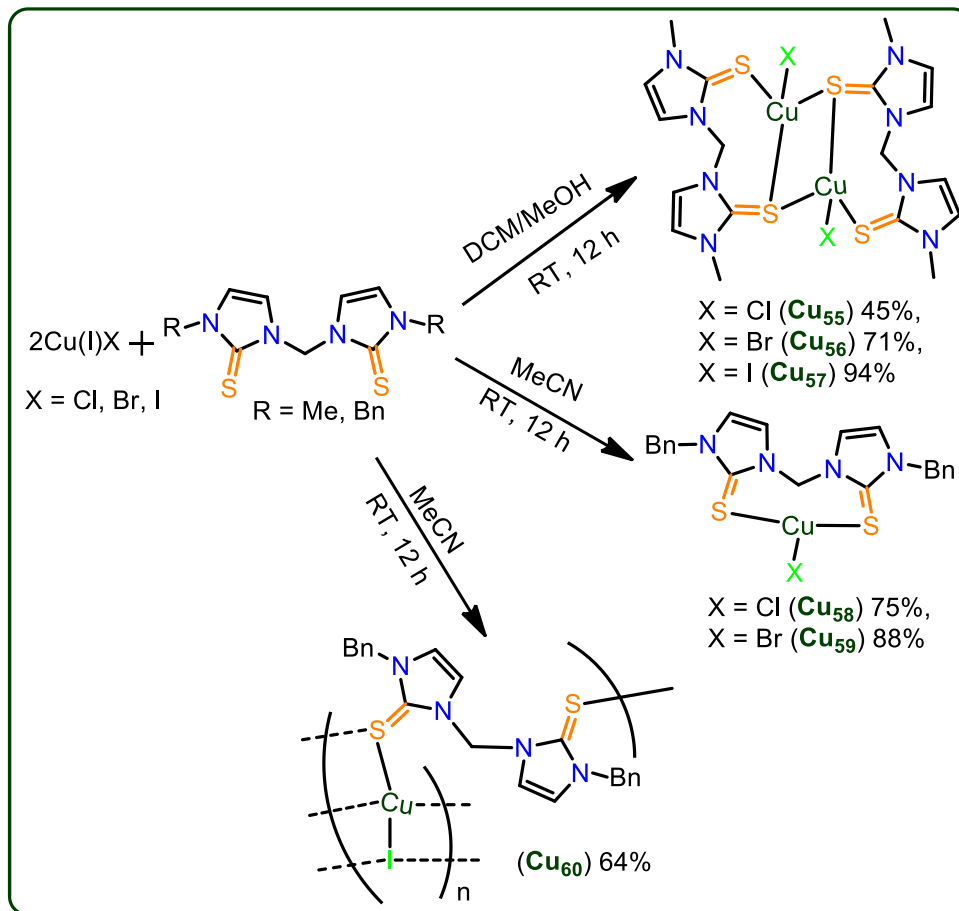


Scheme 1.24: Synthesis of CO^{R} from **Cu₅₁₋₅₄** by demetallation process

Demetallation followed by oxygen atom addition of the CS^{R} ligands takes place in strongly coordinating solvents (DMSO and MeCN) under aerobic conditions to yield CO^{R} moiety, suggesting the weak coordination of the N-heterocyclic carbene to copper(I) centers. Moreover, these complexes utilized for their activities in C–N and C–S cross-coupling reactions. However, these complexes revealed very poor results for cross-coupling of aryl iodides with amides.

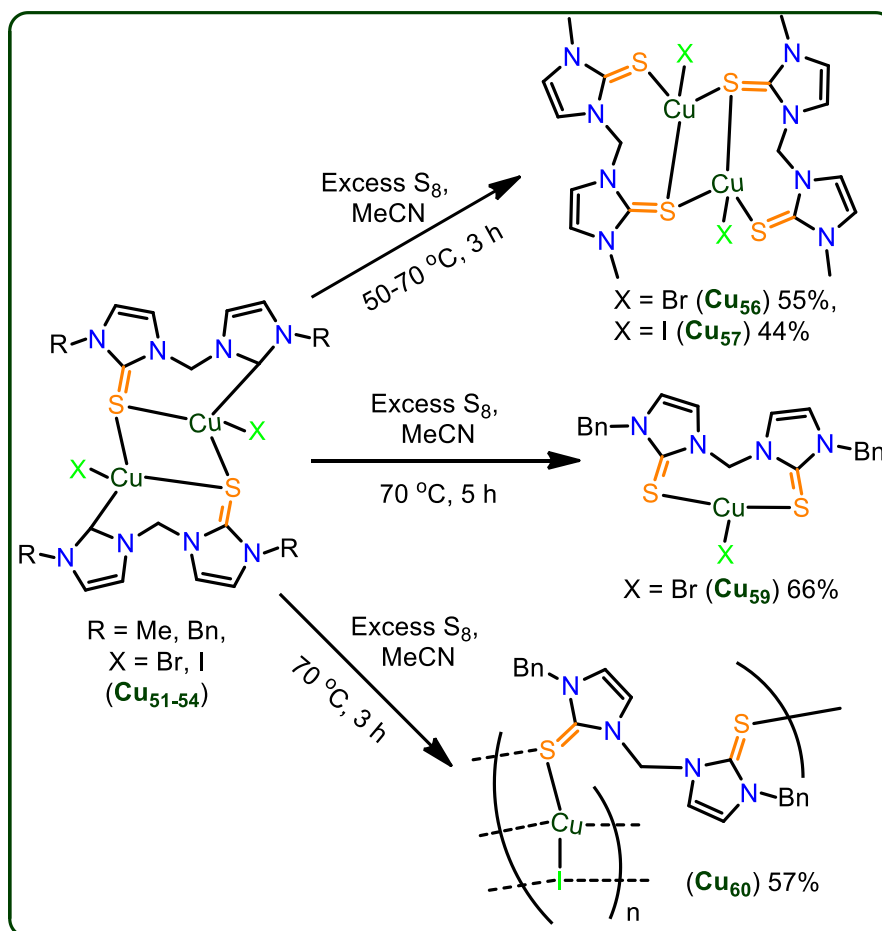
Bis-imidazolin-thione supported copper complexes (**Cu₅₅₋₆₁**) have been synthesized in two different methods. Complexes **Cu₅₅₋₅₇** have been isolated by addition of one equivalent

of a dichloromethane solution of the ligand to a methanol solution of the corresponding copper halide at room temperature, while **Cu**₅₈₋₆₀ were readily prepared by addition of one equivalent of the ligand in acetonitrile to a solution of the corresponding copper(I) halide in acetonitrile.



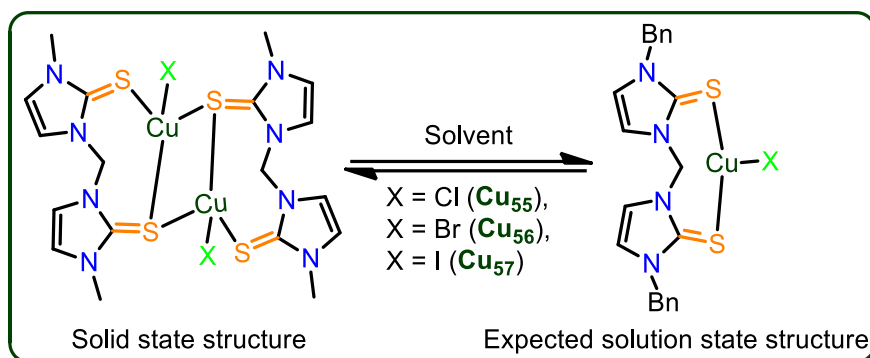
Scheme 1.25: Synthesis of Cu(I) complexes, **Cu**₅₅₋₆₀

Similarly, sulfur atom insertion method is employed during the reaction between $[\text{CuX}(\text{CS}^{\text{R}})]_2$ ($\text{X} = \text{Br, I}$ and $\text{R} = \text{Me, Bn}$) with an excess of S_8 in acetonitrile at elevated temperature to produce the copper complexes, **Cu**_{56-57,59-60} in fairly good yields [87].



Scheme 1.26: Synthesis of Cu(I) complexes, **Cu₅₆₋₆₀** from mixed ligand based copper complexes, **Cu₅₁₋₅₄** by sulfur insertion method

The spectral investigations on three copper(I) halide complexes (**Cu₅₅₋₅₇**) suggested the existence of monomeric form in contrast with the solid state dimeric molecules as presented below. However, in the solid state the copper metal center adopts distorted tetrahedral geometry, and the Cu-S bond distances lie between 2.3221(6) to 2.4602(5) Å. **Cu₅₈₋₅₉** are mononuclear complexes with trigonal planar arrangement around metal center, and the Cu-S bond distances are in between 2.2032(5) to 2.2178(5) Å for **Cu₅₈**, 2.2071(2) to 2.2129(3) Å for **Cu₅₉**. While, **Cu₆₀** is a polymeric complex with different structural arrangement, in which, two sulfur donor atoms connected to different copper atoms. The Cu-S distance for the sulfur donor attached to one copper atom is 2.3393(17) Å, while the other sulfur donor atom attached to two copper atoms is 2.4136(18) to 2.3278(17) Å.



Scheme 1.27: Expected mononuclear complexes from binuclear Cu(I) complexes, \mathbf{Cu}_{55-57}

Similarly, \mathbf{Cu}_{61} has been isolated as single crystals by slow evaporation method by layering the from $\text{Cu}(\text{BF}_4)_2$ hydrate in methanol over dichloromethane solution of mbit (mbit = 1,3-dimethyl-1*H*-imidazole-2(3*H*)-thione).

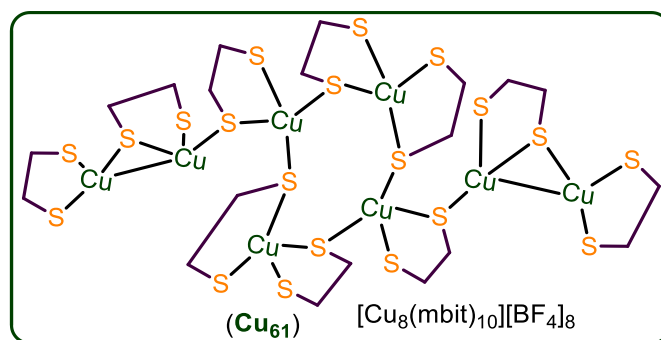
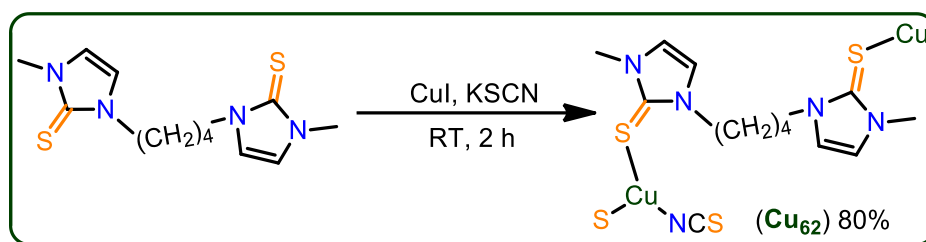


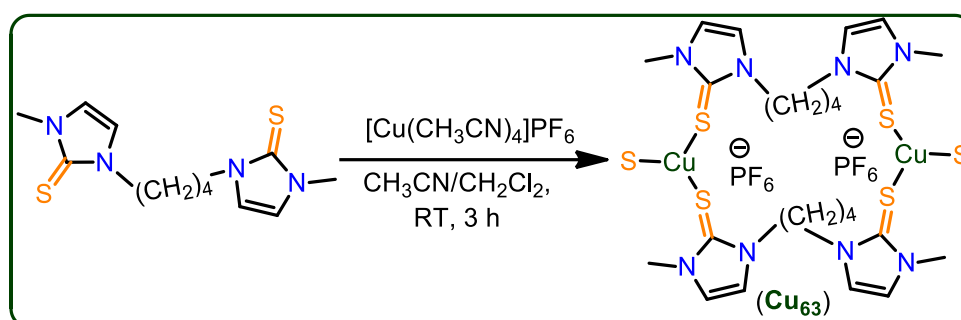
Figure 1.9: Molecular structure of Cu(I) complex, \mathbf{Cu}_{61}

\mathbf{Cu}_{62} is a 2D coordination polymer isolated by mixing equimolar quantities of CuI and KSCN in an acetonitrile solution. The successive addition of respective ligand at room temperature and additional stirring for 2 h produce \mathbf{Cu}_{62} . Each copper metal atom is coordinated by two sulfur atoms with an average Cu-S distance of 2.2414 Å and one nitrogen atom from a terminal N-bonded thiocyanate anion with a Cu-N distance of 1.9172(17) Å. The coordination geometry around the copper atom is a slightly distorted trigonal-planar. Moreover, the \mathbf{Cu}_{62} complex was found to an effective drug for antibacterial activity [88].



Scheme 1.28: Synthesis of Cu(I) coordination polymer complex, **Cu₆₂**

Cu₆₃ is the coordination polymer, which was isolated by treating $\text{Cu}(\text{CH}_3\text{CN})_4\text{PF}_6$ in acetonitrile with excess of bbit (3,3'-(butane-1,4-diyl)bis(1-methyl-1*H*-imidazole-2(3*H*)-thione)) ligand in dichloromethane at room temperature. The copper metal center adopts distorted trigonal planar geometry with sulfur atoms of three bbit ligands, the average C–S bond distance is 1.7144 Å, while the Cu–S bond lengths vary from 2.226(6) to 2.269(6) Å and are in good agreement with the corresponding values in the other trigonal planar CuS_3 geometry. **Cu₆₃** also found to show an interesting features in antibacterial activity [89].



Scheme 1.29: Synthesis of Cu(I) complex, **Cu₆₃**

1.13. ImC-Metal complexes and their applications

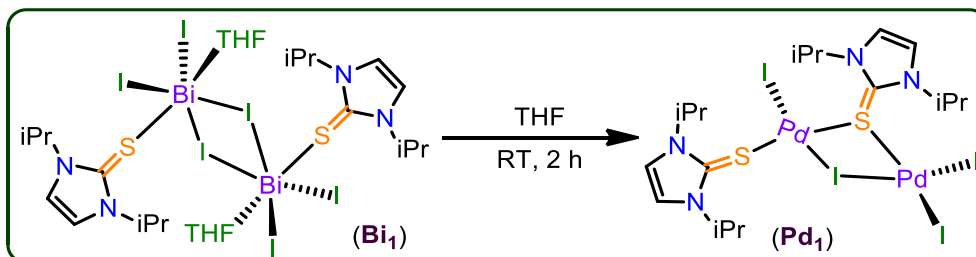
ImC supported metal derivatives find applications in organic transformations, biology and as trans-metallating agents. Although 117 articles were reported, most of them describe the structural investigations and the molecules that are showing interesting applications have described below.

1.13.1. As trans-metallating agents

Particularly, thione derivatives of bismuth(II) and zinc(II) elucidated to be acting as potential synthons for trans-metallation phenomenon.

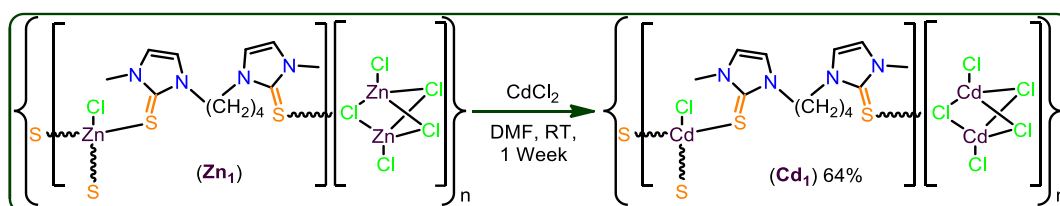
Pd₁ has been isolated from **Bi₁** by trans-metallation route by the dropwise addition of a solution of $[\text{Pd}(\text{OAc})_2]$ in THF to a solid **Bi₁** at room temperature. A dark-red to dark-brown

mixture can be noticed and very few black crystals of **Pd₁** suitable for X-ray diffraction were obtained by slow evaporation of the THF solution at room temperature after several weeks in a tube [90].



Scheme 1.30: Synthesis of Pd(ImC) complex (**Pd₁**) from Bi(ImC) (**Bi₁**) by trans-metallation reaction

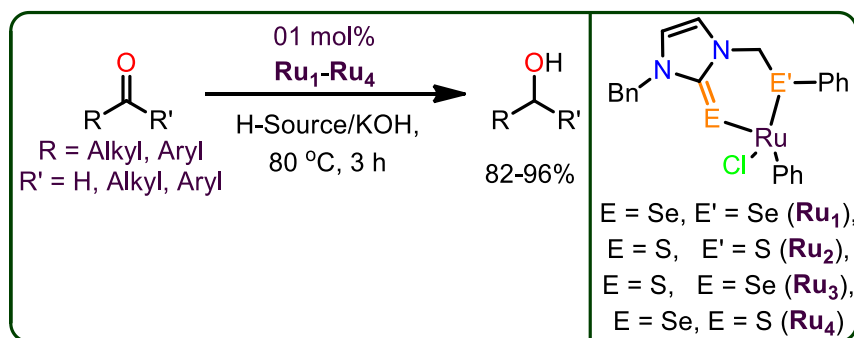
Similarly, **Zn₁** polymer has been treated with CdCl₂ in DMF to isolate **Cd₁** polymer by metal exchange method. Good quality cubic shaped crystals of **Cd₁** were obtained after a week. In addition to this, **Zn₁** and **Cd₁** have shown promising features in inhibiting the activity of bacteria [91].



Scheme 1.31: Synthesis of Cd(ImC) complex (**Cd₁**) from Zn(ImC) complex (**Zn₁**) by trans-metallation reaction

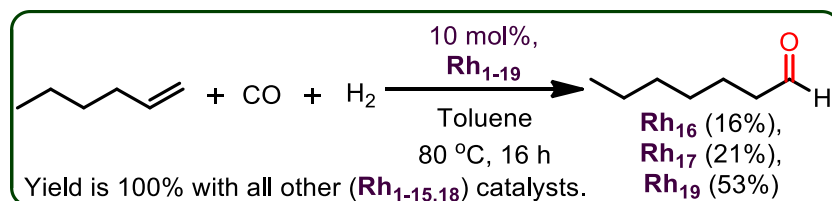
1.13.2. As catalysts in organic transformations

1-Benzyl-3-phenylchalcogenylmethyl-1,3-dihydrobenzoimidazole-2-chalcogenone ligands supported Ru(II) half-sandwich complexes (**Ru₁₋₄**) have been synthesized and discovered their catalytic efficiencies in transfer hydrogenation of carbonyl compounds [92]. Particularly, **Ru₄** has the lowest energy gap between the HOMO and LUMO orbitals, and shows the better catalytic activity among the four complexes.



Scheme 1.32: Catalytic transfer hydrogenation of carbonyl compounds catalyzed by **Ru₁₋₄**

The thione supported rhodium complexes (**Rh₁₋₁₁**) found to be more active catalysts under selected conditions than their corresponding NHC complexes (**Rh_{16,17,19}**) for hydroformylation of 1-hexene despite the fact that their selectivity is low [93].



Scheme 1.33: Hydro-formylation reaction of 1-hexene catalyzed by **Rh₁₋₁₉**

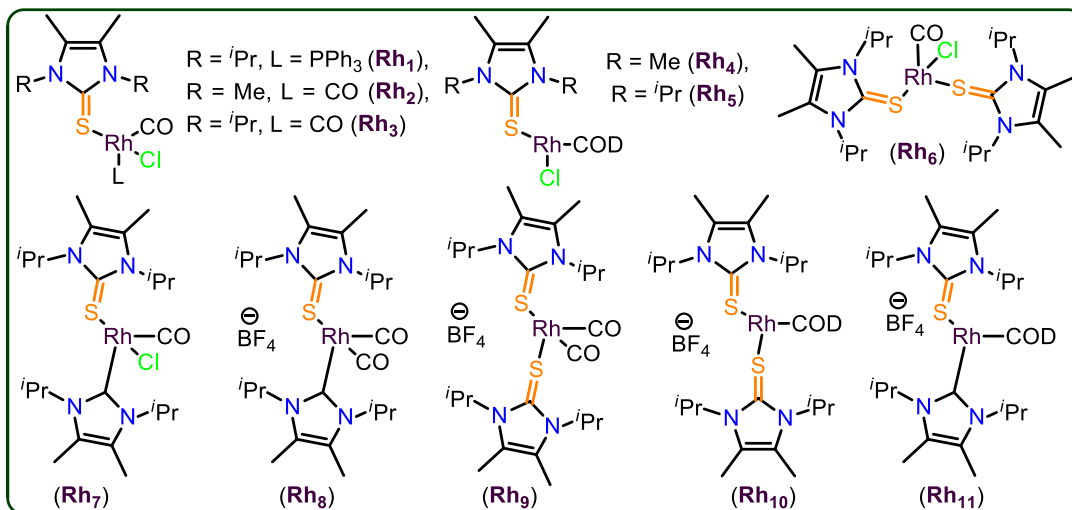


Figure 1.10: Mixed and thio ligands supported Rh complexes used in Hydro-formylation reaction

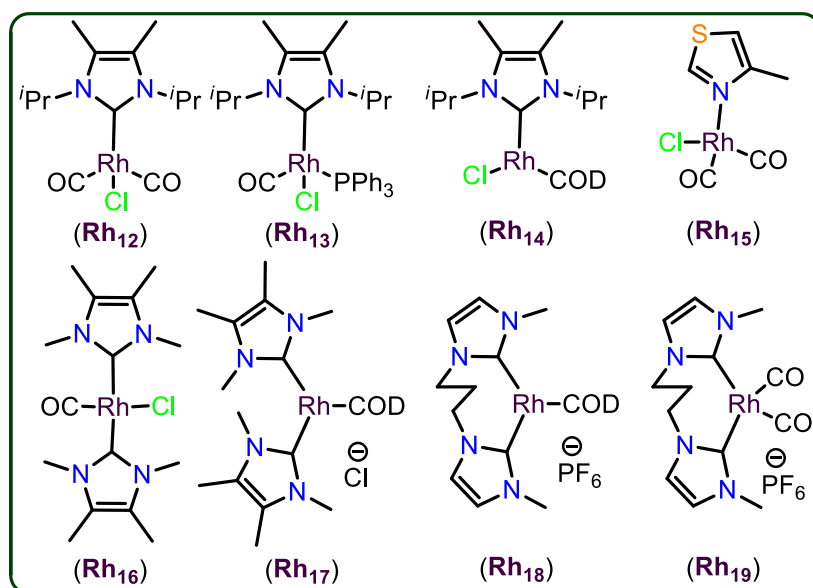
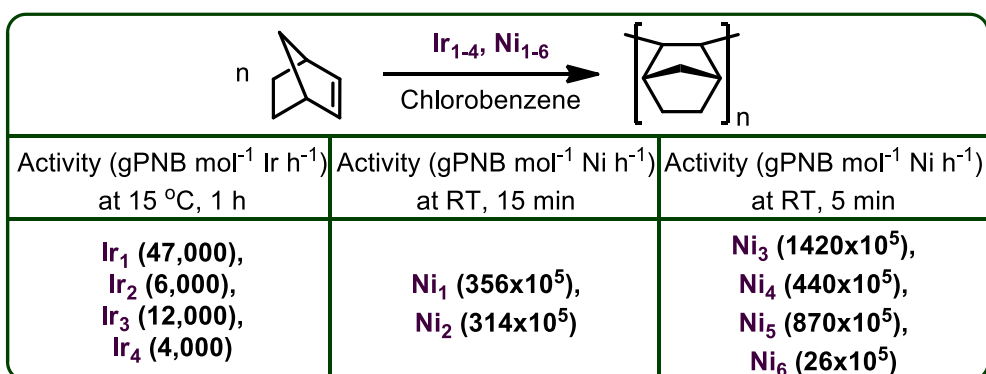


Figure 1.11: NHC supported Rh complexes used in Hydro-formylation reaction

Rhodium (**Rh**₂₀₋₂₃) and Iridium (**Ir**₁₋₄) complexes have been synthesized and structurally characterized. However, Iridium complexes are only moderately active in the vinyl polymerization of norbornene in the presence of methylaluminoxane [94]. Similarly, nickel complexes (**Ni**₁₋₆) have been isolated for the vinyl polymerization of norbornene and are found to exhibit higher activities for norbornene addition polymerization. However, all these catalysts work after the activation with MAO (Methylaluminoxane) and the catalysts **Ni**₃ found to be the best catalysts with higher activity values (1.42×10^8 gPNB mol⁻¹ Ni h⁻¹) at room temperature [57,95].



Scheme 1.34: Vinyl polymerization of norbornene catalyzed by **Ir**₁₋₄, **Ni**₁₋₆

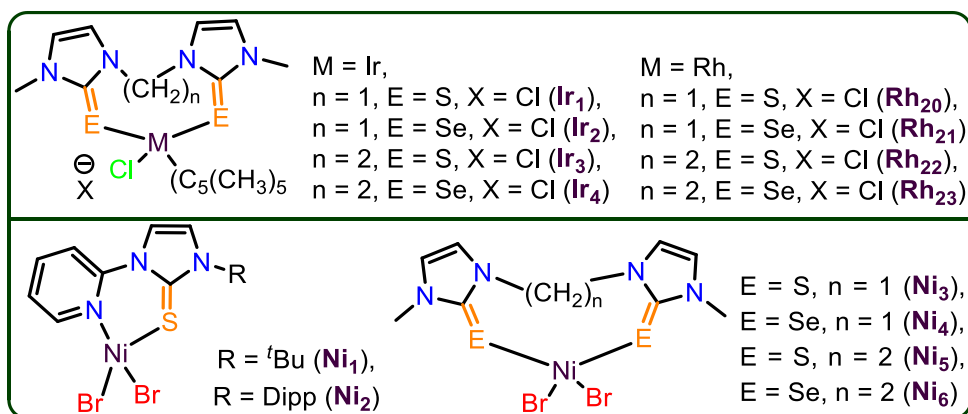
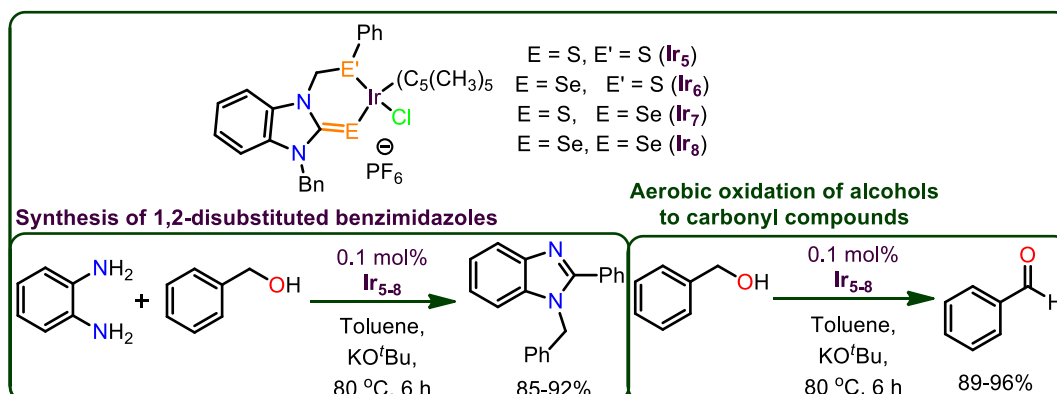


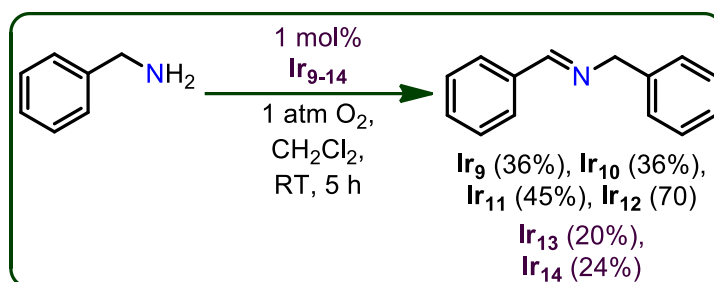
Figure 1.12: Catalysts used for vinyl polymerization of norbornene

Ir₅₋₈ are the first examples of complexes of (E, E') (E and E' = S and Se) ligands with Ir(III). These are efficient catalysts for the one-pot synthesis of 1,2-disubstituted benzimidazoles from alcohols. Similarly, the transfer of hydrogen from alcohols to acetone to yield carbonyl compounds is also been demonstrated by **Ir**₅₋₈ and are displaying the better efficiency than previous reports with minimal catalyst loading [96].



Scheme 1.35: Synthesis of 1,2-disubstituted benzimidazoles and aerobic oxidation of carbonyl compounds by **Ir**₅₋₈

A series of iridium complexes (**Ir**₉₋₁₂) have been isolated with bis thione ligands and studied their efficiencies under visible-light induced oxidative coupling of benzylamine to imine, interestingly, the isolated yields are appreciable with **Ir**₉₋₁₂ than their corresponding NHC derivatives **Ir**₁₃₋₁₄ [70].



Scheme 1.36: Oxidative coupling of benzylamine to imine by **Ir₉₋₁₄**

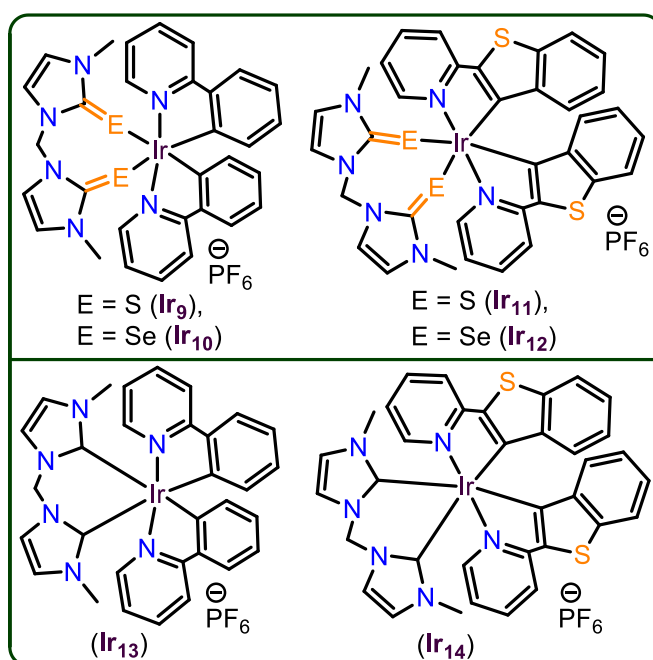
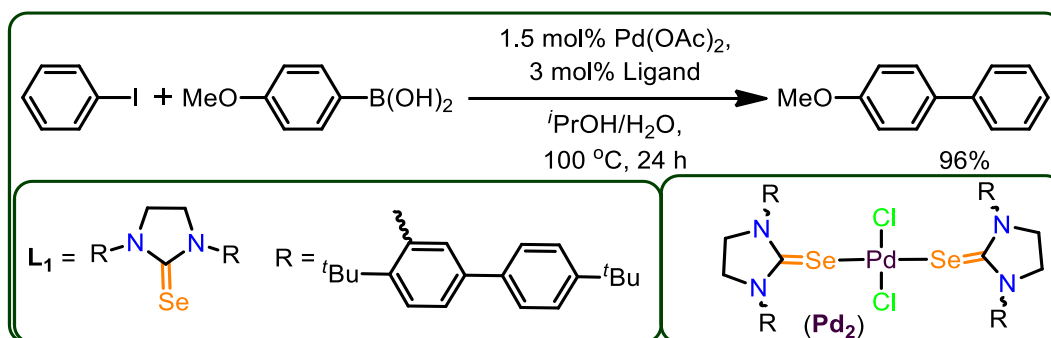
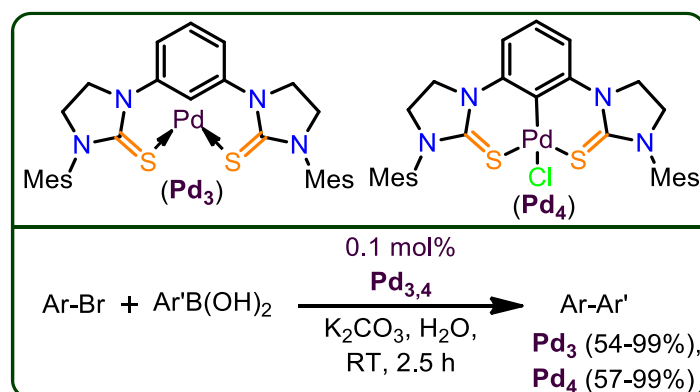


Figure 1.13: Catalysts used for the oxidative coupling of benzylamine

Interestingly, the *in situ* generated catalyst (**Pd₂**) has been demonstrated for the cross-coupling reactions of various aryl halides with arylboronic acid catalysis (Suzuki coupling) under aerobic condition.⁹⁷ However, the ligand **L₁** coordination with palladium has been detected by single crystal x-ray diffraction analysis during the reaction between PdCl₂(CH₃CN)₂ and **L₁** in dichloromethane at room temperature. In addition to this, Pd(0) and Pd(II) complexes (**Pd₃** and **Pd₄**) have been synthesized and compared their catalytic activity in Suzuki coupling reaction [98]. It was investigated that in most cases +2 oxidized catalyst **Pd₄** showed better efficiency than Pd(0) catalyst **Pd₃**.

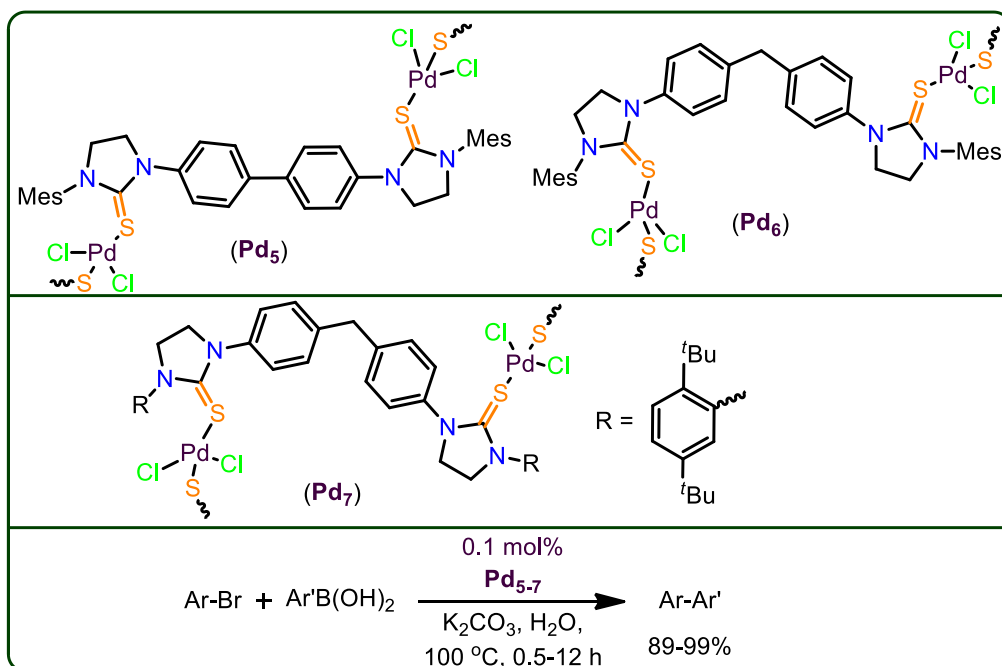


Scheme 1.37: Suzuki coupling catalyzed by *in situ* generated catalyst, **Pd₂**



Scheme 1.38: Suzuki coupling catalyzed by Pd(0) and Pd(II) catalysts, **Pd_{3,4}**

Moreover, the synthesis of self-supported, heterogeneous, thiourea–PdCl₂ catalysts (**Pd₅₋₇**) found applications in Suzuki reaction of aryl bromides and aryl boronic acids [99]. These newly designed bulky and rigid bis-thiourea ligands, acted as efficient heterogeneous catalysts in the Suzuki reaction in neat water under aerobic conditions. Moreover, facile recovery of the heterogeneous catalysts was validated with no deceptive palladium leaching.



Scheme 1.39: Suzuki coupling reactions catalyzed by Pd(II) catalysts, **Pd**₅₋₇

Se–C–Se pincer ligand is been used to derive **Pd**₈ complex and was found to be useful catalyst for the heck coupling of iodobenzene [100]. The selone ligated Pd(II) pincer complex **Pd**₈ was studied for limited substrate scope as a catalyst for the Heck C–C coupling reaction using iodobenzene with alkyl acrylates in DMA (Dimethylacetamide) at 140 °C.

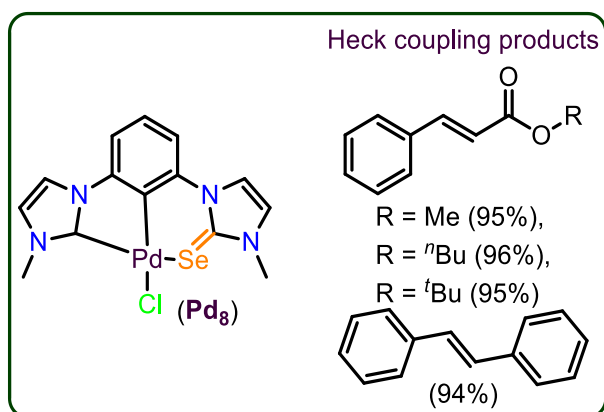


Figure 1.14: Heck coupling products isolated Pd(II) catalyst, **Pd**₈

Similarly, catalyst **Pd**₉ provided the modest to good yields in Heck, Suzuki–Miyaura, and Sonogashira coupling reactions [101]. However, the substrate scope is limited for very few examples as displayed in figure 1.15.

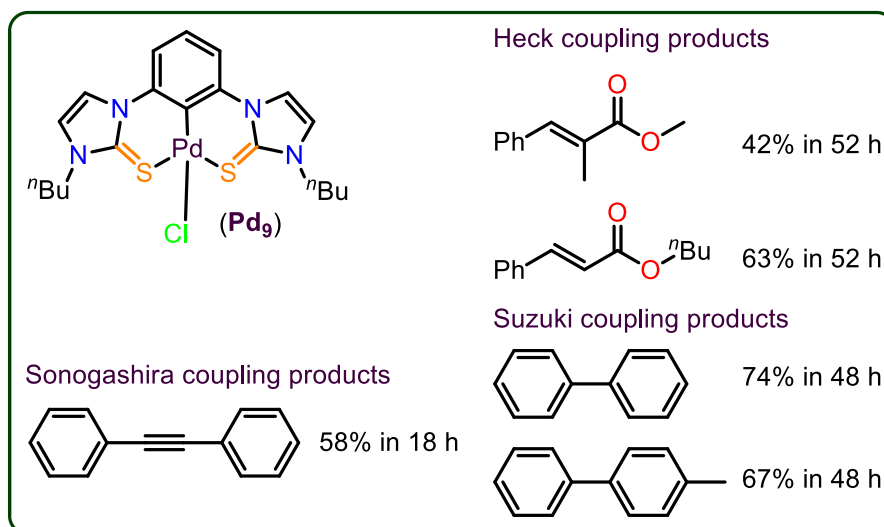
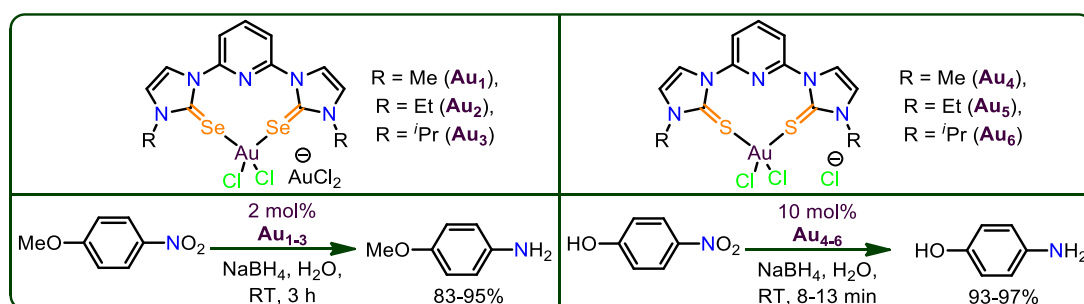


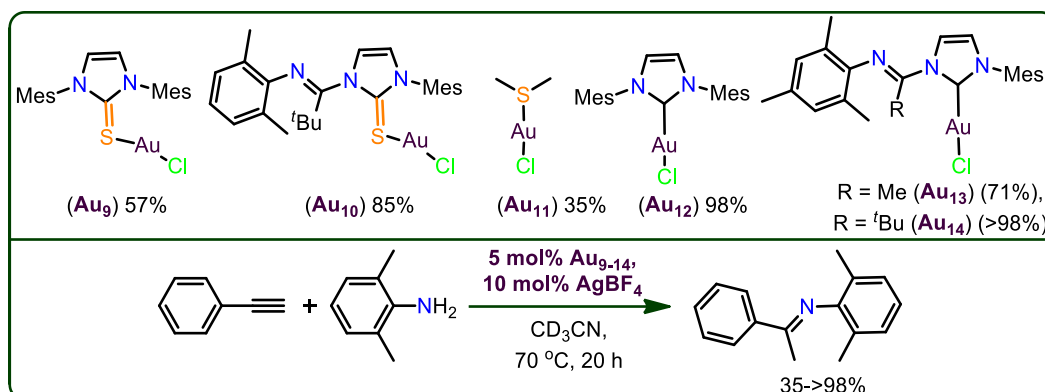
Figure 1.15: Heck, Suzuki–Miyaura, and Sonogashira coupling products isolated by catalyst, **Pd₉**

Au₁₋₃ complexes have been synthesized using pyridine based selone ligand (SeNSE) and are found to be highly an active catalysts in hydrogenation of nitroarenes to aromatic anilines [102]. Similarly, **Au₄₋₆** have been isolated by pyridine based SNS ligands and employed as catalysts in the reduction of 4-nitrophenol to 4-nitroaniline [103]. However, the latter was demonstrated based on UV-visible spectral changes and only on 4-nitro phenol.



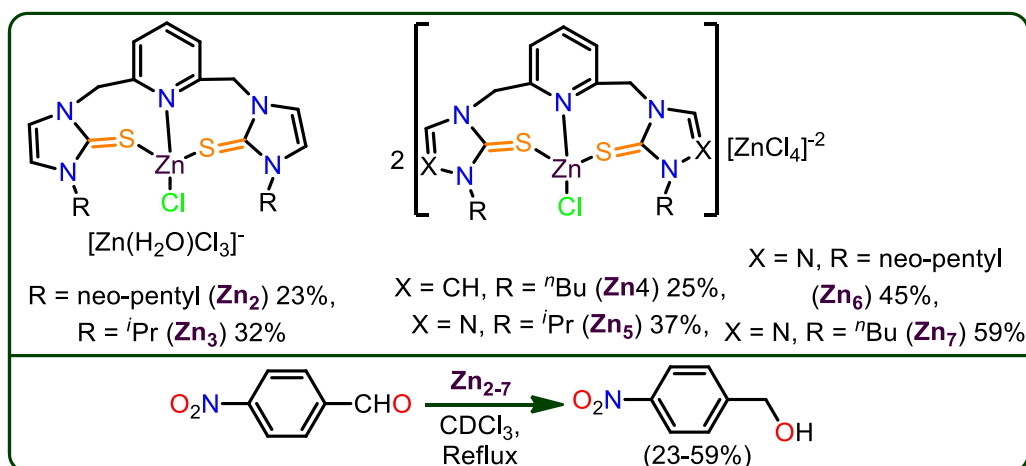
Scheme 1.40: Reduction of nitroarenes to aromatic amines by **Au₁₋₆**

Imidazole-2-thione and 1-imino-3-arylimidazol-2-ylidene gold(I) complexes (**Au₇₋₈**) have been synthesized and discovered their efficiencies in hydroamination of alkynes [67]. NMR reactions were performed in CDCl₃ to evaluate the percentage of conversion and was detected between NHC–Au and ImC–Au as presented in Scheme 1.41.



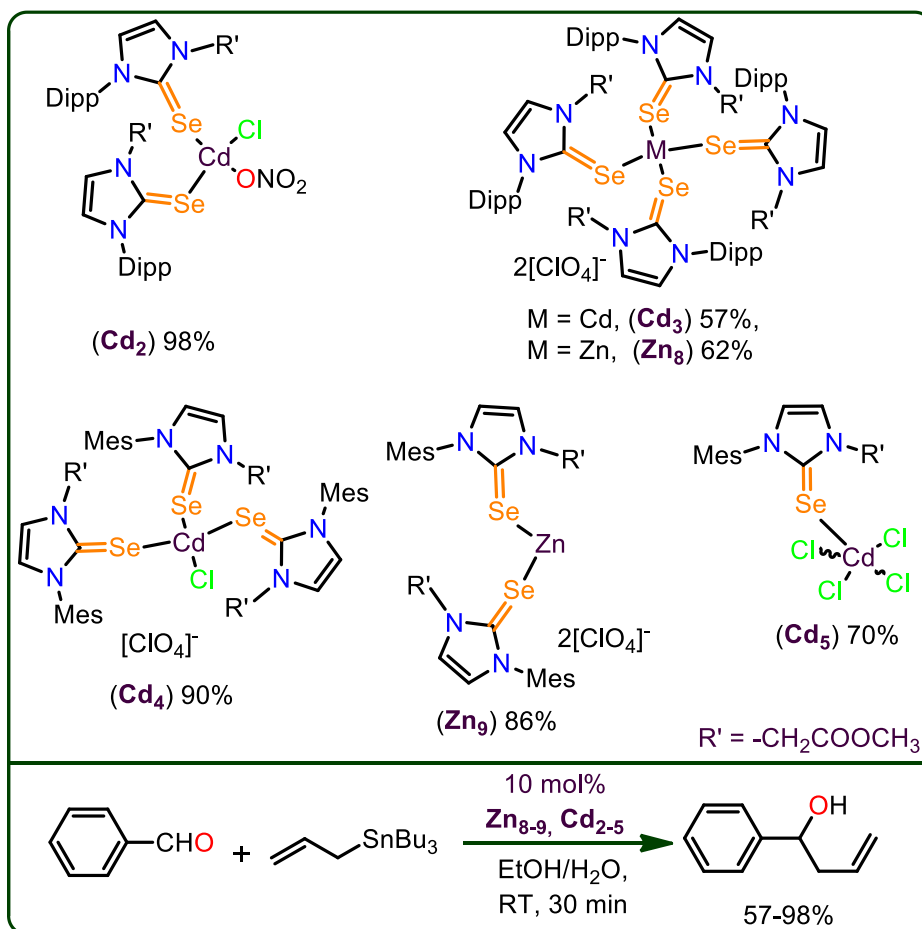
Scheme 1.41: Hydro-amination of alkynes catalyzed by catalysts, **Au**₉₋₁₄

Furthermore **Zn**₂₋₇ have been employed for the reduction of 4-nitrobenzaldehyde in CDCl₃ at reflux [104]. The maximum yield obtained is 59% with **Zn**₇, however, the reaction does not take place without catalyst and the yield is only 15% with commercial ZnCl₂.



Scheme 1.42: Reduction of 4-nitro benzaldehyde catalyzed by **Zn**₂₋₇

Zn₈₋₉ and **Cd**₂₋₅ have been structurally characterized and found to be useful catalysts for Barbier type of reactions [105]. Interestingly, **Cd**_{1,4} displayed better yields over all other catalysts. However, Cd1 examined for the substrate scope and was showing better yields (74-98%) irrespective of substrates.



Scheme 1.43: Barbier type reaction catalyzed by **Zn₈₋₉** and **Cd₂₋₅**

1.13.3. As an antibacterial agents

Silver(I)-based coordination polymers (**Ag**₁₋₅) of the bis-(imidazole-2-thione) ligands with varying dimensionality have been synthesized and found to be promising drugs in antibacterial activity [106] while, **Ag**₆ is a 3D coordination polymer and showed better antibacterial activities [88]. **Cd**₇ is a coordination polymer, investigated for antibacterial activities [107].

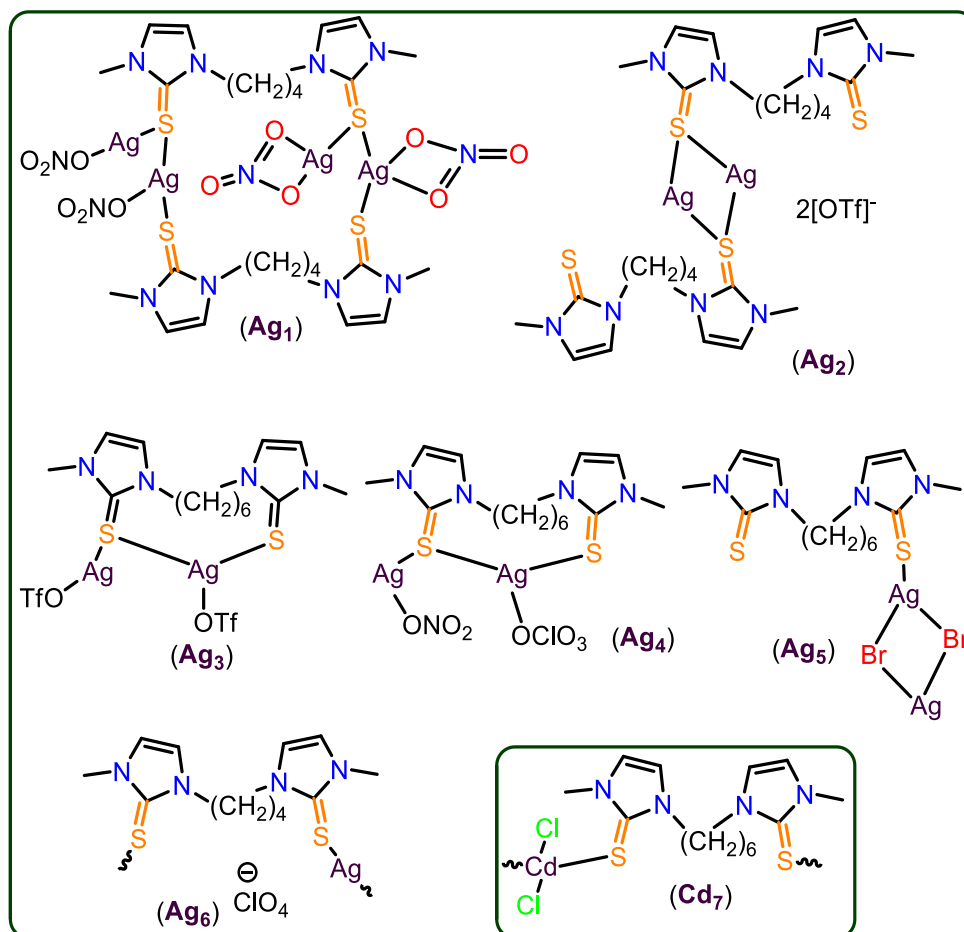
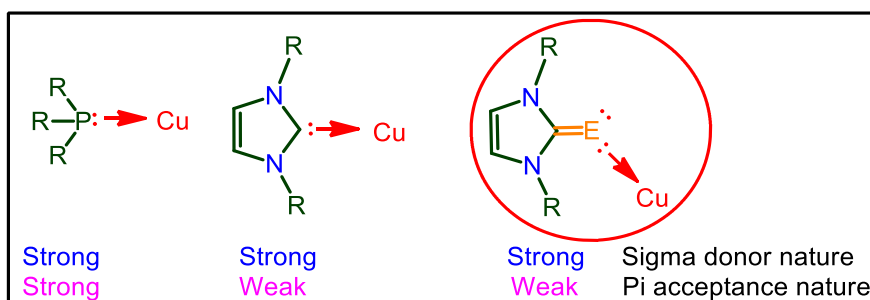


Figure 1.16: ImC-metal complexes used as drugs for antibacterial activities

1.14. Scope of the Work

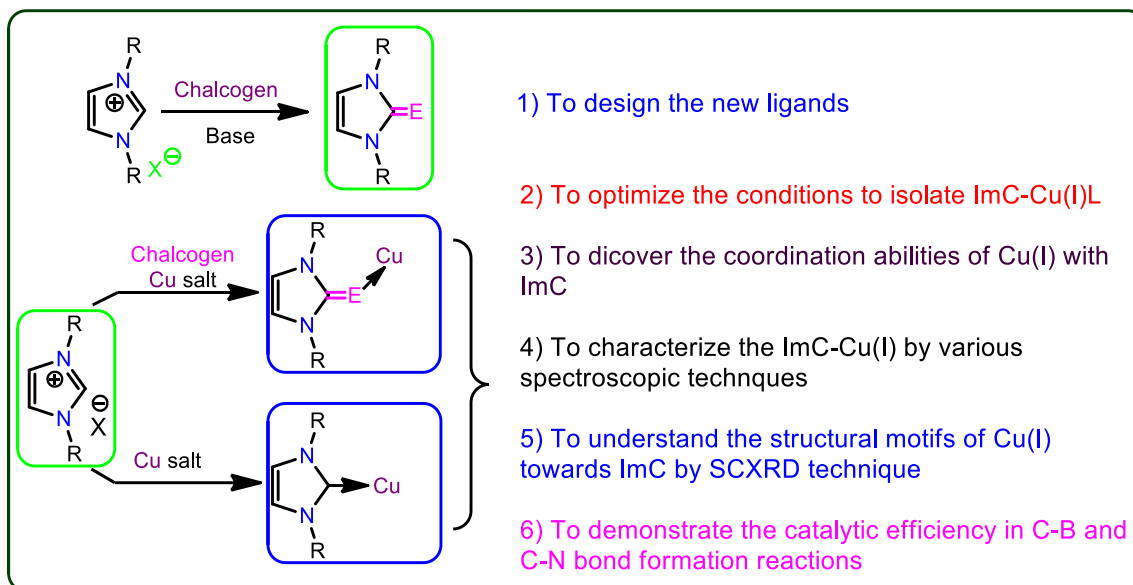
The structural properties and applications of ImC-metal have attracted much attention in recent past. Though, several transition metal-NHC analogues of metal ImC complexes are known, the application of ImC-transition metal derivatives are limited [90-91]. The known applications are limited to catalysis, medicinal chemistry as antibacterial agents [88,106-107] and also as single source precursors for nanomaterial applications [54,108-109].

As discussed in this section (Chapter 1, *vide supra*), only 13 types of organic transformations have been demonstrated using ImC-metal complexes. Out of which only one transformation has been displayed by using ImC-Cu catalyst in 2010 by Son *et al.*, while the applications of NHC-Cu are well known [73]. However, the comparative catalytic applications using both NHC-metal and ImC-metal are limited (only 4 examples are known) to elucidate the alternative ligand behavior of ImC over NHC. Albeit, the efficiency of ImC supported metal complexes in terms of isolated yield and selectivity of desired product is high over NHC-metal complexes [67,70,73,93]. On the other hand, the catalyst reproducibility has not been demonstrated as of now. Although 20 articles have been reported on ImC-Cu derivatives, like [(NHC)₂Cu]X the linear homoleptic chalcogenone derivatives are still scarce.⁸² Moreover, the ImC-Cu clusters are rare [74,87]. Besides, it is worth mentioning that the comparison of efficiencies and reaction pathway studies between phosphine-metal, NHC-metal and ImC-metal are not known [93]. Thus, our thesis focus is to understand the structural and catalytic applications of ImC supported copper(I) complexes. Besides, our target is to compare the catalytic efficiencies of ImC supported copper(I) with their NHC-Cu analogues.



1.15. Objectives

Our objectives are:



1.16. References:

- [1] R. H. Crabtree, *The Organometallic Chemistry of the Transition Metals*, 2005, vol. 18.
- [2] R. Crabtree, *Library (Lond)*, 2009.
- [3] J. J. Schneider, *J. Organomet. Chem.*, 2009, **694**, 2185.
- [4] G. Berton and P. W. N. M. Van Leeuwen, *Understanding the art*, 2008.
- [5] J. Pritchard, G. a. Filonenko, R. van Putten, E. J. M. Hensen, and E. a. Pidko, *Chem. Soc. Rev.*, 2015, **44**, 3808–3833.
- [6] A. Stirling, N. N. Nair, A. Lledós, and G. Ujaque, *Chem. Soc. Rev.*, 2014, **43**, 4940–4952.
- [7] J. Laughner, *Nat. Gas Dev. from Shale*, 2012, **1**, 56.
- [8] C. Contescu, *Chem. Rev.*, 1995, **95**, 475–476.
- [9] Y. Liu, G. Zhao, D. Wang, and Y. Li, *Natl. Sci. Rev.*, 2015, **2**, 150–166.
- [10] R. Schlögl, *Angew. Chemie - Int. Ed.*, 2015, **54**, 3465–3520.
- [11] F. Zaera, *Chem. Soc. Rev.*, 2013, **42**, 2746–2762.
- [12] A. J. Arduengo, III and L. I. Iconaru, *Dalt. Trans.*, 2009, 6903.
- [13] N. Marion, S. Díez-González, and S. P. Nolan, *Angew. Chemie - Int. Ed.*, 2007, **46**, 2988–3000.
- [14] E. Peris, *Chem. Rev.*, 2017, DOI: 10.1021/acs.chemrev.6b00695.
- [15] D. M. Flanigan, F. Romanov-Michailidis, N. a. White, and T. Rovis, *Chem. Rev.*, 2015, **115**, 9307–9387.
- [16] G. Prabusankar, A. Sathyanarayana, P. Suresh, C. Naga Babu, K. Srinivas, and B. P. R. Metla, *Coord. Chem. Rev.*, 2014, **269**, 96–133.
- [17] F. Lazreg, F. Nahra, and C. S. J. Cazin, *Coord. Chem. Rev.*, 2015, **293-294**, 48–79.
- [18] D. J. Nelson and S. P. Nolan, DOI: 10.1021/om5001919.
- [19] W. A. Herrmann, *Angew. Chemie Int. Ed.*, 2002, **41**, 1290–1309.
- [20] V. Nair, S. Bindu, and V. Sreekumar, *Angew. Chemie - Int. Ed.*, 2004, **43**, 5130–5135.
- [21] D. J. Cardin, B. Cetinkaya, M. F. Lappert, M. Sciences, and J. Bighton, *Chem. Rev.*, 1972, **72**, 545.
- [22] M. Kline and R. L. Harlow, *J Am. Chem. Soc.*, 1991, **113**, 363–365.
- [23] F. E. Hahn and M. C. Jahnke, *Angew. Chemie - Int. Ed.*, 2008, **47**, 3122–3172.
- [24] G. Evano, N. Blanchard, and M. Toumi, *Chem. Rev.*, 2008, **108**, 3054–3131.
- [25] P. Wipf, *Synthesis (Stuttg)*, 2002, 2317–2317.

- [26] F. Lazreg, F. Nahra, and C. S. J. Cazin, *Coord. Chem. Rev.*, 2015, **293-294**, 48–79.
- [27] H. G. Raubenheimer, S. Cronje, P. H. Van Rooyen, P. J. Olivier, and J. G. Toerien, *Angew. Chem. Int. Ed. Engl.*, 1994, **7006**, 11–12.
- [28] A. A. D. Tulloch, A. a Danopoulos, S. Kleinhenz, M. E. Light, M. B. Hursthouse, and G. Eastham, *Organometallics*, 2001, 2027–2031.
- [29] P. K. Fraser and S. Woodward, *Tetrahedron Lett.*, 2001, **42**, 2747–2749.
- [30] V. Jurkauskas, J. P. Sadighi, and S. L. Buchwald, *Org. Lett.*, 2003, **5**, 2417–2420.
- [31] S. P. Nolan, *N-Heterocyclic Carbenes in Synthesis*, 2006.
- [32] S. Díez-González, N. Marion, and S. P. Nolan, *Chem. Rev.*, 2009, **109**, 3612–3676.
- [33] R. Singh and S. P. Nolan, *Annu. Reports Sect. 'B' (Organic Chem.)*, 2006, **102**, 168.
- [34] S. Díez-González, E. C. Escudero-Adán, J. Benet-Buchholz, E. D. Stevens, A. M. Z. Slawin, and S. P. Nolan, *Dalt. Trans.*, 2010, **39**, 7595.
- [35] C. a. Citadelle, E. Le Nouy, F. Bisaro, A. M. Z. Slawin, and C. S. J. Cazin, *Dalt. Trans.*, 2010, **39**, 4489.
- [36] J. Chun, H. S. Lee, I. G. Jung, S. W. Lee, H. J. Kim, and S. U. Son, *Organometallics*, 2010, **29**, 1518–1521.
- [37] S. Díez-Gonzalez and S. P. Nolan, *Angew. Chemie - Int. Ed.*, 2008, **47**, 8881–8884.
- [38] F. Lazreg, A. M. Z. Slawin, and C. S. J. Cazin, *Organometallics*, 2012, **31**, 7969–7975.
- [39] G. C. Fortman, A. M. Z. Slawin, and S. P. Nolan, *Organometallics*, 2010, **29**, 3966–3972.
- [40] N. P. Mankad, D. S. Laitar, and J. P. Sadighi, *Organometallics*, 2004, **23**, 3369–3371.
- [41] V. Charra, P. de Frémont, and P. Braunstein, *Coord. Chem. Rev.*, 2017, **341**, 53–176.
- [42] J. P. Canal, T. Ramnial, D. a Dickie, and J. a C. Clyburne, *Chem. Commun. (Camb.)*, 2006, 1809–1818.
- [43] Y. S. Hor, a. Richardella, P. Roushan, Y. Xia, J. G. Checkelsky, a. Yazdani, M. Z. Hasan, N. P. Ong, and R. J. Cava, *Phys. Rev. B - Condens. Matter Mater. Phys.*, 2009, **79**, 2–6.
- [44] T. Topological, B. Te, Y. L. Chen, J. G. Analytis, J.-H. Chu, Z. K. Liu, S.-K. Mo, X. L. Qi, H. J. Zhang, D. H. Lu, X. Dai, Z. Fang, S. C. Zhang, I. R. Fisher, Z. Hussain, and Z.-X. Shen, *Science.*, 2014, **178**, 1–4.
- [45] W. Wang, J. Goebel, L. He, S. Aloni, Y. Hu, and a P. *Nature*, 2010, 17316–17324.
- [46] C. Inorganica and U. Cagliari, *Chalcogenone C = E compounds*, 2004.

- [47] Y. Rong, A. Al-Harbi, B. Kriegel, G. Parkin, *Inorg. Chem.* 2013, **52**, 7172–7182.
- [48] T. Chivers, H. P. a. Mercier, K. M. Mitchell, G. J. Schrobilgen, G. Strohe, P. a. Bianconi, a. Kuhn, and R. Herbst-Irmer, *J. Chem. Soc. Dalt. Trans.*, 1996, **32**, 1185.
- [49] Y. Rong, A. Al-Harbi, B. Kriegel, and G. Parkin, *Inorg. Chem.*, 2013, **52**, 7172–7182.
- [50] D. J. Nelson, F. Nahra, S. R. Patrick, D. B. Cordes, A. M. Z. Slawin, and S. P. Nolan, *Organometallics*, 2014, **33**, 3640–3645.
- [51] S. V. C. Vummaleti, D. J. Nelson, A. Poater, A. Gómez-Suárez, D. B. Cordes, A. M. Z. Slawin, S. P. Nolan, and L. Cavallo, *Chem. Sci.*, 2015, **6**, 1895–1904.
- [52] K. P. Bhabak, K. Satheeshkumar, S. Jayavelu, and G. Mugesh, *Org. Biomol. Chem.*, 2011, **9**, 7343–50.
- [53] D. Manna, G. Roy, G. Mugesh, *Acc. Chem. Res.* 2011, **46**, 2706–2715
- [54] J. Choi, N. Kang, H. Y. Yang, H. J. Kim, and S. U. Son, *Chem. Mater.*, 2010, **22**, 3586–3588.
- [55] J. Choi, S. Y. Park, H. Y. Yang, H. J. Kim, K. Ihm, J. H. Nam, J. R. Ahn, and S. U. Son, *Polym. Chem.*, 2011, **2**, 2512.
- [56] C. Wang, Y. Tong, Y. Huang, H. Zhang, and Y. Yang, *RSC Adv.*, 2015, **5**, 63087–63094.
- [57] W. G. Jia, Y. B. Huang, Y. J. Lin, G. L. Wang, and G. X. Jin, *Eur. J. Inorg. Chem.*, 2008, 4063–4073.
- [58] K. Srinivas, A. Sathyanarayana, C. Naga Babu, and G. Prabusankar, *Dalt. Trans.*, 2016, **45**, 5196–5209.
- [59] K. Srinivas, C. Naga Babu, and G. Prabusankar, *Dalt. Trans.*, 2015, **44**, 15636–15644.
- [60] A. Koner, S. C. Serin, G. Schnakenburg, B. O. Patrick, D. P. Gates, and R. Streubel, *Dalton Trans.*, 2017, 12–14.
- [61] M. Bauer, D. Premužić, G. Thiele, B. Neumüller, R. Tonner, Á. Raya-Barón, I. Fernández, and I. Kuzu, *Eur. J. Inorg. Chem.*, 2016, **2016**, 3756–3766.
- [62] Y. Wang, H. P. Hickox, Y. Xie, P. Wei, S. a. Blair, M. K. Johnson, H. F. Schaefer, and G. H. Robinson, *J. Am. Chem. Soc.*, 2017, **139**, 6859–6862.
- [63] R. Cammi, M. Lanfranchi, L. Marchiò, C. Mora, C. Paiola, and M. A. Pellinghelli, *Inorg. Chem.*, 2003, **42**, 1769–1778.
- [64] M. M. Kimani, J. L. Brumaghim, and D. Vanderveer, *Inorg. Chem.*, 2010, **49**, 9200–9211.

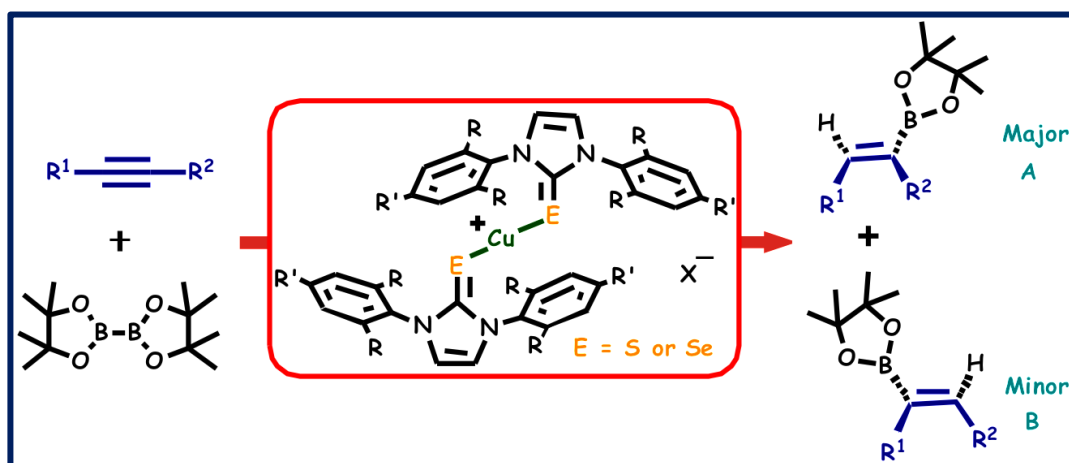
- [65] H.-N. Zhang, W.-G. Jia, Q.-T. Xu, and C.-C. Ji, *Inorg. Chim. Acta*, 2016, **450**, 315–320.
- [66] W.-G. Jia, Y.-B. Huang, Y.-J. Lin, and G.-X. Jin, *J. Chem. Soc. Dalt. Trans.*, 2008, 5612–20.
- [67] E. Alvarado, A. C. Badaj, T. G. Larocque, and G. G. Lavoie, *Chem. - A Eur. J.*, 2012, **18**, 12112–12121.
- [68] C. N. Babu, K. Srinivas, and G. Prabusankar, *Dalt. Trans.*, 2016, 6456.
- [69] N. Ghavale, S. T. Manjare, H. B. Singh, and R. J. Butcher, *Dalt. Trans.*, 2015, **44**, 11893–11900.
- [70] J. Jin, H. W. Shin, J. H. Park, J. H. Park, E. Kim, T. K. Ahn, D. H. Ryu, and S. U. Son, *Organometallics*, 2013, **32**, 3954–3959.
- [71] U. Flörke, A. Ahmida, J. Schröder, H. Egold, and G. Henkel, *Acta Crystallogr. Sect. E Struct. Reports Online*, 2013, **69**, m211–m211.
- [72] J. R. Miecznikowski, M. a. Lynn, J. P. Jasinski, W. Lo, D. W. Bak, M. Pati, E. E. Butrick, A. E. R. Drozdowski, K. a. Archer, C. E. Villa, E. G. Lemons, E. Powers, M. Siu, C. D. Gomes, N. a. Bernier, and K. N. Morio, *Polyhedron*, 2014, **80**, 157–165.
- [73] H. R. Kim, I. G. Jung, K. Yoo, K. Jang, E. S. Lee, J. Yun, and S. U. Son, *Chem. Commun. (Camb.)*, 2010, **46**, 758–760.
- [74] M. M. Kimani, C. a. Bayse, and J. L. Brumaghim, *Dalt. Trans.*, 2011, **40**, 3711.
- [75] M. M. Kimani, D. Watts, L. a. Graham, D. Rabinovich, G. P. a. Yap, and J. L. Brumaghim, *Dalt. Trans.*, 2015, **44**, 16313–16324.
- [76] M. M. Kimani, H. C. Wang, and J. L. Brumaghim, *Dalt. Trans.*, 2012, **41**, 5248.
- [77] M. M. Kimani, C. A. Bayse, B. S. Stadelman, and J. L. Brumaghim, *Inorg. Chem.*, 2013, **52**, 11685.
- [78] M. M. Kimani, C. A. Bayse, B. S. Stadelman, and J. L. Brumaghim, *Inorg. Chem.*, 2013, **52**, 11685–11687.
- [79] S. Yadav, S. T. Manjare, H. B. Singh and R. J. Butcher, *Dalton Trans.*, 2016, **45**, 12015.
- [80] S. Yadav, H. B. Singh, and R. J. Butcher, *Eur. J. Inorg. Chem.*, 2017, **2017**, 2968–2979.
- [81] M. T. Aroz, M. C. Gimeno, M. Kulcsar, A. Laguna, and V. Lippolis, *Eur. J. Inorg. Chem.*, 2011, **2**, 2884–2894.
- [82] S. Groysman and R. H. Holm, *Inorg. Chem.*, 2009, **48**, 621–627.

- [83] N. Parvin, S. Pal, S. Khan, S. Das, S. K. Pati, and H. W. Roesky, *Inorg. Chem.*, 2017, **56**, 1706–1712.
- [84] J. R. Miecznikowski, M. a. Lynn, J. P. Jasinski, E. Reinheimer, D. W. Bak, M. Pati, E. E. Butrick, A. E. R. Drozdowski, K. a. Archer, C. E. Villa, E. G. Lemons, E. Powers, M. Siu, C. D. Gomes, and K. N. Morio, *J. Coord. Chem.*, 2014, **67**, 29–44.
- [85] H. Du, W. Fu, S. Zhang, L. Li, H. Wang, Z. Yue, W. Zhang, Y. Niu, and Y. Zhu, *J. Coord. Chem.*, 2014, **67**, 807–821.
- [86] M. Slivarichova, R. Ahmad, Y. Y. Kuo, J. Nunn, M. F. Haddow, H. Othman, and G. R. Owen, *Organometallics*, 2011, **30**, 4779–4787.
- [87] M. Slivarichova, R. Correa, J. Nunn, R. Ahmad, M. F. Haddow, H. A. Sparkes, T. Gray, and G. R. Owen, *J. Organomet. Chem.*, 2017, **847**, 224–233.
- [88] A. Beheshti, K. Nozarian, S. S. Babadi, S. Noorizadeh, H. Motamedi, P. Mayer, G. Bruno, and H. A. Rudbari, *J. Solid State Chem.*, 2017, **249**, 70–79.
- [89] A. Beheshti, S. S. Babadi, K. Nozarian, F. Heidarizadeh, N. Ghamari, P. Mayer, and H. Motamedi, *Polyhedron*, 2016, **110**, 261–273.
- [90] M. Jagenbrein, K. Y. Monakhov, and P. Braunstein, *J. Organomet. Chem.*, 2015, **796**, 11–16.
- [91] A. Beheshti, M. B. Pour, C. T. Abrahams, and H. Motamedi, *Polyhedron*, 2017, **135**.
- [92] A. K. Sharma, H. Joshi, K. N. Sharma, P. L. Gupta, and A. K. Singh, *Organometallics*, 2014, **33**, 3629–3639.
- [93] A. Neveling, G. R. Julius, S. Cronje, C. Esterhuysen, and H. G. Raubenheimer, *Dalton Trans.*, 2005, 181–192.
- [94] W.-G. Jia, Y.-B. Huang, Y.-J. Lin, and G.-X. Jin, *Dalt. Trans.*, 2008, 5612.
- [95] Y. B. Huang, W. G. Jia, and G. X. Jin, *J. Organomet. Chem.*, 2009, **694**, 86–90.
- [96] A. K. Sharma, H. Joshi, R. Bhaskar, and A. K. Singh, *Dalt. Trans.*, 2017, **46**, 2228–2237.
- [97] H. Li, Z. Wu, M. Yang, and Y. Qi, *Catal. Letters*, 2010, **137**, 69–73.
- [98] A. T. Cawley and U. Flenker, *J. Mass Spectrom.*, 2008, **43**, 854–864.
- [99] W. Chen, R. Li, Y. Wu, L. S. Ding, and Y. C. Chen, *Synthesis (Stuttg.)*, 2006, **2**, 3058–3062.
- [100] N. Ghavale, S. T. Manjare, H. B. Singh, and R. J. Butcher, *Dalt. Trans.*, 2015, **44**, 11893–11900.

- [101] G. E. Tyson, K. Tokmic, C. S. Oian, D. Rabinovich, H. U. Valle, T. K. Hollis, J. T. Kelly, K. a. Cuellar, L. E. McNamara, N. I. Hammer, C. E. Webster, A. G. Oliver, and M. Zhang, *Dalt. Trans.*, 2015, **44**, 14475–14482.
- [102] H. Zhang, W. Jia, Q. Xu, and C. Ji, *Inorganica Chim. Acta*, 2016, **450**, 315–320.
- [103] W. Jia, Y. Dai, H. Zhang, X. Lu, and E. Sheng, *RSC Adv.*, 2015, **5**, 29491–29496.
- [104] J. R. Miecznikowski, W. Lo, M. a. Lynn, S. Jain, L. C. Keilich, N. F. Kloczko, B. E. O’Loughlin, A. P. Dimarzio, K. M. Foley, G. P. Lisi, D. J. Kwiecien, E. E. Butrick, E. Powers, and R. Al-Abbasee, *Inorg. Chim. Acta*, 2012, **387**, 25–36.
- [105] C. N. Babu, K. Srinivas and G. Prabusankar, *Dalton Trans.*, 2016, **45**, 6456.
- [106] A. Beheshti, S. Soleymani-babadi, P. Mayer, C. T. Abrahams, H. Motamedi, and D. Trzybin, *Dalton Trans.*, 2017, 5249.
- [107] A. Beheshti, K. Nozarian, C. T. Abrahams, and H. Motamedi, *J. Coord. Chem.*, 2017, **70**, 3394–3408.
- [108] D. J. Williams, K. M. White, D. VanDerveer, and A. P. Wilkinson, *Inorg. Chem. Commun.*, 2002, **5**, 124–126.
- [109] S. T. Manjare, S. Yadav, H. B. Singh, and R. J. Butcher, *Eur. J. Inorg. Chem.*, 2013, 5344–5357.

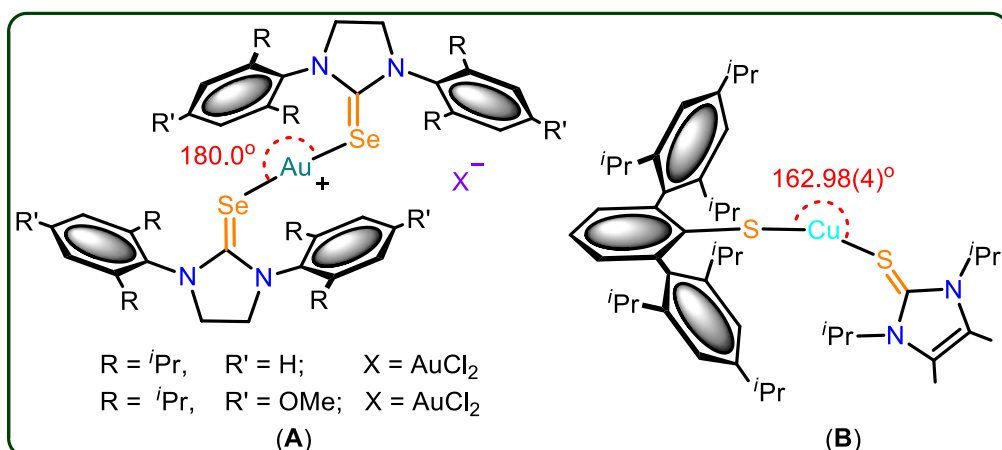
Chapter 2

Linear Cu(I) Chalcogenones: Synthesis and Application in Borylation of Unsymmetrical Alkynes



2.1. Introduction

The focus on copper chalcogenide chemistry is experiencing continuous growth and interest over last few decades owing to their novel properties and significant applications [1,2]. The property of copper chalcogenides is mainly controlled by chalcogen sources. For example, the recent works have also witnessed the active role of decade old ligand system imidazolin-2-chalcogenones for this endeavor [3-6]. Notably, imidazolin-2-chalcogenone ligands have potential to serve as a ligand with copper in medicine [3]. Some other potential applications of these imidazolin-2-chalcogenone ligand supported copper included their use as precursor for nanomaterial synthesis and co-ligand in catalysis. Recently the shape and phase controlled copper-selenide nanoflakes were reported using 1-*n*-butyl-3-ethylimidazolium methylselenite and copper sulphate [4]. Besides, the imidazoline-2-thione tethered copper catalysts were demonstrated for highly regioselective boron addition to internal alkynes [5]. This catalytic study represents the first and only report available to understand the role of imidazoline-2-chalcogenone in catalysis as co-ligand. In this process the catalytic reactions were carried out using *insitu* generated catalysts. The isolation of catalyst from catalytic reaction mixture led to tri coordinated copper imidazoline-2-thione complex with planar metal geometry. Although copper exist in different coordination mode with imidazoline-2-chalcogenones [2d,6], homoleptic two coordinated copper complexes of imidazoline-2-chalcogenones are not reported. Recent efforts have revealed that it is possible to isolate two coordinated homoleptic imidazoline-2-selone gold complexes [(IPr=Se)₂Au][AuCl₂], 1,3-bis(2,6-diisopropyl-phenyl)-imidazoline-2-selone and [(IPr^{OMe}=Se)₂Au][AuCl₂], IPr^{OMe} = 1,3-bis-(2,6-diisopropyl-4-methoxyphenyl)-imidazoline-2-selone, using more π accepting imidazoline-2-selone ligands (Scheme 2.1, **A**) [7]. However, only one *quasi*-linear homoleptic copper imidazolin-2-chalcogenone complex is known (Scheme 2.1, **B**) [8]. Molecule **B** has been isolated using relatively less π -accepting thione ligand.



Scheme 2.1: Known linear/*quasi*-linear homoleptic group 9, imidazoline-2-chalcogenone complexes

However, these recent efforts have not answered the critical questions necessary to clearly realize the formation of linear dicoordinated coinage metal complexes involving imidazolin-2-chalcogenones. For example, do “homoleptic two coordinated” intermediates exist in the catalytic process? How essential is “more π accepting imidazoline-2-selone” to isolate the homoleptic two coordinated coinage metal derivatives? In order to address these above challenges, we have isolated the homoleptic two coordinated copper imidazoline-2-thione/selone complexes using relatively less π accepting imidazoline-2-thiones/selones and studied their role in regioselective borylation of alkynes.

2.2. Experimental Section

2.2.1. General remarks

All manipulations were carried out under argon atmosphere in a glove box using standard Schlenk techniques. The solvents were purchased from commercial sources and purified according to standard procedures and freshly distilled under argon atmosphere prior to use [9]. Unless otherwise stated, the chemicals were purchased from commercial sources. IPrHCl (1,3-bis(2,6-diisopropylphenyl)-1*H*-imidazol-3-ium chloride), IPr=S (1,3-bis(2,6-diisopropylphenyl)-1*H*-imidazole-2(3*H*)-thione), IPr=Se (1,3-bis(2,6-diisopropylphenyl)-1*H*-imidazole-2(3*H*)-selenone), IMesHCl (1,3-dimesityl-1*H*-imidazol-3-ium chloride), IMes=S (1,3-dimesityl-1*H*-imidazole-2(3*H*)-thione), and IMes=Se (1,3-dimesityl-1*H*-imidazole-2(3*H*)-selenone) were prepared as previously reported [10]. Cu(ClO₄)₂·6H₂O and Cu(BF₄) hydrate were purchased from Sigma Aldrich and used as received. FT-IR measurement (neat) was carried out on a Bruker Alpha-P Fourier transform spectrometer. The UV-vis spectra were measured on a T90+ UV-visible spectrophotometer. Thermogravimetric

analysis (TGA) was performed using a TASDT Q600, Tzero-press. NMR spectra were recorded on Bruker Ultrashield-400 spectrometers at 25 °C unless otherwise stated. Chemical shifts are given relative to TMS and were referenced to the solvent resonances as internal standards. Elemental analyses were performed by the Euro EA-300 elemental analyzer. The crystal structures of **1-8** were measured on an Oxford Xcalibur 2 diffractometer. Single crystals of complexes suitable for the single crystal X-ray analysis were obtained from their reaction mixture at room temperature and the suitable single crystals for X-ray structural analysis were mounted at low temperature (150 K) (except **1**, **3** and **5**, measured at 298 K) in inert oil under an argon atmosphere. Using Olex2 [11], the structure was solved with the ShelXS [12] structure solution program using Direct Methods and refined with the olex2.refine refinement package using Gauss-Newton minimization. Absorption corrections were performed on the basis of multi-scans. Non-hydrogen atoms were anisotropically refined. Hydrogen atoms were included in the refinement in calculated positions riding on their carrier atoms. No restraint has been made for any of the compounds. The function minimized was $[\sum w(F_o^2 - F_c^2)^2]$ ($w = 1/[\sigma^2(F_o^2) + (aP)^2 + bP]$), where $P = (\max(F_o^2, 0) + 2F_c^2)/3$ with $\sigma^2(F_o^2)$ from counting statistics. The functions R_1 and wR_2 were $(\sum ||F_o| - |F_c||)/\sum |F_o|$ and $[\sum w(F_o^2 - F_c^2)^2/\sum (wF_o^4)]^{1/2}$, respectively. Structures **1** and **5** contains solvent accessible VOIDS of 143 Å³ and 144 Å³, respectively. This residual voids in a structure may be due to the disordered counter ion density. The counter ions in structures **1**, **2**, **5** and **6** are disordered.

Caution

Perchlorate salts of metal salts and complexes are potentially explosive. Only small amounts of material should be prepared and handled with great care; particular caution must be exercised when they are dried under vacuum.

2.2.2. Synthesis of [(IPr=S)₂Cu]ClO₄ (**1**)

A mixture of IPr=S (0.100 g, 0.238 mmol) and Cu(ClO₄)₂.6H₂O (0.106 g, 0.286 mmol) in methanol (5 mL) was refluxed at 80 °C for 12 h. The clear reaction mixture was brought to room temperature to result the colorless crystals of **1** in 2 days. Yield: 73% (based on Cu(ClO₄)₂.6H₂O). M.p.: 258-260 °C (dec.). Elemental analysis calcd (%) for C₅₄H₇₂ClCuN₄O₄S₂ (1002.4): C, 64.58; H, 7.23; N, 5.58; Found: C, 64.08; H, 7.19; N, 5.50. ¹H NMR (400 MHz, CDCl₃): δ = 7.38-7.34 (t, 2H, CH_{para}), 7.20-7.18 (d, 4H, CH_{meta}), 7.10 (s, 2H, ImH), 2.35-2.28 (sept, 4H, ⁱPrCH), 1.16-1.15, 1.13-1.11 (d, 24H, CH₃) ppm. ¹³C NMR (100 MHz, CDCl₃): δ = 160.07 (NCN), 145.63 (ImC), 131.66, 131.48, 124.99, 122.10 (ArC),

28.91 (*i*PrCH), 24.16, 23.30 (CH₃) ppm. FT-IR (neat): $\bar{\nu}$ = 2933(s), 2839(m), 1554(w), 1458(s), 1424(m), 1379(s), 1334(m), 1214(m), 1180(w), 1094(s) (Cl–O), 981(s), 938(s), 803(s) cm⁻¹.

2.2.3. Synthesis of [(IPr=Se)₂Cu]ClO₄ (2)

2 was prepared in the same manner as described for **1** using IPr=Se (0.100 g, 0.213 mmol) and Cu(ClO₄)₂·6H₂O (0.095 g, 0.256 mmol) in methanol (5 mL). Yield: 70% (based on Cu(ClO₄)₂·6H₂O). M.p.: 276-278 °C (dec.). Elemental analysis calcd (%) for C₅₄H₇₂ClCuN₄O₄Se₂ (1098.2): C, 59.06; H, 6.61; N, 5.10; Found: C, 58.56; H, 6.71; N, 5.08. ¹H NMR (400 MHz, CDCl₃): δ = 7.43-7.39 (t, 2H, CH_{para}), 7.23-7.22 (d, 4H, CH_{meta}), 7.20 (s, 2H, ImH), 2.34-2.28 (sept, 4H, *i*PrCH), 1.20-1.19, 1.12-1.10 (d, 24H, CH₃) ppm. ¹³C NMR (100 MHz, CDCl₃): δ = 154.21 (NCN), 145.50 (ImC), 132.44, 131.55, 124.98, 123.86 (ArC), 28.96 (*i*PrCH), 24.24, 23.32 (CH₃) ppm. FT-IR (neat): $\bar{\nu}$ = 2961(s), 2871(m), 1519(w), 1454(s), 1351(s), 1324(m), 1214(m), 1182(w), 1076(s) (Cl–O), 967(s), 804(s), 750(s) cm⁻¹.

2.2.4. Synthesis of [(IMes=S)₂Cu]ClO₄ (3)

3 was prepared in the same manner as described for **1** using IMes=S (0.100 g, 0.297 mmol) and Cu(ClO₄)₂·6H₂O (0.132 g, 0.356 mmol) in methanol (5 mL). Yield: 74% (based on Cu(ClO₄)₂·6H₂O). M.p.: 263-265 °C (dec.). Elemental analysis calcd (%) for C₄₂H₄₈ClCuN₄O₄S₂ (834.2): C, 60.34; H, 5.79; N, 6.70; Found: C, 60.14; H, 5.87; N, 6.59. ¹H NMR (400 MHz, CDCl₃): δ = 7.04 (s, 4H, ImH), 6.94 (s, 8H, CH_{meta}), 2.25 (s, 12H, CH_{3para}), 1.95 (s, 24H, CH_{3ortho}) ppm. ¹³C NMR (100 MHz, CDCl₃): δ = 157.02 (C=S), 141.08, 134.95, 131.63, 130.10, 121.21 (ArC), 21.10 (*p*-CH₃), 17.59 (*o*-CH₃) ppm. FT-IR (neat): $\bar{\nu}$ = 3169(w), 1607(m), 1554(w), 1481(s), 1442(m), 1374(s), 1232(m), 1095(s), 1072(s) (Cl–O), 925(w), 844(w), 735(s) cm⁻¹.

2.2.5. Synthesis of [(IMes=Se)₂Cu]ClO₄ (4)

4 was prepared in the same manner as described for **1** using IMes=Se (0.100 g, 0.260 mmol) and Cu(ClO₄)₂·6H₂O (0.116 g, 0.312 mmol) in methanol (5 mL). Yield: 67% (based on Cu(ClO₄)₂·6H₂O). M.p.: 278-280 °C (dec.). Elemental analysis calcd (%) for C₄₂H₄₈ClCuN₄O₄Se₂ (930.0): C, 54.26; H, 5.20; N, 6.03; Found: C, 54.06; H, 5.18; N, 5.93. ¹H NMR (400 MHz, CDCl₃): δ = 7.04 (s, 4H, ImH), 6.94 (s, 8H, CH_{meta}), 2.24 (s, 12H, CH_{3para}), 1.95 (s, 24H, CH_{3ortho}) ppm. ¹³C NMR (100 MHz, CDCl₃): δ = 150.28 (C=S), 141.12, 134.81, 132.56, 130.09, 123.04 (ArC), 21.23 (*p*-CH₃), 17.69 (*o*-CH₃) ppm. FT-IR

(neat): $\bar{\nu}$ = 1602(m), 1549(w), 1480(s), 1443(m), 1363(s), 1230(m), 1038(s) (C–O), 926(w), 845(w), 735(s) cm^{-1} .

2.2.6. Synthesis of [(IPr=S)₂Cu]BF₄ (5)

5 was prepared in the same manner as described for **1** using IPr=S (0.100 g, 0.238 mmol) and Cu(BF₄)₂ (0.068 g, 0.286 mmol) in methanol (5 mL). Yield: 69% (based on Cu(BF₄)₂). M.p.: 296-298 °C (dec.). Elemental analysis calcd (%) for C₅₄H₇₂BCuN₄F₄S₂ (991.6): C, 65.40; H, 7.32; N, 5.65; Found: C, 64.86; H, 7.18; N, 5.43. ¹H NMR (400 MHz, CDCl₃): δ = 7.53-7.50 (t, 2H, CH_{para}), 7.33-7.32 (d, 4H, CH_{meta}), 7.21 (s, 2H, ImH), 2.65-2.55 (sept, 4H, ⁱPrCH), 1.40-1.38, 1.20-1.18 (d, 24H, CH₃) ppm. ¹³C NMR (100 MHz, CDCl₃): δ = 159.99 (C=S), 145.63, 131.62, 131.50, 124.97, 122.11 (ArC), , 28.90 (ⁱPrCH), 24.13, 23.30 (CH₃) ppm. ¹¹B{¹H} NMR (128.4 MHz, CDCl₃): δ = -0.98 ppm. ¹⁹F{¹H} NMR (376.4 MHz, CDCl₃): δ = -154.30 ppm. FT-IR (neat): $\bar{\nu}$ = 3540(b), 2963(s), 1632(m), 1556(w), 1462(s), 1375(s), 1257(w), 1214(w), 1040(s) (B–F), 939(w), 802(m), 746(s), 693(s), 570(m) cm^{-1} .

2.2.7. Synthesis of [(IPr=Se)₂Cu]BF₄ (6)

6 was prepared in the same manner as described for **1** using IPr=Se (0.100 g, 0.213 mmol) and Cu(BF₄)₂ (0.060 g, 0.256 mmol) in methanol (5 mL). Yield: 77% (based on Cu(BF₄)₂). M.p.: 260-262 °C (dec.). Elemental analysis calcd (%) for C₅₄H₇₂BCuN₄F₄Se₂ (1085.4): C, 59.75; H, 6.69; N, 5.16; Found: C, 59.66; H, 6.72; N, 5.21. ¹H NMR (400 MHz, CDCl₃): δ = 7.61-7.57 (t, 2H, CH_{para}), 7.38-7.36 (d, 4H, CH_{meta}), 7.14 (s, 2H, ImH), 2.56-2.46 (sept, 4H, ⁱPrCH), 1.28-1.26, 1.15-1.14 (d, 24H, CH₃) ppm. ¹³C NMR (100 MHz, CDCl₃): δ = 154.21 (C=Se), 145.50, 132.44, 131.55, 124.99, 123.86 (ArC), , 28.96 (ⁱPrCH), 24.25, 23.32 (CH₃) ppm. ¹¹B{¹H} NMR (128.4 MHz, CDCl₃): δ = -0.99 ppm. ¹⁹F{¹H} NMR (376.4 MHz, CDCl₃): δ = -154.14 ppm. FT-IR (neat): $\bar{\nu}$ = 3552(b), 2963(m), 1631(m), 1554(w), 1462(m), 1425(m), 1359(s), 1212(w), 1176(w), 1044(s) (B–F), 939(m), 803(s), 749(s), 689(m) cm^{-1} .

2.2.8. Synthesis of [(IMes=S)₂Cu]BF₄ (7)

7 was prepared in the same manner as described for **1** using IMes=S (0.100 g, 0.297 mmol) and Cu(BF₄)₂ (0.085 g, 0.356 mmol) in methanol (5 mL). Yield: 75% (based on Cu(BF₄)₂). M.p.: 288-290 °C (dec.). Elemental analysis calcd (%) for C₄₂H₄₈BCuN₄F₄S₂ (823.3): C, 61.27; H, 5.88; N, 6.80; Found: C, 61.06; H, 5.18; N, 5.93. ¹H NMR (400 MHz, CDCl₃): δ = 7.17 (s, 4H, ImH), 6.94 (s, 8H, CH_{meta}), 2.28 (s, 12H, CH_{3para}), 1.94 (s, 24H, CH_{3ortho}) ppm. ¹³C NMR (100 MHz, CDCl₃): δ = 156.94 (C=S), 141.05, 134.96, 131.66,

130.08, 121.23 (ArC), 21.10 (*p*-CH₃), 17.57 (*o*-CH₃) ppm. ¹¹B{¹H} NMR (128.4 MHz, CDCl₃): δ = -0.97 ppm. ¹⁹F{¹H} NMR (376.4 MHz, CDCl₃): δ = -154.13 ppm. FT-IR (neat): $\bar{\nu}$ = 3531(b), 1632(m), 1552(w), 1480(m), 1442(m), 1374(s), 1287(m), 1231(m), 1028(s) (B-F), 923(w), 842(w), 733(s), 691(s), 602(s), 570(m) cm⁻¹.

2.2.9. Synthesis of [(IMes=Se)₂Cu]BF₄ (**8**)

8 was prepared in the same manner as described for **1** using IMes=Se (0.100 g, 0.260 mmol) and Cu(BF₄)₂ (0.075 g, 0.312 mmol) in methanol (5 mL). Yield: 63% (based on Cu(BF₄)₂). M.p.: 235-237 °C (dec.). Elemental analysis calcd (%) for C₄₂H₄₈BCuN₄F₄Se₂ (917.2): C, 55.00; H, 5.28; N, 6.11; Found: C, 54.86; H, 5.23; N, 5.98. ¹H NMR (400 MHz, CDCl₃): δ = 7.26 (s, 4H, ImH), 7.02 (s, 8H, CH_{meta}), 2.36 (s, 12H, CH_{3para}), 2.02 (s, 24H, CH_{3ortho}) ppm. ¹³C NMR (100 MHz, CDCl₃): δ = 150.07 (C=Se), 141.06, 134.81, 132.58, 130.06, 123.08 (ArC), 21.23 (*p*-CH₃), 17.67 (*o*-CH₃) ppm. ¹¹B{¹H} NMR (128.4 MHz, CDCl₃): δ = -1.01 ppm. ¹⁹F{¹H} NMR (376.4 MHz, CDCl₃): δ = -153.76 ppm. FT-IR (neat): $\bar{\nu}$ = 3525(b), 1630(m), 1550(w), 1480(m), 1448(m), 1369(s), 1288(m), 1234(m), 1022(s) (B-F), 825(w), 793(w), 735(w), 689(s), 566(m) cm⁻¹.

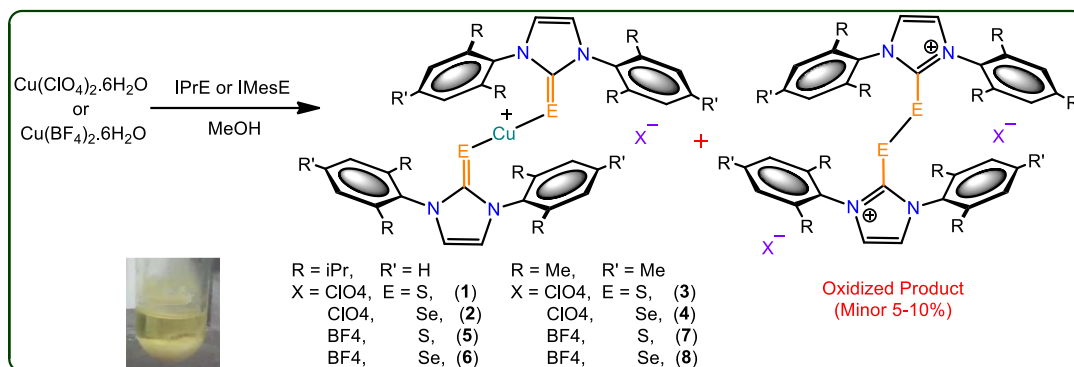
2.2.10. **1-8** catalyzed regioselective boron addition to unsymmetrical alkynes

The catalytic reactions were carried out under very mild conditions using newly synthesized copper(I) catalysts (**1-8**) for the regioselective boron addition of unsymmetrical alkynes in THF using previously reported synthetic procedure [5]. Copper(I) complex (0.050 mmol) was taken in a Schlenk flask along with NaO^t-Bu (0.100 mmol) in THF (0.40 mL) under the brisk flow of nitrogen. After the mixture was stirred at room temperature for 30 min, bis(pinacolato)diboron (B₂pin₂) (0.55 mmol) in THF (0.30 mL) was added. The reaction mixture was stirred further for 20-30 min. Then, alkyne (0.50 mmol) was added, followed by MeOH (1 mmol). The Schlenk flask was washed with THF (0.40 mL), sealed, and allowed to stir at room temperature. The progress of reaction was monitored by TLC. After the completion, 5-10 mL hexane was added and the reaction mixture was filtered through Celite and concentrated. The products were purified by column chromatography to produce an oily liquids. The fading of the starting materials and appearance of products were conveniently examined by ¹H NMR spectroscopy.

2.3. Result and discussion

2.3.1. Synthesis and characterization of 1-8

The linear mononuclear copper(I) thiones and selones, **1-8** were isolated in excellent yield from the reduction of corresponding copper(II) salts using imidazoline-2-thiones/selones (Scheme 2.2). The reduction of copper(II) to copper(I) using imidazoline-2-chalcogenones, R=E (E = S, Se and Te) is one of the rare reaction. Only two reports demonstrate the reduction of Cu²⁺ to Cu⁺ by chalcogenones. The first Cu²⁺ to Cu⁺ reduction was demonstrated by Brumaghim and co-workers [2b]. Later, the reduction of CuCl₂ using 2,6-bis{[N-isopropyl-N'-methylene]-imidazoline-2-thione}-pyridine or 2,6-bis{[N-isopropyl-N'-methylene]triazole-2-thione}pyridine was reported [13].



Scheme 2.2: Synthesis of **1-8**

The formation of **1-8** were confirmed by elemental analysis, FT-IR, multinuclear (¹H, ¹³C, ¹¹B and ¹⁹F) NMR, UV-vis, TGA and single crystal X-ray diffraction techniques. All these compounds are soluble in common organic solvents like CH₂Cl₂, CHCl₃, acetone, THF, and acetonitrile. In ¹³C NMR, the carbene carbon chemical shift value of **1-8** were upfield shifted (about $\delta = 5-8$ ppm) from those of the corresponding ligands IPr=E and IMes=E, respectively (Figure 2.4 and 2.9). This could be due to a decrease in the π -acceptance nature of the carbene carbon upon coordination. In ¹H NMR, the signals of protons, which are in weak interactions with counter anions are clearly shuffled (Figure 2.5 and 2.10). The FT-IR spectra of **1-8** showed stretching frequencies in the range of 1022 to 1094 cm⁻¹ for uncoordinated perchlorate/tetra fluoro borate anions (Figure 2.3 and 2.8). In addition, the tetra fluoro borate complexes (**4-8**) were further confirmed by ¹⁹F and ¹¹B NMR spectroscopy. The ¹¹B NMR spectra of **5-8** showed a sharp signal in the range of -0.97 to -1.01 ppm (Figure 2.11) and ¹⁹F NMR spectra of **5-8** showed a sharp signal in the range of -153.76 to -154.30 ppm (Figure 2.12). The solid state structures of **1-8** were further confirmed by single crystal X-ray diffraction study.

2.3.2. Single crystal X-ray structure of 1-8

The molecules **1-3** and **5-8** crystallized in the monoclinic space group, $C2/c$, while molecule **4** crystallized in the orthorhombic space group, $P2_12_12_1$ (Figure 2.1-2.2 and 2.6-2.7). The crystallographic data for **1-8** are furnished in table 2.2, 2.3. The molecular drawing with selected bond lengths and bond angles are reported in scheme 2.3 and table 2.1. Molecules **1-8** are isolated as homoleptic cation with corresponding anion. **1-3** and **5-8** are the rare examples of structurally characterized perfect linear homoleptic copper(I) chalcogenone derivatives, while **4** is in *quasi-linear* geometry.

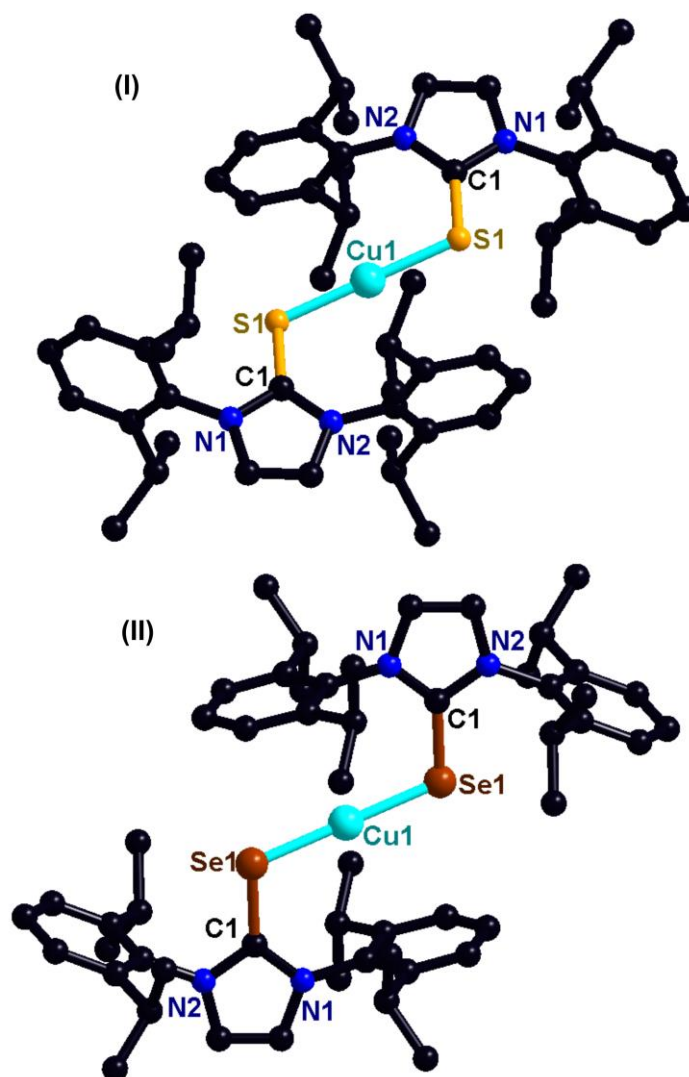


Figure 2.1: (I); Molecular structure of **1**. (II); Molecular structure of **2**. Hydrogen atoms and perchlorate counter ions have been omitted for clarity

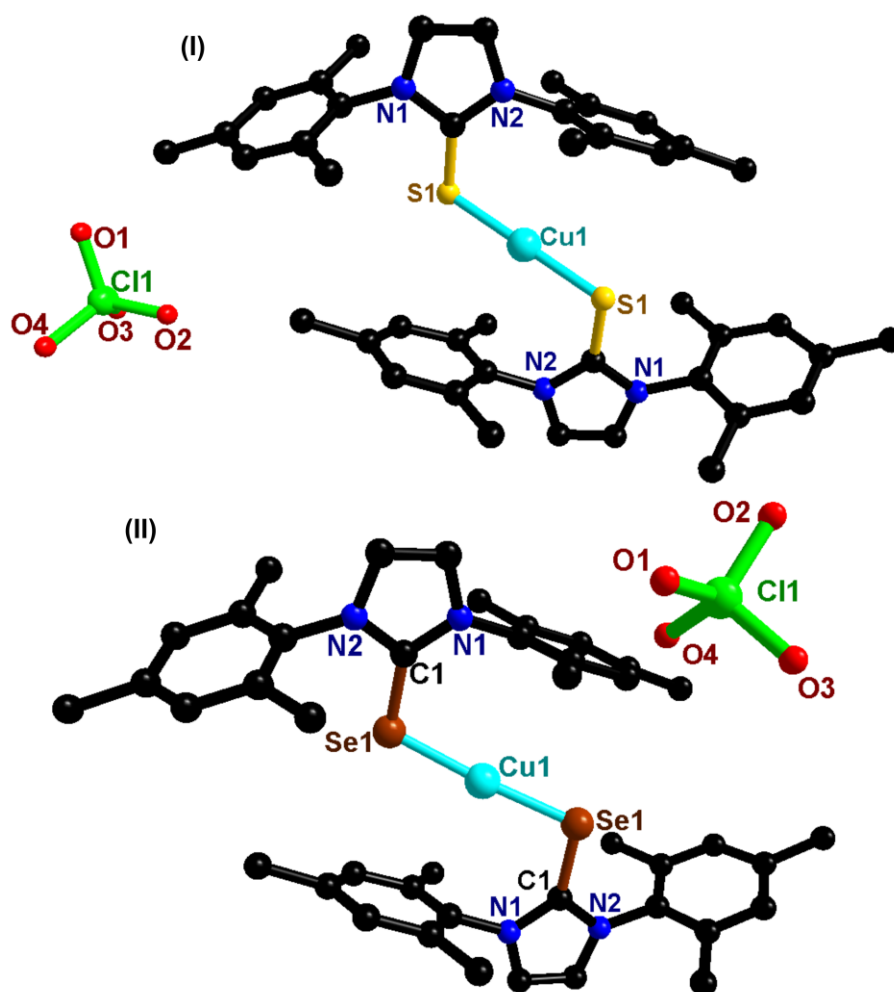
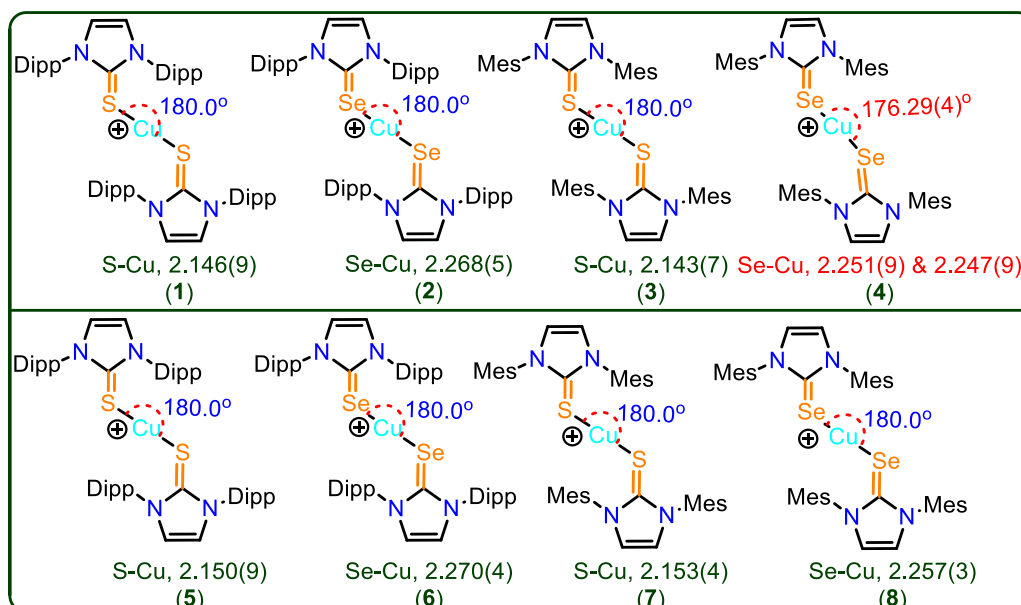


Figure 2.2: (I); Molecular structure of **3**. (II) Molecular structure of **4**. Hydrogen atoms have been omitted for clarity

The copper(I) center in **1-8** is two coordinated with two imidazole-2-thiones/selones and valency is satisfied by one perchlorate/tetra fluoro borate counter anion. Similar such linearly coordinated copper(I) compounds are very rare. In particular, only two nonlinear copper(I) thione derivatives $[\text{Cu}(\text{dptu})_2](\text{SO}_4)_{0.5}$ (dptu = N,N'-diphenylthiourea) ($\text{S}-\text{Cu}-\text{S}$ is $162.18(2)^\circ$) and $[\text{Cu}(\text{SAr}^*)(\text{S}=\text{C}(\text{N}^i\text{Pr})_2(\text{CMe})_2)]$ (Ar^*S = 2,6-bis(2,4,6-triisopropylphenyl)benzenethiolate) ($\text{S}-\text{Cu}-\text{S}$ is $162.98(4)^\circ$) were reported with thiourea type of ligands (*vide supra*, Scheme 2.1, B) [14]. Among coinage metals, only linearly coordinated gold(I) imidazoline-2-chalcogenone complexes are known (*vide supra*, Scheme 2.1). However, few non imidazole class of ligands coordinated *quasi*-linear or linear group 9 thio derivatives, $[\text{Ph}_4\text{P}][\text{Cu}(\text{SC}\{\text{O}\}\text{Me})_2]$ ($176.6(2)^\circ$), $[\text{NEt}_4][\text{Cu}(\text{SAd})_2]$ (Ad = adamantanyl) (180°), *fac*- $[\text{Mn}(\text{CN}^i\text{Bu})(\text{CO})_3\{(\text{PPh}_2)_2\text{C}(\text{H})\text{SC}(\text{S})\text{NMe}_2\}]_2\text{Cu}][\text{BF}_4]$ (180°),

[Ph₄P][Ag(SC{O}Me)₂] (178.9(5)^o) and [Ph₄P][Ag(SC{O}Ph)₂] (161.1(4)^o) were reported [15,16].



Scheme 2.3: Vital bond lengths [Å] and angles [°] of compounds **1-8**

The C=S bond lengths and C=Se bond lengths are increased upon coordinating with copper compared to their corresponding ligands IPr=S (1.670(3) Å), IMes=S (1.675(18) Å), IPr=Se (1.822(4) Å), and IMes=Se (1.830(6) Å) (Scheme 2.3) [10]. The Cu–S bond lengths in **1**, **3**, **5** and **7** are almost comparable with that of [NEt₄][Cu(SAd)₂] (Ad = adamantanyl) (2.147(1) Å) [15]. The E–Cu–E bond angle in **1-3** and **5-8** is exactly 180°, while molecule **4** is in *quasi*-linear form with Se–Cu–Se angle of 176.29(4)°. Similar such linear and *quasi*-linear thio derivatives of copper complexes are limited, which are known with different types of thio ligands [15,16]. Thus Cu–E bond lengths in **1-3** and **5-8** are comparable, while Cu–Se bond lengths in **4** are not comparable (Cu(1)–Se(1), 2.251(9) Å and Cu(1)–Se(1'), 2.248(9) Å).

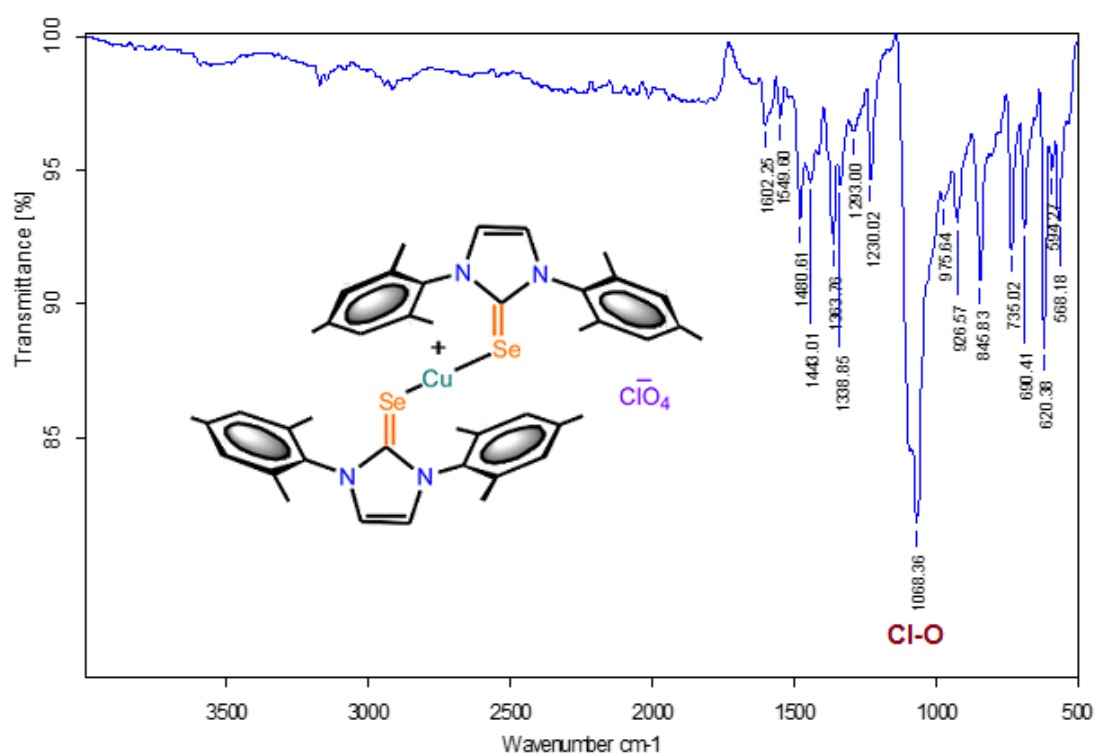


Figure 2.3: Neat FT-IR spectrum of **4**

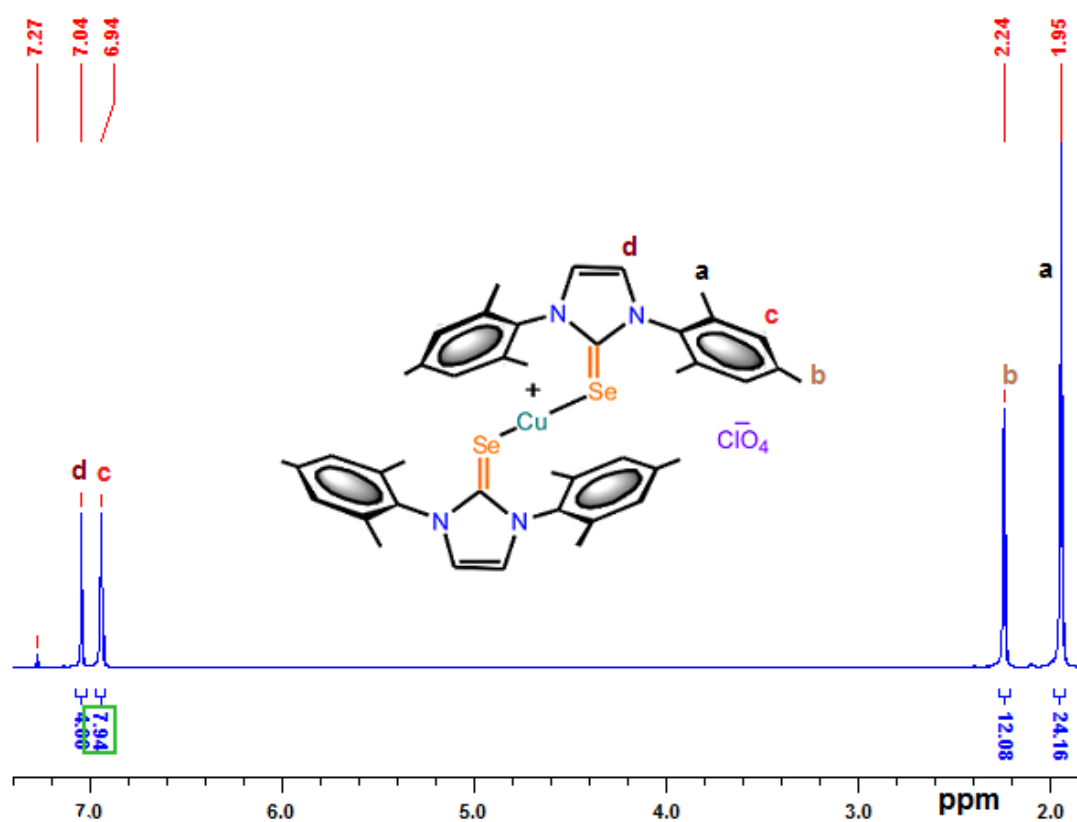


Figure 2.4: ¹H NMR spectrum of **4** in CDCl₃ at room temperature

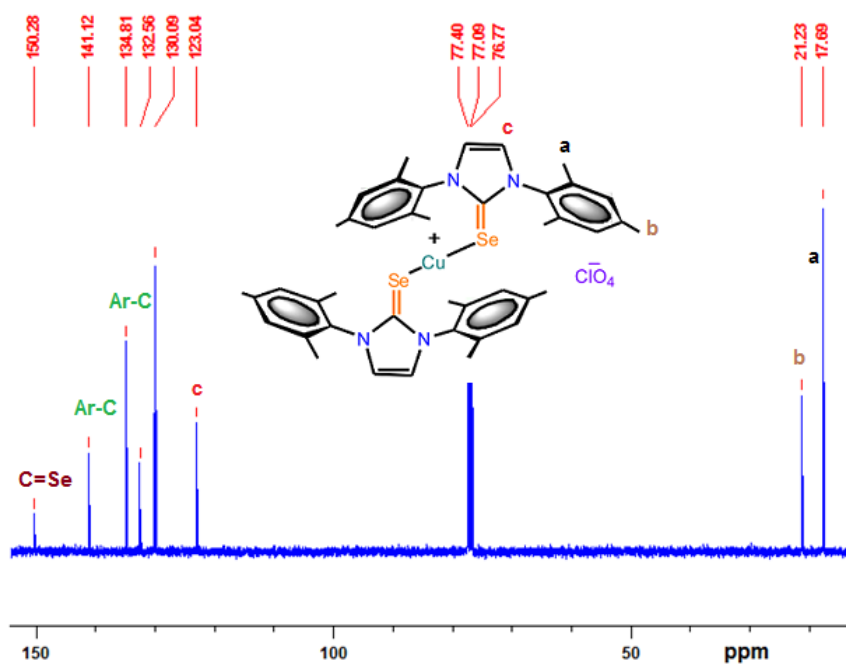


Figure 2.5: ^{13}C NMR spectrum of **4** in CDCl_3 at room temperature

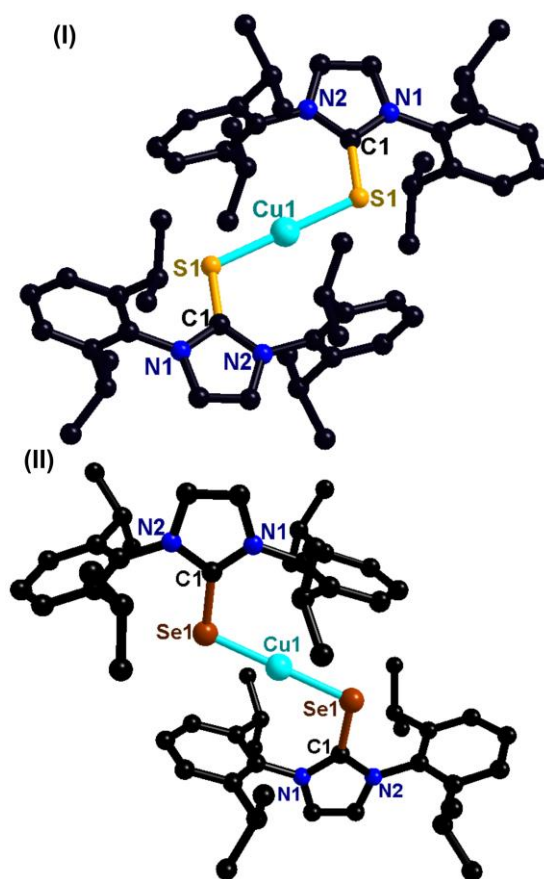


Figure 2.6: (I); Molecular structure of **5**. (II); Molecular structure of **6**. Hydrogen atoms and tetra fluoro borate counter ions have been omitted for clarity

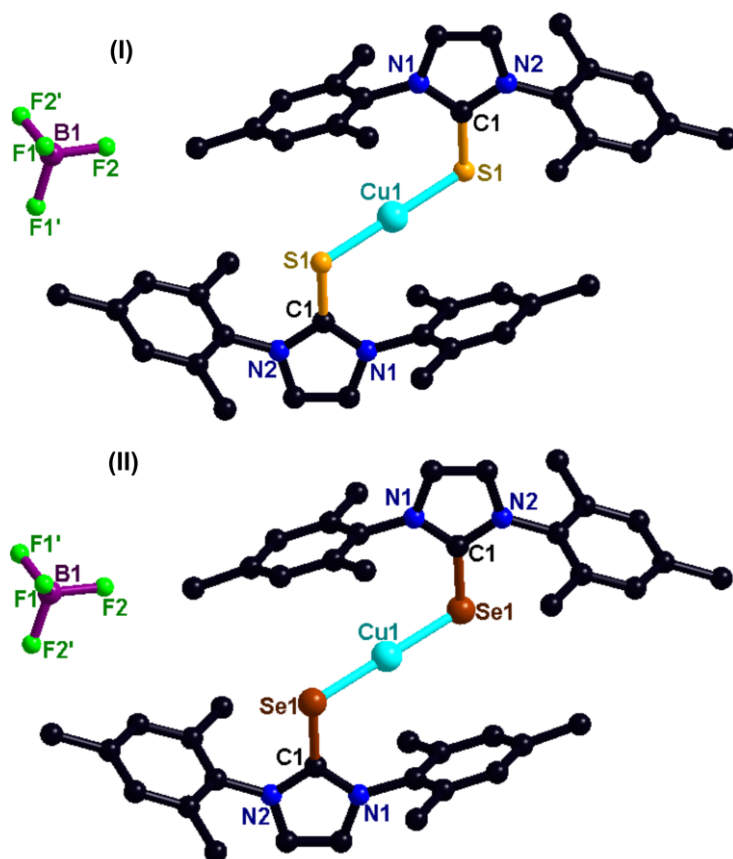


Figure 2.7: (I); Molecular structure of **7**. (II); Molecular structure of **8**. Hydrogen atoms have been omitted for clarity

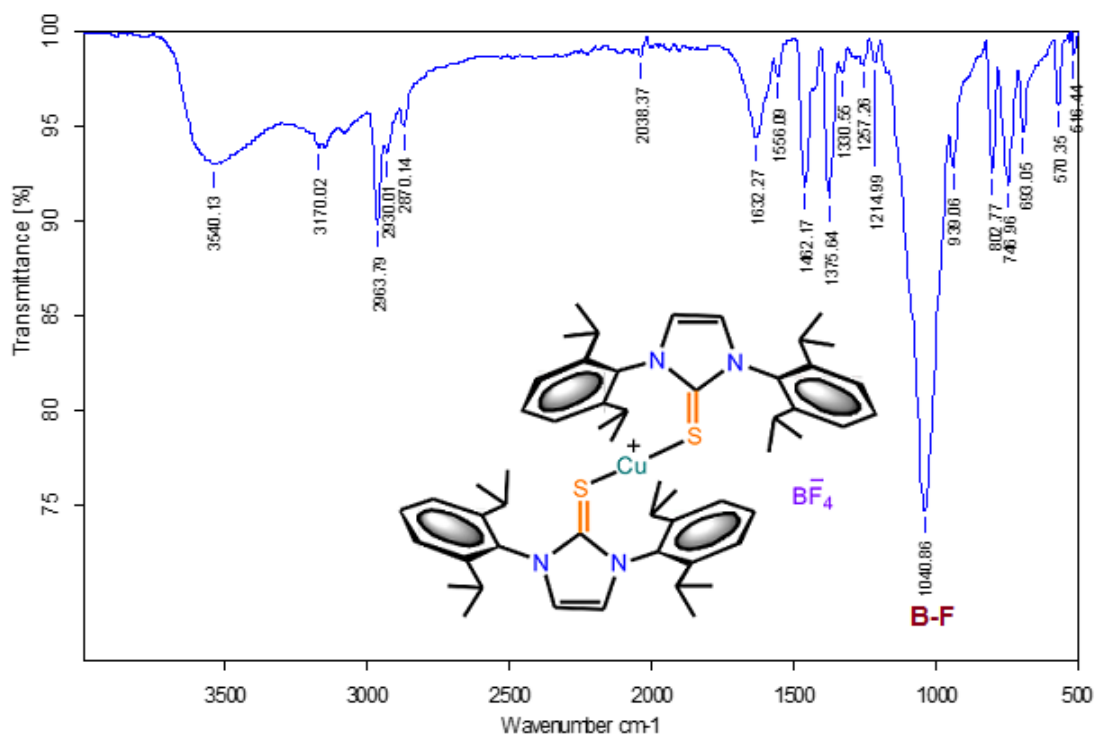


Figure 2.8: Neat FT-IR spectrum of **5** in CDCl_3 at room temperature

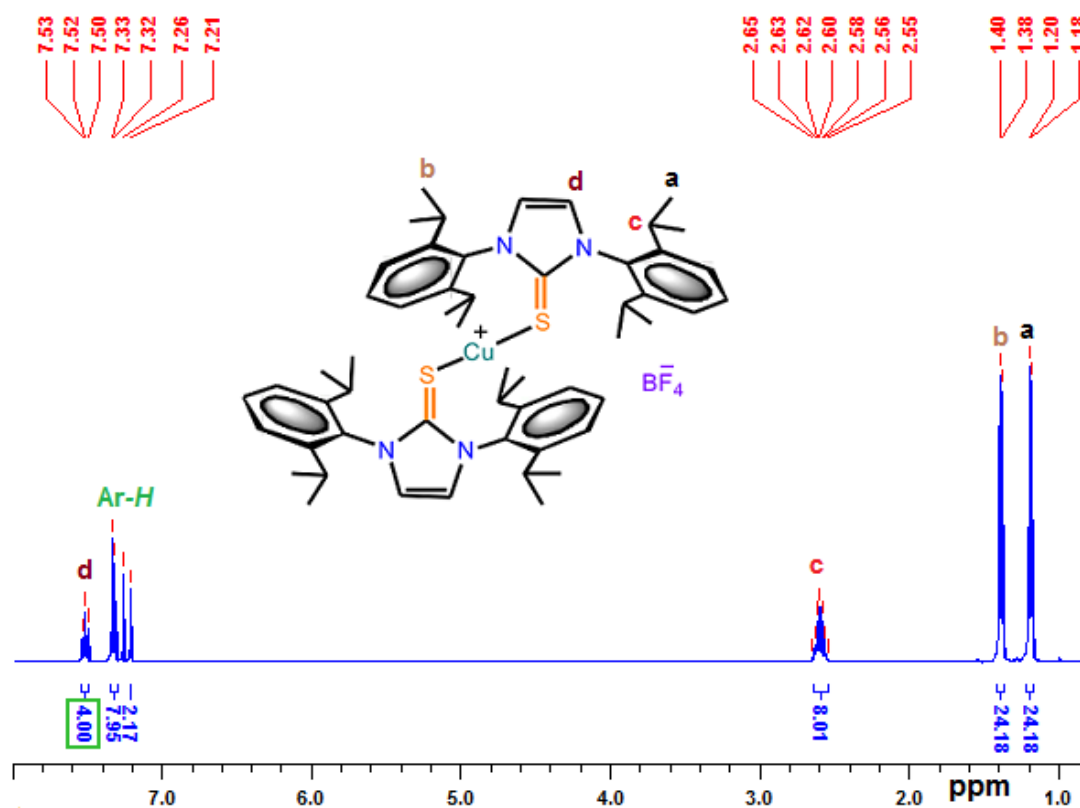


Figure 2.9: ^1H NMR spectrum of **5** in CDCl_3 at room temperature

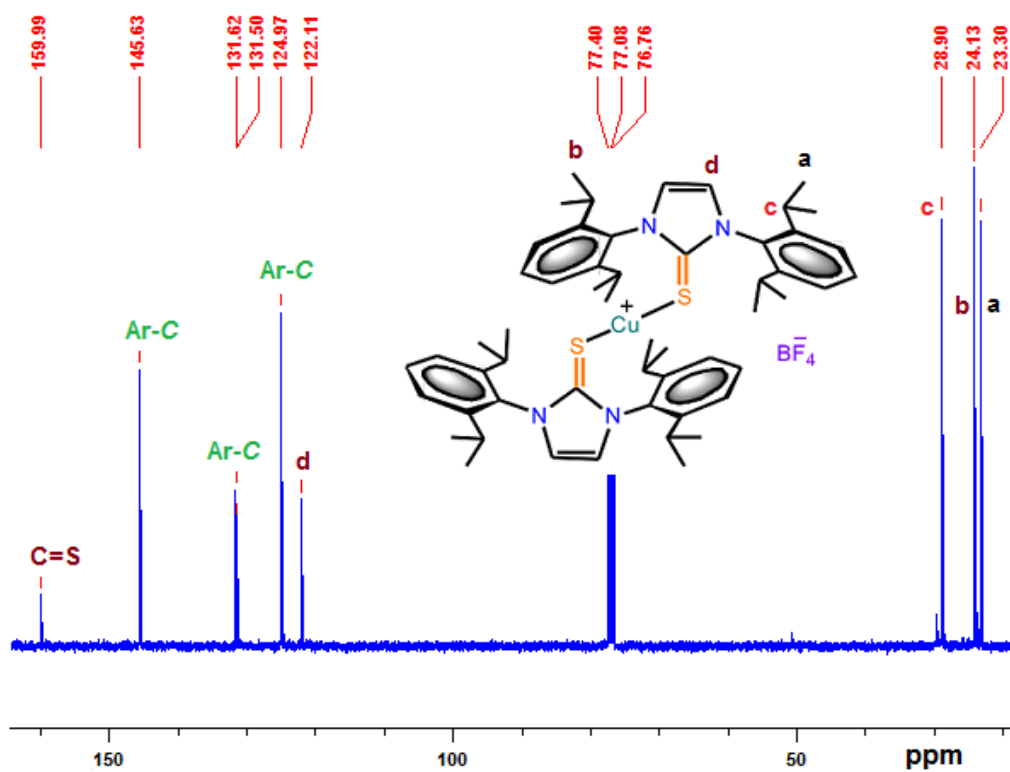


Figure 2.10: ^{13}C NMR spectrum of **5** in CDCl_3 at room temperature

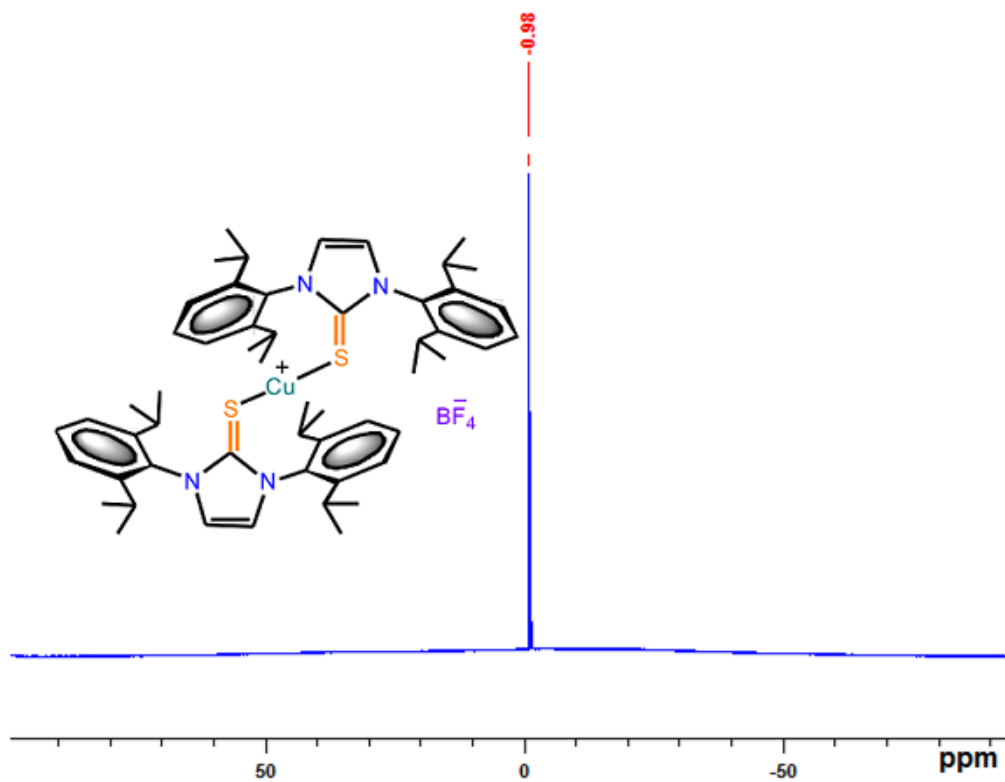


Figure 2.11: ^{11}B NMR spectrum of **5** in CDCl_3 at room temperature

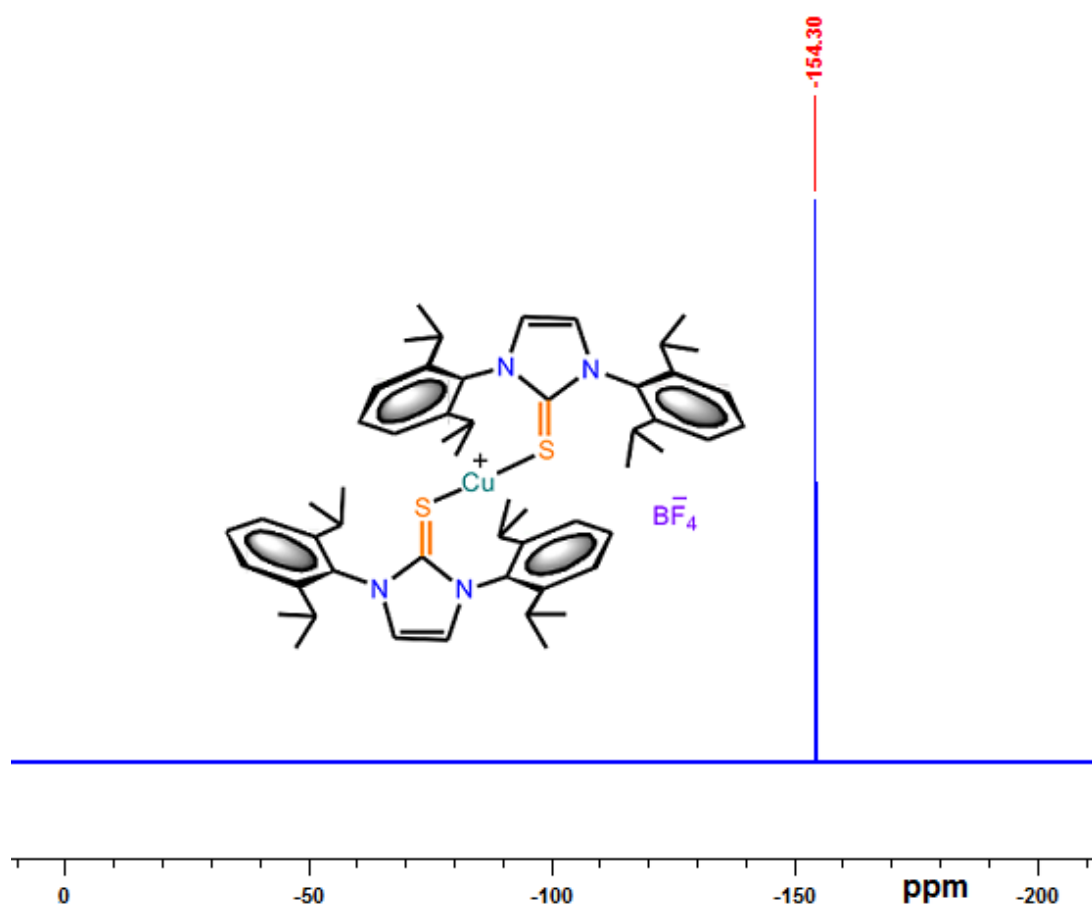


Figure 2.12: ^{19}F NMR spectrum of **5** in CDCl_3 at room temperature

Table 2.1: Selected bond lengths (\AA) and bond angles ($^\circ$) in **1-8**.

	Cu(1)–E(1)	C(1)–E(1)	E(1)–Cu(1)–E(1)	C(1)–E(1)–Cu(1)
1	2.146(9)	1.702(4)	180.0	109.44(13)
2	2.268(5)	1.857(4)	180.0	105.09(14)
3	2.143(7)	1.701(3)	180.0	107.19(9)
4	2.247(9)	1.864(5)	176.29(4)	103.23(15)
5	2.150(9)	1.700(4)	180.0	109.65(13)
6	2.270(4)	1.862(4)	180.0	105.07(13)
7	2.153(4)	1.705(18)	180.0	106.70(6)
8	2.257(3)	1.860(3)	180.0	103.04(7)

Table 2.2: Structural parameters of compounds **1-4**.

	1	2	3	4
Empirical formula	C ₅₄ H ₆₉ ClCuN ₄ O ₄ S ₂	C ₅₄ H ₇₂ N ₄ O ₄ ClCuSe ₂	C ₄₂ H ₄₈ N ₄ O ₄ ClCuS ₂	C ₄₂ H ₄₈ N ₄ CuSe ₂ ClO ₄
Formula weight	1001.25	1098.12	835.96	929.79
Temperature (K)	298	150	298	150
Crystal system	Monoclinic	Monoclinic	Monoclinic	Orthorhombic
Space group	<i>C2/c</i>	<i>C2/c</i>	<i>C2/c</i>	<i>P2₁2₁2₁</i>
<i>a</i> /Å	19.8863(14)	19.5343(15)	21.1509(9)	8.3174(3)
<i>b</i> /Å	15.9337(4)	16.1976(6)	8.2603(3)	17.8053(5)
<i>c</i> /Å	20.405(3)	21.4008(15)	24.586(1)	28.9437(7)
α°	90	90	90	90
β°	114.235(8)	121.691(10)	101.678(4)	90
γ°	90	90	90	90
Volume (Å ³)	5895.8(10)	5761.7(9)	4206.5(3)	4286.4(2)
<i>Z</i>	4	4	4	4
$\rho_{\text{calc}}/\text{mg mm}^{-3}$	1.128	1.2658	1.3200	1.4407
Absorption coefficient (μ/mm^{-1})	1.931	2.744	2.602	3.586
<i>F</i> (000)	2124.0	2272.4	1752.6	1887.5
Reflections collected	12751	10957	8849	11109
<i>R</i> _{int}	0.0308	0.0354	0.0277	0.0363
GOF on <i>F</i> ²	1.650	1.039	1.030	1.035
<i>R</i> ₁ (<i>I</i> > 2 σ (<i>I</i>))	0.0868	0.0766	0.0481	0.0480
w <i>R</i> ₂ (<i>I</i> > 2 σ (<i>I</i>))	0.2510	0.233171	0.145660	0.140271
<i>R</i> ₁ values (all data)	0.1097	0.0866	0.0642	0.0551
<i>R</i> ₂ values (all data)	0.2710	0.2332	0.1457	0.1403

Table 2.3: Structural parameters of compounds **5-8**.

	5	6	7	8
Empirical formula	C ₅₄ H ₇₂ N ₄ S ₂ CuBF ₄	C ₅₄ H ₇₂ BN ₄ F ₄ CuSe ₂	C ₄₂ H ₄₈ BN ₄ F ₄ S ₂ Cu	C ₄₂ H ₄₈ BCuF ₄ N ₄ Se ₂
Formula weight	991.70	1085.44	823.32	917.16
Temperature (K)	298	150	150	150
Crystal system	Monoclinic	Monoclinic	Monoclinic	Monoclinic
Space group	<i>C2/c</i>	<i>C2/c</i>	<i>C2/c</i>	<i>C2/c</i>
<i>a</i> /Å	19.9289(11)	19.6185(8)	20.0772(7)	19.9268(8)
<i>b</i> /Å	15.8882(5)	16.1577(3)	8.2488(3)	8.3983(3)
<i>c</i> /Å	20.3741(16)	21.2244(9)	24.7461(10)	24.7922(10)
α /°	90	90	90	90
β /°	114.824(8)	121.810(6)	101.745(4)	100.413(4)
γ /°	90	90	90	90
Volume (Å ³)	5855.1(7)	5717.4(5)	4012.5(3)	4080.6(3)
<i>Z</i>	4	4	4	4
$\rho_{\text{calc}}/\text{mg mm}^{-3}$	1.1249	1.2609	1.3629	1.4928
Absorption coefficient (μ/mm^{-1})	1.574	2.385	2.188	3.235
<i>F</i> (000)	2104.4	2239.3	1719.5	1854.4
Reflections collected	11826	10507	6872	6844
<i>R</i> _{int}	0.0346	0.0221	0.0220	0.0240
GOF on <i>F</i> ²	1.067	1.031	1.049	1.052
<i>R</i> ₁ (<i>I</i> > 2 σ (<i>I</i>))	0.0865	0.0736	0.0383	0.0391
w <i>R</i> ₂ (<i>I</i> > 2 σ (<i>I</i>))	0.2953	0.2354	0.1080	0.1061
<i>R</i> ₁ values (all data)	0.1127	0.0763	0.0442	0.0433
<i>R</i> ₂ values (all data)	0.2953	0.2354	0.1080	0.1061

2.4. UV-vis solid and solution state absorption study of 1-8

The solution state UV-vis absorption spectra of **1-8** were measured in CHCl₃ (Figure 2.13(I) and 2.13(III)). In solution state UV-vis absorption spectra, IPr=S (L₁), IPr=Se (L₂), IMes=S (L₃), IMes=Se (L₄), and **1-8** shows nearly comparable absorption patterns. The absorption band observed around 240-250 nm can be attributed to $\pi \rightarrow \pi^*$ transition, while the absorption band observed around 260-310 nm can be assigned to $n \rightarrow \pi^*$ transition. In general, the absorption intensity of **1-8** are considerably lower (hypochromic) along with bathochromic shift compared to corresponding chalcogenone ligands. As shown in Figure 2.13(II) and 2.13(IV), the solid state UV-vis absorption spectra of **1-8** are not comparable with solution state absorption spectra of **1-8**. In the case of solid state absorption spectra, the $\pi \rightarrow \pi^*$ and $n \rightarrow \pi^*$ transitions are merged together to give a broad absorption band.

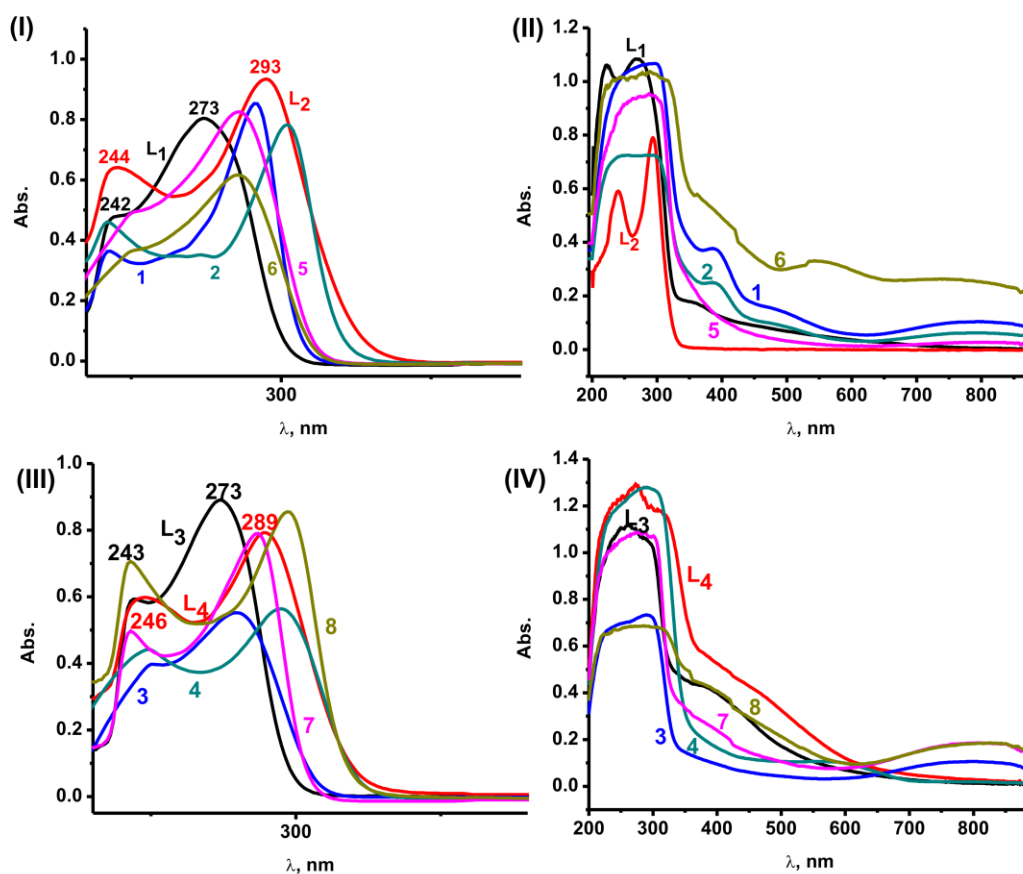


Figure 2.13: (I) Solution state UV-vis spectra of (IPr=S) L₁, (IPr=Se) L₂, **1**, **2**, **5** and **6** in CHCl₃ at 25 °C (1.8 X 10⁻⁵ M); (II) Solid state UV-vis spectra of (IPr=S) L₁, (IPr=Se) L₂, **1**, **2**, **5** and **6**. (III) Solution state UV-vis spectra of (IMes=S) L₃, (IMes=Se) L₄, **3**, **4**, **7** and **8** in CHCl₃ at 25 °C (1.8 X 10⁻⁵ M); (IV) Solid state UV-vis spectra of (IMes=S) L₃, (IMes=Se) L₄, **3**, **4**, **7** and **8**

2.5. TGA analysis of 1-8

The thermal stability of molecules **1-8** are analyzed by TGA. Figure 2.14 reveals the thermal breakdown pathway of **1-8** based on thermal investigation in a flowing nitrogen atmosphere ($10\text{ }^{\circ}\text{C min}^{-1}$, $30\text{-}900\text{ }^{\circ}\text{C}$). Complexes **1-5** show enough stability till $370\text{-}390\text{ }^{\circ}\text{C}$ then sudden weight loss in a single step in the region of $40\text{-}70\%$, which can be endorsed for the decomposition of organic moieties. Subsequently, the gradual weight loss was observed till $850\text{ }^{\circ}\text{C}$ with $9\text{-}12\%$ residue for the metal chalcogenides. Whereas, complex **2** displayed an extreme stability till $370\text{ }^{\circ}\text{C}$ and showed gradual weight loss till $850\text{ }^{\circ}\text{C}$ with 12% residue. The complexes **6-8** were fairly stable up to $400\text{ }^{\circ}\text{C}$ and showed gradual decrease till $800\text{ }^{\circ}\text{C}$ but the complex **6** lost its weight gradually up to $600\text{ }^{\circ}\text{C}$ and remains unchanged till $900\text{ }^{\circ}\text{C}$ with 18% residue. The black residues obtained from the thione compounds (**1, 3, 5** and **7**) were almost in concord with the calculated values for the copper mono sulfide (CuS). Similarly, the residues obtained from the selenone compounds (**2, 4, 6** and **8**) were in concord with the calculated values for the copper mono selenide (CuSe).

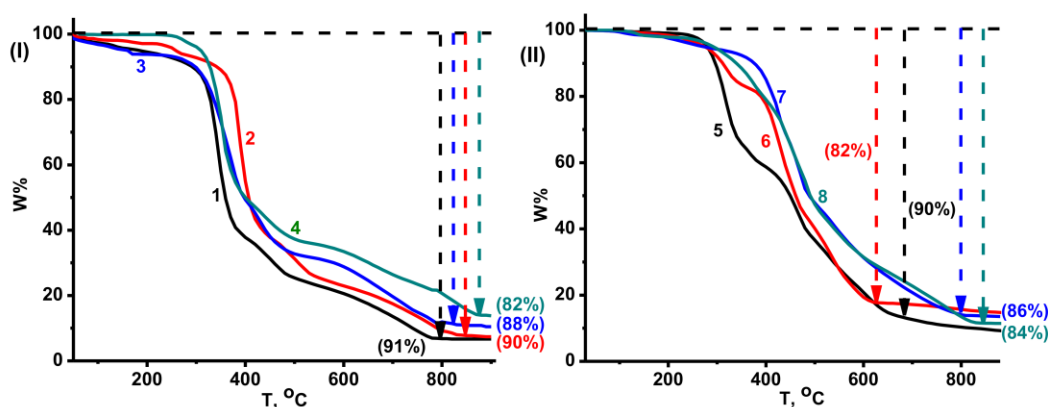
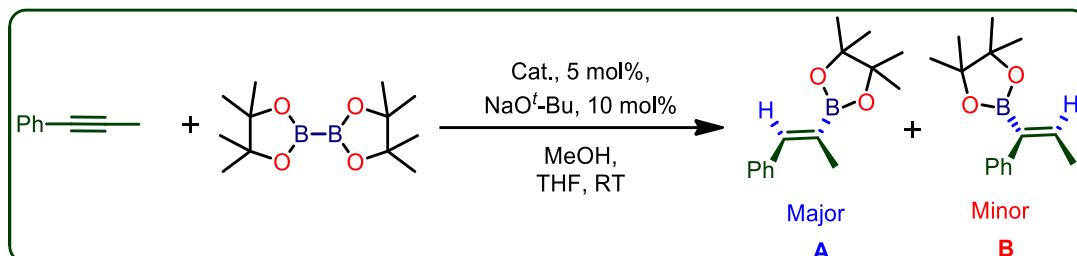


Figure 2.14: TGA curve of **1-4** (I) and **5-8** (II) from $30\text{-}900\text{ }^{\circ}\text{C}$ under nitrogen atmosphere with heating rate of $10\text{ }^{\circ}\text{C min}^{-1}$. Left: **1** residual wt. 9% , calc. wt is 10% ; **3** residual wt. 12% , calc. wt. 12% ; **5** residual wt. 10% , calc. wt is 9% and **7** residual wt. 14% , calc. wt. 12% . Right: **2** residual wt. 10% , calc. wt is 12% ; **4** residual wt. 18% , calc. wt. 16% ; **6** residual wt. 18% , calc. wt is 15% and **8** residual wt. 16% , calc. wt. 15%

2.6. Copper(I) catalyzed borylation of unsymmetrical alkynes

The copper(I) mediated selective borylation of alkyne is consider to be one of the key reaction in multi step organic synthesis [17,18]. The catalytic reaction were demonstrated with copper using NHC [17] or phosphine [18] as ligand. For example, the imidazole chalcogenones supported copper catalysts for borylation of alkyne is rare [5,18d]. Thus,

molecules **1-8** are used as catalyst for regioselective borylation of alkyne under mild conditions (Table 2.4). The borylation of 1-phenyl-1-propyne using bis(pinacolato)diboron in THF was probed in the presence of MeOH as a proton source at ambient temperature using catalysts **1-8** (Scheme 2.4).



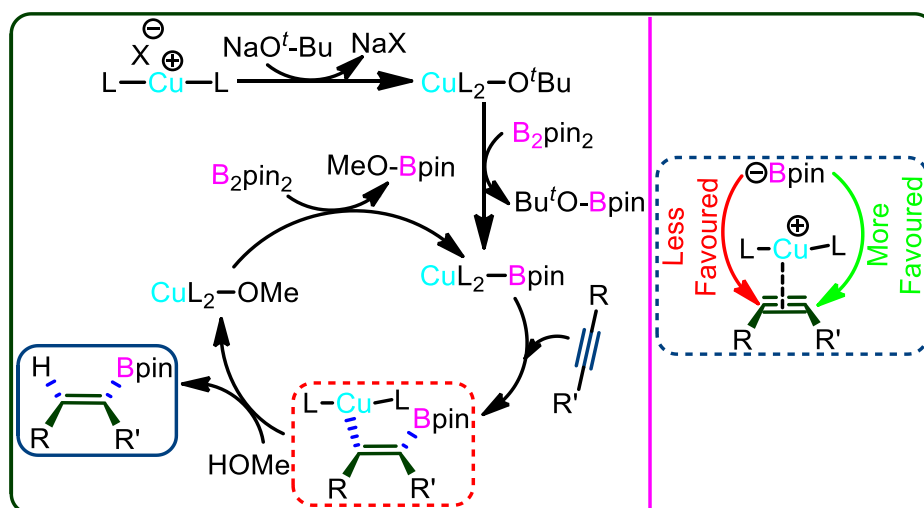
Scheme 2.4: Regioselective borylation of 1-phenyl-1-propyne using **1-8**

The catalysts **1-8** are active towards borylation of 1-phenyl-1-propyne over a period of 24 h to 36 h. Among **1-8**, catalyst **4** is very active (yield, 96%) and highly regioselective (100% major product) (Table 2.4, entry 4). The catalyst **2** shows poor selectivity (Entry 2), while catalyst **6** gives poor conversion (Entry 6). Notably, the regioselectivity (98%-100% major product) of **3** (Entry 3), **5** (Entry 5), **7** (Entry 7) and **8** (Entry 8) is appreciable, however the yield is considerably lower than entry 4. In order to understand the role of ancillary ligands, the catalytic reaction was performed using only IMes=Se (Entry 9), Cu(ClO₄)₂.6H₂O (Entry 10), Cu(BF₄)₂.H₂O (Entry 11) and IMes=Se/Cu(ClO₄)₂.6H₂O (Entry 12). As expected, no catalytic reaction was noticed in the presence of IMes=Se (Entry 9). The reaction was very slow in the case of Cu(ClO₄)₂.6H₂O with poor yield (Entry 10). Interestingly, the regioselectivity and yield are nearly comparable for Cu(BF₄)₂.H₂O (Entry 11) and IMes=Se/Cu(ClO₄)₂.6H₂O (Entry 12). Therefore, the well define catalyst **4** (Entry 4) is very active than the *insitu* catalyst (Entry 12).

Table 2.4: Regioselective borylation of 1-phenyl-1-propyne using **1-8**.^a

E	Catalyst	Time (h)	Selectivity (%) ^b		SMC (%) ^b	Y (%) ^c
			A	B		
1	1	24	90	10	90	80
2	2	36	86	14	75	70
3	3	24	99	01	74	68
4	4	24	100	ND	>99	96
5	5	36	100	ND	64	62
6	6	36	94	06	40	38
7	7	24	98	02	76	70
8	8	36	99	01	90	82
9	IMes=Se	48	0	0	NR	NR
10	Cu(ClO ₄) ₂ .6H ₂ O	48	99	01	45	40
11	Cu(BF ₄) ₂ .H ₂ O	36	98	02	65	60
12	IMes=Se and Cu(ClO ₄) ₂ .6H ₂ O	36	94	06	70	64

^aReaction conditions: 0.50 mmol 1-phenyl-1-propyne, 0.55 mmol bis(pinacolato)diboron, 5 mol% copper(I) catalyst, 10 mol% NaO^t-Bu and 1.0 mmol MeOH were used at room temperature. E-entry, ^b%-Based on ¹H NMR spectroscopy, ^c%-Isolated yield by column chromatography, NR-No reaction, ND-Not detected, SMC-starting material conversion and Y-yield



Scheme 2.5: Plausible reaction pathway shows the nucleophilic attack by Bpin anion from less hindered side followed by protonation

Subsequently, the temperature and solvent choice were optimized using catalyst **4** (Table 2.5). The regioselectivity and yield are not appreciable when the reaction was carried out using **4** in THF at 75 °C (Entry 2) or in 1,4-dioxane at 25 °C (Entry 3) or in hexane at 25 °C (Entry 4). The mid polar solvents like toluene, diethyl ether and dichloromethane gave considerable selectivity with good yield (Entry 5-7, respectively). Therefore the best possible conversion and regioselectivity can be obtained using catalyst **4** in THF at room temperature (Entry 1 and 4). As proposed in scheme 2.5, the nucleophilic attack by Bpin anion take place at the electrophilic centre; followed by protonation led to an expected product. The most efficient catalytic nature of **4** can be attributed to the more Lewis acidic nature of copper centre: *i.e.*, poor σ -donor and strong π -accepting nature of ligand coordinated with a strong cationic nature of metal centre [7] and deviation in bond angle also facilitates the intermediate formation followed by greater conversion of substrates.

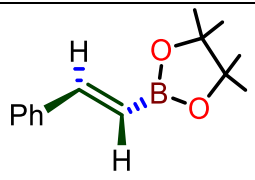
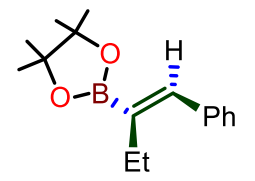
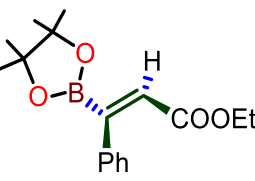
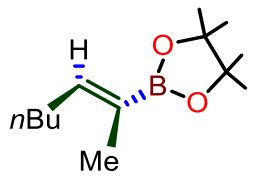
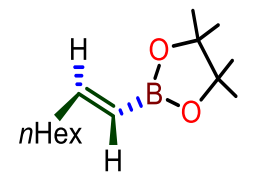
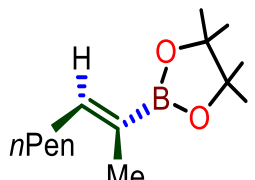
Consequently, the scope of catalyst **4** was analyzed for unsymmetrical alkynes (Table 2.6). The aromatic alkynes like phenyl acetylene, 1-phenyl-1-butyne and ethyl 3-phenylpropionate gave 100% selectivity with very good yield (Table 2.6, entries 1-2 for product A and entry 3 for product B) [19]. Whereas, the aliphatic alkynes like 2-hexyne, 1-octyne and 2-octyne gave considerably less selectivity compared to aromatic alkynes (Table 2.6, entries 4-6). However, the product yield for both aliphatic and aromatic alkynes are comparable.

Table 2.5: Optimization of regioselective borylation of 1-phenyl-1-propyne by **4** in 24 h.^a

E	Solvent	T (°C)	Selectivity (%) ^b		SMC (%) ^b	Y (%) ^c
			A	B		
1	THF	25	100	ND	>99	96
2	THF	75	95	05	76	70
3	1,4-dioxane	25	90	10	37	35
4	Hexane	25	90	10	46	40
5	Toluene	25	98	02	85	78
6	Et ₂ O	25	95	05	90	85
7	CH ₂ Cl ₂	25	99	01	80	76

^aReaction conditions: 0.50 mmol 1-phenyl-1-propyne, 0.55 mmol bis(pinacolato)diboron, 5 mol% copper(I) catalyst (**4**), 10 mol% NaO^t-Bu and 1.0 mmol MeOH were used in 1.0 mL of solvent. E-entry, ^b%-Based on ¹H NMR spectroscopy, ^c%-Isolated yield by column chromatography, ND-Not detected, SMC-starting material conversion and Y-yield

Table 2.6: Regioselective borylation of unsymmetrical alkynes by **4** at 25 °C in THF.^a

E	Starting material	Major product	Selectivity (%) ^b		SMC (%) ^b	Y (%) ^c
			A	B		
1	$\text{H}-\text{C}\equiv\text{C}-\text{Ph}$		100	ND	75	69
2	$\text{Ph}-\text{C}\equiv\text{C}-\text{Et}$		100	ND	82	78
3	$\text{Ph}-\text{C}\equiv\text{C}-\text{COEt}$		ND	100	80	72
4	$n\text{Bu}-\text{C}\equiv\text{C}-\text{Me}$		78	22	85	76
5	$n\text{Hex}-\text{C}\equiv\text{C}-\text{H}$		85	15	90	80
6	$n\text{Pen}-\text{C}\equiv\text{C}-\text{Me}$		90	10	95	82

^aReaction conditions: 0.50 mmol alkyne, 0.55 mmol bis(pinacolato)diboron, 5 mol% copper(I) catalyst (**4**), 10 mol% NaO^t-Bu and 1.0 mmol MeOH were used in 1.0 mL of THF at room temperature for 24 h. E-entry, ^b-Based on ¹H NMR spectroscopy, ^c%-Isolated yield by column chromatography, ND-Not detected, SMC-starting material conversion and Y-yield

2.7. Summary

The copper(I) thione (**1**, **3**, **5** and **7**) complexes along with a rare homoleptic two coordinated copper(I) selenone (**2**, **4**, **6** and **8**) complexes were synthesized and structurally characterized. The molecules **1-8** were isolated from copper(II) to copper(I) reduction by chalcogenones. The molecules **1-3** and **5-8** are in perfect linear geometry, while **4** is in *quasi*-linear geometry. These newly isolated molecules **1-8** were used as catalyst for boron addition to alkynes. The catalysts **1-8** were active for regioselective boron addition to alkynes. Moreover, (i) we assume that the homoleptic two coordinated intermediate do not exist in the catalytic process, (ii) the π -accepting nature of imidazoline-2-chalcogenone do play less role in isolating homoleptic two coordinated coinage metal derivatives, (iii) complex **4** showed the best catalytic activity, (iv) well define catalyst is much more active than the *in-situ* generated catalyst, for example catalyst **4**, (v) IMes=Se based copper(I) complexes (**4** and **8**) were more selective and efficient than **3** and **5-7**, and (vi) the more Lewis acidic nature of copper centre in **4** enhances the catalytic activity. The excellent selectivity of the reactions at room temperature, especially with **4**, makes this strategy viable for borylation of symmetrical/unsymmetrical alkynes. Nevertheless the investigation towards highly selective catalysts with reduced reaction time is in progress.

2.8. References

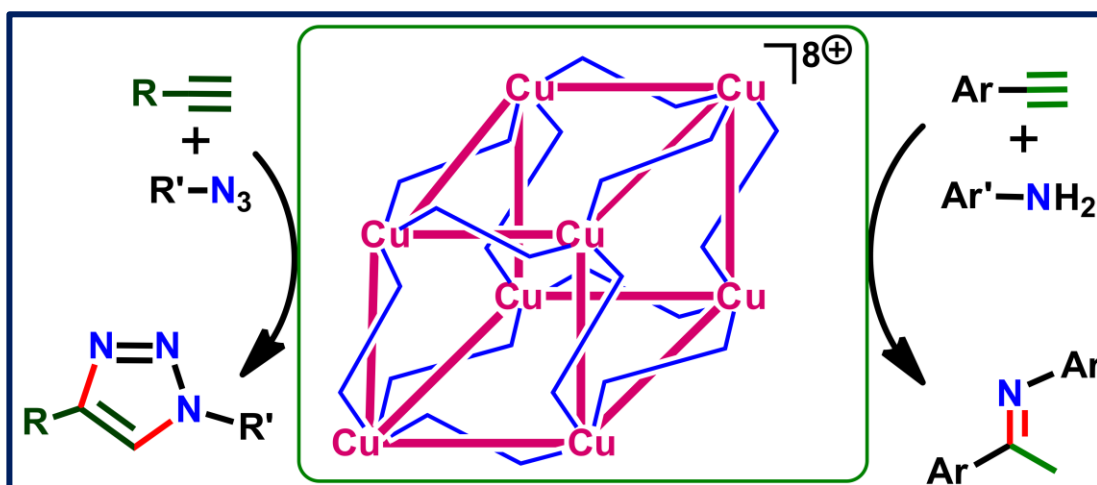
- [1] For selected recent examples: (a) A. Singh, A. Singh, J. Ciston, K. Bustillo, D. Nordlund and D. J. Milliron, *J. Am. Chem. Soc.*, 2015, **137**, 6464–6467; (b) K. Miszta, R. Brescia, M. Prato, G. Bertoni, S. Marras, Y. Xie, S. Ghosh, M. R. Kim and L. Manna, *J. Am. Chem. Soc.*, 2014, **136**, 9061–9069; (c) X. Q. Chen, Z. Li, Y. Bai, Q. Sun, L. Z. Wang and S. X. Dou, *Chem. – Eur. J.*, 2015, **21**, 1055–1063; (d) X.-J. Wu, X. Huang, X. Qi, H. Li, B. Li and H. Zhang, *Angew. Chem., Int. Ed.*, 2014, **53**, 8929–8933; (e) A. Comin and L. Manna, *Chem. Soc. Rev.*, 2014, **43**, 3957–3975; (f) P. L. Saldanha, R. Brescia, M. Prato, H. Li, M. Povia, L. Manna and V. Lesnyak, *Chem. Mater.*, 2014, **26**, 1442–1449; (g) L. Liu, H. Zhong, Z. Bai, T. Zhang, W. Fu, L. Shi, H. Xie, L. Deng and B. Zou, *Chem. Mater.*, 2013, **25**, 4828–4834; (h) O. Fuhr, S. Dehnen and D. Fenske, *Chem. Soc. Rev.*, 2013, **42**, 1871–1906; (i) O. Mayasree, C. R. Sankar, K. M. Kleinke and H. Kleinke, *Coord. Chem. Rev.*, 2012, **256**, 1377–1383; (j) J. Chang and E. R. Waclawik, *RSC Adv.*, 2014, **4**, 23505–23527; (k) M. V. Kovalenko, M. Scheele and D. V. Talapin, *Science*, 2009, **324**, 1417–1420.

- [2] (a) R. H. Holm, P. Kennepohl and E. I. Solomon, *Chem. Rev.*, 1996, **96**, 2239–2314; (b) A. V. Davis and T. V. O’Halloran, *Nat. Chem. Biol.*, 2008, **4**, 148–151; (c) E. E. Battin and J. L. Brumaghim, *Cell Biochem. Biophys.*, 2009, **55**, 1–23; (d) E. E. Battin, N. R. Perron and J. L. Brumaghim, *Inorg. Chem.*, 2006, **45**, 499–501; (e) R. R. Ramoutar and J. L. Brumaghim, *J. Inorg. Biochem.* 2007, **101**, 1028–1035.
- [3] (a) M. M. Kimani, C. A. Bayse, B. S. Stadelman and J. L. Brumaghim, *Inorg. Chem.*, 2013, **52**, 11685–11687; (b) M. M. Kimani, H. C. Wang and J. L. Brumaghim, *Dalton Trans.*, 2012, **41**, 5248–5259; (c) M. M. Kimani, J. L. Brumaghim and D. VanDerveer, *Inorg. Chem.*, 2010, **49**, 9200–9211; (d) M. M. Kimani, C. A. Bayse and J. L. Brumaghim, *Dalton Trans.*, 2011, **40**, 3711–3723; (e) E. E. Battin, M. T. Zimmerman, R. R. Ramoutar, C. E. Quarles and J. L. Brumaghim, *Metallomics*, 2011, **3**, 503–512.
- [4] X. D. Liu, X. C. Duan, P. Peng and W. Zheng, *Nanoscale*, 2011, **3**, 5090–5095.
- [5] H. R. Kim II, G. Jung, K. Yoo, K. Jang, E. S. Lee, J. Yun and S. U. Son, *Chem. Commun.*, 2010, **46**, 758–760.
- [6] (a) M. T. Aroz, M. C. Gimeno, M. Kulcsar, A. Laguna and V. Lippolis, *Eur. J. Inorg. Chem.*, 2011, 2884–2894; (b) T. S. Lobana, R. Sultana, R. J. Butcher, A. Castineiras, T. Akitsu, F. J. Fernandez and M. C. Vega, *Eur. J. Inorg. Chem.*, 2013, 5161–5170.
- [7] D. J. Nelson, F. Nahra, S. R. Patrick, D. B. Cordes, A. M. Z. Slawin and S. P. Nolan, *Organometallics*, 2014, **33**, 3640–3645.
- [8] S. Groysman and R. H. Holm, *Inorg. Chem.*, 2009, **48**, 621–627.
- [9] D. D. Perrin and W. L. F. Armarego, *Purification of laboratory chemicals*, Pergamon Press, London, 3rd edn, 1988.
- [10] (a) L. Jafarpour, E. D. Stevens and S. P. Nolan, *J. Organomet. Chem.*, 2000, **606**, 49–54; (b) J. Huang, H. J. Schanz, E. D. Stevens and S. P. Nolan, *Inorg. Chem.*, 2000, **39**, 1042–1045; (c) M. Tretiakov, Y. G. Shermolovich, A. P. Singh, P. P. Samuel, H. W. Roesky, B. Niepötter, A. Visschera and D. Stalke, *Dalton Trans.*, 2013, **42**, 12940–12946; (d) K. Srinivas, P. Suresh, C. N. Babu, A. Sathyanarayana and G. Prabusankar, *RSC Adv.*, 2015, **5**, 15579–15590; (e) A. Liske, K. Verlinden, H. Buhl, K. Schaper and C. Ganter, *Organometallics*, 2013, **32**, 5269–5272; (f) D. J. Nelson, A. Collado, S. Manzini, S. Meiries, A. M. Z. Slawin, D. B. Cordes and S. P. Nolan, *Organometallics*, 2014, **33**, 2048–2058.

- [11] O. V. Dolomanov, L. J. Bourhis, R. J. Gildea, J. A. K. Howard and H. Puschmann, *J. Appl. Crystallogr.*, 2009, **42**, 339–341.
- [12] (a) G. M. Sheldrick, *Acta Crystallogr. Sect. A: Fundam. Crystallogr.*, 1990, **46**, 467–473; (b) G. M. Sheldrick, SHELXL-97, *Program for Crystal Structure Refinement*, Universität Göttingen, Göttingen, 1997.
- [13] J. R. Miecznikowski, M. A. Lynn, J. P. Jasinski, E. Reinheimer, D. W. Baki, M. Pati, E. E. Butrick, A. E. R. Drozdowski, K. A. Archer, C. E. Villa, E. G. Lemons, E. Powers, M. Siu, C. D. Gomes and K. N. Morio, *J. Coord. Chem.*, 2014, **67**, 29–44.
- [14] G. A. Bowmaker, N. Chaichit, J. V. Hanna, C. Pakawatchai, B. W. Skelton and A. H. White, *Dalton Trans.*, 2009, 8308–8316.
- [15] K. Fujisawa, S. Imai, N. Kitajima and Y. Moro-oka, *Inorg. Chem.*, 1998, **37**, 168–169.
- [16] For example: (a) S. Groysman, A. Majumdar, S.-L. Zheng and R. H. Holm, *Inorg. Chem.*, 2010, **49**, 1082–1089; (b) J. Ruiz, R. Quesada, V. Riera, S. Garcia-Granda and M. R. Diaz, *Chem. Commun.*, 2003, 2028–2029; (c) G. Pilloni, B. Longato, G. Bandoli and B. Corain, *Dalton Trans.*, 1997, 819–825; (d) S. Zeevi and E. Y. Tshuva, *Eur. J. Inorg. Chem.*, 2007, 5369–5376; (e) M. Y. Chiang, R. Bau, G. Minghetti, A. L. Bandini, G. Banditelli and T. F. Koetzle, *Inorg. Chem.*, 1984, **23**, 122–124; (f) J. T. Sampanthar, J. J. Vittal and P. A. W. Dean, *J. Chem. Soc., Dalton Trans.*, 1999, 3153–3156.
- [17] For the selected examples: (a) H. Yoshida, Y. Takemoto and K. Takaki, *Chem. Commun.*, 2014, **50**, 8299–8302; (b) R. Barbeyron, E. Benedetti, J. Cossy, J.-J. Vasseur, S. Arseniyadis and M. Smietana, *Tetrahedron*, 2014, **70**, 8431–8452; (c) Y. D. Bidal, F. Lazreg and C. S. J. Cazin, *ACS Catal.*, 2014, **4**, 1564–1569; (d) N. Miyaura and A. Suzuki, *Chem. Rev.*, 1995, **95**, 2457–2483.
- [18] For the selected examples: (a) D. Li, Y. E. Kimand and J. Yun, *Org. Lett.*, 2015, **17**, 860–863; (b) A. L. Moure, R. G. Arrayás, D. J. Cárdenas, I. Alonso and J. C. Carretero, *J. Am. Chem. Soc.*, 2012, **134**, 7219–7222; (c) H. Yoshida, S. Kawashima, Y. Takemoto, K. Okada, J. Ohshita and K. Takaki, *Angew. Chem., Int. Ed.*, 2012, **51**, 235–238; (d) H. R. Kim and J. Yun, *Chem. Commun.*, 2011, **47**, 2943–2945.
- [19] J.-E. Lee, J. Kwon and J. Yun, *Chem. Commun.*, 2008, 733–734.

Chapter 3

Large Cu^{I}_8 Chalcogenone Cubic Cages with Non-interacting Counter Ion



3.1. Introduction

The chemistry of copper-NHC (NHC = N-heterocyclic carbene) has attracted much attention in the past two decades invoking requirements in catalysis [1]. The most of the known copper-NHC molecules are mononuclear, dinuclear, trinuclear or tetranuclear [2]. Though, more than twelve hundred articles have been reported (according to the SciFinder search on “Copper Carbene”) related to the copper carbene chemistry, the NHC–Cu clusters are rare [3]. Unlike phosphine based copper clusters [4], the penta⁵ or higher nuclear copper–NHC derivatives and their catalytic applications are limited due to strong σ donor and poor π -accepting nature of NHC along with steric hindrance [6]. The search for the suitable NHC or analogues of NHC type ligands to isolate the polynuclear copper clusters or cages are in great demand [7]. Therefore it is one of the most challenging tasks to design the synthetic strategy using NHC or NHC analogues for clusters or cages of specific nuclearity with shape. Recently, the NHC analogues of imidazole-2-chalcogenone copper(I) complexes have been reported with promising features in catalysis due to the tunable σ -donor and π -accepting nature of imidazole-2-chalcogenone [8]. Surprisingly, the catalytic efficiency of copper-imidazole-2-chalcogenone complexes is better than copper–NHC complexes. This chapter describes the first perfect Cu_8^{I} cubic cages $[\{\text{Cu}(\text{Btp})\}_8(\text{PF}_6^-)](\text{PF}_6^-)_7$ (**9**) and $[\{\text{Cu}(\text{Bpsp})\}_8(\text{PF}_6^-)](\text{PF}_6^-)_7$ (**10**) supported by imidazole-2-chalcogenone ligands (Btp = 2,6-bis(1-isopropylimidazole-2-thione)pyridine or Bpsp = 2,6-bis(1-isopropylimidazole-2-selone)pyridine). To the best of our knowledge, **9** and **10** are the large copper cubic cages isolated as of now.

3.2. Experimental Section

3.2.1. General remarks

All manipulations were carried out under argon atmosphere using standard Schlenk techniques. The solvents were purchased from commercial sources and purified according to standard procedures and freshly distilled under argon atmosphere prior to use [9]. Unless otherwise stated, the chemicals were purchased from commercial sources. 1,1'-(pyridine-2,6-diyl)bis(3-isopropyl-1*H*-imidazol-3-ium)bromide, 2,6-Bis(1-isopropylimidazole-2-thione)pyridine (Btp) [10] and 2,6-bis(1-isopropylimidazole-2-selone)pyridine (Bpsp) ligands were synthesized as reported [11]. 2,6-dibromo pyridine, Sulphur powder, selenium powder and $[\text{Cu}(\text{CH}_3\text{CN})_4]\text{PF}_6$ were purchased from Sigma Aldrich and used as received.

FT-IR measurement (neat) was carried out on a Bruker Alpha-P Fourier transform spectrometer. The UV-vis spectra were measured on a T90+ UV-visible spectrophotometer. Thermogravimetric analysis (TGA) was performed using a TASDT Q600, Tzero-press. NMR spectra were recorded on Bruker Ultrashield-400 spectrometers at 25 °C unless otherwise stated. Chemical shifts are given relative to TMS and were referenced to the solvent resonances as internal standards. Elemental analyses were performed by the Euro EA-300 elemental analyzer. The crystal structures of **9** and **10** were measured on an Oxford Xcalibur 2 diffractometer. Single crystals of complexes suitable for the single crystal X-ray analysis were obtained from their reaction mixture at room temperature and the suitable single crystals for X-ray structural analysis were mounted at room temperature (298 K) in inert oil under an argon atmosphere. Using Olex2 [12], the structure was solved with the ShelXS [13] structure solution program using Direct Methods and refined with the olex2.refine refinement package using Gauss-Newton minimization. Absorption corrections were performed on the basis of multi-scans. Non-hydrogen atoms were anisotropically refined. Hydrogen atoms were included in the refinement in calculated positions riding on their carrier atoms. No restraint has been made for any of the compounds.

3.2.2. Synthesis of **9**

[Cu(CH₃CN)₄]PF₆ (0.069 g, 0.185 mmol) was dissolved in acetonitrile (3 mL) in an oven dried Schlenk flask under inert atmosphere, to which Bptp (0.100 g, 0.278 mmol) in chloroform was added dropwise and was allowed to stir for 12 h. Yield: 93% (0.128 g, based on [Cu(CH₃CN)₄]PF₆). M.p.: 220-223 °C (melting). Elemental analysis calcd (%) for C_{23.5}H_{32.5}N_{7.5}S₃Cu₁P₁F₆ (724.76): C, 38.94; H, 4.52; N, 14.49; S, 13.27; Found: C, 38.8; H, 4.5; N, 14.7; S, 13.3. ¹H NMR (DMSO-*d*₆, 400 MHz): δ = 1.37-1.39 (d, 2((CH₃)₂CH), 12H), 4.90-4.94 (m, 2(CH₃)₂CH, 2H), 7.74 (d, imidazole, 2H), 7.86 (d, imidazole, 2H), 8.07-8.08 (d, pyridine, 2H), 8.39-8.43 (t, pyridine, 1H) ppm. ¹³C NMR (DMSO-*d*₆, 100 MHz): δ = 21.03 ((CH₃)₂CH), 49.40 ((CH₃)₂CH), 116.88 (pyridine), 119.99 (imidazole), 120.36 (imidazole), 142.97 (pyridine), 147.56 (pyridine), 155.87 (C=S) ppm. ³¹P NMR (DMSO-*d*₆, 161 MHz): -157.36 to -131.02 (sept, PF₆) ppm. ¹⁹F NMR (DMSO-*d*₆, 376 MHz): δ = -71.05 to -69.16 (d, PF₆) ppm. FT-IR (neat): $\bar{\nu}$ 3156(w), 2978(w), 1671(w), 1596(m), 1459(s), 1400(s), 1342(m), 1279(w), 1221(s), 1130(m) (C=S), 1070(w), 995(w), 828(vs) (P-F), 730(m), 682(m), 553(s) (P-F) cm⁻¹.

3.2.3. Synthesis of 10

[Cu(CH₃CN)₄]PF₆ (0.055 g, 0.146 mmol) was dissolved in acetonitrile (3 mL) in an oven dried Schlenk flask under inert atmosphere, to which B₂sp (0.100 g, 0.220 mmol) in chloroform was added dropwise and was allowed to stir for 12 h. Yield: 81% (0.105 g, based on [Cu(CH₃CN)₄]PF₆). M.p.: 215-216 °C (melting). Elemental analysis calcd (%) for C_{23.5}H_{32.5}N_{7.5}Se₃Cu₁P₁F₆ (865.45): C, 32.61; H, 3.79; N, 12.14; Found: C, 32.7; H, 3.8; N, 12.8. ¹H NMR (DMSO-*d*₆, 400 MHz): 1.36-1.37 (d, 2((CH₃)₂CH), 12H), 4.92 (m, 2(CH₃)₂CH, 2H), 7.88 (d, imidazole, 2H), 8.01 (d, imidazole, 2H), 8.14-8.15 (d, pyridine, 2H), 8.45 (t, pyridine, 1H) ppm. ¹³C NMR (DMSO-*d*₆, 100 MHz): 21.20 ((CH₃)₂CH), 51.57 ((CH₃)₂CH), 118.79 (pyridine), 122.26 (imidazole), 122.71 (imidazole), 143.71 (pyridine), 148.51 (pyridine), 154.19 (C=Se) ppm. ³¹P NMR (DMSO-*d*₆, 161 MHz): -157.32 to -130.98 (sept, PF₆) ppm. ¹⁹F NMR (DMSO-*d*₆, 376 MHz): -71.06 to -69.17 (d, PF₆) ppm. FT-IR (neat): $\bar{\nu}$ 3156(w), 2977(w), 1692(w), 1574(m), 1458(s), 1420(s), 1341(m), 1217(w), 1116(m) (C=Se), 1073(w), 1045(w), 829(vs) (P-F), 758(m), 732(m), 677(m), 586(m), 554(s) (P-F) cm⁻¹.

3.2.4. Synthesis of 9@AuCl

Molecule **9** (0.01g, 1 equiv) and an excess (dms)AuCl (0.07g, 16 equiv) were mixed together and evacuated for 10 minutes, after which 1 mL of acetonitrile was added under argon flow and allowed to stir at room temperature for 12h. ¹H NMR (DMSO-*d*₆, 400 MHz): 1.39 (s, 2((CH₃)₂CH), 12H), 4.98 (m, 2(CH₃)₂CH, 2H), 7.65-7.73 (m, imidazole, 4H), 8.27 (m, pyridine, 3H) ppm.

3.2.5. Synthesis of 9@Perylene

Molecule **9** (0.01g, 1 equiv) and an excess perylene (0.03g, 8 equiv) were mixed together and evacuated for 10 minutes, after which 1 mL of acetonitrile was added under argon flow and was allowed to stir at reflux for 4 h. ¹H NMR (DMSO-*d*₆, 400 MHz): 1.39-1.41 (d, 2((CH₃)₂CH), 12H), 4.93-5.02 (m, 2(CH₃)₂CH, 2H), 7.53-7.57 (t, perylene, 2H), 7.73 (d, imidazole, 2H), 7.79-7.81 (d, perylene, 2H), 7.86 (d, imidazole, 2H), 8.18-8.20 (d, pyridine, 2H), 8.35-8.42 (m, perylene, 2H and pyridine 1H) ppm.

3.2.6. Synthesis of 9@Pyrene

Molecule **9** (0.01g, 1 equiv) and an excess pyrene (0.03g, 8 equiv) were mixed together and evacuated for 10 minutes, after which 1 mL of acetonitrile was added under argon flow and was allowed to stir at reflux for 4h. ¹H NMR (DMSO-*d*₆, 400 MHz): 1.39-1.41 (d,

2((CH₃)₂CH), 12H), 4.95-4.98 (m, 2(CH₃)₂CH, 2H), 7.74 (d, imidazole, 2H), 7.87 (d, imidazole, 2H), 8.07-8.30 (m, pyrene, 10H), 8.32-8.40 (m, pyrene, 3H) ppm.

3.2.7. Cu(I) catalysts catalysed azide–alkyne cycloaddition reactions (CuAAC)

Catalyst **9** or **10** (1 mol%), azide (1 mmol) and terminal alkyne (1.2 mmol) were placed in an oven dried Schlenk flask. The reaction mixture was then allowed to stir at room temperature and the progress of the reaction was monitored by thin layer chromatography. The solid mass obtained was dissolved in ethyl acetate and passed through silica gel column. The solvent has been removed by rotary evaporator and the residue washed several times with n-hexane yielded pure desired products. All the isolated products were well characterized by ¹H and ¹³C NMR and few products (**Ia**, **Ib**, **IIa** and **IIbB**) were also characterized by single crystal X-ray diffraction technique.

3.2.8. Cu(I) catalysts mediated hydroamination of terminal alkynes

Catalysts **9** or **10** (1 mol %) and AgBF₄ (1 mol %) were placed together in an oven dried Schlenk flask. The Schlenk flask was then evacuated and refilled with nitrogen two to three times. Subsequently, acetonitrile (1 mL) was added to the mixture and was allowed to stir at room temperature for 5-10 minutes. After which, the corresponding arylamine (0.6 mmol) and terminal alkyne (0.50 mmol) were added successively. The resulting mixture was allowed to stir at 70 °C for the appropriate time and the progression of the reactions were determined by thin layer chromatography. The isolated imines were well characterized by ¹H and ¹³C NMR spectroscopy.

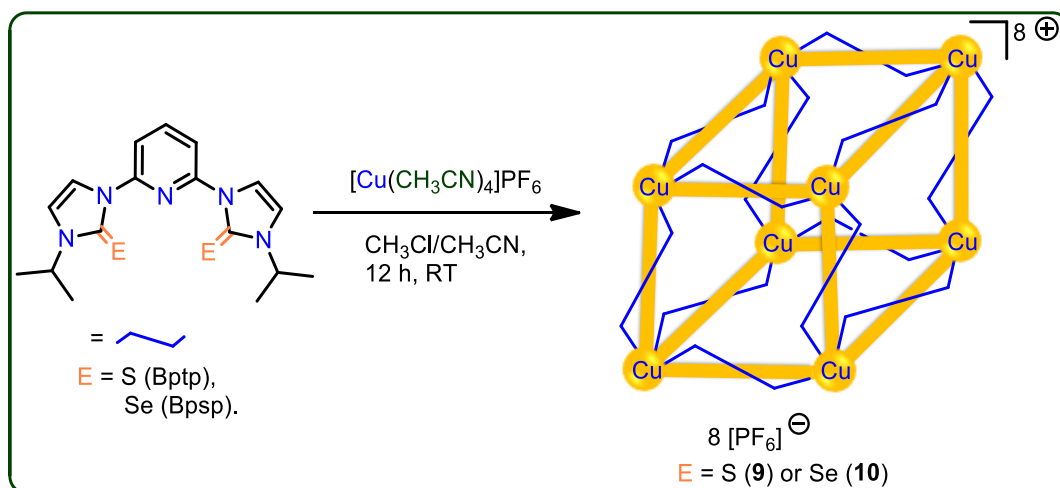
3.3. Result and discussion

3.3.1. Synthesis and characterization

The octanuclear copper(I) cubic clusters **9** and **10** were isolated in excellent yield by treating [Cu(CH₃CN)₄]PF₆ with an appropriate amount of Bptp or Bpsp in acetonitrile and chloroform mixture (Scheme 3.1). Pyridine-based organo dichalcogenone ligands Bptp and Bpsp were synthesized in a single step *via* the reactions of pyridine bridged imidazolium dibromide derivatives with elemental chalcogen powder in the presence of K₂CO₃ in good yield.

The ionic salts **9** and **10** were confirmed by FT-IR, multinuclear (¹H, ¹³C, ³¹P and ¹⁹F) NMR, UV-vis, TGA, CHN analysis, BET, single crystal X-ray diffraction and powder X-ray diffraction techniques. **9** and **10** are stable under ambient conditions for several months and soluble in polar solvents such as acetonitrile and DMSO. In ¹H NMR, the isopropyl CH signal

is upfield shifted by around 0.3 ppm, while imidazole *CH* signals are downfield shifted by 0.4 to 0.9 ppm. The hydrogen at 4th position in the pyridine unit appeared to be downfield shifted by 0.4 ppm, while the other protons at 3rd and 5th position in pyridine moiety appears to be upfield shifted by 0.4 to 0.6 ppm compared to free ligands. The ¹³C NMR spectra of the copper(I) complexes **9** and **10** are mostly the same with very little shift in the resonances when compared to the respective ligand precursors (Figure 3.2 and 3.8). In ¹³C NMR, the C=S and C=Se signal in **9** and **10** appeared to be upfield shifted (5 ppm for **9** and 1 ppm for **10** compared to corresponding ligand), respectively (Figure 3.3 and 3.9). This can be attributed to the strong σ -donor and poor π -accepting nature of the carbene carbon upon complexation with copper(I). The ³¹P NMR spectra shows a septet for the presence of PF₆ counter ions in **9** and **10** (Figure 3.4 and 3.10). The ¹⁹F NMR spectra depicts a doublet for PF₆ counter ions in **9** and **10** (Figure 3.5 and 3.11).



Scheme 3.1: Synthesis of **9** and **10**

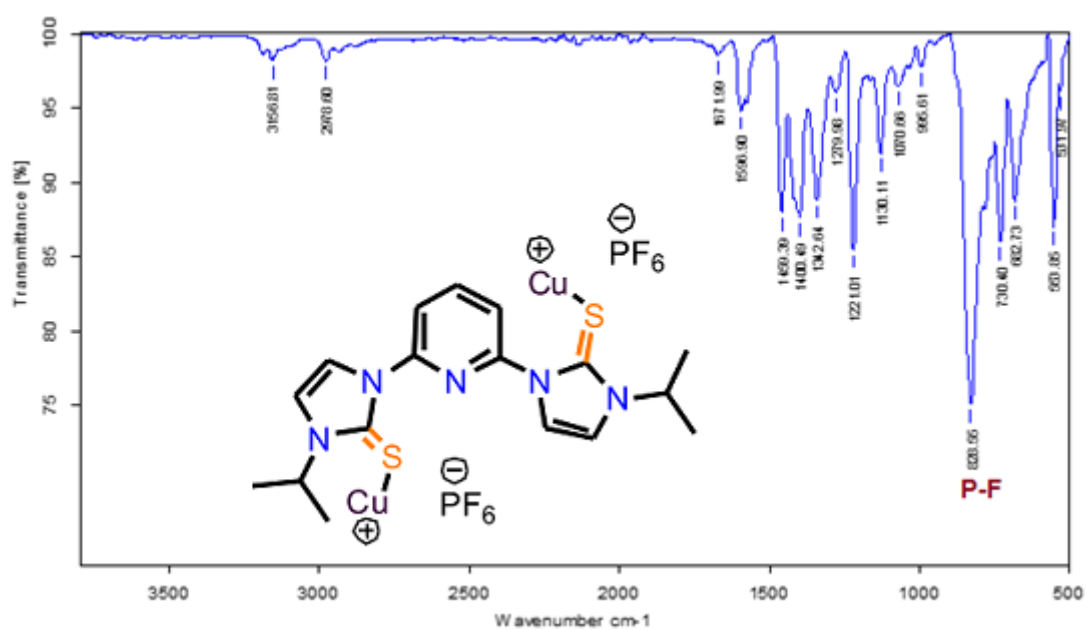


Figure 3.1: Neat FT-IR spectrum of **9** at room temperature

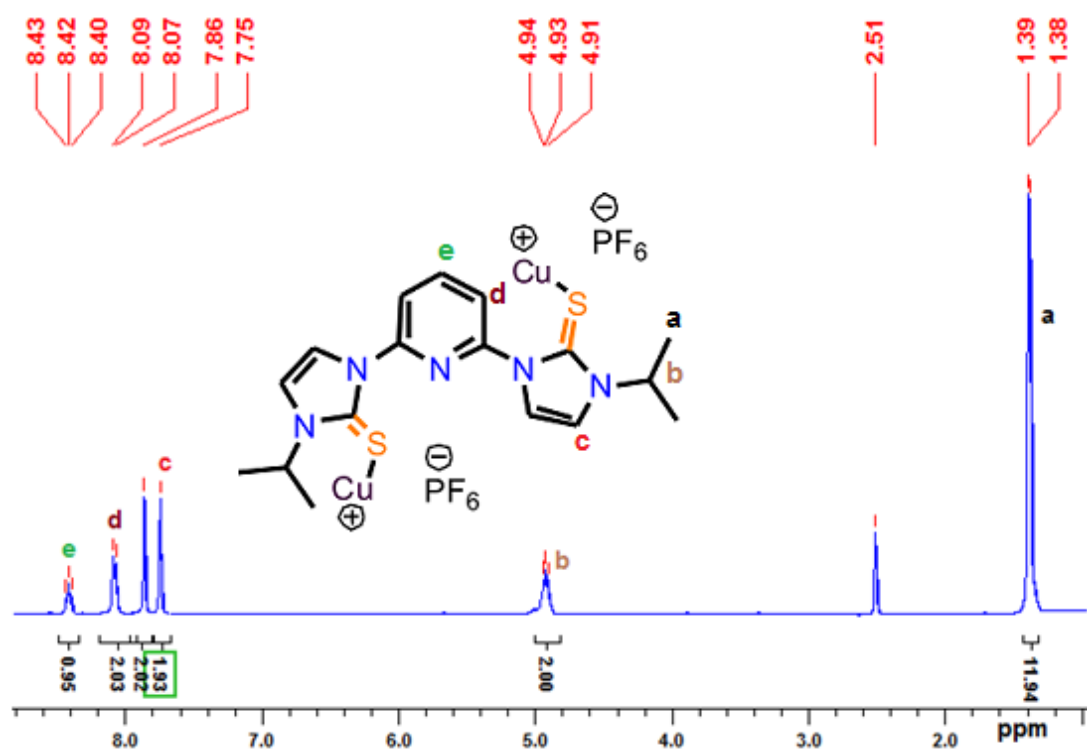


Figure 3.2: ^1H NMR spectrum of **9** in $\text{DMSO-}d_6$ at room temperature

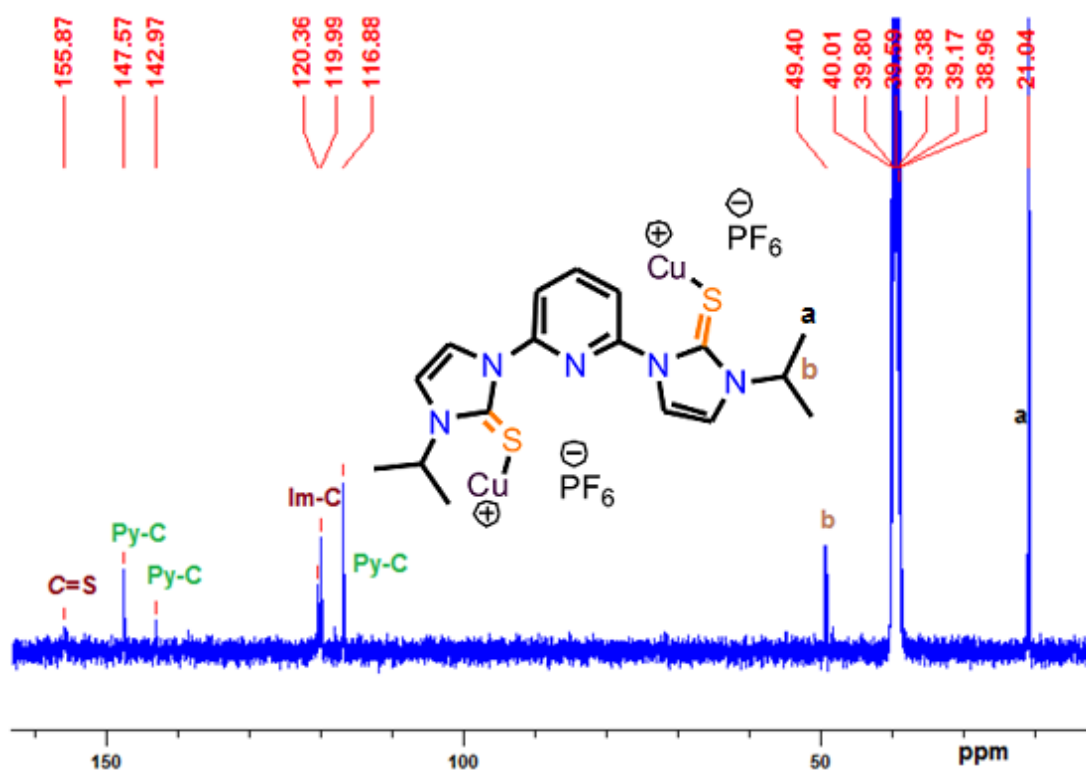


Figure 3.3: ^{13}C NMR spectrum of **9** in $\text{DMSO-}d_6$ at room temperature

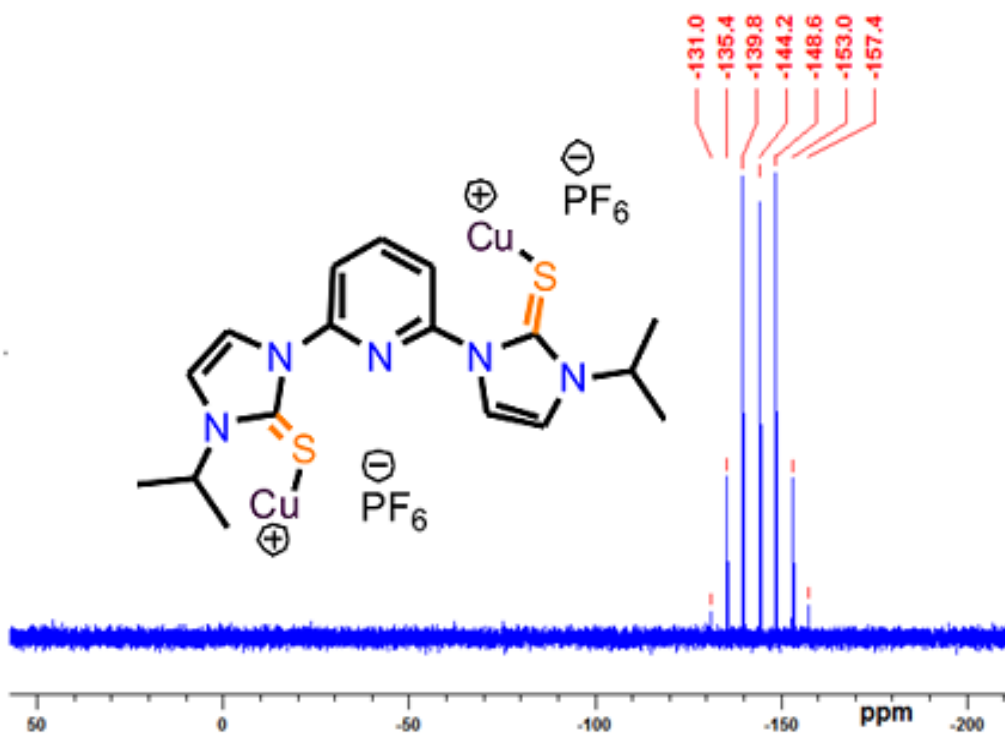


Figure 3.4: ^{31}P NMR spectrum of **9** in $\text{DMSO-}d_6$ at room temperature

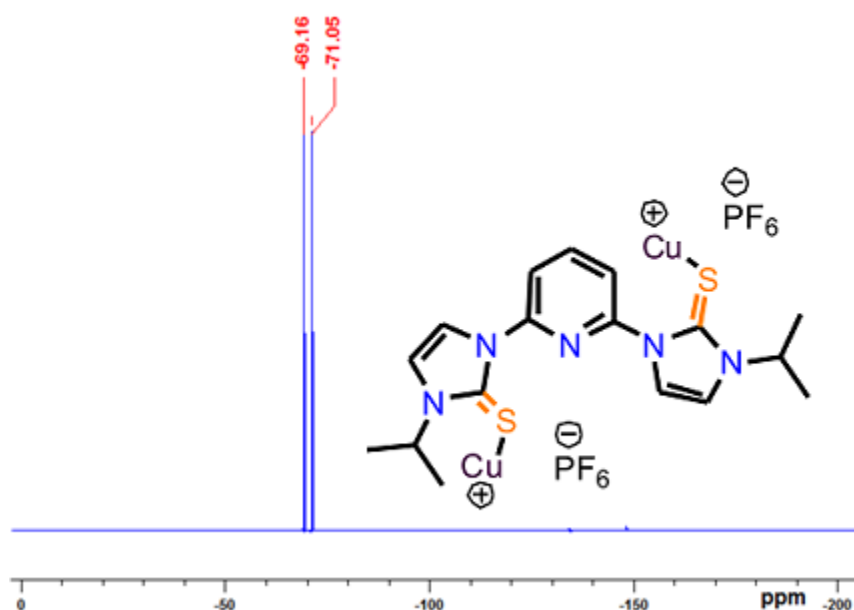


Figure 3.5: ^{19}F NMR spectrum of **9** in $\text{DMSO-}d_6$ at room temperature

The ionic salts **9** and **10** crystallized in the cubic space group, $Pn-3n$. The crystallographic data for **9** and **10** are furnished in table 3.2. The solid-state structures with selected bond lengths and bond angles are reported in figures 3.1. Liu and co-workers have reported several octanuclear copper(I) clusters using phosphorus-chalcogenide as suitable ligand, where the presence of interacting elementary ion into the center of a centrosymmetric copper cluster or cubic cage is very essential to retains the original symmetry of the cluster [14]. Notably, a tremendous efforts have been made to alter the size of the octanuclear copper core [15]. The size of the metal core can be altered based on the size and charge of anion present in the center of cage [16]. In all these aforementioned $\text{Cu}_8(\text{I})$ cubic cages, the edge length between $\text{Cu}(\text{I})\cdots\text{Cu}(\text{I})$ in octanuclear copper cubic cage ranges from 2.859 Å to 3.225 Å [16c]. Surprisingly, the known $\text{Cu}_8(\text{I})$ cubic cages were isolated only using $[(i\text{PrO})_2\text{PE}_2]^-$ ($\text{E} = \text{Se}$ or S) ligands. However it appears that the (i) similar such cages have never been reported with any other ligands; (ii) octanuclear copper cubic cages with larger than $\text{Cu}(\text{I})\cdots\text{Cu}(\text{I})$ edge length of 3.225 Å have never been isolated. Thus, the neutral donor ligand, imidazole-2-chalcogenone can be an ideal replacement for anionic ligand $[(i\text{PrO})_2\text{PSe}_2]^-$ to generate octanuclear copper(I) clusters. Though several copper(I) cubic cages have been isolated with centered atom (mainly halogen or chalcogen or hydride etc), only one copper(I) cubic cage, $[\text{Cu}_8\{\text{Se}_2\text{P}(\text{O}^i\text{Pr})_2\}_6](\text{PF}_6)_2$ has been reported without centered atom [16a], where the $\text{Cu}\cdots\text{Cu}$

separations are not equal (3.216(1) and 3.220(1) Å). **9** and **10** are the first examples of perfect copper(I) cubic cages known without non-interacting centered atom or molecule.

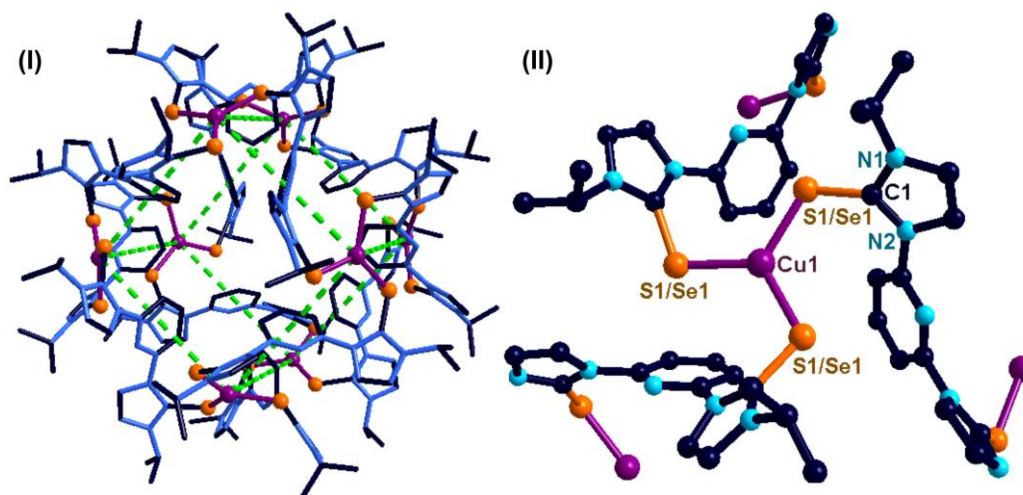


Figure 3.6: (I); The solid state structures of **9** and **10**. Hydrogen atoms and PF₆ counter anions have been omitted for the clarity. Dotted lines between copper centres are imaginary lines. (II); Coordination environment of copper(I) in **9** and **10**

Table 3.1: Selected bond lengths (Å) and angles (°) in **9** and **10**.

	9	10
C(1)–E(1)	1.700(2)	1.856(5)
E(1)–Cu(1)	2.249(6)	2.338(5)
E(1)–Cu(1)–E(1)	120.0	120.0
C(1)–E(1)–Cu(1)	112.72(8)	109.45(14)
N(1)–C(1)–N(2)	105.07(19)	105.0(4)
N(1)–C(1)–E(1)	125.17(18)	124.5(4)
N(2)–C(1)–E(1)	129.74(18)	130.4(4)

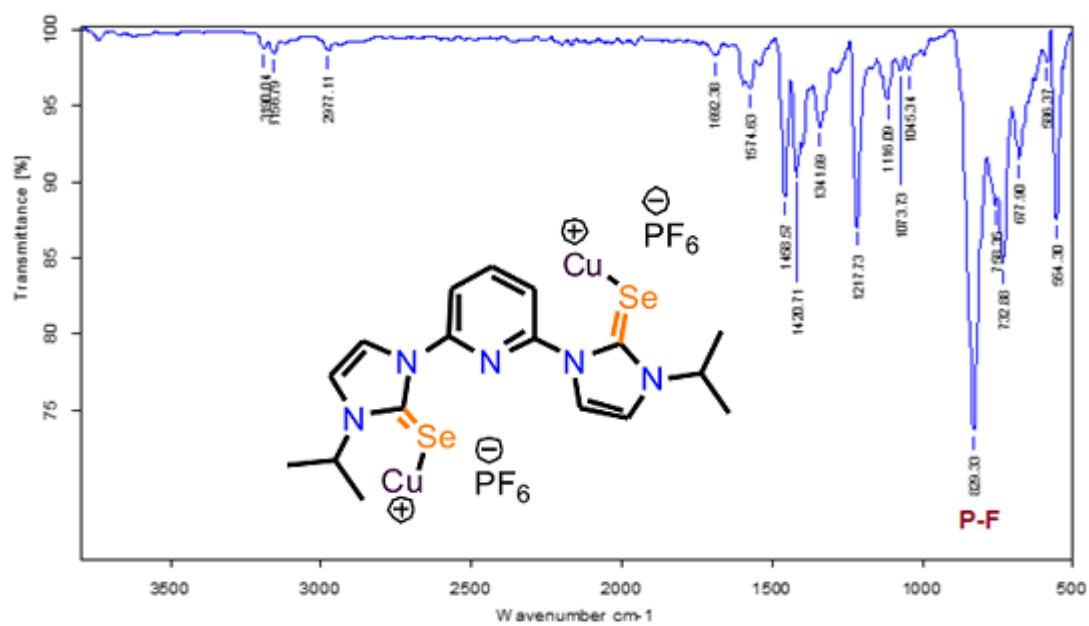


Figure 3.7: Neat FT-IR spectrum of **10** at room temperature

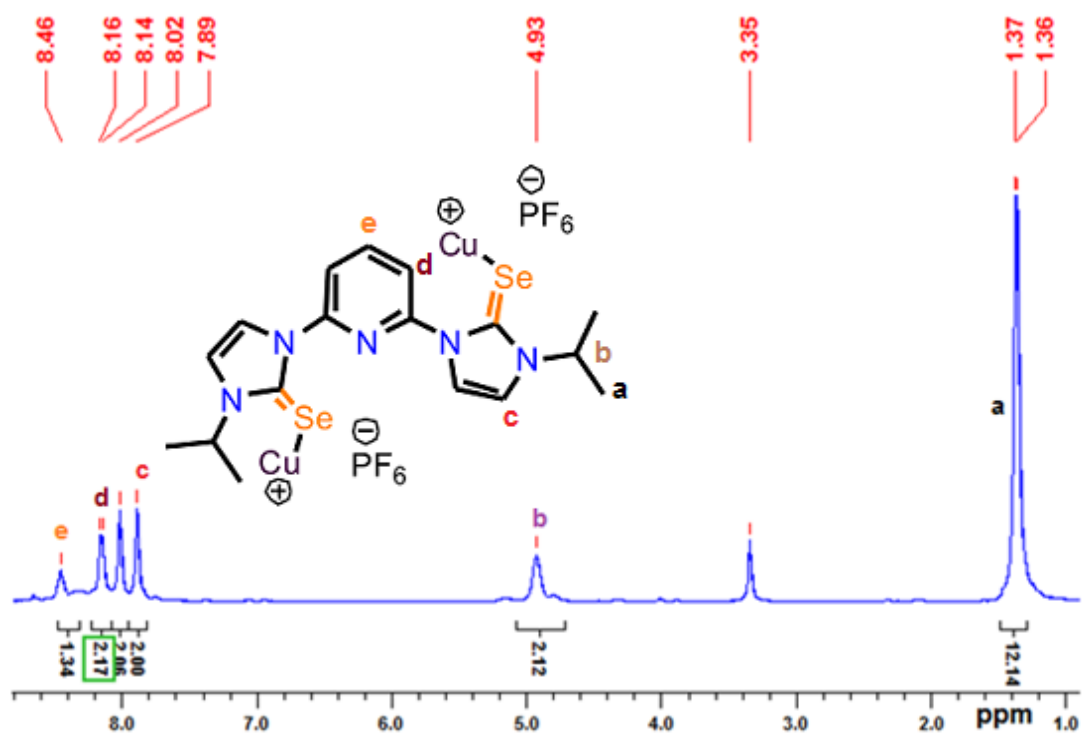


Figure 3.8: ^1H NMR spectrum of **10** in $\text{DMSO-}d_6$ at room temperature

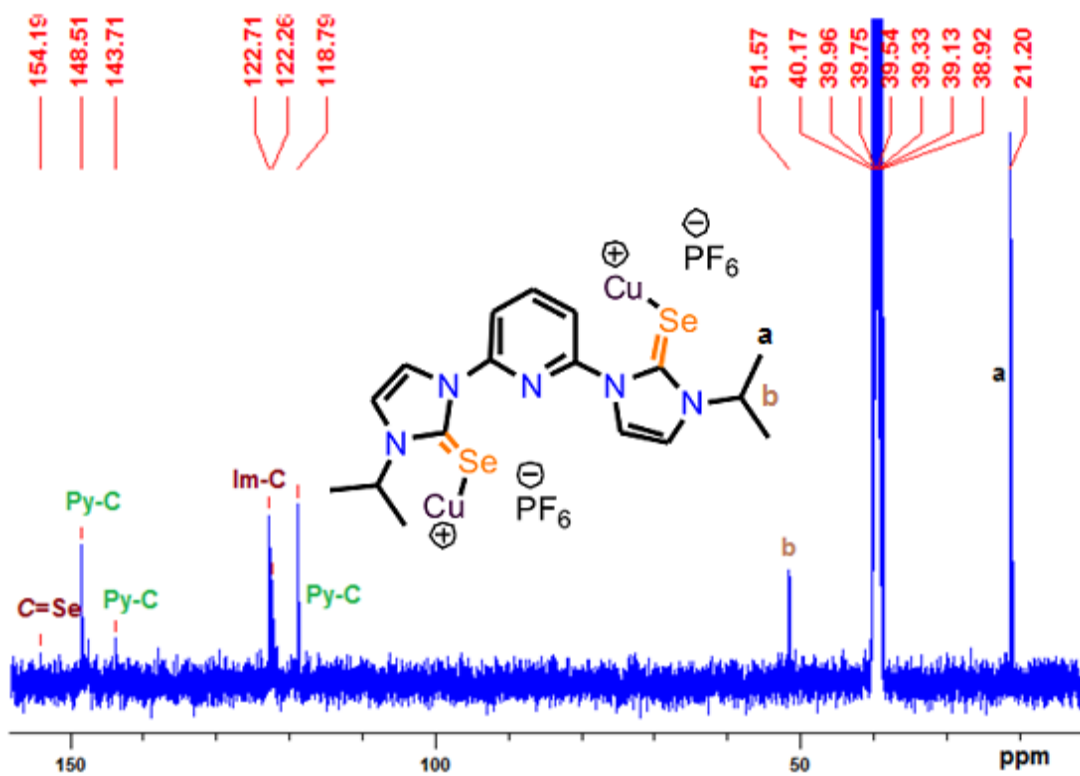


Figure 3.9: ^{13}C NMR spectrum of **10** in $\text{DMSO-}d_6$ at room temperature

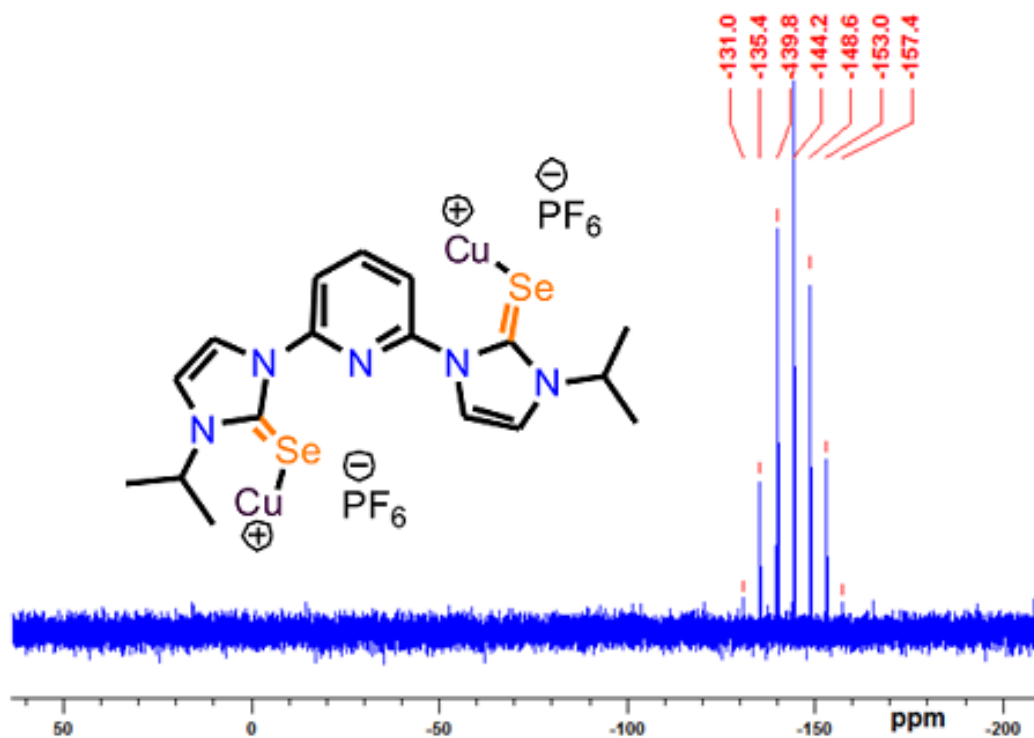


Figure 3.10: ^{31}P NMR spectrum of **10** in $\text{DMSO-}d_6$ at room temperature

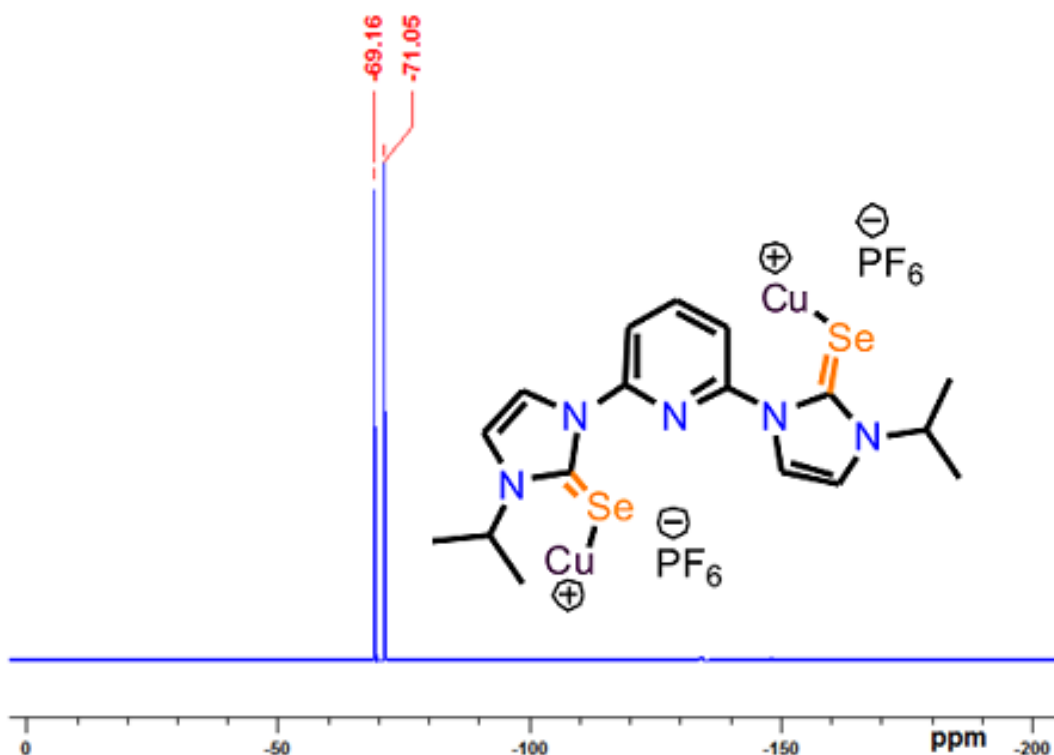


Figure 3.11: ^{19}F NMR spectrum of **10** in $\text{DMSO-}d_6$ at room temperature

The faces of the cubanes **9** and **10** are open. Notably, the distance between copper atoms in **9** (8.413 Å) and **10** (8.593 Å) are equal. The diagonal distance between $\text{Cu}\cdots\text{Cu}$ is 14.571 Å (for **9**) and 14.883 Å (for **10**). The $\text{Cu}\cdots\text{Cu}$ diagonal distance found in **9** and **10** are nearly 50% shorter than the diagonal $\text{Fe}\cdots\text{Fe}$ distance found in the large $\text{Fe}^{\text{II}}/\text{Ni}^{\text{II}}$ face capped cubic box (25.622 Å) [17]. The solid-state structures of complexes **9** and **10** consists of one cubic $[\text{Cu}_8(\text{Bptp}/\text{Bpsp})_{12}]^{8+}$ cation and eight $[\text{PF}_6]^-$ anions, in which each copper center is linked by three ligands. The E–Cu–E bond angles around copper centers in **9** and **10** are in favour of trigonal planar arrangement.

The carbon–sulfur bond lengths in **9** is 1.700(2) Å, which is closer to that of (C=S, 1.61 Å) double bond [18a] than a single bond distance (C–S, 1.83 Å) [18b]. The carbon–selenium bond length in **10** is 1.856(5) Å, which is closer to that of a C–Se single bond distance (1.94 Å) [19a] than a C=Se double bond distance (1.74 Å) [19b]. The S–Cu distance (2.249 (6) Å) in complex **9** is slightly shorter than that of dichloro- $[(\eta^3\text{-S,S,N})(2,6\text{-bis}\{[\text{N-isopropyl}]\text{imidazole-1-ylidene-2-thione}\})\text{-pyridine copper(II)}]$ (2.30–2.32 Å) [20]. The Se–Cu bond length (2.338(5) Å) found in **10** is slightly elongated than that of $[(\text{IPr}=\text{Se})_2\text{Cu}]\text{X}$ and $[(\text{IMes}=\text{Se})_2\text{Cu}]\text{X}$ (Where X = BF_4 and ClO_4) (2.24–2.27 Å) [8c].

Table 3.2: Structural parameters of compounds **9** and **10**.

	9	10
Empirical formula	C ₇₂ H ₈₈ N ₂₄ F ₄₈ P ₈ S ₂₄ Cu ₈	C ₇₂ H ₈₈ N ₂₄ F ₂₄ P ₁₆ Cu ₈ Se ₁₆
Formula weight	5837.38	6817.85
Temperature (K)	298	298
Crystal system	Cubic	Cubic
Space group	<i>Pn-3n</i>	<i>Pn-3n</i>
<i>a</i> /Å	24.4090(3)	24.82051(14)
<i>b</i> /Å	24.4090(3)	24.82051(14)
<i>c</i> /Å	24.4090(3)	24.82051(14)
α /°	90	90
β /°	90	90
γ /°	90	90
Volume (Å ³)	14542.9(3)	15290.87(15)
<i>Z</i>	2	2
ρ_{calc} /mg mm ⁻³	1.3329	14807
Absorption coefficient (μ /mm ⁻¹)	3.301	4.785
<i>F</i> (000)	5995.9	6666.0
Reflections collected	10421	12189
<i>R</i> _{int}	0.0266	0.0288
GOF on <i>F</i> ²	1.005	1.011
<i>R</i> ₁ (<i>I</i> >2 σ (<i>I</i>))	0.0410	0.0359
w <i>R</i> ₂ (<i>I</i> >2 σ (<i>I</i>))	0.1338	0.0893
<i>R</i> ₁ values (all data)	0.0496	0.0478
<i>R</i> ₂ values (all data)	0.1432	0.0979

3.4. PXRD and Thermogravimetric analysis

The PXRD pattern of bulk samples of **9** and **10** are nearly comparable with calculated PXRD pattern of corresponding single crystal data (Figure 3.12), which clearly supports the phase purity of bulk samples of **9** and **10**.

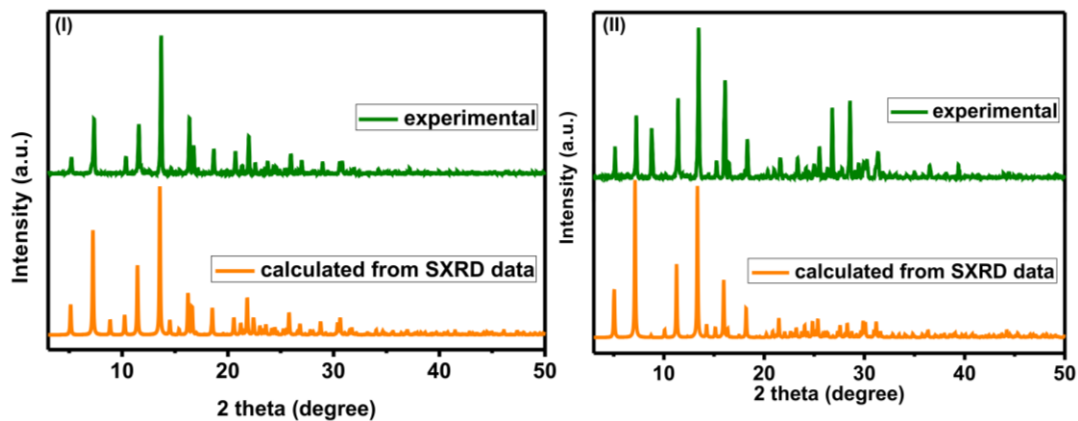


Figure 3.12: (I); Experimental powder X-ray diffraction pattern (A) of **9** vs simulated powder pattern (B) for **9**. (II); Experimental powder X-ray diffraction pattern (A) of **10** vs simulated powder pattern (B) for **10**

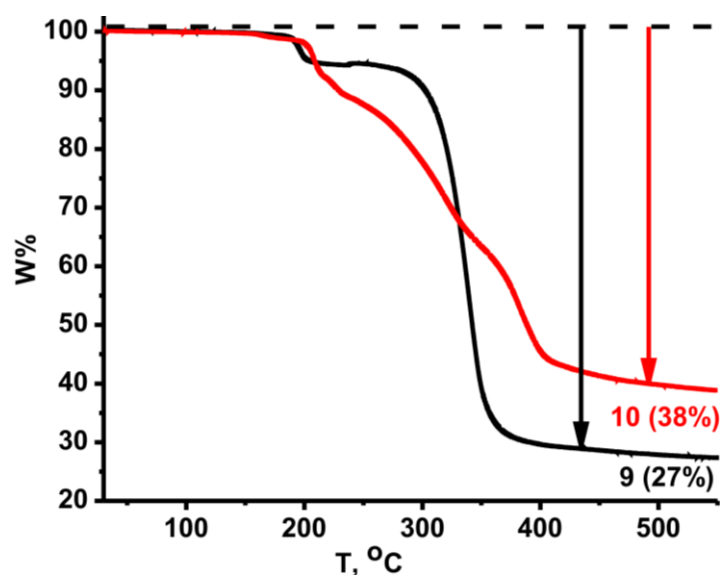


Figure 3.13: TGA curves of **9** and **10** from 30 to 550 °C under a nitrogen atmosphere with a heating rate of 10 °C min⁻¹. For **9**: residual wt 26%, calc. wt 23%; For **10**: residual wt 39%, calc. wt 40%

Moreover, the thermal stability of **9** and **10** is not comparable (Figure 3.13). The thermal decomposition pathway of **9** is much clearer than **10**. **9** and **10** depicted enough stability until 200 °C. Then compound **9** shows a little weight loss (5%), which can be attributed to the

phase change in **9**. Subsequently **9** shows enough stability until 305 °C then observed a sudden weight loss in a single step to give Cu₂S residue (26%, Calcd. 23%), which can be attributed to the decomposition of organic moieties in **9**. Besides, **10** depicts gradual weight loss from its melting point (210 °C) through minor phase transformations along with the organic moieties decomposition to yield Cu₃Se₂ residue (39%, Calcd. 40%).

3.5. UV-visible absorption studies

The solution state and solid state UV-visible absorption spectra of **9** and **10** are compared with Bptp and Bpsp, respectively (Figure 3.14). Almost similar absorption patterns for $\pi \rightarrow \pi^*$ (200-300 nm) and $n \rightarrow \pi^*$ (300–350 nm) transitions are observed in the solution state UV-vis spectroscopy for both the ligands and their copper(I) complexes (**9** and **10**). Bathochromic shift was noticed for Bpsp and **10** compared to Bptp and **9**. Interestingly, in the solid state UV-vis study, complexes **9** and **10** depicted the bathochromic shift along with broadening of absorption band due to a strong molecular association in solid state form compared to their solution state study.

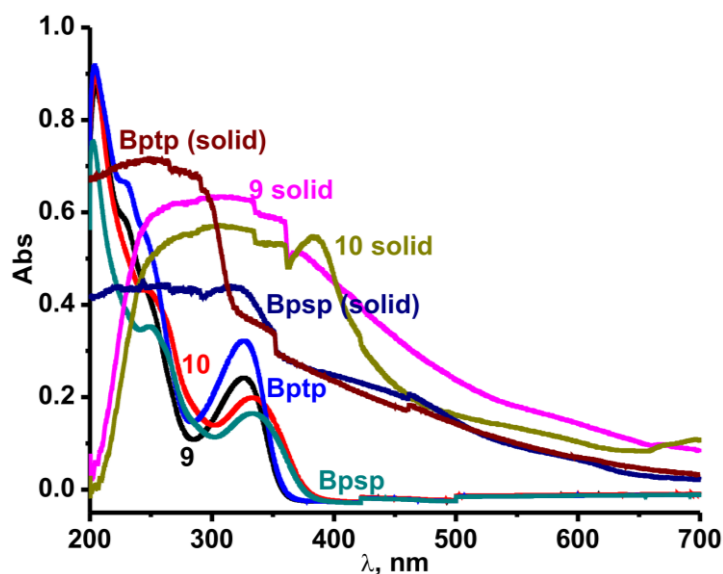


Figure 3.14: UV-vis spectra of Bptp, Bpsp, **9** and **10** (Solution state in acetonitrile at 25 °C, 2.8×10^{-5} M)

3.6. Miscellaneous investigations

Considering the size of these cages, **9** was subjected to BET analysis. The maximum quantity adsorbed at STP is $1.45 \text{ cm}^3/\text{g}$, which is not very impressive. However, the molecule was subjected to trans-metallation, host-guest interactions with pyrene, perylene and fullerene and the obtained results have been presented below.

3.6.1. Trans-metallation reaction with molecule **9**.

Besides, the attempts to transmetallate copper in **9** by gold using $(\text{dms})\text{AuCl}$ were unproductive (Figure 3.15). Both **9** and **10** undergoes dissociation to result the starting materials by depositing gold metal on the surface of the flask.

The compound **9** and $(\text{dms})\text{AuCl}$ were dissolved completely in acetonitrile and was colorless in the beginning, after 10 minutes the reaction mixture turns violet in color and then after 30 minutes the reaction mixture contains blue precipitate in a colorless solution. After which the reaction mixture was dried in *vacuo* and subjected to NMR measurements. The ^1H NMR measurement supports the presence of ligand (Btp) moiety in the crude product of trans-metallation reaction (Figure 3.16).

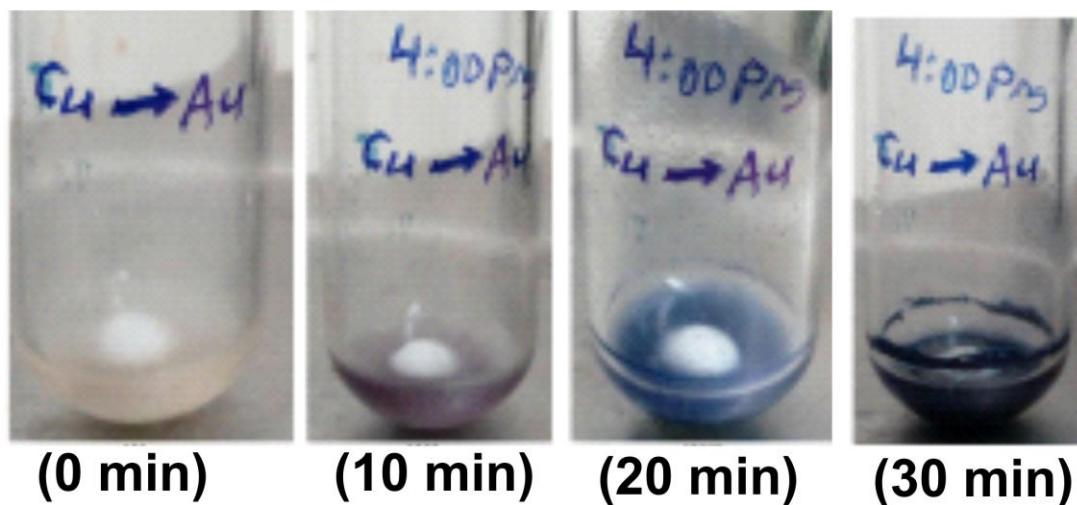


Figure 3.15: Reaction progress during trans-metallation reaction

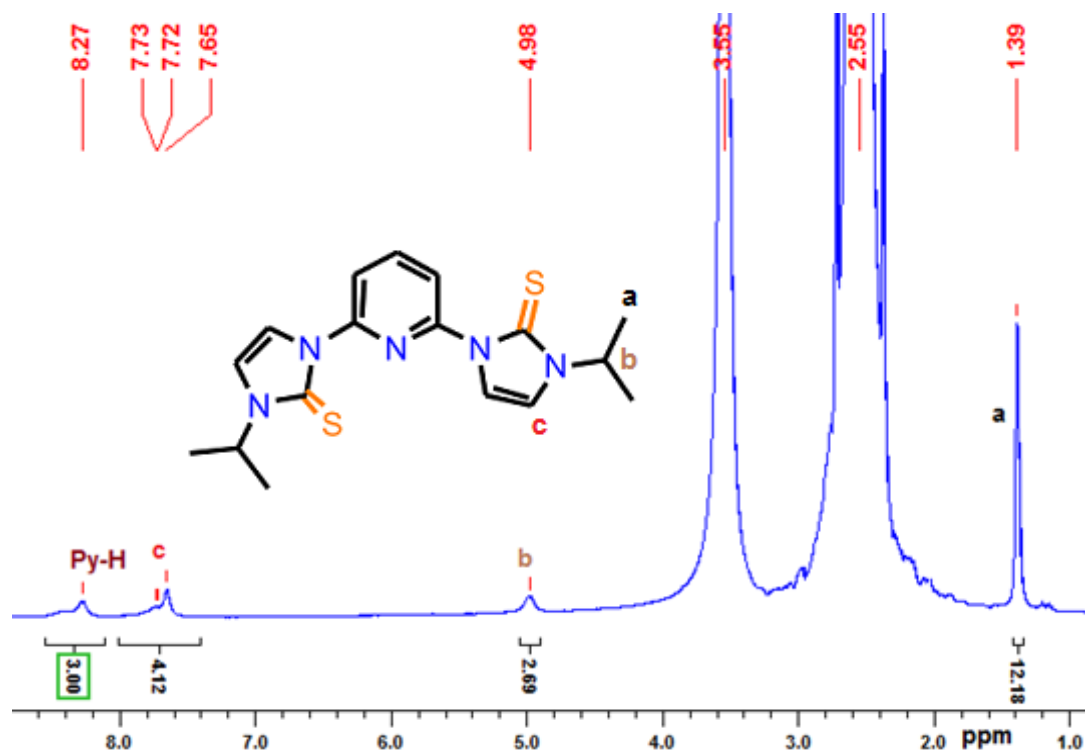
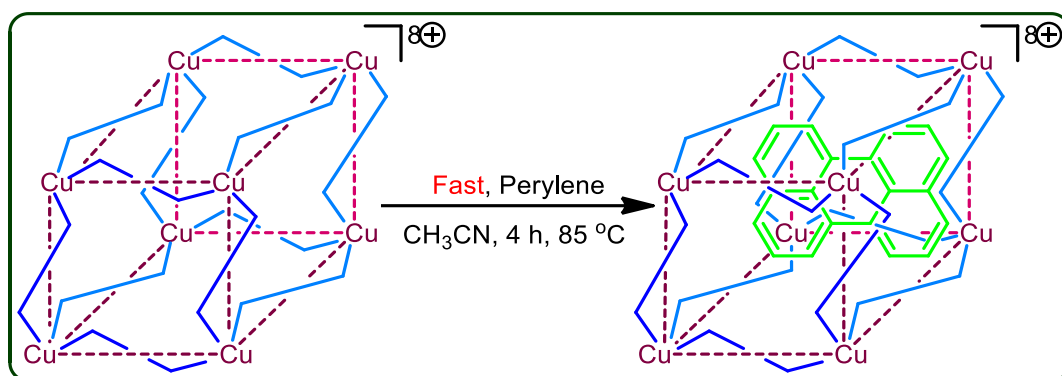


Figure 3.16: ¹H NMR spectrum of trans-metallation reaction mixture in DMSO-d₆ at room temperature

In order to understand the host-guest property of these cages, the preliminary studies were carried out between **9** and pyrene or perylene (Scheme 3.2-3.3). **9** act as a host for both perylene and pyrene to result **9**@perylene (Figure 3.17-3.19) and **9**@pyrene (Figure 3.20-3.22), respectively. Notably the perylene uptake by **9** is much faster than pyrene. Attempt to introduce C₆₀ into **9** was not successful (Figure 3.23).

3.6.2. Host-Guest interactions on molecule **9** with perylene.

The compound **9** and perylene were not dissolved completely in acetonitrile and has a yellow turbid solution in the beginning and was allowed to stir at 85 °C, the reaction mixture forms a yellow crystalline solid in a clear colorless solution after 4 h, and then the reaction mixture was dried in vacuo and subjected to spectroscopic measurements, which evidently displays the existence of **9**@perylene molecule.



Scheme 3.2: Synthesis of **9@Perylene** molecule by host-guest interactions

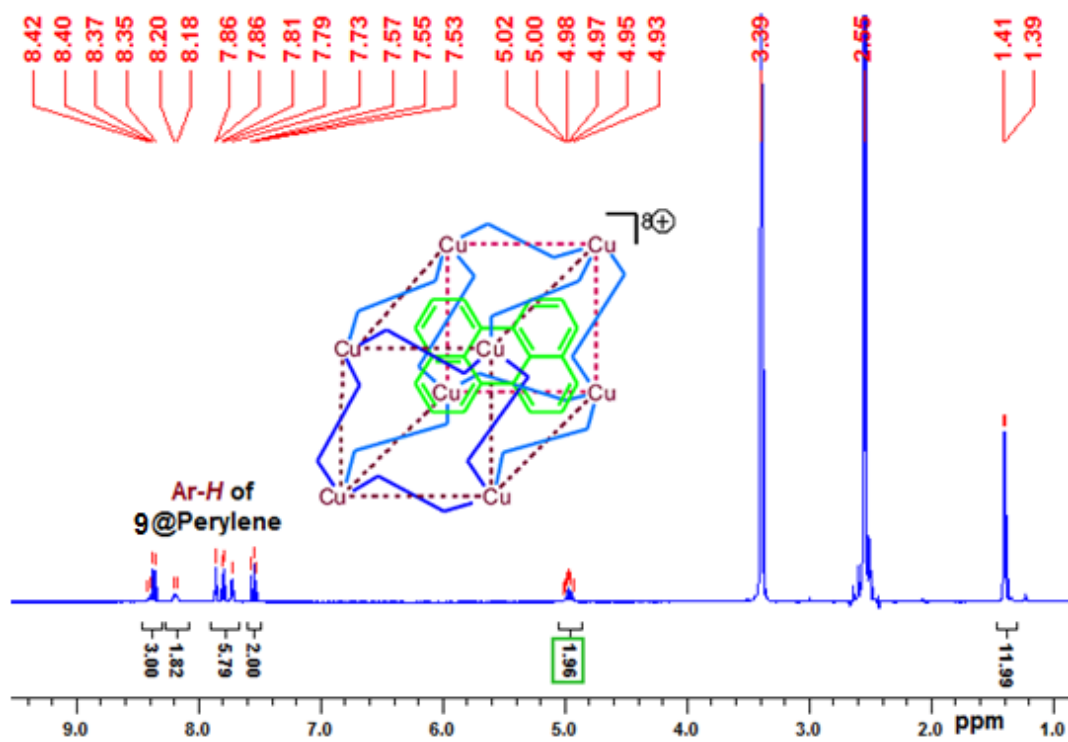


Figure 3.17: ¹H NMR spectrum of **9@perylene** in DMSO-*d*₆ at room temperature

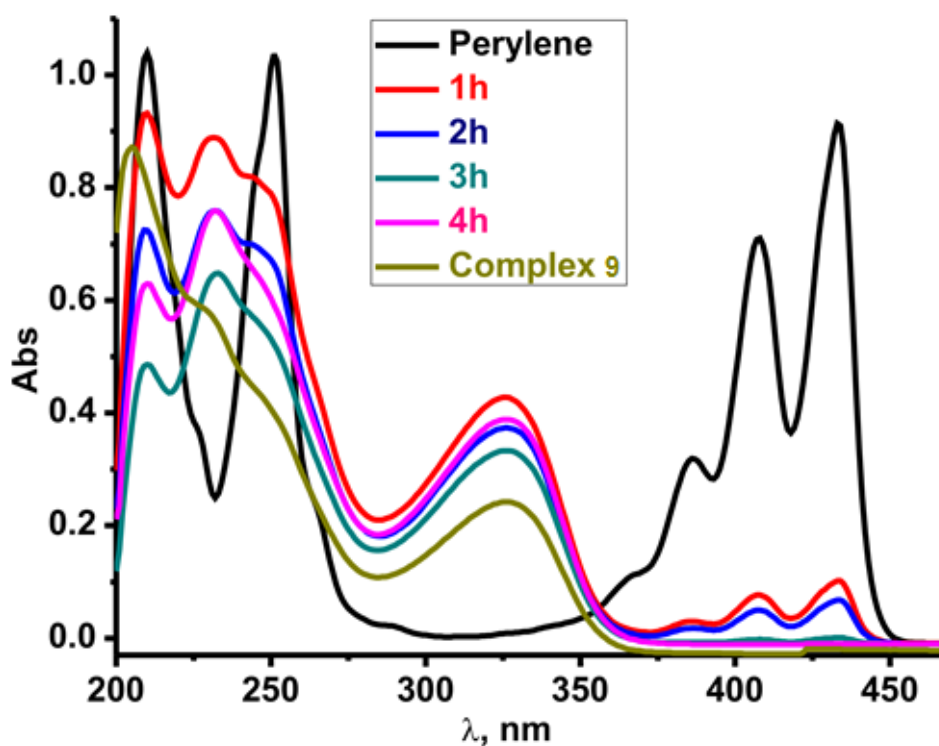


Figure 3.18: Solution state UV-visible spectral analysis of **9** and the reaction mixture of **9**@perylene in acetonitrile at elevated temperature with 1 h interval, measured at 298K with 2.8×10^{-5} M acetonitrile solution

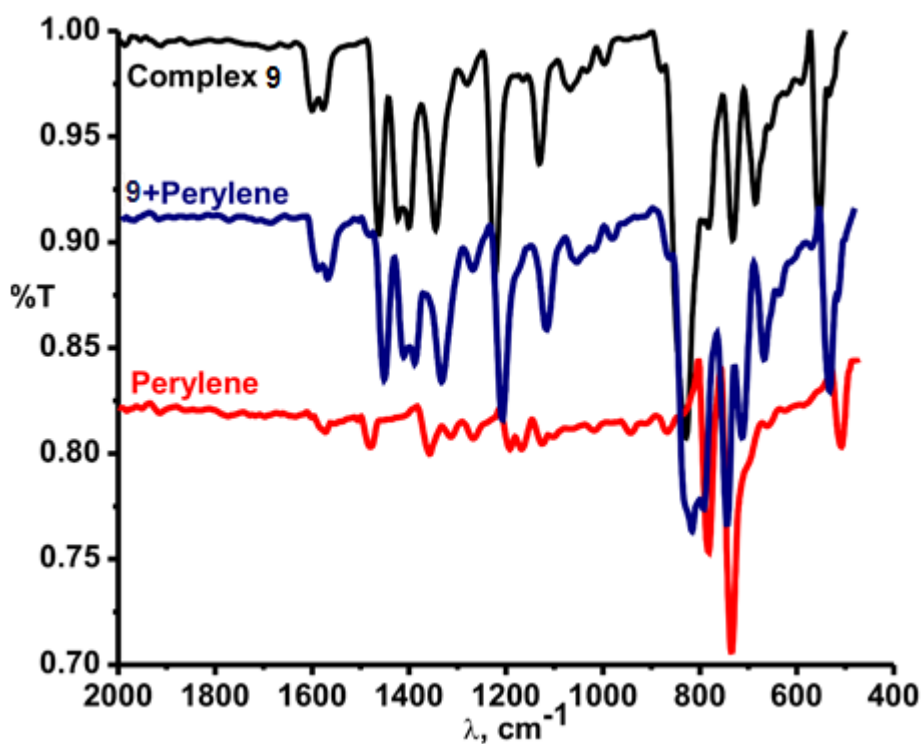
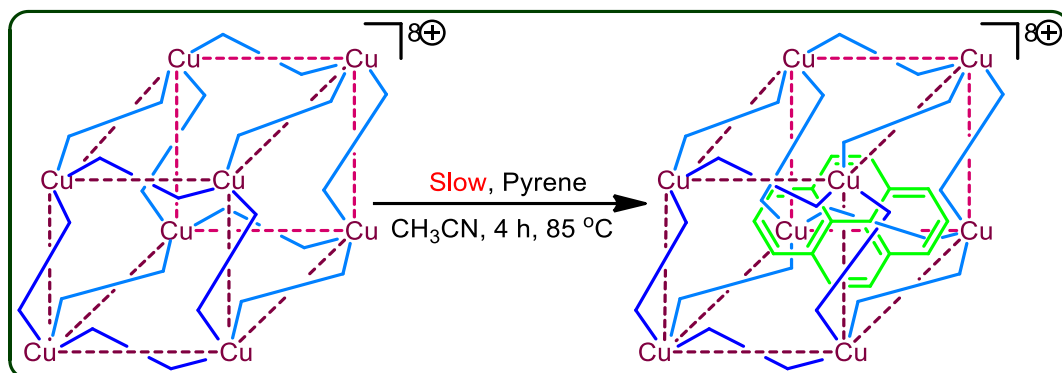


Figure 3.19: Neat FT-IR spectrum of **9** (Black), a reaction mixture of **9** and perylene (Blue) and perylene (Red) after 4 h in acetonitrile

3.6.3. Host-Guest interactions on Molecule 9 with Pyrene.

The compound **9** and pyrene were not dissolved completely in acetonitrile and was a little yellow turbid solution in the beginning, after 10 minutes at 85 °C, the reaction mixture turns as clear yellow solution after 4 h, and the reaction mixture was dried in vacuo and subjected to spectroscopic measurements, which clearly shows the existence of **9**@pyrene molecule.



Scheme 3.3: Synthesis of **9**@Pyrene molecule by host-guest interactions

As presented in Figure 3.21, the reaction mixture represents only pyrene absorption spectra in solution UV-vis spectroscopy up to 2 h, while broadening of the absorption bands noticed after 3 h is due to the association of pyrene with molecule **9**, and the final (4 h) absorption spectra of the reaction mixture is fairly altered from the molecule **9** alone, suggesting the complete incorporation/association of pyrene into the molecule **9**.

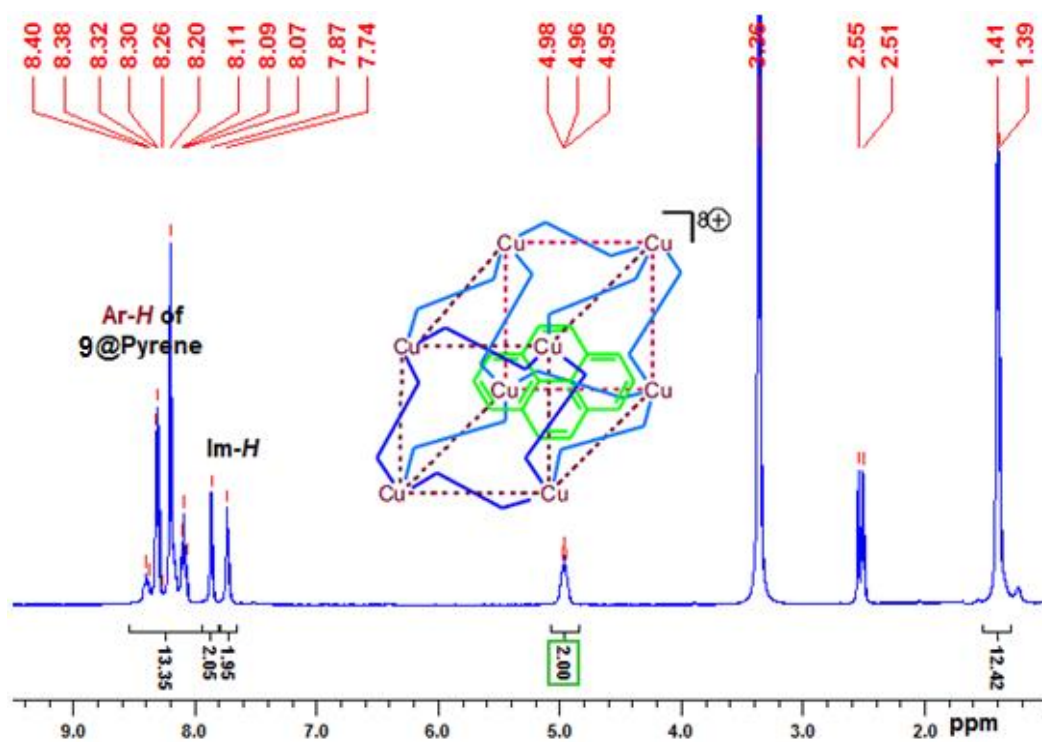


Figure 3.20: ^1H NMR spectrum of **9@pyrene** in $\text{DMSO-}d_6$ at RT

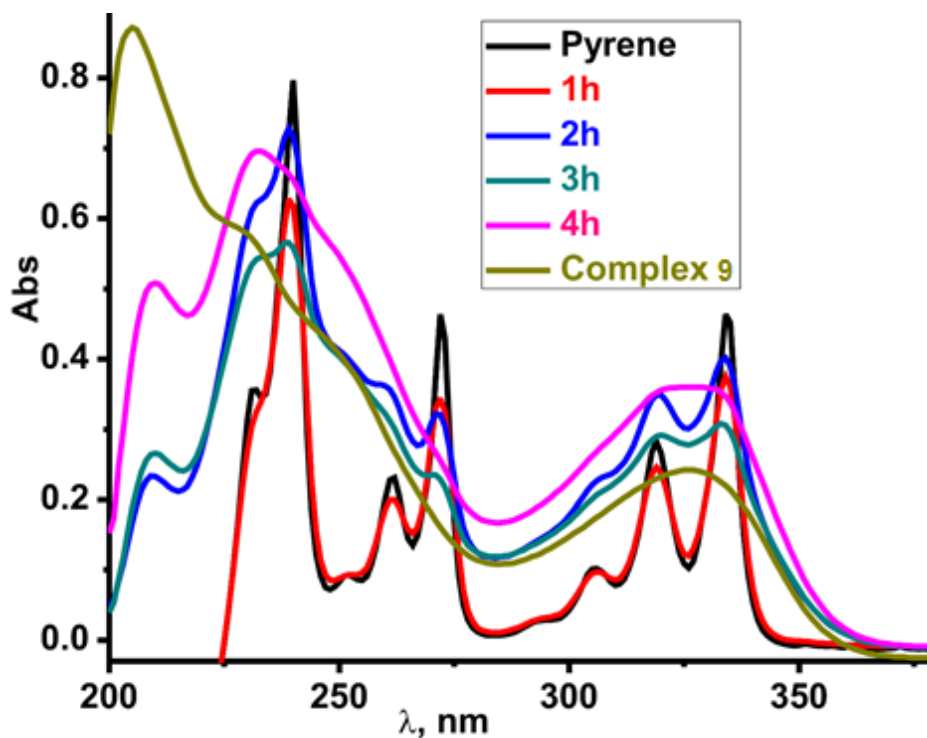


Figure 3.21: Solution state UV-visible spectral analysis of **9** and the reaction mixture of **9** and pyrene in acetonitrile at elevated temperature with 1 h interval, measured at 298K with 2.8×10^{-5} M acetonitrile solution

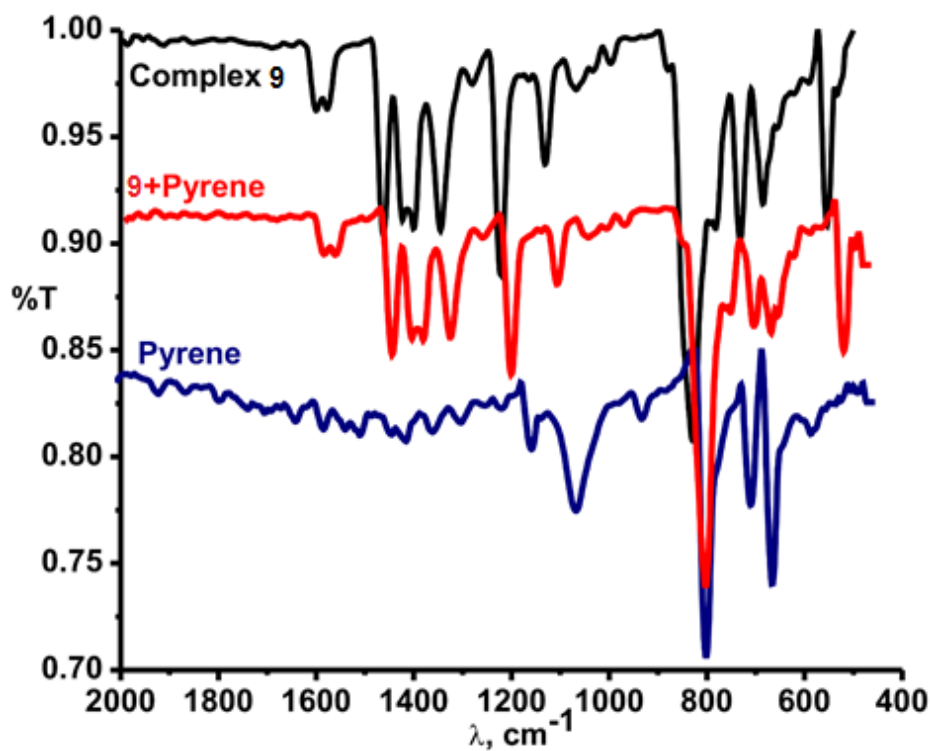


Figure 3.22: Neat FT-IR spectrum of **9** (Black), a reaction mixture of **9** and pyrene (Red) and pyrene (Blue) after 4 h in acetonitrile

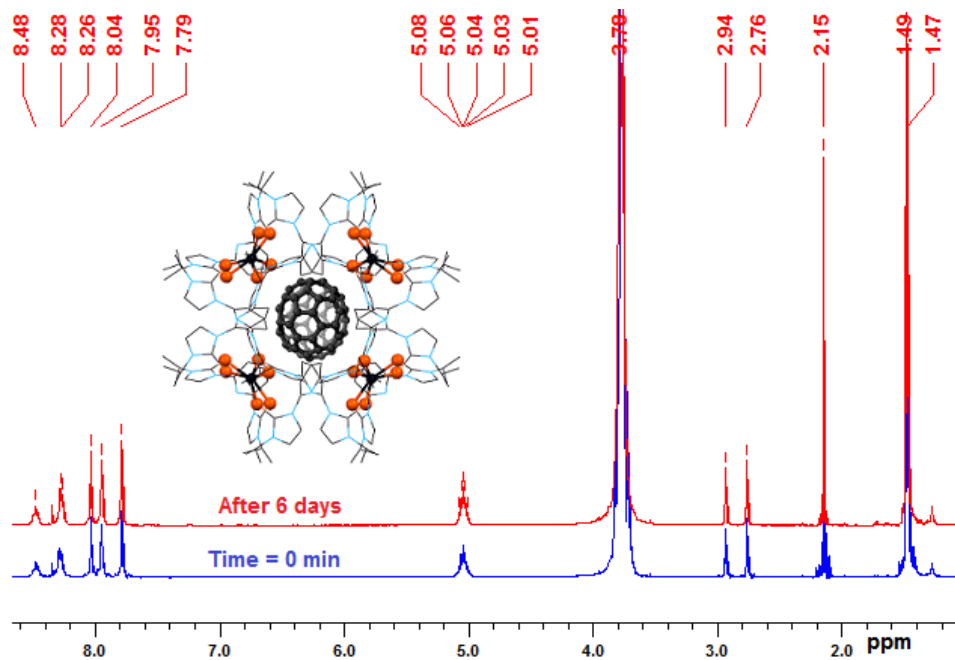
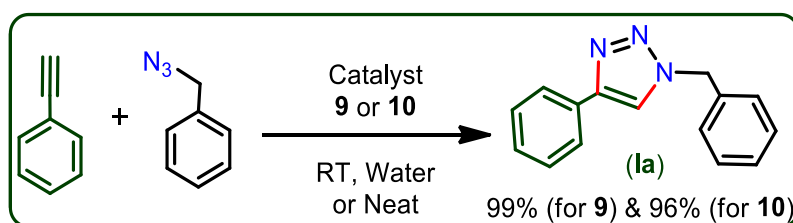


Figure 3.23: ^1H NMR comparison of molecule **9**@ C_{60} host-guest interactions in $\text{DMF-}d_7$ at RT

Molecule **9** (0.014g, 1 equiv) and C₆₀ (0.02g, 1 equiv) were mixed together under argon flow in an NMR tube and was dissolved in DMF-*d*₇ (0.5 mL), then it was subjected to NMR measurement at time 0 minutes. After which it was allowed to stay at 85 °C and then ¹H NMR was measured every day to investigate the incorporation/association of C₆₀ into the cavity of molecule **9**. ¹H NMR (DMF-*d*₇, 400 MHz): 1.47-1.49 (d, 2((CH₃)₂CH), 12H), 5.01-5.08 (m, 2(CH₃)₂CH, 2H), 7.78-7.79 (d, imidazole, 2H), 7.95 (d, imidazole, 2H), 8.27-8.29 (m, pyridine, 2H), 8.46-8.50 (m, pyridine, 1H) ppm.

3.7. Catalytic Investigations

Subsequently, **9** and **10** were employed for azide-alkyne cycloaddition reactions to produce 1,2,3-triazoles under mild conditions (Scheme 3.4, Table 3.3). Though, the catalytic reactions were promising both in water medium (entry 1) and under neat conditions (entry 2), less reaction time was noticed for the solvent free reaction over the water media reaction.



Scheme 3.4: Catalysts **9** and **10** mediated one-pot synthesis of triazoles

Table 3.3: Optimization studies for CuAAC reaction mediated by Copper(I) catalysts **9** and **10**.^a

Entry	Catalyst	Cat. (mol%)	Solvent	Time (min)	Yield (%) ^b
1	9	1	water	30	>99
2	9	1	neat	15	>99
3	9	0.5	neat	60	98
4	9	0.1	neat	180	94
5	9	2	neat	15	>99
6	10	1	neat	20	>99
7	[Cu(CH ₃ CN) ₄]PF ₆	1	neat	60	45

^aReaction conditions: phenyl acetylene (0.6 mmol), benzyl azide (0.5 mmol) and solvent (2 mL). ^bIsolated yield

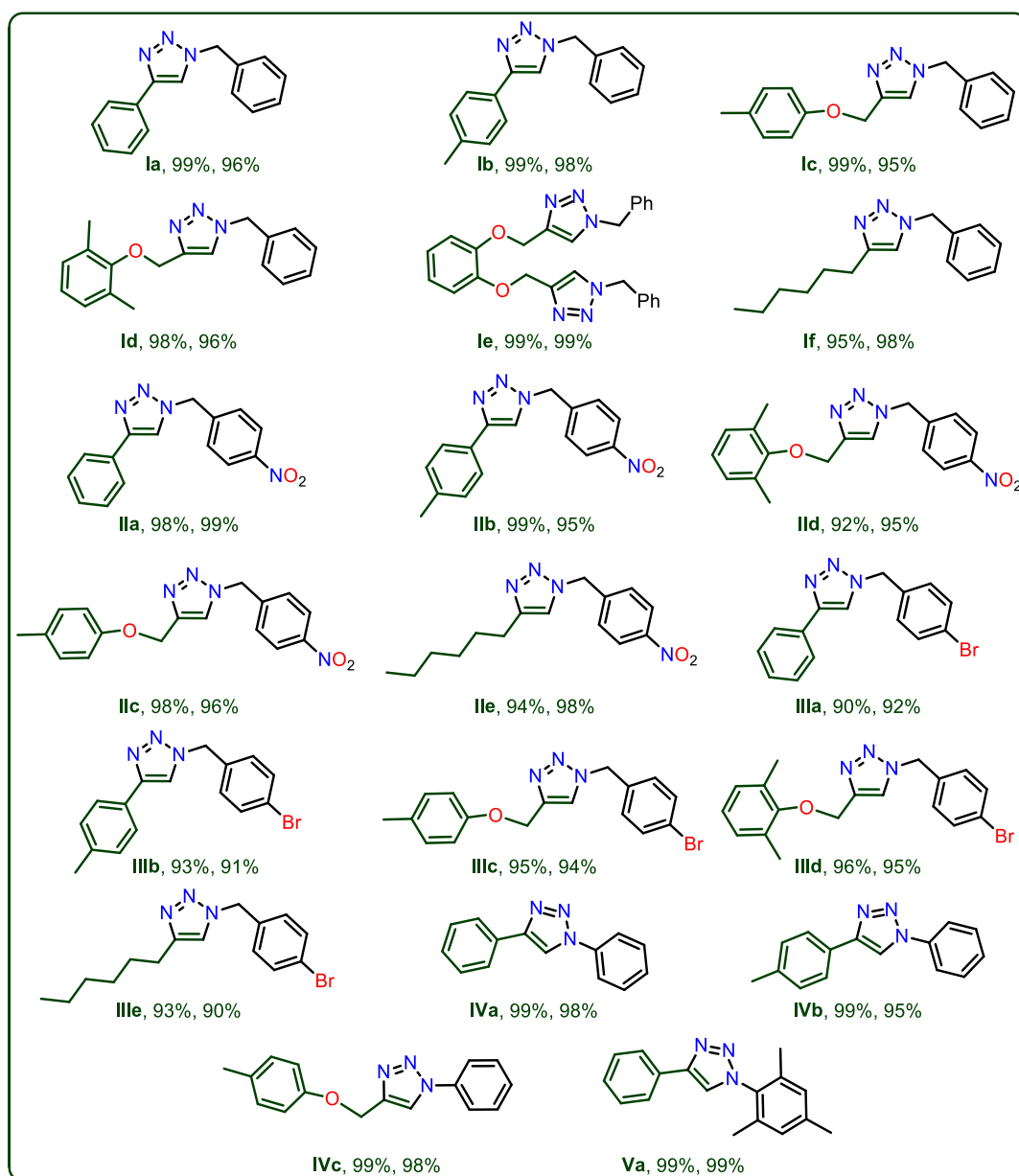


Chart 3.1: ^aReaction conditions: alkyne (1.2 mmol), azide (1 mmol), Catalyst **9** and/or **10** (1 mol%), neat, isolated yield

Besides, the yield of **Ia** was decreased, when the catalyst mol% was decreased (for 0.5 mol%, see entry 3 and for 0.1 mol%, see entry 4). However, the extension of time led to the isolation of quantitative yield of **Ia**. On the other hand, not much improvement in the yield was observed by reducing the time or increasing catalyst loading (2 mol%, entry 5). Notably, catalyst **10** requires little longer time than the catalyst **9** (entry 6). In addition, less amount of product formation (**Ia**) was observed under solvent free conditions using only $[\text{Cu}(\text{CH}_3\text{CN})_4](\text{PF}_6)$ (entry 7). Further, we have explored the scope of the reactions using

benzyl azide, 4-nitrobenzylazide, 4-bromobenzylazide, phenylazide and 2,4,6-trimethyl phenylazide with a varieties of terminal alkynes using 1 mol% of **9** and/or **10** as catalysts under solvent free conditions. The yield of the product was excellent (>95%, Chart 3.1).

The isolated products were characterized by ^1H and ^{13}C NMR spectroscopy. The solid state structures of isolated products **Ia**, **Ib**, **IIa**, and **IIb** were additionally evaluated by single crystal X-ray diffraction analysis (Figure 3.24).

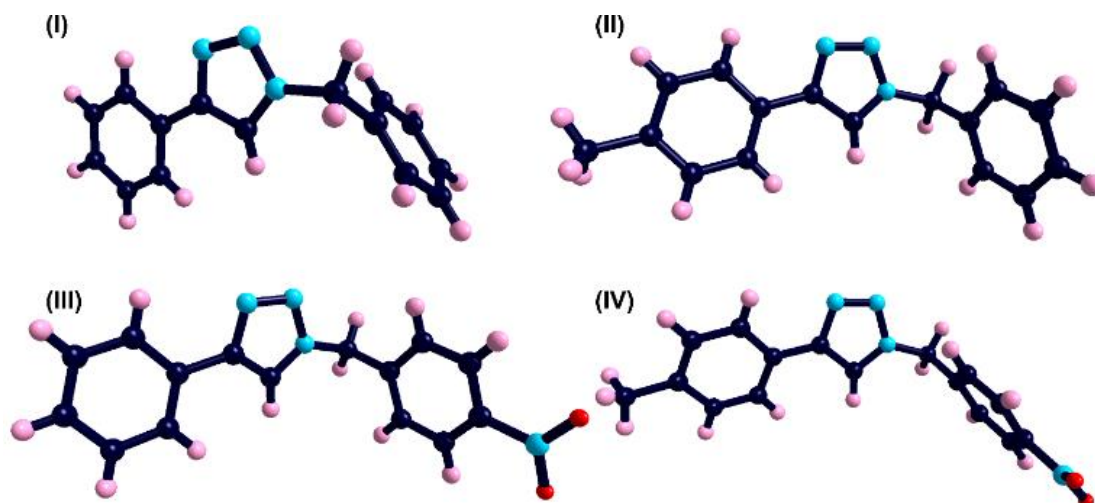


Figure 3.24: (I) The solid state structure of **Ia**. (II) The solid state structure of **Ib**. (III) The solid state structure of **IIa**. (IV) The solid state structure of **IIb**. Atom Colours: Dark Blue; Carbon, Sky Blue; Nitrogen, Red; Oxygen and Rose; Hydrogen

Table 3.4: Structural parameters of compounds **Ia**, **Ib**, **IIa** and **IIb**.

	Ia	Ib	IIa	IIb
Empirical formula	C ₁₅ H ₁₃ N ₃	C ₁₆ H ₁₄ N ₃	C ₁₅ H ₁₂ N ₄ O ₂	C ₁₆ H ₁₄ N ₄ O ₂
Formula weight	235.29	249.32	280.29	294.32
Temperature (K)	298	298	298	298
Crystal system	Monoclinic	Monoclinic	Orthorhombic	Monoclinic
Space group	<i>P2₁/c</i>	<i>P2₁</i>	<i>P2₁2₁2₁</i>	<i>P2₁/c</i>
<i>a</i> /Å	6.0383(13)	8.0688(12)	5.7169(7)	9.5421(9)
<i>b</i> /Å	8.0923(17)	5.8237(6)	13.9426(17)	5.7049(4)
<i>c</i> /Å	25.709(8)	14.4259(17)	17.101(3)	27.128(3)
α /°	90	90	90	90
β /°	93.516(19)	100.683(13)	90	98.745(10)
γ /°	90	90	90	90
Volume (Å ³)	1253.9(5)	666.13(15)	1363.1(3)	1459.6(2)
<i>Z</i>	4	2	4	4
$\rho_{\text{calc}}/\text{mg mm}^{-3}$	1.2463	1.2429	1.3657	1.3392
Absorption coefficient (μ/mm^{-1})	0.076	0.076	0.095	0.092
<i>F</i> (000)	496.2	264.1	584.3	616.3
Reflections collected	10726	2967	3974	6410
<i>R</i> _{int}	0.0743	0.0457	0.0430	0.0333
GOF on <i>F</i> ²	1.040	1.035	1.066	1.069
<i>R</i> ₁ (<i>I</i> > 2 σ (<i>I</i>))	0.0688	0.0736	0.0884	0.0688
w <i>R</i> ₂ (<i>I</i> > 2 σ (<i>I</i>))	0.1682	0.1638	0.2247	0.1538
<i>R</i> ₁ values (all data)	0.1497	0.1494	0.1699	0.1375
<i>R</i> ₂ values (all data)	0.2335	0.2281	0.2989	0.1999

In addition to this the catalysts longevity has been investigated using 1 mol% of catalyst **9** with benzyl azide and phenyl acetylene in neat conditions at room temperature and it was found that the same catalyst can produce appreciable yields for eight successive cycles (Figure 5.26). Moreover, PXRD studies on reused catalyst revealed that the catalyst exists as an intact octa-nuclear cage rather than dissociated molecules (Figure 3.25).

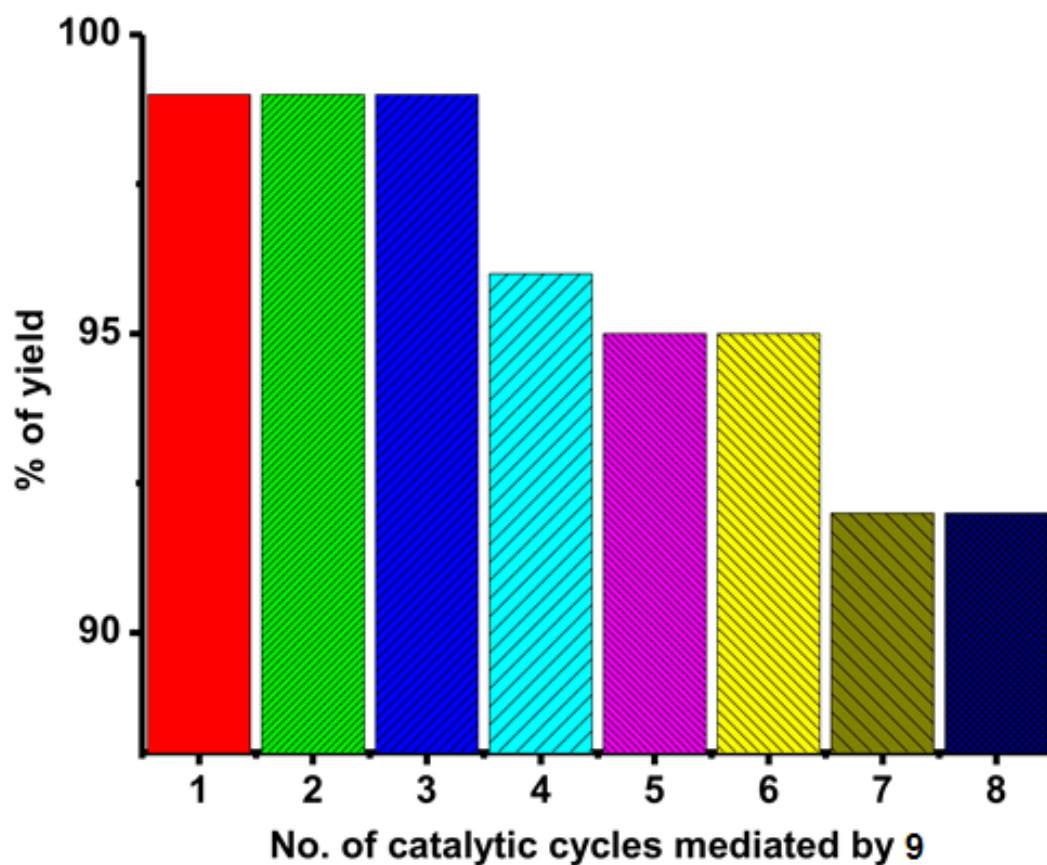


Figure 3.25: Longevity studies on catalyst **9** (1 mol%) in click catalysis using benzyl azide (1 mmol) and phenyl acetylene (1.2 mmol) under neat conditions at room temperature

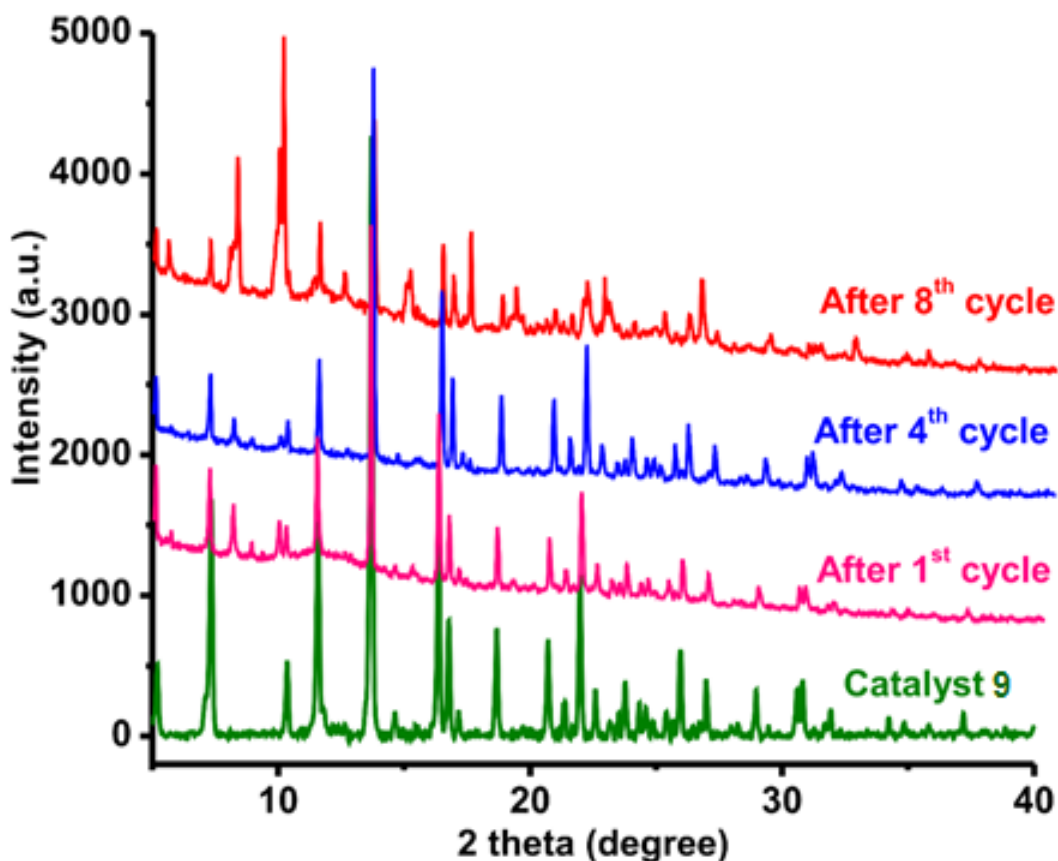
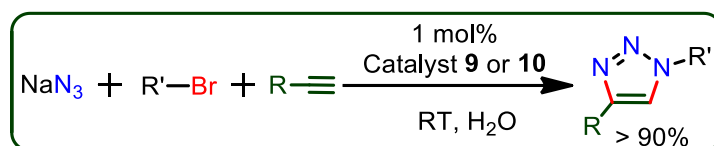


Figure 3.26: PXRD studies on reused catalyst **9**

Since the copper catalyzed one-pot synthesis of triazoles, by a three-component reaction (organic bromide, sodium azide and an alkyne; in order to avoid azide isolation) is very much demanding [21], the **9** and **10** mediated one-pot reactions were performed in water (Scheme 3.5).



Scheme 3.5: Catalysts **9** and **10** mediated one-pot synthesis of triazoles

The catalysts **9** and **10** gave remarkable yield (> 90%) from reactants with electron-rich or electron-poor azides and alkynes (Chart 3.2). The catalytic efficiency of **9** and **10** are comparable with cationic $[\text{Cu}(\text{NHC})_2]^+$ systems [22]. Thus, it was realized that the co-ordinatively unsaturated Cu(I) centers with trigonal planar arrangement along with open face cubic arrangement allow the CuAAC reaction substrates to conveniently approach the metal center on cubic surface to trigger the reaction.

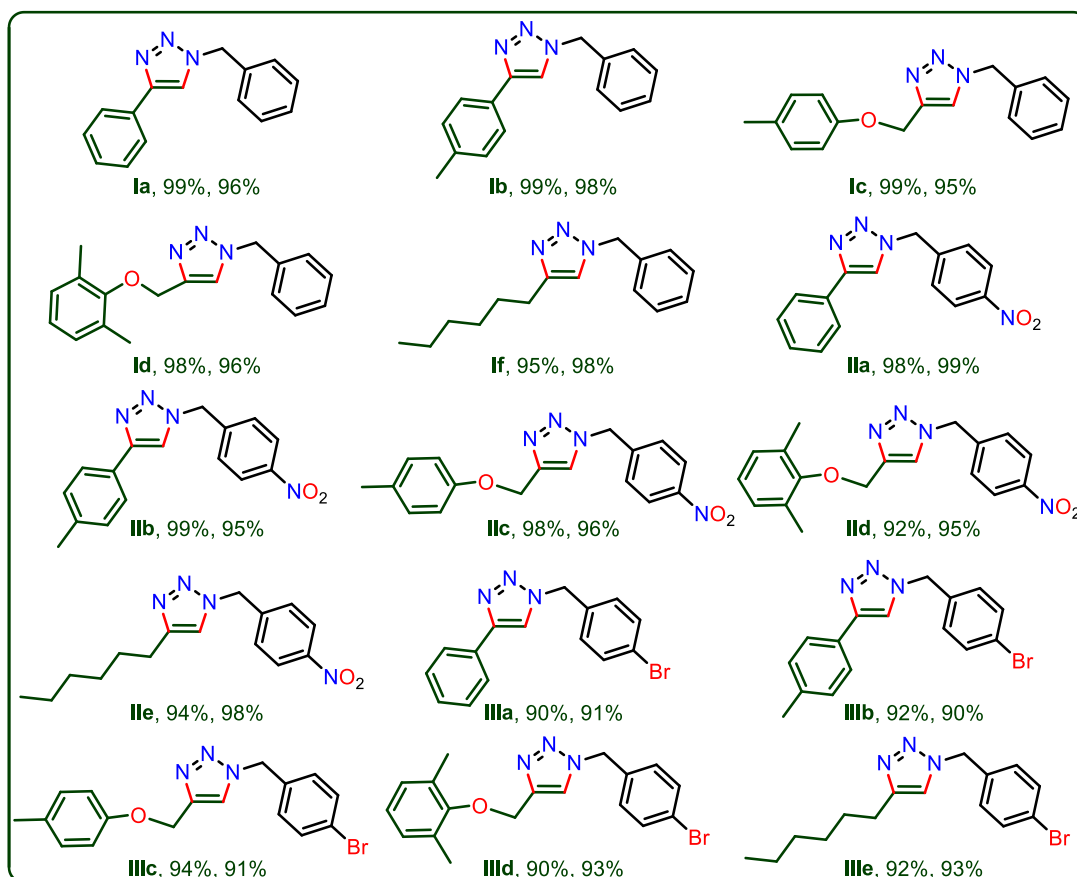
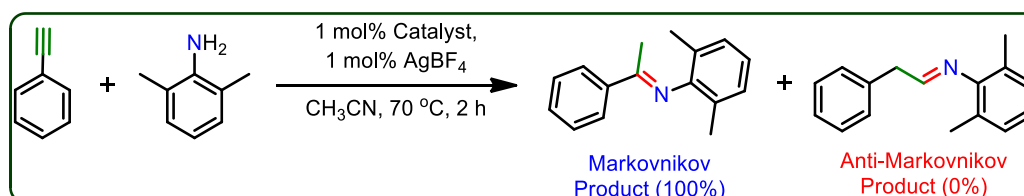


Chart 3.2: ^aReaction conditions: alkyne (1.2 mmol), azide (1 mmol), Catalyst **9** and/or **10** (1 mol%), neat, isolated yield

Moreover, the catalysts **9** and **10** were highly active and selective (Markovnikov's product) for the hydroamination of terminal alkynes with arylamines (Scheme 3.6, Table 3.5). The reaction was performed between phenyl acetylene and 2,6-dimethyl aniline in acetonitrile using 1 mol% catalyst **9** or **10** along with 1 mol% AgBF₄ as cocatalyst.



Scheme 3.6: Hydroamination of alkynes by catalysts **9** and **10**

Table 3.5: Optimization studies for hydroamination reaction mediated by Copper(I) catalysts **9** and **10**^a.

Entry	Catalyst	Cat. (mol%)	Solvent	Time (h)	Yield (%) ^b
1	9	1	CH ₃ CN	2	>99
2	10	1	CH ₃ CN	2	>99
3 ^c	9	1	CH ₃ CN	3	98
4 ^d	9	1	CH ₃ CN	12	72
5	9	1	Benzene	2	20
6	9	1	CH ₃ OH	2	70
7	9	1	THF	2	65
8 ^e	9	1	CH ₃ CN	2	90
9	AgBF₄	1	CH ₃ CN	12	30
10	Ag(OTf)	1	CH ₃ CN	12	25

^aReaction conditions: phenyl acetylene (0.5 mmol), 2,6-dimethylaniline (0.6 mmol) and solvent (2 mL). ^bIsolated yield, ^cwithout AgBF₄, ^dreaction performed at room temperature, ^ewith Ag(OTf)

The reaction proceeds very smoothly with both the catalysts in presence of AgBF₄ in 2 h (entry 1 and 2). Besides the absence of AgBF₄ required slightly longer time (3 h) for the completion of hydroamination reaction (entry 3). On the other hand, moderate yield was noticed for the same reaction performed at RT for 12 h (entry 4). However, benzene (entry 5), methanol (entry 6) and tetrahydrofuran (entry 7) produced moderate yields. The presence of Ag(OTf) along with catalyst **9** gave fairly good yield (entry 8). However, AgBF₄ presence is significant in this transformation. The starting material conversion was not appreciable only with AgBF₄ (entry 9) or Ag(OTf) (entry 10) under longer reaction times. Therefore acetonitrile was anticipated to be the best solvent for this transformation with quantitative yields. The catalysts were highly active (yield, from 92 to 99%) with excellent functional group tolerance (Chart 3.3) and the catalytic efficiency of **9** or **10** are on par with Cu–NHC catalysts [22b, 23].

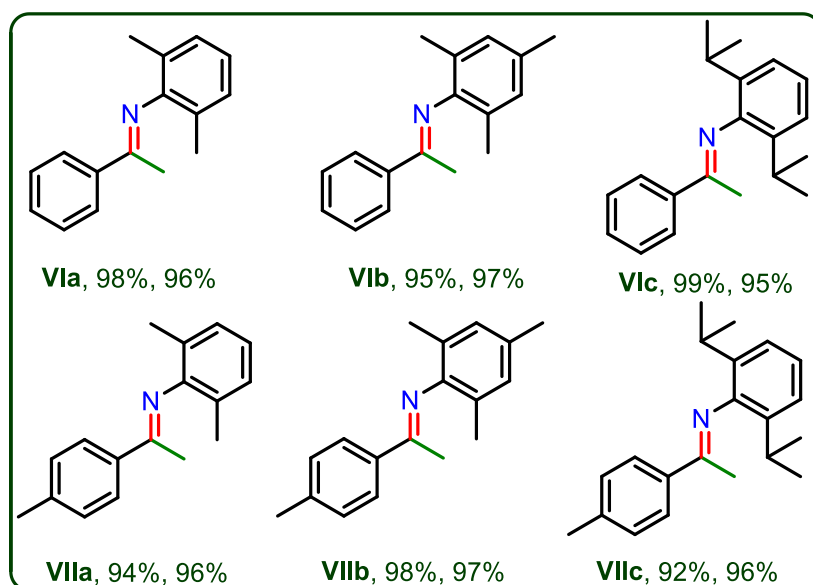


Chart 3.3: Products isolated in hydroamination reaction. Reaction conditions: alkyne (0.5 mmol), substituted aniline (0.6 mmol) and solvent (2 mL)

3.8. Summary

In summary, the large octanuclear Cu(I) cubic cages (**9** and **10**) supported by organo dichalcogenones were synthesized and characterized. **9** and **10** are the first examples of perfect Cu(I) cubic cage with Cu(I)⋯Cu(I) distance of 8.413 Å (for **9**) and 8.593 Å (for **10**). Formation of cationic cubic cages were accompanied by the association of twelve ligands (Btp or Bpsp) with eight trigonal planar [CuSe₃] vertex. The cationic charge of cubic cages were satisfied by eight PF₆⁻ counter anions, in which one of the PF₆⁻ anion occupies at the centre of Cu₈ cube without any interaction. Moreover, **9** and **10** are found to be very active catalysts in click chemistry under mild condition, one pot synthesis of triazoles as well as the selective hydroamination of terminal alkynes.

3.9. References

- [1] For selected examples: (a) J. Wang, X. Cao, S. Lv, C. Zhang, S. Xu, M. Shi and J. Zhang, *Nat. Commun.* 2017, **14625**, 1-10; (b) F. Lazreg, F. Nahra and C. S. J. Cazin, *Coord. Chem. Rev.* 2015, **293-294**, 48-79; (c) S. Díez-González and S. P. Nolan, *Acc. Chem. Res.* 2008, **41**, 349–358; (d) E. A. Romero, R. Jazzar and G. Bertrand, *Chem. Sci.* 2017, **8**, 165; (e) J. D. Egbert, C. S. J. Cazin and S. P. Nolan, *Catal. Sci. Technol.* 2013, **3**, 912–926; (f) W. Kirmse, *Angew. Chem. Int. Ed.* 2003, **42**, 1088–1093; (g) S. Gaillard, C. S. J. Cazin and S. P. Nolan, *Acc. Chem. Res.*

- 2012, **45**, 778–787; (h) N. Marion, *NHC-copper, silver and gold complexes in catalysis*, *RSC Catalysis Series* (2011), 6(N-Heterocyclic Carbenes), 317–344; (i) V. Charra, P. Frémont and P. Braunstein, *Coord. Chem. Rev.* 2017, **341**, 53-176.
- [2] (a) X. Hu, I. Castro-Rodriguez and K. Meyer, *J. Am. Chem. Soc.* 2003, **125**, 12237-12245; (b) X. Liu and W. Chen, *Organometallics* 2012, **31**, 6614–6622; (c) M. Nonnenmacher, D. Kunz, F. Rominger, *Organometallics* 2008, **27**, 1561–1568; (d) B. Liu, S. Pan, B. Liu and W. Chen, *Inorg. Chem.* 2014, **53**, 10485-10497; (e) B. Liu, B. Liu, Y. Zhou and W. Chen, *Organometallics* 2010, **29**, 1457-1464; (f) X. Hu, I. Castro-Rodriguez and K. Meyer, *J. Am. Chem. Soc.* 2003, **125**, 12237-12245; (g) A. Biffis, C. Tubaro, E. Scattolin, M. Basato, G. Papini, C. Santini, E. Alvarez and S. Conejero, *Dalton Trans.* 2009, **35**, 7223-7229; (h) N. Sinha, F. Roelfes, A. Hepp, C. Mejuto, E. Peris and F.E. Hahn, *Organometallics* 2014, **33**, 6898-6904.
- [3] (a) A. Makarem, R. Berg, F. Rominger and B. F. Straub, *Angew. Chem. Int. Ed.* 2015, **54**, 7431–7435; (b) S. Simonovic, A. C. Whitwood, W. Clegg, R. W. Harrington, M. B. Hursthouse, L. Male, R. E. Douthwaite. *Eur. J. Inorg. Chem.* 2009, 1786–1795; (c) H. Sun, K. Harms and J. Sundermeyer. *J. Am. Chem. Soc.* 2004, **126**, 9550–9551; (d) A. Makarem, R. Berg, F. Rominger and B. F. Straub, *Angew. Chem. Int. Ed.* 2015, **54**, 7431–7435; (e) S. Gu, J. Huang, X. Liu, H. Liu, Y. Zhou and W. Xu, *Inorg. Chem. Commun.* 2012, **21**, 168–172; (f) W. J. Humenny, S. Mitzinger, C. B. Khadka, B. K. Najafabadi, I. Vieiraa and J. F. Corrigan, *Dalton Trans.* 2012, **41**, 4413-4422; (g) A. Sathyanarayana, B. P. R. Metla, N. Sampath and G. Prabusankar, *J. Organomet. Chem.* 2014, **772-773**, 210-216.
- [4] For selected examples: (a) R. S. Dhayal, W. E. van Zyl and C. W. Liu, *Acc. Chem. Res.*, 2016, **49**, 86–95; (b) M. Shieh, C.-Y. Miu, Y.-Y. Chu and C.-N. Lin, *Coord. Chem. Rev.*, 2012, **256**, 637-694; (c) C. Femoni, M. C. Iapalucci, F. Kaswalder, G. Longoni and S. Zacchini, *Coord. Chem. Rev.*, 2006, **250**, 1580-1604; (d) R. Ahlrichs, A. Eichhöfer, D. Fenske, K. May and H. Sommer, *Angew. Chem. Int. Ed.*, 2007, **46**, 8254-8257; (e) R. Ahlrichs, D. Fenske, M. McPartlin, A. Rothenberger, C. Schrodtr and S. Wieber, *Angew. Chem. Int. Ed.*, 2005, **44**, 3932–3936.
- [5] Z. Han, G. Zhang, M. Zeng, D. Yuan, Q. Fang, J. Li, J. Ribas and H. Zhou, *Inorg. Chem.*, 2010, **49**, 769–771.
- [6] (a) G. Kong, X. Xu, C. Zou and C. Wu, *Chem. Commun.* 2011, **47**, 11005–11007; (b) K. Oisaki, Q. Li, H. Furukawa, A. U. Czaja and O. M. Yaghi, *J. Am. Chem. Soc.*

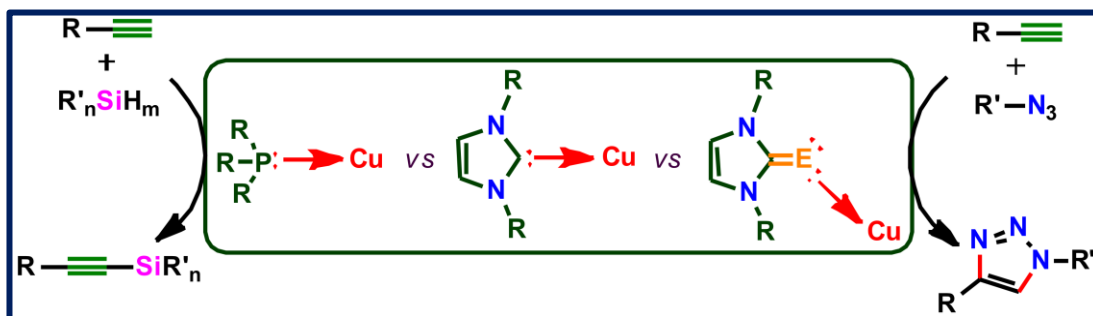
- 2010, **132**, 9262–9264; (c) J. Chun, H. S. Lee, H. G. Jung, S. W. Lee, H. J. Kim and S. U. Son, *Organometallics* 2010, **29**, 1518–1521; (d) J. Luo, J. Wang, G. Li, Q. Huo and Y. Liu, *Chem. Commun.*, 2013, **49**, 11433–11435; (e) C. Tubaro, A. Biffis, R. Gava, E. Scattolin, A. Volpe, M. Basato, M. M. Díaz-Requejo and P. J. Perez, *Eur. J. Org. Chem.* 2012, 1367–1372.
- [7] E. For selected examples: (a) T. Bollermann, G. Prabusankar, C. Gemel, M. Winter, R. W. Seidel and R. A. Fischer, *Chem. Eur. J.* 2010, **16**, 8846–8853; (b) A. Makarem, R. Berg, F. Rominger and B. F. Straub, *Angew. Chem. Int. Ed.* 2015, **54**, 7431–7435; (c) M. A. Fard, T. I. Levchenko, C. Cadogan, W. J. Humenny and J. F. Corrigan, *Chem. Eur. J.* 2016, **22**, 4543–4550; (d) J. Guo, Y. –W. Xu, K. Li, L. –M. Xiao, S. Chen, K. Wu, X. –D. Chen, Y–Z. Fan, J. –M. Liu and C. –Y. Su, *Angew. Chem. Int. Ed.* 2017, **56**, 1–6; (e) S. Durot, J. Taesch and V. Heitz, *Chem. Rev.*, 2014, **114**, 8542–8578; (f) W. M. Bloch and G. H. Clever, *Chem. Commun.*, 2017, **53**, 8506–8516; (g) M. Tegoni and M. Remelli, *Coord. Chem. Rev.*, 2012, **256**, 289–315; (h) A. Schmidt, A. Casini and F. E. Kühn, *Coord. Chem. Rev.*, 2014, **275**, 19–36; (i) W. Wang, Y. –X. Wang and H. –B. Yang, *Chem. Soc. Rev.*, 2016, **45**, 2656–2693; (j) Y. Bai, Q. Luo and J. Liu, *Chem. Soc. Rev.*, 2016, **45**, 2756–2767; (k) H. Li, Z. –J. Yao, D. Liu and G. –X. Jin, *Coord. Chem. Rev.*, 2015, **293–294**, 139–157; (l) K. Byrne, M. Zubair, N. Zhu, X. –P. Zhou, D. S. Fox, H. Zhang, B. Twamley, M. J. Lennox, T. Düren and W. Schmitt, *Nat. Commun.* 2017, **8**, 15268; (m) D. Fujita, Y. Ueda, S. Sato, N. Mizuno, T. Kumasaka and M. Fujita *Nature* 2016, **540**, 563–566; (n) B. M. Schmidt, T. Osuga, T. Sawada, M. Hoshino and M. Fujita, *Angew. Chem. Int. Ed.* 2016, **55**, 1561–1564; (o) M. M. Conn and J. Rebek, Jr. *Chem. Rev.*, 1997, **97**, 1647–1668; (p) P. Ballester, M. Fujita and J. Rebek Jr. *Chem. Soc. Rev.*, 2015, **44**, 392–393; (q) M. Yoshizawa, J. K. Klosterman and M. Fujita, *Angew. Chem. Int. Ed.*, 2009, **48**, 3418–3438; (r) L.-J. Chen, H.-B. Yang and M. Shionoya, *Chem. Soc. Rev.*, 2017, **46**, 2555–2576.
- [8] (a) H. R. Kim II, G. Jung, K. Yoo, K. Jang, E. S. Lee, J. Yun and S. U. Son, *Chem. Commun.* 2010, **46**, 758–760; (b) M. K. Barman, A. K. Sinha and S. Nembenna, *Green Chem.*, 2016, **18**, 2534–2541; (c) K. Srinivas, C. N. Babu and G. Prabusankar, *Dalton Trans.* 2015, **44**, 15636–15644; (d) M. Melaimi, R. Jazzar, M. Soleilhavoup and G. Bertrand, *Angew. Chem. Int. Ed.*, 2017, **56**, 10046–10068; (e) D. J. Nelson, F. Nahra, S. R. Patrick, D. B. Cordes, A. M. Z. Slawin and S. P. Nolan, *Organometallics* 2014, **33**, 3640–3645.

- [9] D. D. Perrin and W. L. F. Armarego, *Purification of laboratory chemicals*, Pergamon Press, London, 3rd edn, 1988.
- [10] W. Jia, Y. Dai, H. Zhang, X. Lu and E. Sheng, *RSC Adv.*, 2015, **5**, 29491–29496.
- [11] H. Zhang, W. Jia, Q. Xu and C. Ji, *Inorg. Chim. Acta*, 2016, **450**, 315–320.
- [12] O. V. Dolomanov, L. J. Bourhis, R. J. Gildea, J. A. K. Howard and H. Puschmann, *J. Appl. Cryst.* 2009, **42**, 339–341.
- [13] (a) G. M. Sheldrick, *Acta Crystallogr. Sect. A*, 1990, **46**, 467–473; (b) G. M. Sheldrick, SHELXL-97, *Program for Crystal Structure Refinement*, Universität Göttingen, Göttingen, 1997.
- [14] (a) J. Galy, A. Mosset, I. Grenthe, I. Puigdomènech, B. Sjöberg and F. Hultèn, *J. Am. Chem. Soc.* 1987, **109**, 380–386; (b) D. Armentano, T. F. Mastropietro, M. Julve, R. Rossi, P. Rossi and G. D. Munno, *J. Am. Chem. Soc.* 2007, **129**, 2740–2741.
- [15] R. S. Dhayal, W. E. van Zyl and C. W. Liu, *Acc. Chem. Res.* 2016, **49**(1), 86–95.
- [16] (a) C. W. Liu, B. Sarkar, Y. Huang, P. Liao, J. Wang, J. Saillard and S. Kahlal, *J. Am. Chem. Soc.* 2009, **131**, 11222–11233; (b) C. W. Liu, C. -M. Hung, B. K. Santra, H. -C. Chen, H. -H. Hsueh and J. -C. Wang, *Inorg. Chem.*, 2003, **42**, 3216–3220; (c) C. W. Liu, C. -M. Hung, B. K. Santra, Y. H. Chu, J. -C. Wang and Z. Lin, *Inorg. Chem.*, 2004, **43**, 4306–4314; (d) C. W. Liu, H.-C. Chen, J. -C. Wang and T. -C. Keng, *Chem. Commun.* 1998, 1831–1832; (e) C. W. Liu, M. D. Irwin, A. A. Mohamed and J. P. Fackler, *Inorg. Chim. Acta* 2004, **357**, 3950–3956; (f) C. W. Liu, C. -M. Hung, H. -C. Chen, J. -C. Wang, T. -C. Keng and K. Guo, *Chem. Commun.* 2000, 1897–1898; (g) T. S. Lobana, J. -C. Wang and C. W. Liu, *Coord. Chem. Rev.* 2007, **251**, 91–110; (h) J. P. Fackler, *Inorg. Chem.* 2002, **41**, 6959–6972; (i) C. W. Liu, C. -M. Hung, B. K. Santra, J. -C. Wang, H. -M. Kao and Z. Lin, *Inorg. Chem.*, 2003, **42** (25), 8551–8556.
- [17] W. Meng, B. Breiner, K. Rissanen, J. D. Thoburn, J. K. Clegg and J. R. Nitschke, *Angew. Chem. Int. Ed.* 2011, **50**, 3479–3483.
- [18] (a) B.V. Trzhtsinskaya and N.D. Abramova, *J. Sulfur Chem.* 1991, **10**, 389; (b) W. Jia, Y. Huang and G. Jin, *J. Organomet. Chem.* 2009, **694**, 4008–4013.
- [19] (a) M. M. Kimani, C. A. Bayse and J. L. Brumaghim, *Dalton Trans.*, 2011, **40**, 3711–3723; (b) M. M. Kimani, D. Watts, L. A. Graham, D. Rabinovich, G. P. A. Yap and J. L. Brumaghim, *Dalton Trans.*, 2015, **44**, 16313–16324.
- [20] (a) J. R. Miecznikowski, M. A. Lynn, J. P. Jasinski, W. Lo, D. W. Bak, M. Pati, E. E. Butrick, A. E. R. Drozdowski, K. A. Archer, C. E. Villa, E. G. Lemons, E. Powers,

- M. Siu, C. D. Gomes, N. A. Bernier and K. N. Morio, *Polyhedron* 2014, **80**, 157–165; (b) J. R. Miecznikowski, M. A. Lynn, J. P. Jasinski, E. Reinheimer, D. W. Bak, M. Pati, E. E. Butrick, A. E. R. Drozdowski, K. A. Archer, C. E. Villa, E. G. Lemons, E. Powers, M. Siu, C. D. Gomes and K. N. Morio, *J. Coord. Chem.* 2014, **67**, 29–44.
- [21] C. Wang, D. Ikhlef, S. Kahlal, J. Saillard and D. Astruc, *Coord. Chem. Rev.* 2016, **316**, 1-20.
- [22] (a) S. Díez-González and S. P. Nolan, *Angew. Chem., Int. Ed.* 2008, **47**, 8881-8884; (b) J. D. Egbert, C. S. J. Cazin and S. P. Nolan, *Catal. Sci. Technol.* 2013, **3**, 912-926; (c) F. Lazreg, A. M. Z. Slawin and C. S. J. Cazin, *Organometallics*, 2012, **31**, 7969-7975.
- [23] M. J. Pouy, S. A. Delp, J. Uddin, V. M. Ramdeen, N. A. Cochrane, T. B. Gunnoe, T. R. Cundari, M. Sabat and W. H. Myers, *ACS Catalysis* 2012, **2**, 2182-2193.

Chapter 4

Copper(I) complexes of C, S, Se and P donor ligands for C–N and C–Si bond formation



4.1. Introduction

The chemistry of “soft” Lewis donors such as imidazolin-2-chalcogenones (ImC or NHC=E, E = S and Se) supported metal complexes have gained much attention during past two decades in catalysis due to their tuneable σ -donor and π -accepting properties [1-3]. Thus, the metal will be more electrophilic when attached with more π -acceptor ligands (PPh₃), while, it becomes relatively less electrophilic when attached to weak π -acceptors such as NHC and ImC (Chart 4.1) [4].

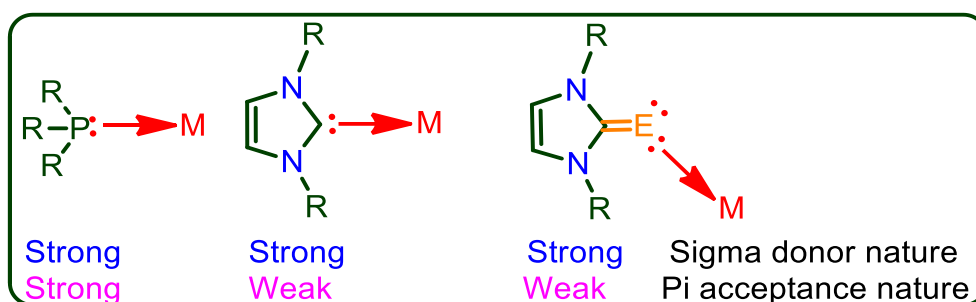


Chart 4.1: σ -donor and π -accepting nature of PPh₃, NHC and ImC ligands

Notably, the stronger σ -donor abilities, over π -accepting nature of ImC compared to both phosphine and NHC is due to the existence of larger contribution (66%) of zwitterionic form (NHC⁺-E⁻) [5]. Although, the coordination chemistry of transition metals with ImC is well known [6], the catalytic applications of these complexes are limited [7]. Notably, the catalytic efficiency NHC=E metal complexes is significantly remarkable compared to NHC-metal complexes (Chart 4.2) [7]. For example in copper chemistry, ImC supported copper(I) complexes {[(IMS)₂CuCl]; IMS = 1,3-dimethylimidazoline-2-thione, and [(IMes=Se)₂Cu][BF₄]; IMes=Se = 1,3-bis(2,4,6-trimethylphenyl)imidazolin-2-selone} were found to be more regioselective in hydroborylation of alkynes over NHC-Cu [7d-e]. Most recently, we have investigated the efficiency of [(Btp/Bpsp)₁₂Cu₈][PF₆]₈ (Btp = 3,3'-(pyridine-2,6-diyl)bis(1-isopropyl-1*H*-imidazole-2(3*H*)-thione), Bpsp = 3,3'-(pyridine-2,6-diyl)bis(1-isopropyl-1*H*-imidazole-2(3*H*)-selenone)) in click catalysis as well as in hydroamination of alkynes, and are found to be as best as NHC-Cu catalyst [8]. However, as of our knowledge, the catalytic comparisons of copper phosphines with NHC-Cu, ImC-Cu have never been investigated.

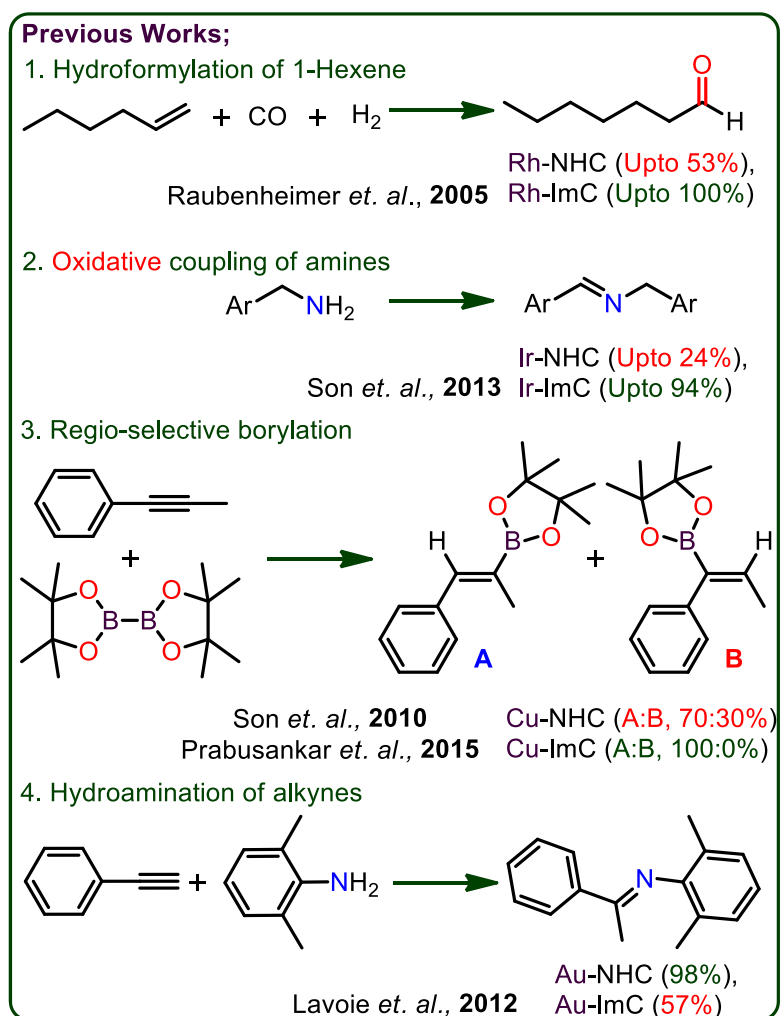


Chart 4.2: Known catalytic comparisons between ImC–metal and NHC–metal supported Cu(I) complexes

Indeed, herein we present the first comparative study of copper–NHC’s, copper-ImC’s and copper-phosphines. The coordination properties of ligands, structural features of copper(I) complexes and catalytic efficiency of new copper(I) complexes are reported in detail.

4.2. Experimental section

4.2.1. General remarks

The necessary manipulations were carried out under argon atmosphere in a glove box or using standard Schlenk techniques. The solvents were purchased from commercial sources and purified according to standard procedures and freshly distilled under argon atmosphere

prior to use [9]. IMes.HCl (1,3-dimesityl-1*H*-imidazol-3-ium chloride), IMes=S (1,3-dimesityl-1*H*-imidazole-2(3*H*)-thione), IMes=Se (1,3-dimesityl-1*H*-imidazole-2(3*H*)-selenone), IPr=Se (1,3-bis(2,6-diisopropylphenyl)-1*H*-imidazole-2(3*H*)-selenone), Ebis (3,3'-(ethane-1,2-diyl)bis(1-methyl-1*H*-imidazole-2(3*H*)-selenone)) and Ebpis (3,3'-(ethane-1,2-diyl)bis(1-isopropyl-1*H*-imidazole-2(3*H*)-selenone)) were prepared as previously reported [7k-l]. Unless otherwise stated, the chemicals were purchased from commercial sources. CuCl, CuBr, CuI, [Cu(CH₃CN)₄]PF₆, KPF₆ and NH₄BF₄ were purchased from Sigma Aldrich and used as received. FT-IR measurement (neat) was carried out on a Bruker Alpha-P Fourier transform spectrometer. The UV-vis spectra were measured on a T90+ UV-visible spectrophotometer. NMR spectra were recorded on Bruker Ultrashield-400 spectrometers at 25 °C unless otherwise stated. Chemical shifts are given relative to TMS and were referenced to the solvent resonances as internal standards. Elemental analyses were performed by the Euro EA-300 elemental analyzer. The crystal structures of **11-24** were measured on an Oxford Supernova diffractometer. Single crystals of complexes suitable for the single crystal X-ray analysis were mounted on Goniometer KM4/Xcalibur equipped with Sapphire2 (large Be window) detector (CuK α radiation source, $\lambda = 1.5418 \text{ \AA}$) at ambient temperature (298 K) in inert oil under an argon atmosphere. Using Olex2 [10], the structure was solved with the ShelXS [11] structure solution program using Direct Methods and refined with the olex2.refine refinement package using Gauss-Newton minimization. Absorption corrections were performed on the basis of multi-scans. Non-hydrogen atoms were anisotropically refined. H atoms were included in the refinement in calculated positions riding on their carrier atoms. No restraint has been made for any of the compounds.

4.2.2. Synthesis of [(IMes=S)Cu]Cl (**11**)

A mixture of IMes=S (0.100 g, 0.297 mmol) and CuCl (0.035 g, 0.356 mmol) in methanol (5 mL) was refluxed at 80 °C for 12 h. The obtained clear solution was brought to an ambient temperature, led to the formation of colorless crystals of **11**. Yield: 78% (based on CuCl). M.p.: 207-209 °C (dec.). Elemental analysis calcd (%) for C₂₁H₂₄ClCuN₂S (435.50): C, 57.92; H, 5.55; N, 6.43; Found: C, 57.84; H, 5.57; N, 6.39. ¹H NMR (400 MHz, DMSO-*d*₆): $\delta = 7.66$ (s, 2H, ImH), 7.07 (s, 4H, CH_{meta}), 2.26 (s, 6H, CH_{3para}), 1.95 (s, 12H, CH_{3ortho}) ppm. ¹³C NMR (100 MHz, DMSO-*d*₆): $\delta = 155.66$ (C=S), 140.04, 134.65, 131.85, 129.61, 121.67 (ArC), 20.69 (*p*-CH₃), 17.11 (*o*-CH₃) ppm. FT-IR (neat): $\bar{\nu} = 3148$ (w), 3112(w), 3082(w), 2917(m), 1605(m), 1558(w), 1482(s), 1449(m), 1382(s), 1290(m),

1235(s), 1167(w) (C=S), 1140(w), 1034(m), 925(w), 853(s), 750(s), 693(s), 666(w), 606(m), 572(m), 520(m) cm⁻¹.

4.2.3. Synthesis of [(IMes=S)Cu]Br (**12**)

12 was prepared in the same manner as described for **11** using IMes=S (0.100 g, 0.297 mmol) and CuBr (0.051 g, 0.356 mmol) in methanol (5 mL). Yield: 84% (based on CuBr). M.p.: 220-222 °C (dec.). Elemental analysis calcd (%) for C₂₁H₂₄BrCuN₂S (479.93): C, 52.55; H, 5.04; N, 5.84; Found: C, 52.54; H, 5.07; N, 5.79. ¹H NMR (400 MHz, DMSO-*d*₆): δ = 7.31 (s, 2H, ImH), 6.97 (s, 4H, CH_{meta}), 2.22 (s, 6H, CH_{3para}), 1.93 (s, 12H, CH_{3ortho}) ppm. ¹³C NMR (100 MHz, DMSO-*d*₆): δ = 159.87 (C=S), 138.59, 135.02, 133.21, 128.87, 119.70 (ArC), 20.62 (*p*-CH₃), 17.32 (*o*-CH₃) ppm. FT-IR (neat): $\bar{\nu}$ = 3147(w), 3113(w), 3084(w), 2916(m), 1604(m), 1556(w), 1481(s), 1449(m), 1382(s), 1345(w), 1289(m), 1234(s), 1167(w) (C=S), 1141(w), 1033(m), 924(w), 885(s), 851(m), 748(s), 693(s), 644(w), 605(m), 573(m), 519(m) cm⁻¹.

4.2.4. Synthesis of [(IMes=S)Cu]I (**13**)

A mixture of IMes=S (0.100 g, 0.297 mmol) and CuI (0.068 g, 0.356 mmol) in methanol (5 mL) was refluxed at 80 °C for 12 h. The obtained white precipitate was dissolved in hot acetonitrile and allowed to crystallize at ambient condition in 2 days. Yield: 71% (based on CuI). M.p.: 232-234 °C (melting). Elemental analysis calcd (%) for C₂₁H₂₄CuIN₂S (526.95): C, 47.87; H, 4.59; N, 5.32; Found: C, 47.84; H, 4.57; N, 5.29. ¹H NMR (400 MHz, DMSO-*d*₆): δ = 7.61 (s, 2H, ImH), 7.08 (s, 4H, CH_{meta}), 2.28 (s, 6H, CH_{3para}), 1.98 (s, 12H, CH_{3ortho}) ppm. ¹³C NMR (100 MHz, DMSO-*d*₆): δ = 156.55 (C=S), 139.76, 134.78, 132.17, 129.50, 121.27 (ArC), 20.69 (*p*-CH₃), 17.23 (*o*-CH₃) ppm. FT-IR (neat): $\bar{\nu}$ = 3145(w), 3111(w), 3084(w), 2913(m), 1597(m), 1556(w), 1478(s), 1445(m), 1380(s), 1286(m), 1230(s), 1165(w) (C=S), 1138(w), 1028(m), 921(w), 848(s), 743(s), 690(s), 604(m), 570(m) cm⁻¹.

4.2.5. Synthesis of [(IMes=Se)Cu]Br (**14**)

14 was prepared in the same manner as described for **11** using IMes=Se (0.100 g, 0.260 mmol) and CuBr (0.048 g, 0.312 mmol) in methanol (5 mL). Yield: 87% (based on CuBr). M.p.: 227-229 °C (melting). Elemental analysis calcd (%) for C₂₁H₂₄BrCuN₂Se (526.85): C, 47.88; H, 4.59; N, 5.32; Found: C, 47.91; H, 4.57; N, 5.29. ¹H NMR (400 MHz, DMSO-*d*₆): δ = 7.73 (s, 2H, ImH), 7.02 (s, 4H, CH_{meta}), 2.25 (s, 6H, CH_{3para}), 1.95 (s, 12H, CH_{3ortho}) ppm. ¹³C NMR (100 MHz, DMSO-*d*₆): δ = 148.22 (C=Se), 139.24, 134.58, 133.32,

129.13, 123.30 (ArC), 20.68 (*p*-CH₃), 17.57 (*o*-CH₃) ppm. FT-IR (neat): $\bar{\nu}$ = 3145(w), 3108(w), 3078(w), 2916(m), 1605(m), 1553(w), 1480(s), 1447(m), 1371(s), 1337(w), 1291(m), 1232(s), 1166(w) (C=Se), 1125(w), 1032(m), 925(w), 851(s), 752(s), 688(s), 594(w), 568(s), 520(m) cm⁻¹.

4.2.6. Synthesis of [(IMes=Se)Cu]I (**15**)

15 was prepared in the same manner as described for **13** using IMes=Se (0.100 g, 0.260 mmol) and CuI (0.060 g, 0.312 mmol) in methanol (5 mL). Yield: 77% (based on CuI). M.p.: 224-226 °C (melting). Elemental analysis calcd (%) for C₂₁H₂₄CuIN₂Se (573.85): C, 43.95; H, 4.22; N, 4.88; Found: C, 43.91; H, 4.17; N, 4.89. ¹H NMR (400 MHz, DMSO-*d*₆): δ = 7.79 (s, 2H, ImH), 7.08 (s, 4H, CH_{meta}), 2.30 (s, 6H, CH_{3para}), 1.97 (s, 12H, CH_{3ortho}) ppm. ¹³C NMR (100 MHz, DMSO-*d*₆): δ = 149.14 (C=Se), 139.85, 134.57, 132.94, 129.53, 123.31 (ArC), 20.77 (*p*-CH₃), 17.38 (*o*-CH₃) ppm. FT-IR (neat): $\bar{\nu}$ = 3143(w), 3107(w), 3079(w), 2913(m), 1599(m), 1551(m), 1477(s), 1443(m), 1369(s), 1334(w), 1289(m), 1228(s), 1163(w) (C=Se), 1123(m), 1026(m), 922(w), 849(s), 746(s), 684(s), 599(w), 566(m) cm⁻¹.

4.2.7. Synthesis of [(IMes=Se)₂Cu][CuCl₂] (**17**)

Method 1: **17** can be prepared in the same manner as described for **11** using IMes=Se (0.100 g, 0.260 mmol) and CuCl (0.031 g, 0.312 mmol) in methanol (5 mL). Yield: 75% (based on CuCl). **Method 2:** IMes=Se (0.100 g, 0.260 mmol) was treated with excess [(IMes)CuCl] (0.16g, 0.426 mmol) in acetone at reflux for overnight yielding the desired product **17** as major product. Yield: 65% (based on IMesCuCl). M.p.: 218-220 °C (melting). Elemental analysis calcd (%) for C₄₂H₄₈Cl₂Cu₂N₄Se₂ (964.79): C, 52.29; H, 5.01; N, 5.81; Found: C, 52.30; H, 5.07; N, 5.84. ¹H NMR (400 MHz, DMSO-*d*₆): δ = 7.81 (s, 2H, ImH), 7.07 (s, 4H, CH_{meta}), 2.28 (s, 6H, CH_{3para}), 1.94 (s, 12H, CH_{3ortho}) ppm. ¹³C NMR (100 MHz, DMSO-*d*₆): δ = 148.59 (C=Se), 140.00, 134.46, 132.76, 129.58, 123.45 (ArC), 20.74 (*p*-CH₃), 17.21 (*o*-CH₃) ppm. FT-IR (neat): $\bar{\nu}$ = 3146(w), 3106(w), 3076(w), 2915(m), 1607(m), 1553(w), 1482(s), 1448(m), 1371(s), 1338(m), 1292(m), 1233(s), 1165(w) (C=Se), 1125(w), 1033(s), 925(w), 852(s), 754(s), 688(s), 595(s), 569(s) cm⁻¹.

4.2.8. Synthesis of [(IMes)₂Cu][Cl] (**18**)

18 can be prepared as by-product during the synthesis of **17** in method 2. Yield: 30% (based on [(IMes)CuCl]. M.p.: 277-279 °C (dec.). Elemental analysis calcd (%) for C₄₂H₄₈ClCuN₄ (707.85): C, 71.26; H, 6.83; N, 7.91; Found: C, 71.30; H, 6.87; N, 7.94. ¹H NMR (400 MHz, CDCl₃): δ = 7.00 (s, 4H, ImH), 6.89 (s, 8H, CH_{meta}), 2.41 (s, 12H, CH_{3para}),

1.66 (s, 24H, CH_{3ortho}) ppm. ^{13}C NMR (100 MHz, $CDCl_3$): δ = 177.35 (C–Cu), 139.39, 134.53, 134.45, 129.16, 122.78 (ArC), 21.18 ($p-CH_3$), 16.95 ($o-CH_3$) ppm. FT-IR (neat): $\bar{\nu}$ = 2912(m), 1604(m), 1542(w), 1483(s), 1400(m), 1266(s), 1230(s), 1163(m), 1069(m), 1036(m), 929(m), 857(s), 733(s), 641(m), 573(m) cm^{-1} .

4.2.9. Synthesis of [(IMes=Se) $_2$ Cu][PF $_6$] (**19**)

Method 1: **19** can be prepared in the same manner as described for **11** using IMes=Se (0.100 g, 0.260 mmol) and $[Cu(CH_3CN)_4]PF_6$ (0.097 g, 0.260 mmol) in methanol (5 mL). Yield: 80% (based on $[Cu(CH_3CN)_4]PF_6$). **Method 2:** IMes=Se (0.100 g, 0.260 mmol) was treated with [(IMes)CuCl] (0.208g, 0.520 mmol) and an excess of KPF_6 (0.239 g, 1.300 mmol) in acetone at reflux for overnight yielding the desired product **19** as major product. Yield: 68% (based on [(IMes)CuCl]. M.p.: 259 °C (dec.). Elemental analysis calcd (%) for $C_{42}H_{48}CuF_6N_4PSe_2$ (975.28): C, 51.72; H, 4.96; N, 5.74; Found: C, 51.73; H, 4.97; N, 5.80. 1H NMR (400 MHz, $CDCl_3$): δ = 7.36 (s, 4H, ImH), 7.04 (s, 8H, CH_{meta}), 2.37 (s, 12H, CH_{3para}), 2.10 (s, 24H, CH_{3ortho}) ppm. ^{13}C NMR (100 MHz, $CDCl_3$): δ = 142.28 (C=Se), 140.96, 134.70, 132.53, 129.88, 124.58 (ArC), 21.35 ($p-CH_3$), 18.47 ($o-CH_3$) ppm. ^{31}P NMR ($CDCl_3$, 161 MHz): -157.59 to -131.22 (sept, PF_6) ppm. ^{19}F NMR ($CDCl_3$, 376 MHz): -74.72 to -72.83 (d, PF_6) ppm. FT-IR (neat): $\bar{\nu}$ = 1484(m), 1435(m), 1264(s), 1185(m) (C=Se), 1121(m), 834(s) (P–F $_{stretching}$), 731(s), 697(s), 549(s) cm^{-1} .

4.2.10. Synthesis of [(IMes) $_2$ Cu][PF $_6$] (**20**)

20 can be prepared as by-product during the synthesis of **19** and also **21** by method 2. Yield: 28% along with **19** and 25% along with **21** (based on [(IMes)CuCl]. M.p.: 238-240 °C (melting). Elemental analysis calcd (%) for $C_{42}H_{48}Cu_2F_6N_4P$ (817.36): C, 61.72; H, 5.92; N, 6.85; Found: C, 61.73; H, 5.97; N, 6.84. 1H NMR (400 MHz, $CDCl_3$): δ = 7.01 (s, 4H, ImH), 6.89 (s, 8H, CH_{meta}), 2.41 (s, 12H, CH_{3para}), 1.66 (s, 24H, CH_{3ortho}) ppm. ^{13}C NMR (100 MHz, $CDCl_3$): δ = 177.35 (C–Cu), 139.40, 134.52, 134.45, 129.16, 122.78 (ArC), 21.18 ($p-CH_3$), 16.96 ($o-CH_3$) ppm. ^{31}P NMR ($CDCl_3$, 161 MHz): -157.59 to -131.21 (sept, PF_6) ppm. ^{19}F NMR ($CDCl_3$, 376 MHz): -74.73 to -72.84 (d, PF_6) ppm. FT-IR (neat): $\bar{\nu}$ = 2920(w), 1608(w), 1482(s), 1454(m), 1372(m), 1341(w), 1265(s), 1234(m), 1035(m), 840(s) (P–F $_{stretching}$), 734(s), 700(m), 557(s) cm^{-1} .

4.2.11. Synthesis of [(IPr=Se) $_2$ Cu][PF $_6$] (**21**)

Method 1: **21** can be prepared in the same manner as described for **11** using IPr=Se (0.10 g, 0.213 mmol) and $[Cu(CH_3CN)_4]PF_6$ (0.040 g, 0.106 mmol) in methanol (5 mL).

Yield: 78% (based on $[\text{Cu}(\text{CH}_3\text{CN})_4]\text{PF}_6$). **Method 2:** $\text{IPr}=\text{Se}$ (0.100 g, 0.213 mmol) was treated with $[(\text{IMes})\text{CuCl}]$ (0.160g, 0.426 mmol) and an excess of KPF_6 (0.19 g, 1.065 mmol) in acetone at reflux for overnight yielding the desired product **21** as major product. Yield: 70% (based on $[(\text{IMes})\text{CuCl}]$). M.p.: 268-270 °C (dec.). Elemental analysis calcd (%) for $\text{C}_{54}\text{H}_{72}\text{CuF}_6\text{N}_4\text{PSe}_2$ (1143.60): C, 56.71; H, 6.35; N, 4.90; Found: C, 56.70; H, 6.37; N, 4.89. ^1H NMR (400 MHz, CDCl_3): $\delta = 7.43\text{--}7.39$ (t, 2H, CH_{para}), $7.23\text{--}7.22$ (d, 4H, CH_{meta}), 7.20 (s, 2H, ImH), 2.34–2.28 (sept, 4H, $^i\text{PrCH}$), 1.20–1.19, 1.12–1.10 (d, 24H, CH_3) ppm. ^{13}C NMR (100 MHz, CDCl_3): $\delta = 155.76$ ($\text{C}=\text{Se}$), 145.79 (ImC), 133.11, 131.11, 124.61, 123.37 (ArC), 29.22 ($^i\text{PrCH}$), 24.95, 23.44 (CH_3) ppm. ^{31}P NMR (CDCl_3 , 161 MHz): -157.59 to -131.21 (sept, PF_6) ppm. ^{19}F NMR (CDCl_3 , 376 MHz): -74.82 to -72.82 (d, PF_6) ppm. FT-IR (neat): $\bar{\nu} = 2962(\text{m})$, $2867(\text{m})$, $1558(\text{w})$, $1463(\text{s})$, $1420(\text{m})$, $1345(\text{s})$, $1265(\text{m})$, $1212(\text{w})$, $1181(\text{m})$ ($\text{C}-\text{Se}$), $1120(\text{w})$, $1060(\text{m})$, $937(\text{m})$, $839(\text{s})$ ($\text{P}-\text{F}_{\text{stretching}}$), $803(\text{w})$, $737(\text{s})$, $555(\text{s})$ cm^{-1} .

4.2.12. Synthesis of $[(\text{PPh}_3)_4\text{Cu}_4\text{I}_4]$ (**22**)

CuI (0.50g, 0.263 mmol) and excess of PPh_3 (1.38g, 0.526 mmol) was mixed together in acetonitrile (20 mL) and was allowed to stir at 85 °C for overnight yielding a colourless clear solution which upon cooling to room temperature produces white crystalline solid of **22**. Yield: 82% (based on CuI). M.p.: 221-223 °C (melting). Elemental analysis calcd (%) for $\text{C}_{72}\text{H}_{60}\text{Cu}_4\text{I}_4\text{P}_4$ (1810.94): C, 47.75; H, 3.34; Found: C, 47.80; H, 3.37. ^1H NMR (400 MHz, CDCl_3): $\delta = 7.30\text{--}7.25$ (m, 3H, ArH), $7.17\text{--}7.13$ (m, 2H, CH_{ortho}) ppm. ^{13}C NMR (100 MHz, CDCl_3): $\delta = 134.09$, 133.94 , 133.79 , 133.58 , 129.46 , 128.47 , 128.38 (ArC) ppm. ^{31}P NMR (CDCl_3 , 161 MHz): -4.96 (s, PPh_3) ppm. FT-IR (neat): $\bar{\nu} = 1677(\text{w})$, $1562(\text{w})$, $1475(\text{m})$, $1429(\text{s})$, $1212(\text{w})$, $1178(\text{m})$, $1093(\text{m})$, $1025(\text{w})$, $995(\text{w})$, $744(\text{s})$, $691(\text{s})$, $521(\text{m})$ cm^{-1} .

4.2.13. Synthesis of $[(\text{Ebis})\text{CuI}]_n$ (**23**)

Method 1: **22** (0.26g, 0.143 mmol) and **Ebis** (3,3'-(ethane-1,2-diyl)bis(1-methyl-1*H*-imidazole-2(3*H*)-selenone)) (0.10g, 0.287 mmol) were mixed together and evacuated for 10 minutes in high vacuo followed by the addition of acetonitrile (5 mL), and was allowed to stir at 85 °C for 12 h, yielding a clear colourless solution, which upon cooling to ambient temperature produced colourless crystalline solid of **23**. Yield: 75% (based on **22**). **Method 2:** CuI (0.05 g, 0.299 mmol) and PPh_3 (0.15 g, 0.599 mmol) were mixed together in acetonitrile (5 mL), and was allowed to stir at 85 °C for 3 h. To the obtained clear solution **Ebis** (0.10 g, 0.299 mmol) was added and was further stirred at reflux for 12 h to obtain a clear solution, which on further cooling to room temperature yields compound **23**. M.p.: 220-

222 °C (dec.). Elemental analysis calcd (%) for C₁₀H₁₄Cu₂I₂N₄Se₂ (729.06): C, 16.47; H, 1.94; N, 7.68; Found: C, 16.43; H, 1.97; N, 7.64. ¹H NMR (400 MHz, CDCl₃): δ = 6.80-6.79 (d, 2H, ImH), 6.76 (d, 2H, ImH), 4.57 (s, 4H, CH₂-CH₂), 3.66 (s, 6H, CH₃) ppm. ¹³C NMR (100 MHz, CDCl₃): δ = 155.73 (C=Se), 119.95, 119.75 (ImC), 47.22 (CH₂-CH₂), 37091 (CH₃) ppm. FT-IR (neat): $\bar{\nu}$ = 2932(m), 1679(s), 1561(m), 1479(m), 1436(m), 1405(m), 1244(m), 1180(m) (C=Se), 1115(s), 1046(m), 924(w), 808(m), 751(w), 717(s), 690(s), 533(s) cm⁻¹.

4.2.14. Synthesis of [(Ebpis)_{1.5}Cu][BF₄]_n (**24**)

Method 1: **24** was synthesized in the same method as described for **23** using **22** (0.22g, 0.123 mmol) and **Ebpis** (3,3'-(ethane-1,2-diyl)bis(1-isopropyl-1*H*-imidazole-2(3*H*)-selenone)) (0.10, 0.247 mmol). The successive addition of excess NH₄BF₄ (0.13 g, 1.235 mmol) to the reaction mixture after 12 h, produced a clear solution. The reaction mixture was filtered and concentrated in vacuo to isolate **24** in very good yield. Yield: 78% (based on **22**).

Method 2: CuI (0.05 g, 0.299 mmol) and PPh₃ (0.15 g, 0.599 mmol) were mixed together in acetonitrile (5 mL), and was allowed to stir at 85 °C for 3 h. To the obtained clear solution **Ebpis** (0.12 g, 0.299 mmol) was added and was further stirred at reflux for 12h to obtain an orange precipitate, then NH₄BF₄ (0.06 g, 0.599 mmol) which on further cooling to room temperature yields compound **24**. M.p.: 229-231 °C (dec.). Elemental analysis calcd (%) for C₂₁H₃₃B₁Cu₁F₄N₆Se₃ (756.75): C, 33.33; H, 4.40; N, 11.11; Found: C, 33.30; H, 4.37; N, 11.14. ¹H NMR (400 MHz, CDCl₃): δ = 6.79-6.76 (m, 4H, ImH), 5.26-5.07 (m, 2H, N-CH), 4.60 (s, 4H, CH₂-CH₂), 1.34-1.32 (d, 12H, CH₃) ppm. ¹³C NMR (100 MHz, CDCl₃): δ = 154.13 (C=Se), 120.38, 114.77, 50.96, 46.71, 21.95 (CH₃) ppm. ¹¹B{¹H} NMR (128.4 MHz, CDCl₃): δ = -0.99 ppm. ¹⁹F{¹H} NMR (376.4 MHz, CDCl₃): δ = -154.02 ppm. FT-IR (neat): $\bar{\nu}$ = 3170(w), 3141(w), 2977(w), 1567(m), 1453(m), 1418(s), 1325(s), 1218(m), 1175(m) (C=Se), 1135(m), 1036(s) (B-F_{stretching}), 741(s), 684(s), 640(m), 518(m) cm⁻¹.

4.2.15. General synthetic procedure for the [3+2] cycloaddition of azides and terminal alkynes

Azide (1.0 mmol), alkyne (1.2 mmol), catalyst (1 mol%) and water (1 mL) were loaded. The solution was stirred at room temperature for 1 h and the conversion was noticed by TLC to ensure the completion of reaction. After the complete conversion water (5 mL) was added followed by the addition of ethyl acetate (5 mL). The reaction mixture was allowed to stir at room temperature for further 5-10 minutes. After which the ethyl acetate layer was collected and the volatiles were evaporated to obtain the solid compound. The acquired solids were

further washed with *n*-hexane and dried under *vacuo* to yield the desired product. The isolated 1,2,3-triazole products in all the experiments were estimated to be extremely pure.

4.2.16. General procedure for the synthesis of C–Si bonding

Catalyst (1 mol%) was placed in an oven dried Schlenk flask and was evacuated for 5 minutes then refilled with an argon gas. CH₃CN (1 mL) was added to the flask under argon, followed by terminal alkyne (1.0 mmol), hydrosilane (1.2 mmol) and pyridine (0.2 mmol). The resulting mixture was allowed to stir at 100 °C for 12 h. After the completion of the reaction, a saturated aqueous NH₄Cl solution (10 mL) was added to the mixture, and the aqueous phase was extracted with ethyl acetate (5 mL x 3). The combined organic layer was washed with brine (10 mL) and then dried over anhydrous sodium sulfate. Filtration and evaporation of the solvent followed by column chromatography on silica gel gave the corresponding product.

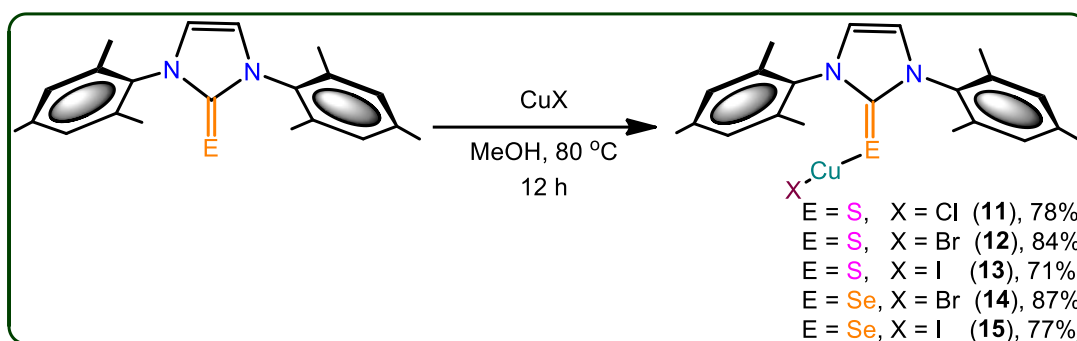
4.3. Result and discussion

The N-heterocyclic thione and selone ligands such as IMes=S, IMes=Se, IPr=Se, Ebis and Ebpis were synthesized in fairly good yields from their corresponding imidazolium salts using elemental chalcogen powders in the presence of potassium carbonate [7k-l]. These organochalcogen ligands were demonstrated as promising ligands to investigate the coordination abilities with copper metal. The copper(I) complexes isolated herein are found to be organized in three different categories such as neutral monomeric copper(I) complexes [12], cationic monomeric copper(I) complexes, neutral 2D copper(I) sheet and cationic 2D copper(I) sheet.

4.3.1. Synthesis and characterization of 11-15

Neutral mononuclear copper(I) complexes, **11-15** were synthesized by treating copper(I) halides with one equivalent of IMes=E in methanol (Scheme 4.1). The monomeric copper(I) complexes **11-15** were isolated in excellent yield. The crystalline solids **11-15** are soluble only in hot acetonitrile and in DMSO. The formation of these compounds were established by elemental analysis, FT-IR, multi nuclear NMR spectroscopy, UV-vis and single crystal X-ray diffraction techniques.

In ¹H NMR, the aryl hydrogens are slightly downfield shifted upon complexation, while the imidazole hydrogens are largely downfield shifted due to hydrogen bonding interactions. The C=E signal in ¹³C NMR is up-field shifted by 5-10 ppm due to the decrease in π -acceptance nature of carbene carbon upon complexation. FT-IR spectra of molecules **11-15** show the existence of C=E stretching frequency at 1163-1167 cm⁻¹, which is in agreement with the complex formation.



Scheme 4.1: Synthesis of **11-15**

4.3.2. Single crystal X-ray structures of **11-15**

The solid state structures of **11-15** were unambiguously determined by single crystal x-ray diffraction technique (Figure 4.1). **11-15** crystallized in the monoclinic space group, $P2_1/c$. The crystallographic data for **11-14** are listed out in table 4.1, while **15** is listed in table 4.2 and the important bond parameters are assembled in table 4.4. The molecular structures of **11-15** are isostructural and are neutral monomeric copper(I) chalcogenone complexes with a copper:chalcogen ratio of 1:1. The copper(I) centre in **11-15** is two coordinated with one imidazole thione/selone and one halogen atom. Interestingly, the molecular structures of **11-15** are comparable with NHC analogues of [(IMes)CuX].

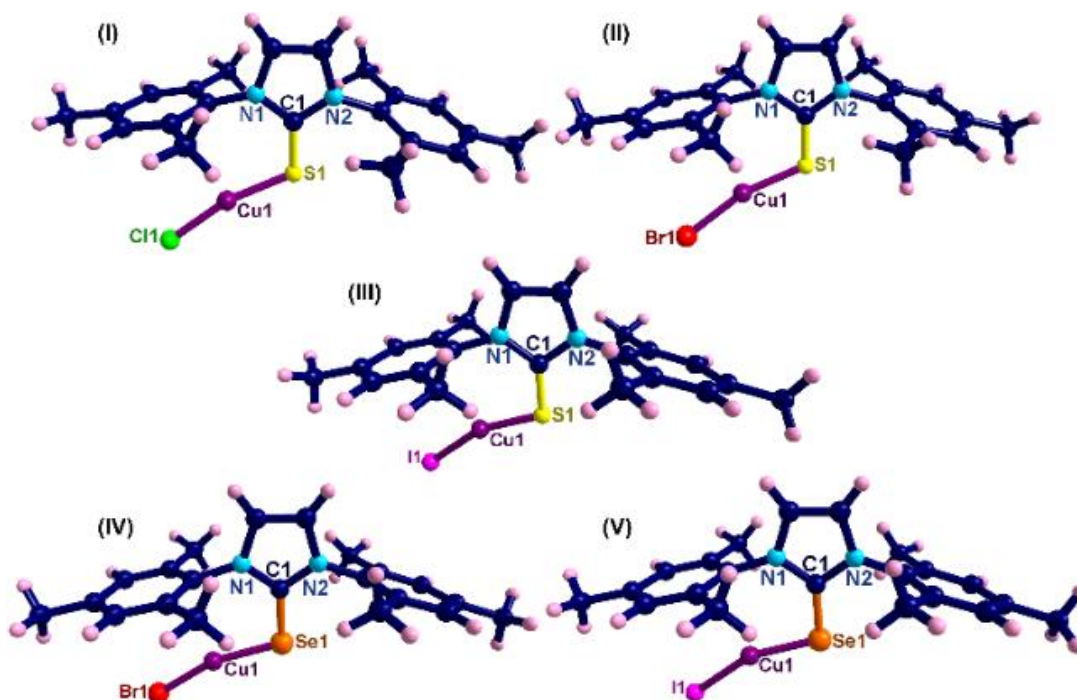


Figure 4.1 Molecular structures of **11-15**

Upon coordination, the C=S bond length (1.699(3) Å for **11**, 1.699(3) Å for **12**, 1.699(8) Å for **13**) and C=Se bond length (1.855(5) Å for **14**, 1.842(9) Å for **15**) are marginally increased related to their corresponding ligands (IMes=S (1.675(18) Å) and IMes=Se (1.830(6) Å)) [5k]. The E–Cu–X bond angle in molecules **11-15** lies between 159.60(4)-165.94(6)°, suggesting the quasi-linear arrangement around metal centre.

4.3.3. Molecular packing and Hydrogen bonding interactions in **11-15**

Molecules **11-15** show quite a strong C–H···Cl, and also moderately strong C–H···S and C–H···Se hydrogen bonding interactions in their solid state structures as evidenced by single crystal X-ray diffraction analysis (Chart 4.3). Surprisingly, the molecular packing of **11** is not comparable with **12-15**. The hydrogen bonded polymeric chain through C(3)–H(3)···Cl (2.8116(2) Å, 164.549(3)°) interactions are observed in **11**, and are marginally stronger than the C–H···Cl interactions reported for [(IPr=S)BiCl₃]·CHCl₃ (C(2)–H(2)···Cl(1); 2.871 Å, 145.32°) [5k].

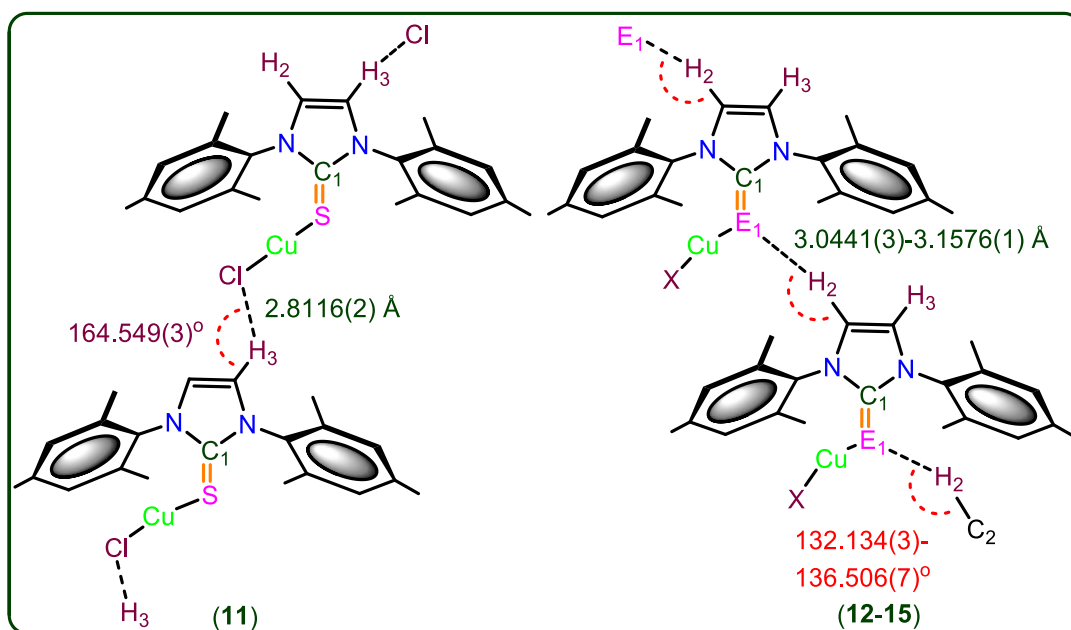


Chart 4.3: The representation of H(3)···Cl(1) bond distances in **11** and H(2)···E(1) bond distances and C(2)–H(2)–E(1) bond angles in molecules **12-15**

The solid state structure elucidated from single crystal X-ray diffraction technique revealed the oppositely arranged molecular layers in molecule **11**. While, all the other molecules (**12-15**) are arranged in AA'AA'AA'AA'AA' (Figure 4.2-4.3) fashion in their solid states structures. In addition to this, an unusual C–H···S bonding is noticed in **12**

(3.101(1) Å, 134.84(1)°) and **13** (3.044(3) Å, 136.51(7)°), while the very rare C–H···Se bonding observed in **14** (3.158(1) Å, 132.74(3)°) and **15** (3.1241(1) Å, 132.134(3)°) [5k]. The observed C–H···S interactions in **12** and **13** are quite weak compared to the interactions reported for [(IPr)S]BiCl₃·CHCl₃ (H···S; 2.797 Å, 175.23°) [5k], while C–H···S interactions in **12** and **13** are stronger than the interactions reported for *N,N'*-dimethylthioformamide (H···S; 3.781(7) Å, 175.4(7)°) [13].

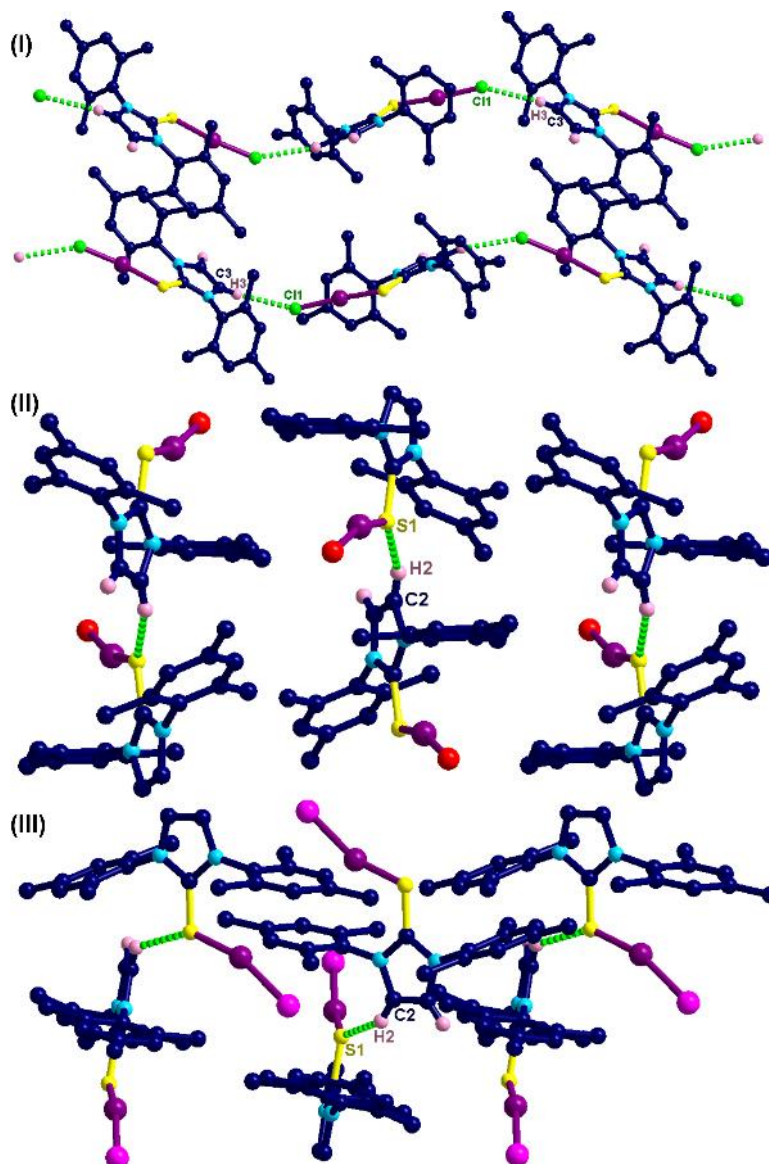


Figure 4.2: (I) Molecular packing arrangement of **11** with extended C–H···Cl hydrogen bonding interactions. Non-interacting hydrogen atoms have been omitted for the clarity. D···A distances [Å]: H(3)···Cl(1), 2.8116(2); C–D···A angles [°]:

C(3)–H(3)···Cl(1), 164.549(3). (II) Molecular packing arrangement of **12** with extended C–H···S hydrogen bonding interactions. Non-interacting hydrogen atoms have been omitted for the clarity. D···A distances [Å]: H(2)···S(1), 3.1008(1); C–D···A angles [°]: C(2)–H(2)···S(1), 134.838(1); C(1)–S(1)···H(2), 106.654(1). (III) Molecular packing arrangement of **13** with extended C–H···S hydrogen bonding interactions. Non-interacting hydrogen atoms have been omitted for the clarity. D···A distances [Å]: H(2)···S(1), 3.0441(3); C–D···A angles [°]: C(2)–H(2)···S(1), 136.506(7); C(1)–S(1)···H(2), 106.816(4)

Besides, the imidazole protons signal appeared to be down field shifted (about 0.3-0.7 ppm) for molecules **11-15** due to the existence of hydrogen bonding (Figure 4.4). Moreover, the C(1)–E(1)–Cu(1) bond angles are almost comparable. The existing E···H bond distances (3.0441(3)-3.1576(1) Å) and bond angles (132.134(3)-136.506(7)°) additionally supports the moderately strong hydrogen bonding (Chart 4.3) [7k,14].

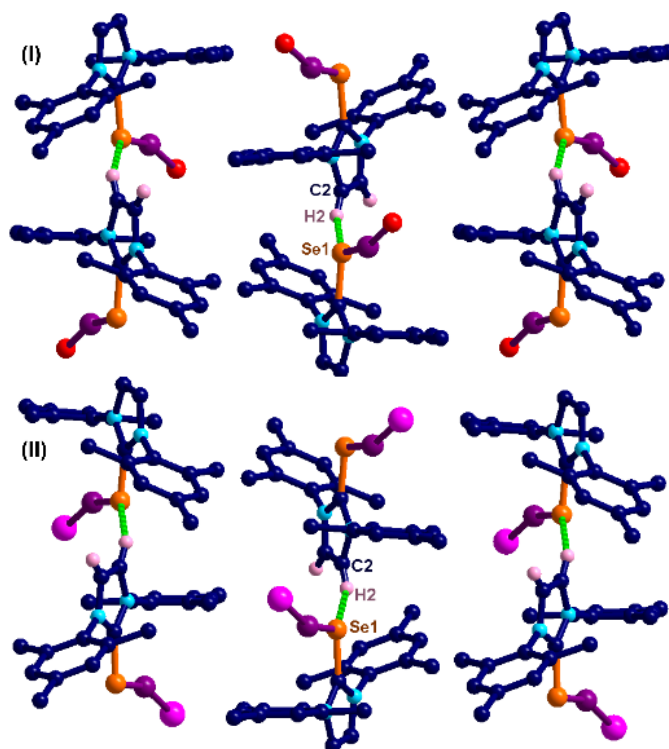


Figure 4.3: (I) Molecular packing arrangement of **14** with extended C–H···Se hydrogen bonding interactions. Non-interacting hydrogen atoms have been omitted for the clarity.

D···A distances [Å]: H(2)···Se(1), 3.1576(1); C–D···A angles [°]: C(2)–H(2)···Se(1), 132.740(3); C(1)–Se(1)···H(2), 105.844(2). (II) Molecular packing arrangement of **15** with extended C–H···Se hydrogen bonding interactions. Non-interacting hydrogen atoms have been omitted for the clarity. D···A distances [Å]: H(2)···Se(1), 3.1241(1); C–D···A angles [°]: C(2)–H(2)···Se(1), 132.134(3); C(1)–Se(1)···H(2), 104.541(1)

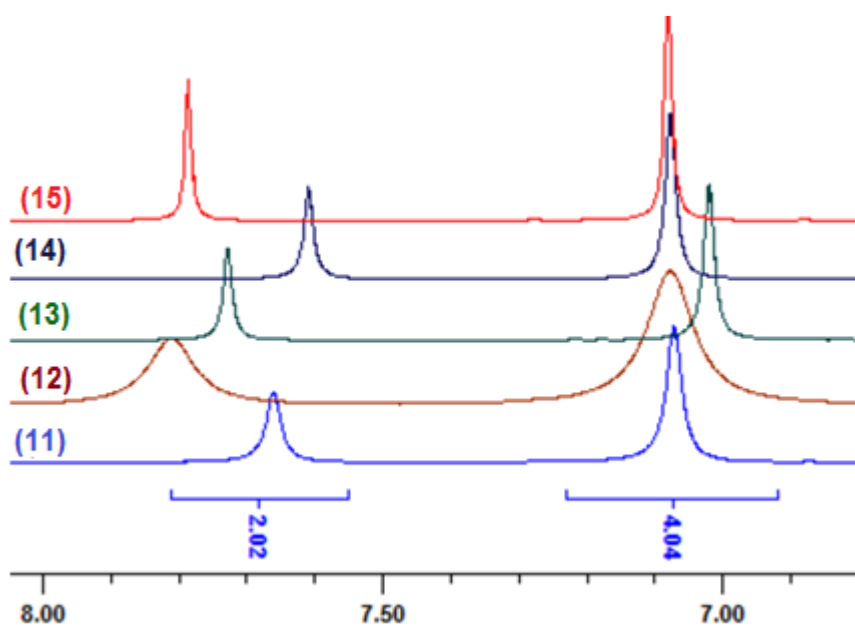


Figure 4.4: Section of ¹H NMR spectra (400 MHz, DMSO-*d*₆) displays the aryl region among **11-15**

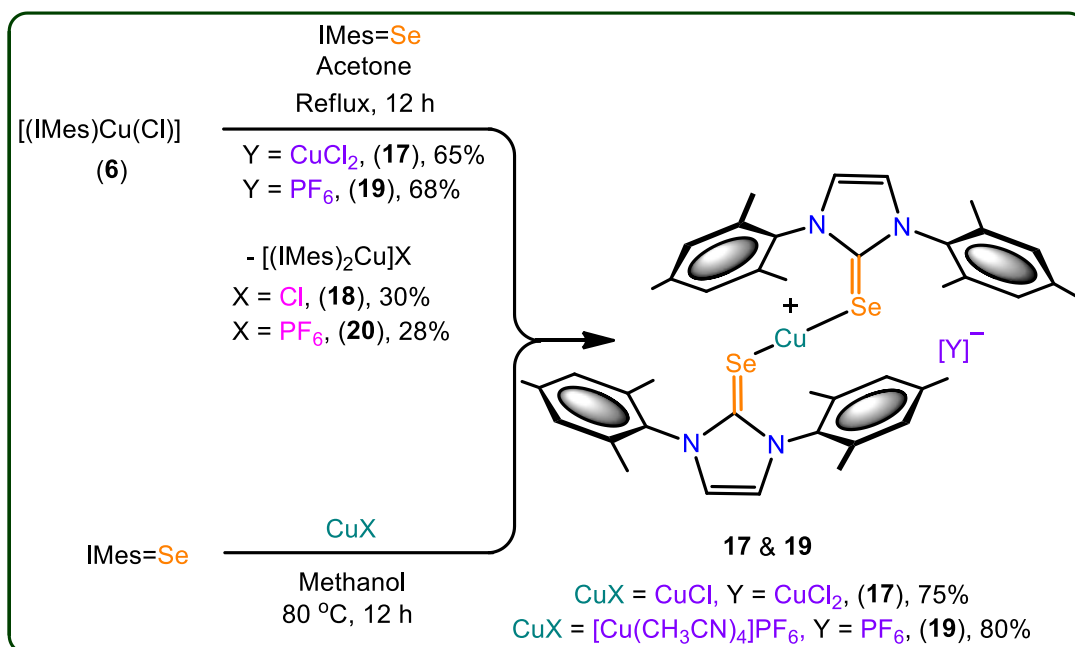
Table 4.1: Structural parameters of compounds **11-14**.

	11	12	13	14
Empirical formula	C ₂₁ H ₃₁ N ₂ S CuCl	C ₂₁ H ₂₄ N ₂ S CuBr	C ₂₁ H ₂₄ N ₂ Se CuBr	C ₂₁ H ₂₄ N ₂ S CuI
Formula weight	435.50	479.93	526.85	526.95
Temperature (K)	298	298	298	298
Crystal system	Monoclinic	Monoclinic	Monoclinic	Monoclinic
Space group	P2 ₁ /c	P2 ₁ /c	P2 ₁ /c	P2 ₁ /c
<i>a</i> /Å	11.062(5)	11.203(4)	11.204(2)	11.502(12)
<i>b</i> /Å	15.367(6)	15.375(6)	15.341(2)	15.412(14)
<i>c</i> /Å	13.707(6)	13.620(6)	13.774(11)	13.615(16)
α /°	90	90	90	90
β /°	113.378(5)	112.795(5)	112.61(15)	112.63(13)
γ /°	90	90	90	90
Volume (Å ³)	2139.1(18)	2163.1(14)	2185.3(6)	2227.9(5)
<i>Z</i>	4	4	4	4
$\rho_{\text{calc}}/\text{mg mm}^{-3}$	1.352	1.474	1.601	1.570
Absorption coefficient (μ/mm^{-1})	3.540	4.529	5.495	13.179
<i>F</i> (000)	900.7	976.0	1036.0	1042.9
Reflections collected	5620	8986	5465	8950
<i>R</i> _{int}	0.0214	0.0242	0.0206	0.0442
GOF on <i>F</i> ²	1.062	1.054	1.017	1.063
<i>R</i> ₁ (<i>I</i> >2 σ (<i>I</i>))	0.0506	0.0458	0.0556	0.0850
w <i>R</i> ₂ (<i>I</i> >2 σ (<i>I</i>))	0.1450	0.1207	0.2110	0.3193
<i>R</i> ₁ values (all data)	0.0656	0.0546	0.0674	0.1158
<i>R</i> ₂ values (all data)	0.1700	0.1309	0.2111	0.3194

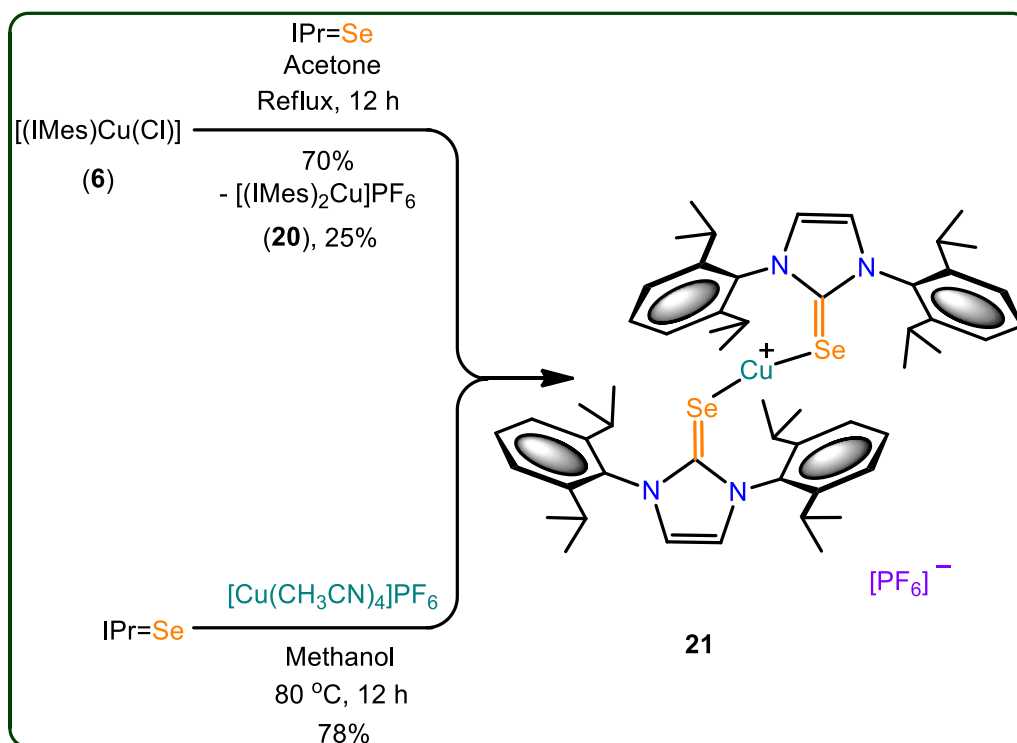
4.3.4. Synthesis and characterization of 17-21

The cationic copper(I) complexes (**17-21**) were isolated in very good yields by treating IMes=Se (for **17** and **19**) and IPr=Se (for **21**) with [Cu(CH₃CN)₄]PF₆ in methanol (Scheme 4.2-4.3). Interestingly, these complexes can also be isolated in very good yield along with cationic NHC-copper(I) complexes **18** and **20** by ligand transfer method from [(IMes)CuCl] (**16**) [15]. The ligand exchange reaction signifies the improved donor abilities of ImC over NHC ligands to stabilize metal center [16]. Compounds **17**, **19** and **21** were crystallized at ambient temperature. The compounds **18** and **20** were separated by hand picking method from the mixture and purified by recrystallization from saturated dichloromethane solutions. The

formation of **17**, **19** and **21** were established by elemental analysis, FT-IR, multi nuclear NMR spectroscopy and single crystal X-ray diffraction techniques. The PF₆ counter anion in molecules, **19** (834 cm⁻¹), **20** (840 cm⁻¹) and **21** (839 cm⁻¹) were confirmed by IR spectroscopy. The ³¹P NMR display septet for the presence of PF₆ (-131.21 to -157.59 ppm) ion and the ¹⁹F NMR show doublet for PF₆ (-72.82 to -74.82 ppm) ion. The C=Se is shifted up field for **16** (178.98 ppm), for **17** (148.59 ppm), for **19** (142.28 ppm) and for **21** (154.21 ppm) respectively. Molecules **17** and **19** display (10-15 ppm) up field shift after complexation, compared to their corresponding ligand (IMes=Se, 157.49 ppm). **21** shows up field shift around 8 ppm, compared to its ligand (IPr=Se, 162.14 ppm), suggesting a strong σ-donor nature of NHC=E over NHC [7d,k-l].



Scheme 4.2: Synthesis of **17-20**



Scheme 4.3: Synthesis of **21**

4.3.5. Single crystal X-ray structure of 17-21

The solid state structures of **17**, **19** and **21** were confirmed by single crystal X-ray diffraction technique (Figure 4.5). **17**, **19** and **21** crystallized in the monoclinic space group, $P2_1/n$ (for **17** and **19**), $C2/c$ (for **21**). The crystallographic data for **17**, **19** and **20** are fitted out in table 4.2 and the important bond parameters are listed table 4.4. The molecular structures of **17**, **19** and **21** are cationic homoleptic mononuclear copper(I) selones. The copper(I) centre in **17**, **19** and **21** are ceremoniously two coordinated with two imidazolin-2-selones and its valence satisfied with one counter anion, particularly, $[\text{CuCl}_2]^-$ for **17**, $[\text{PF}_6]^-$ ion for **19** and **21**. The cation salt **17** represent the first copper–ImC salt with loosely bound $[\text{CuCl}_2]^-$ salt.

The C=Se bond lengths in **17** (1.856(3) Å), **19** (1.853(3) Å) and **21** (1.849(3) Å) are considerably longer than that of corresponding ligands [IMes=Se (1.830(6) Å) and IPr=Se (1.822(4) Å)] [7d,k-l]. The Se–Cu bond distances are almost similar and the Se–Cu–Se bond angles found in **17**, **19** and **21** are perfectly linear as reported for linear copper(I) chalcogenones by our group [7d]. The molecules **18** and **20** produced poor quality crystals, however, the bonding modes of NHC to the copper(I) metal centre is clearly established by single crystal X-ray measurement.

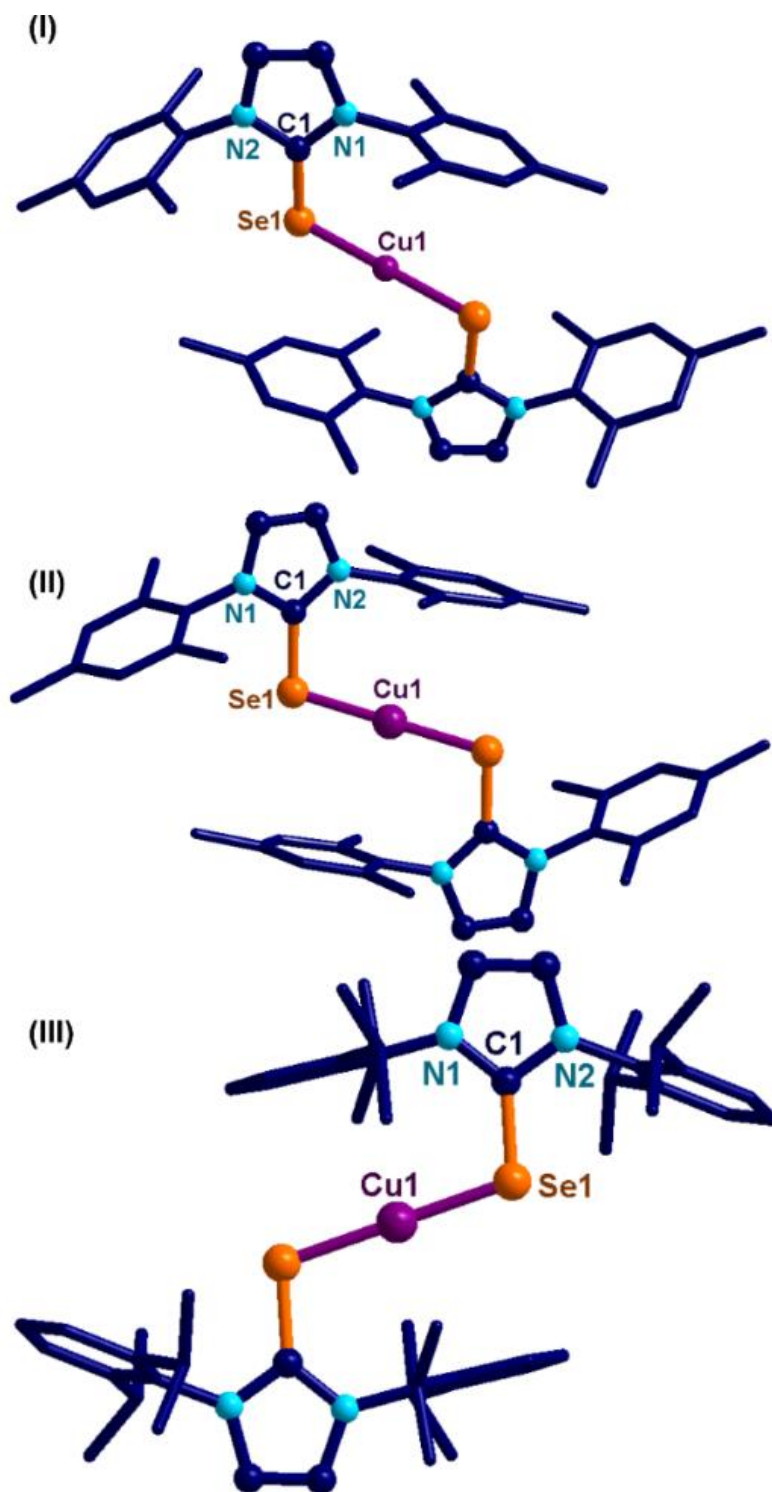
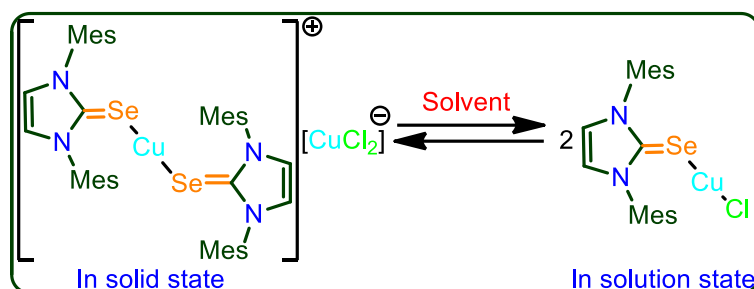


Figure 4.5: (I) Molecular structure of **17**. Hydrogen atoms and dichlorocuprate counter ions have been omitted for clarity; (II) Molecular structure of **19**. Hydrogen atoms and hexafluoro phosphate counter anions have been omitted for clarity; (III) Molecular structure of **21**. Hydrogen atoms and hexafluoro phosphate counter anions have been omitted for clarity

Interestingly, the presence of dichlorocuprate counter ion in **17** is responsible for the expected existence of mononuclear complex as shown in scheme 4.4. The NMR studies (^1H , ^{13}C , HMBC and HSQC) on molecule **17** and its comparative spectral changes with **11** suggests that the existence of mononuclear complex without any counter ion (Figures 4.6-4.10). As of our knowledge, this is the first example of imidazolin-2-selone that shows the dynamic equilibrium between homoleptic and heteroleptic species.



Scheme 4.4: Expected solution state structure of molecule **17** in solution state as suggested by NMR studies

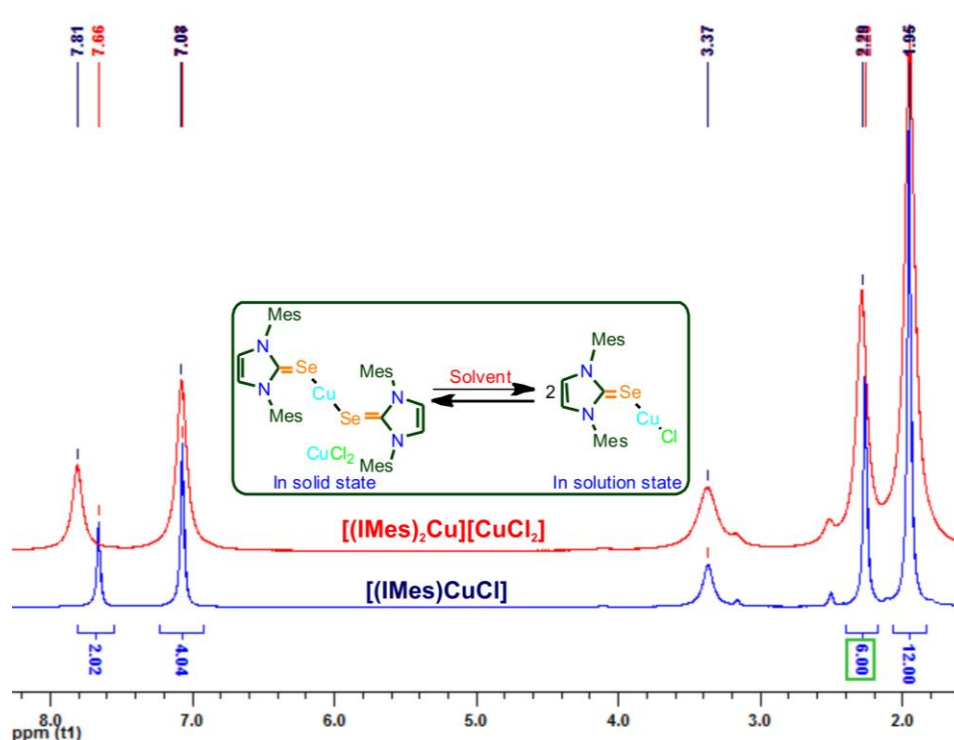


Figure 4.6: Comparison of ^1H NMR between molecules **11** and **17** in $\text{DMSO-}d_6$ at

RT

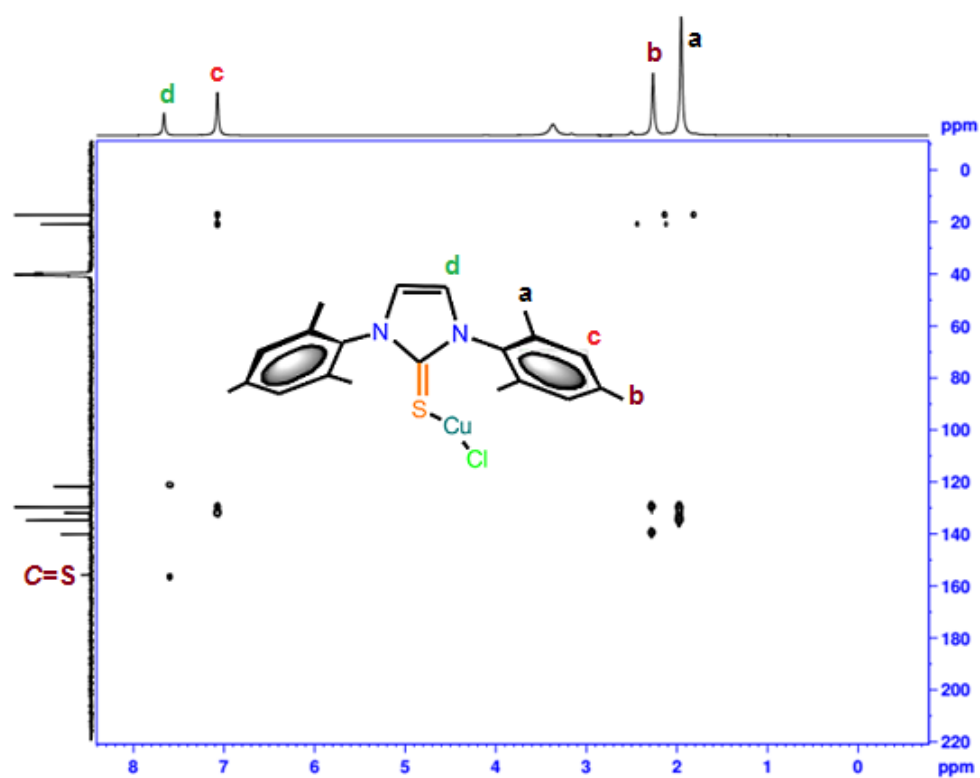


Figure 4.7: HMBC spectrum of (IMes=S)CuCl (**11**) in DMSO- d_6 at RT

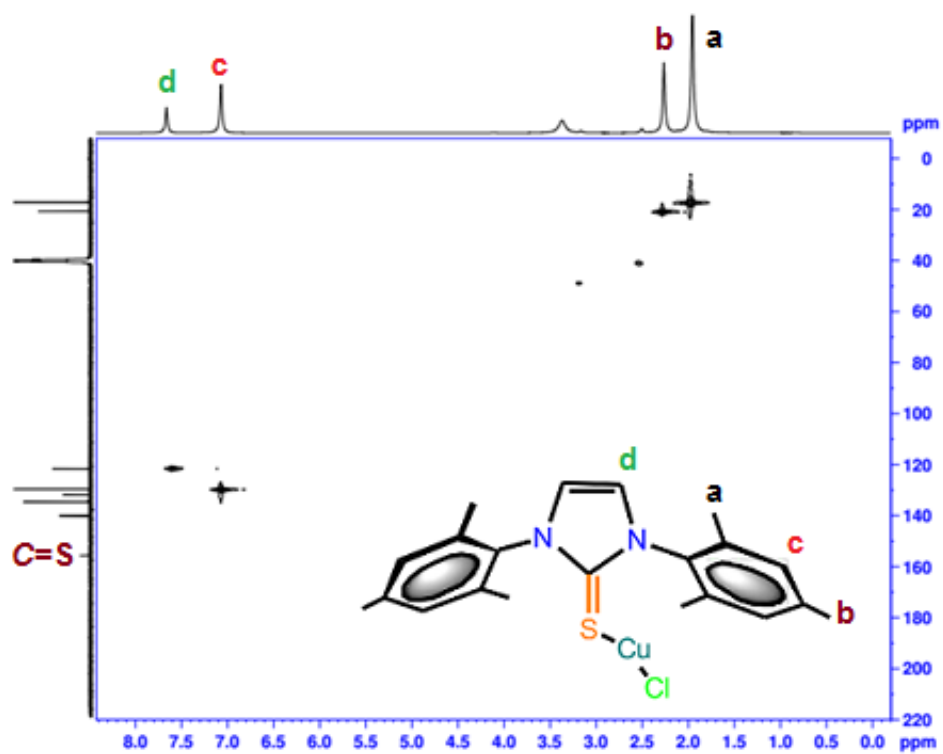


Figure 4.8: HSQC spectrum of (IMes=S)CuCl (**11**) in DMSO- d_6 at RT

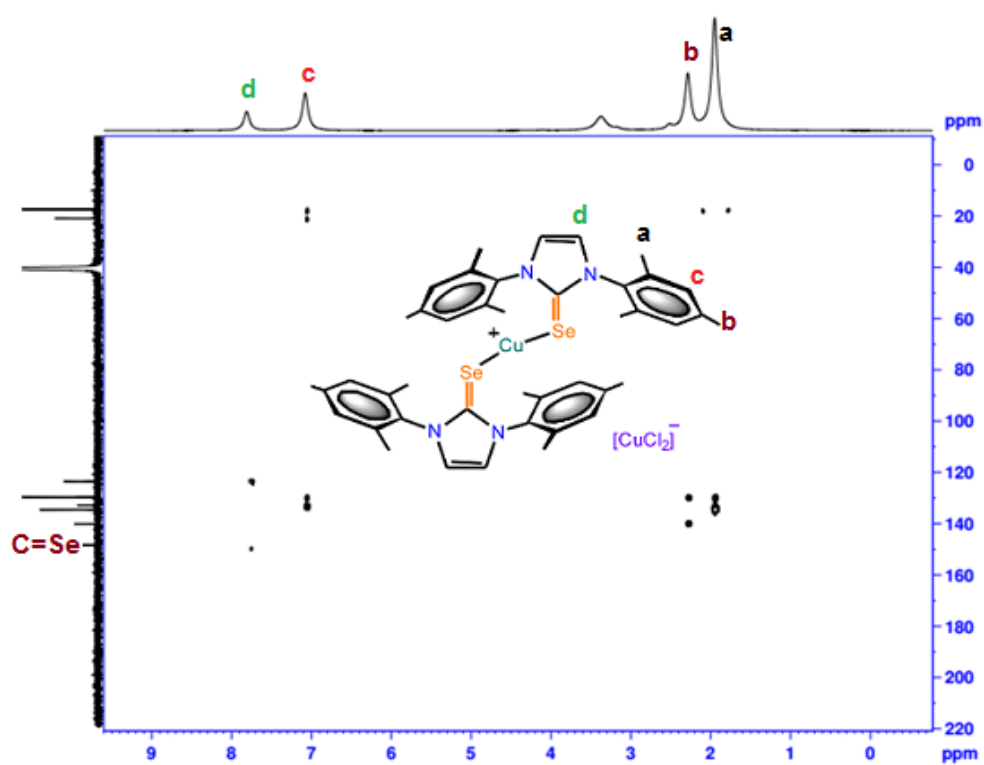


Figure 4.9: HMBC spectrum of $[(\text{IMes}=\text{Se})_2\text{Cu}][\text{CuCl}_2]$ (**17**) in $\text{DMSO-}d_6$ at RT

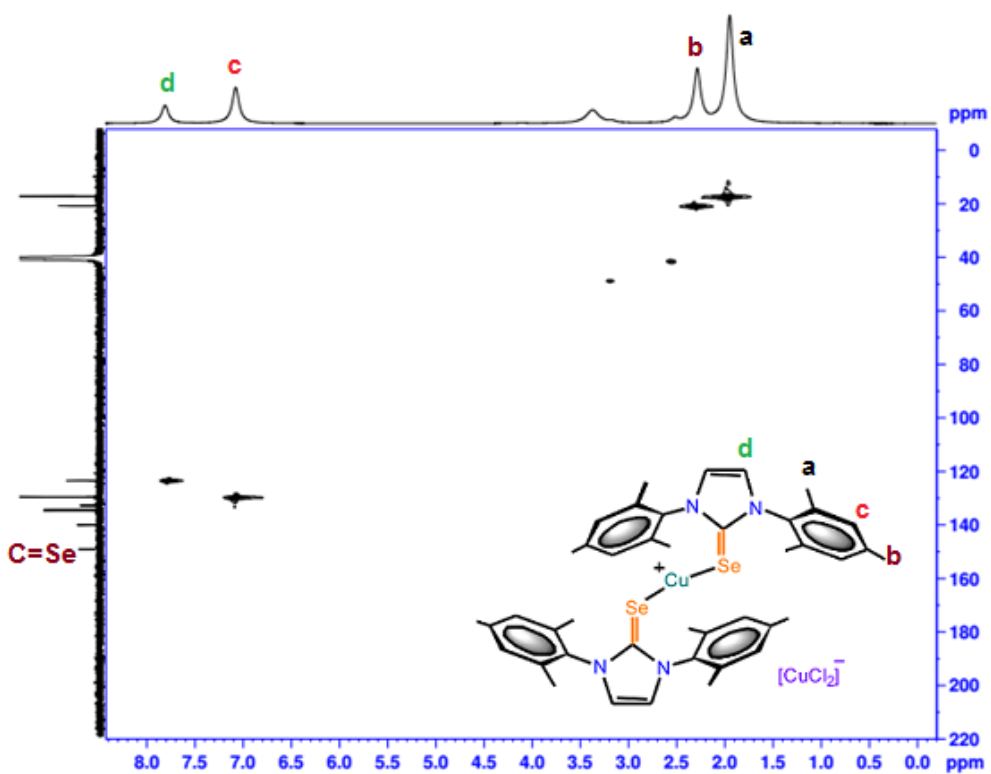


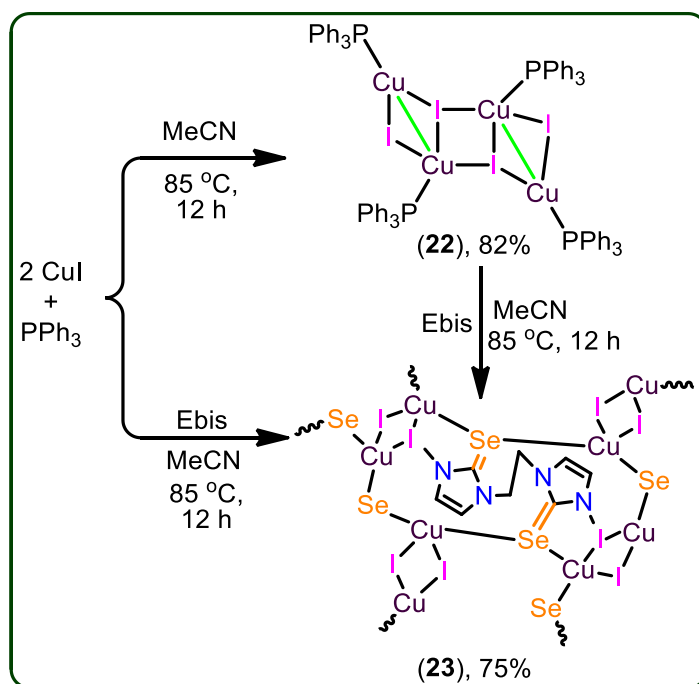
Figure 4.10: HSQC spectrum of $[(\text{IMes}=\text{Se})_2\text{Cu}][\text{CuCl}_2]$ (**17**) in $\text{DMSO-}d_6$ at RT

Table 4.2: Structural parameters of compounds **15**, **17**, **19** and **20**.

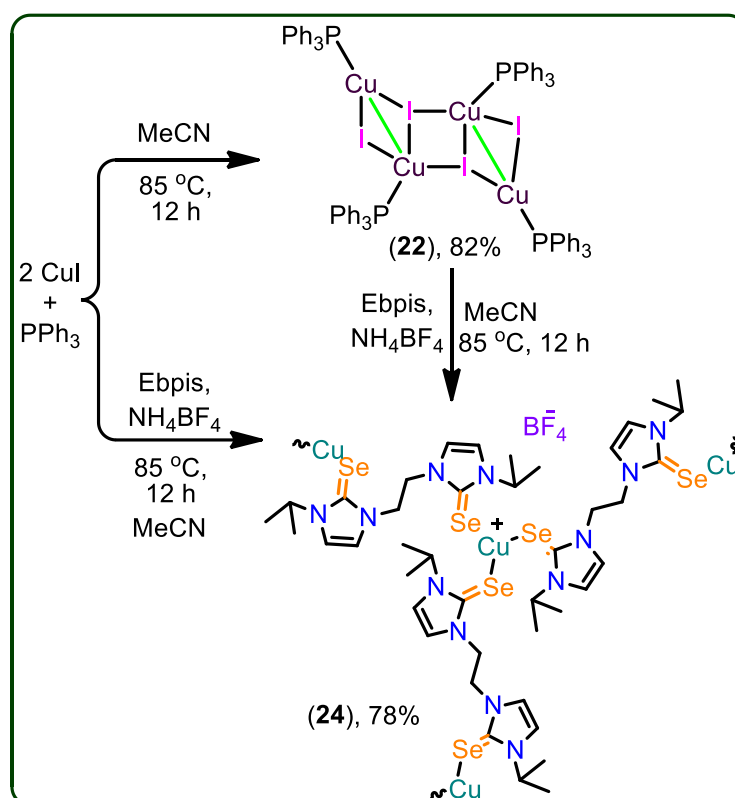
	15	17	19	21
Empirical formula	C ₂₁ H ₂₄ N ₂ Se	C ₄₂ H ₄₈ N ₄ Cl ₂	C ₄₂ H ₄₈ N ₄ F ₆	C ₅₄ H ₇₂ N ₄ F ₆
	CuI	Cu ₂ Se ₂	PCuSe ₂	PCuSe ₂
Formula weight	573.85	964.79	975.30	1143.63
Temperature (K)	298	298	298	298
Crystal system	Monoclinic	Monoclinic	Monoclinic	Monoclinic
Space group	P2 ₁ /c	P2 ₁ /n	P2 ₁ /n	C2/c
<i>a</i> /Å	11.5428(5)	8.3465(2)	8.4401(2)	19.575(8)
<i>b</i> /Å	15.3915(8)	19.3330(5)	18.3180(4)	16.342(4)
<i>c</i> /Å	13.7448(7)	13.4761(3)	14.4474(3)	20.431(10)
α /°	90	90	90	90
β /°	112.36(5)	96.74(2)	98.02(2)	113.63(5)
γ /°	90	90	90	90
Volume (Å ³)	2258.3(2)	2159.5(10)	2211.8(9)	5987.8(5)
<i>Z</i>	4	2	2	4
$\rho_{\text{calc}}/\text{mg mm}^{-3}$	1.6877	1.4836	1.4644	1.2685
Absorption coefficient (μ/mm^{-1})	13.981	4.531	3.421	2.601
<i>F</i> (000)	1110.4	968.2	984.1	2353.1
Reflections collected	9201	8771	7598	10607
<i>R</i> _{int}	0.0314	0.0497	0.0193	0.0223
GOF on <i>F</i> ²	1.021	1.046	1.040	1.045
<i>R</i> ₁ (<i>I</i> > 2 σ (<i>I</i>))	0.0490	0.0463	0.0472	0.0542
w <i>R</i> ₂ (<i>I</i> > 2 σ (<i>I</i>))	0.1503	0.1347	0.1319	0.1516
<i>R</i> ₁ values (all data)	0.0623	0.0545	0.0588	0.0665
<i>R</i> ₂ values (all data)	0.1504	0.1525	0.1522	0.1697

4.3.6. Synthesis of copper(I) coordination polymers **23** and **24**

The 2D copper(I) layer **23** was isolated in good yield by treating $[(PPh_3)_3Cu_4I_4]$ with Ebis. **23** can also be isolated from the direct reaction between CuI, PPh₃ and Ebis (Scheme 4.5). The two dimensional ionic coordination polymer of **24** was isolated from the one pot reaction between CuI, PPh₃, Ebpis and NH₄BF₄ or by treating **22** with Ebpis and NH₄BF₄ (Scheme 4.6). These experiments signifies the higher σ -donor strength of NHC=Se over PPh₃ [16]. The formation of **23** and **24** were established by elemental analysis, FT-IR, multi nuclear NMR spectroscopy and single crystal X-ray diffraction techniques. The FT-IR spectrum of **24** display the existence of BF₄ counter ion ($B-F_{stretching}$, $\bar{\nu} = 1036\text{ cm}^{-1}$), and was also approved by a signal at -0.99 ppm in ¹¹B NMR and a signal at -154.02 ppm in ¹⁹F NMR. The carbene carbon signal in **23** (155.73 ppm) and **24** (154.13 ppm) are in the up field shifted as expected after the coordination to copper [7d].



Scheme 4.5: Synthesis of **22** and **23**



Scheme 4.6: Synthesis of **24**

4.3.7. Single crystal X-ray structures of **22-24**

The solid state structures of **22-24** were determined by single crystal X-ray diffraction technique (Figure 4.11 and 4.13). Molecule **22** crystallized in monoclinic space group, C_2/c , while, **23** crystallized in the monoclinic space group, $P2_1/c$ and **24** crystallized in tetragonal space group, $P4_12_12$. The crystallographic data for **22**, **23** and **24** are listed out in table 4.3 and the important bond parameters are listed in table 4.4.

The copper(I) centre in **22** shows two types of coordination environments such as tetra and penta coordination with μ_2 and μ_3 bridging iodides. The coordination environment of penta coordinated copper in **22** is fulfilled by three iodine atoms, one phosphine and one copper atom. The coordination environment of tetra coordinated copper is fulfilled by two iodine, one phosphorus and one copper atoms. The μ_3 bridged iodine and copper distances are established to be longer than the distance noted between μ_2 bridged iodine and copper centres. The μ_3 bonded Cu–I distances (2.713(14) Å) are found to be slightly longer than the μ_2 bonded Cu–I distances (2.645(14) Å). The Cu–P bond lengths [Cu(1)–P(1), 2.248(2) Å, Cu(2)–P(2) Å, 2.227(2)] are comparable. The Cu–Cu distances in molecule **22** found to be 2.843(19) Å, which is comparable with the sum of van der Waals radii for copper (2.8 Å) [17].

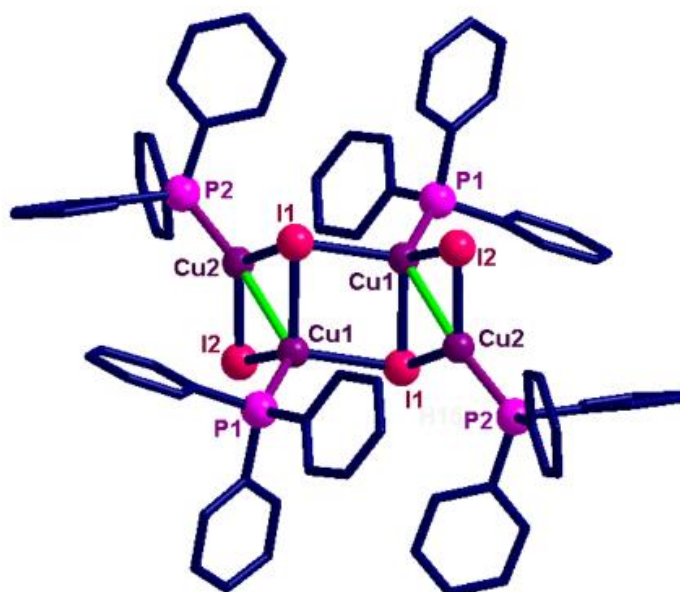


Figure 4.11: Solid state structure of **22**. Hydrogen atoms and dichlorocuprate counter ions have been omitted for clarity. Selected bond lengths (Å) and angles (°): Cu(1)–P(1), 2.248(2), Cu(2)–P(2), 2.227(2), Cu(1)–Cu(2), 2.843(19), Cu(1)–I(1), 2.713(14), Cu(1)–I(2), 2.645(14), Cu(2')–I(1), 2.590(14), Cu(2)–I(2), 2.533(14), Cu(1)–I(1)–Cu(2'), 105.86(4), Cu(1)–I(2)–Cu(2), 66.57(4), Cu(1')–I(2)–Cu(2'), 64.72(2)

The molecule **23** is a two dimensional sheet consists of Cu_2I_2 core. Each Cu_2I_2 core is further connected by Ebis ligands to form an interesting 2D layer of **23** (Figure 4.12-4.13). The copper(I) centre in **23** adopts tetrahedral geometry ($106.384(0)^\circ$ - $113.202(1)^\circ$) by two selone units and with two iodides. The bridging Cu–I distances ($2.650(12)$ Å to $2.660(13)$ Å) are in the expected range. The Se–Cu distance is ($2.553(14)$ Å) considerably longer than that of **14**, **15**, **17**, **19**, **20** and **24**. This is a rare structural evidence for the μ_2 bridging mode of bis-imidazolin-2-chalcogenone ligands [6d,e,17b].

The molecule **24** exists as two dimensional sheet through tricoordinated homoleptic copper selenide ($114.60(4)^\circ$ to $126.86(4)^\circ$). The geometry of copper(I) centre in **24** can be described as trigonal planar. The coordination environment around copper(I) is satisfied by μ_3 bridging Ebpis ligands. The Se–Cu distances in **24** are slightly elongated ($2.323(10)$ Å- $2.336(9)$ Å) due to the formation of extended coordination (Figure 4.12).

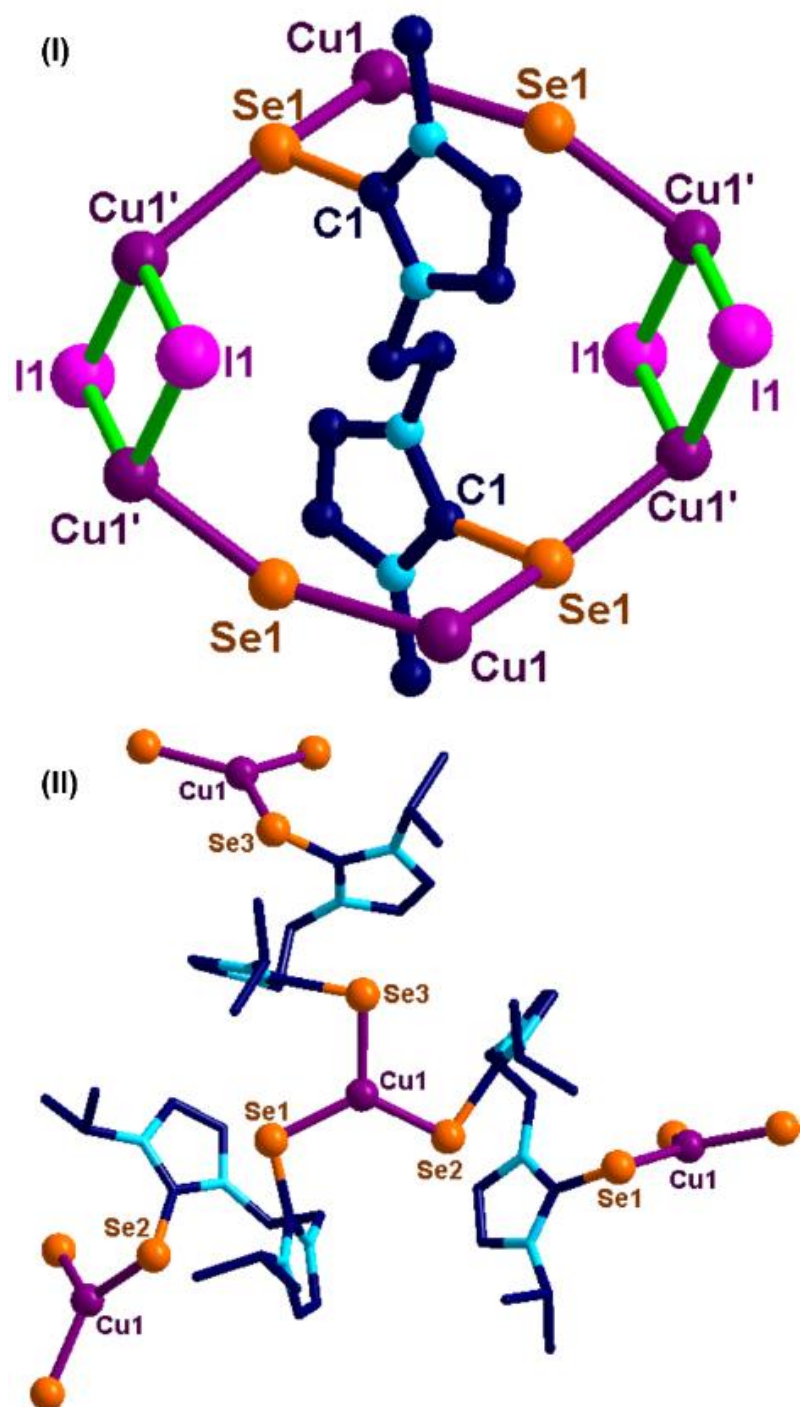


Figure 4.12: (I) Solid state structure of **23**. Hydrogen atoms have been omitted for clarity; (II) Solid state structure of **24**. Hydrogen atoms and tetrafluoroborate counter ions have been omitted for clarity

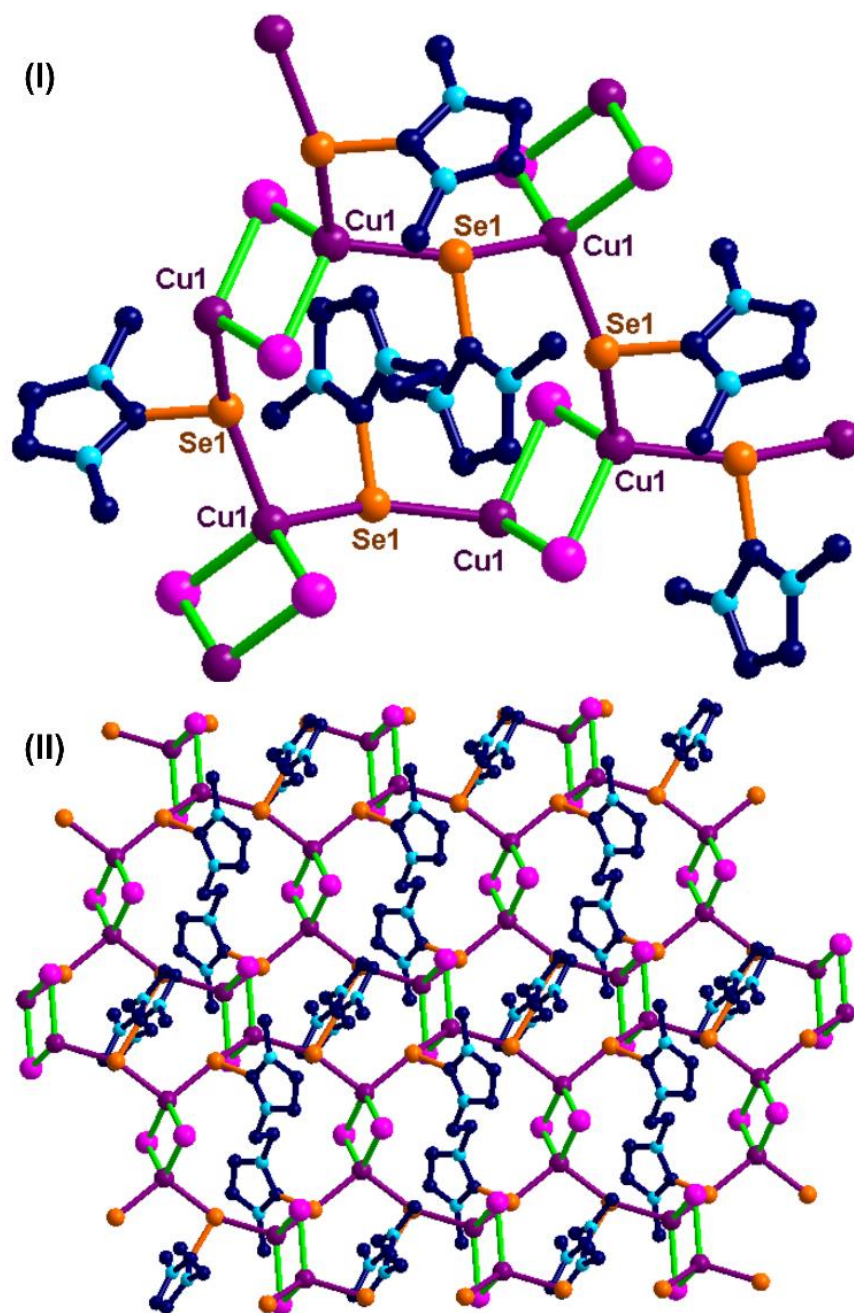


Figure 4.13: Packing arrangement of molecule 23

Table 4.3: Structural parameters of compounds **22**, **23-24**.

	22	23	24
Empirical formula	C ₇₄ H ₆₃ NP ₄ Cu ₄ I ₄	C ₅ H ₇ CuIN ₂ Se	C ₂₁ H ₃₃ N ₆ BF ₄ CuSe ₃
Formula weight	1887.03	364.53	756.78
Temperature (K)	298	298	298
Crystal system	Monoclinic	Monoclinic	Tetragonal
Space group	C2/c	P2 ₁ /c	P4 ₁ 2 ₁ 2
<i>a</i> /Å	26.6333(12)	9.8486(4)	16.4174(2)
<i>b</i> /Å	16.1396(6)	10.7720(3)	16.4174(2)
<i>c</i> /Å	18.2784(8)	8.0970(3)	22.1831(4)
<i>α</i> [°]	90	90	90
<i>β</i> [°]	110.048(5)	103.735(4)	90
<i>γ</i> [°]	90	90	90
Volume (Å ³)	7380.9(6)	834.44(5)	5979.02(16)
<i>Z</i>	4	4	8
$\rho_{\text{calc}}/\text{mg mm}^{-3}$	1.6980	2.9015	1.6813
Absorption coefficient (μ/mm^{-1})	15.579	10.604	5.613
<i>F</i> (000)	3650.2	667.7	2955.9
Reflections collected	13446	3108	12308
<i>R</i> _{int}	0.0691	0.0326	0.0230
GOF on <i>F</i> ²	1.027	1.007	1.047
<i>R</i> ₁ (<i>I</i> >2 σ (<i>I</i>))	0.0790	0.0443	0.0395
w <i>R</i> ₂ (<i>I</i> >2 σ (<i>I</i>))	0.2104	0.1237	0.1025
<i>R</i> ₁ values (all data)	0.0917	0.0572	0.0478
<i>R</i> ₂ values (all data)	0.2419	0.1395	0.1121

Table 4.4: Key bond angles and bond distances in molecules **11-24**.

	C=E (Å)	E-Cu (Å)	¹³ C (C=E)	¹³ C (C-M)	NC(Se)N (°)	E-Cu-X (°)
11^a	1.699(3)	2.129(11)	155.6	-	109.2(3)	165.94(6)
12^a	1.699(3)	2.135(9)	159.87	-	106.4(2)	163.97(4)
13^a	1.699(8)	2.142(3)	156.55	-	105.4(7)	160.72(10)
14^a	1.855(5)	2.241(11)	148.21	-	106.6(5)	163.34(6)
15^a	1.842(4)	2.252(9)	149.14	-	105.9(4)	159.60(4)
						E-Cu-E (°)
16^b	-	-	-	177.66	105.1(1)	-
17^a	1.856(3)	2.253(3)	148.59	-	106.1(3)	180.0
18^b	-	-	-	177.35	100.6(19), 105.4(17)	180.0
19^b	1.853(3)	2.252(3)	142.28	-	106.0(3)	180.0
20^b	-	-	-	177.35	93.5(16), 102.4(13)	179.1(9)
21^b	1.849(3)	2.267(3)	154.21	-	105.7(2)	180.0
23^b	1.867(7)	2.553(14)	155.73	-	106.8(6)	160.72(10)
24^b	2.336(9)	2.323(10)- 2.336(9)	154.13	-	106.0(5), 106.0(5), 108.7(12)	114.60(4)- 126.86(4)

^a [¹³C] NMR measured in DMSO-*d*₆, ^b [¹³C] NMR measured in CDCl₃

4.4. UV-vis solid and solution state absorption study of **11-24**

The solution state UV-vis absorption spectra of **11-24** were measured in CH₃CN at 25 °C (Figure 4.14).

The solid state UV-visible spectra of **11-24** are broad compared to their solution state UV-visible spectra, mainly due to the molecular association in the solid state. The selone derivatives (**14** and **15**) of IMes=E show slight bathochromic shift compared to the thione derivatives (**11-13**).

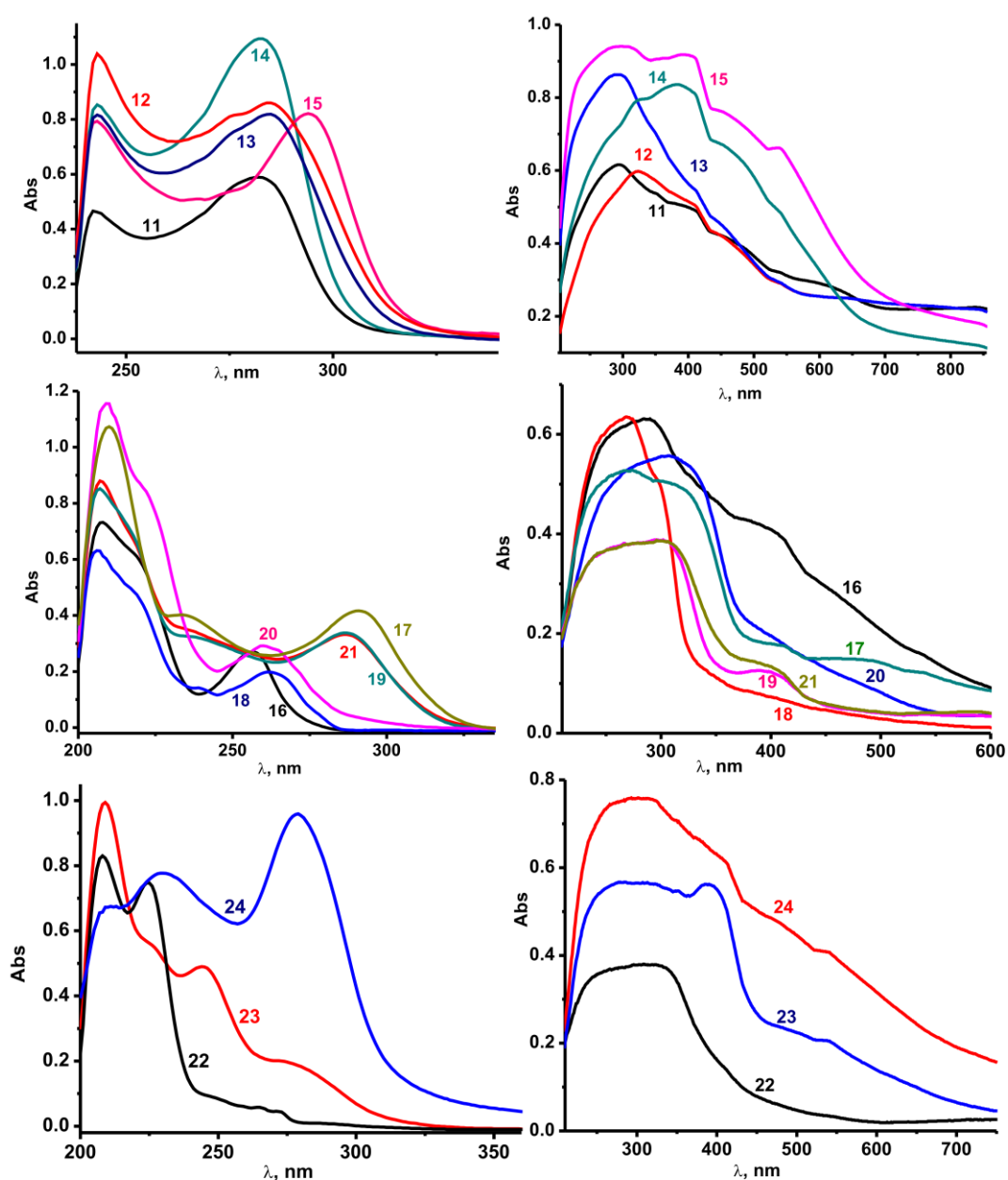


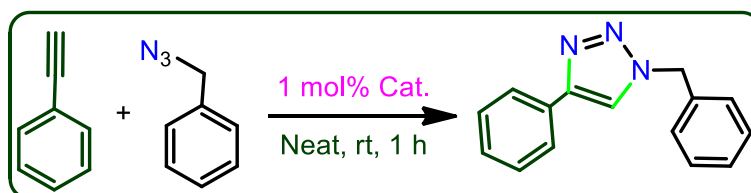
Figure 4.14: (I) Solution UV-vis spectra of complexes **11-15** in acetonitrile at 298 k with 1.2×10^{-5} M solutions; (II) Solid state UV-vis spectra of complexes **11-15** at 298 k; (III) Solution UV-vis spectra of complexes **16-21** in acetonitrile at 298 k with 1.2×10^{-5} M solutions; (IV) Solid state UV-vis spectra of complexes **16-21** at 298 k; (V) Solution UV-vis spectra of complexes **22-24** in acetonitrile at 298 k with 1.2×10^{-5} M solutions; (VI) Solid state UV-vis spectra of complexes **22-24** at 298 k.

Besides, all the complexes show absorption at higher wavelength than corresponding ligands IMes=S (243, 273 nm), IMes=Se (246, 290 nm) [7k]. The solution state spectra is

almost identical except for **15**, which shows slight red shift. Molecules, **18** and **20** shows slight red shift for $n-\pi^*$ transitions, while in the solid state $\pi-\pi^*$ and $n-\pi^*$ transitions are merged together to show a broad absorption range to support the molecular association. Upon coordination, **17**, **19** and **21** depicts about 50 nm shift for $n-\pi^*$ transitions due to the influence of selone moiety. Besides, the solid state UV-visible spectra of complexes **22-24** displayed a broad signal in the range of 200-400 nm, while the same appears to be distinct signals for $\pi-\pi^*$ and $n-\pi^*$ transitions in solution state UV-visible study. The absorption band appeared at 274 nm (for **23**) and 278 nm (for **24**) can be assigned to ligand-metal charge transfer.

4.5. Copper catalysts mediated cycloaddition of azides and terminal alkynes

The application of newly isolated catalysts (**11-15**, **17**, **19** and **21-24**) were investigated for the click reaction of azides with terminal alkynes [18-21]. Besides, the well-known catalyst, such as [(IMes)CuCl] (**16**) together with its homoleptic NHC derivatives such as [(IMes)₂Cu][Cl] (**18**) and [(IMes)₂Cu][PF₆] (**20**) were also tested for comparison. Therefore, we have demonstrated the click catalysis using ImC supported copper(I) complexes and compared the catalytic efficiency with NHC and phosphine supported copper(I) complexes for the first time. To the best of our knowledge, the significance of ancillary ligands such as PPh₃, NHC, NHC=S and NHC=Se have never been compared in any catalysis [7d-e,6,20].



Scheme 4.7: [3+2] cycloaddition of benzylazide with phenyl acetylene

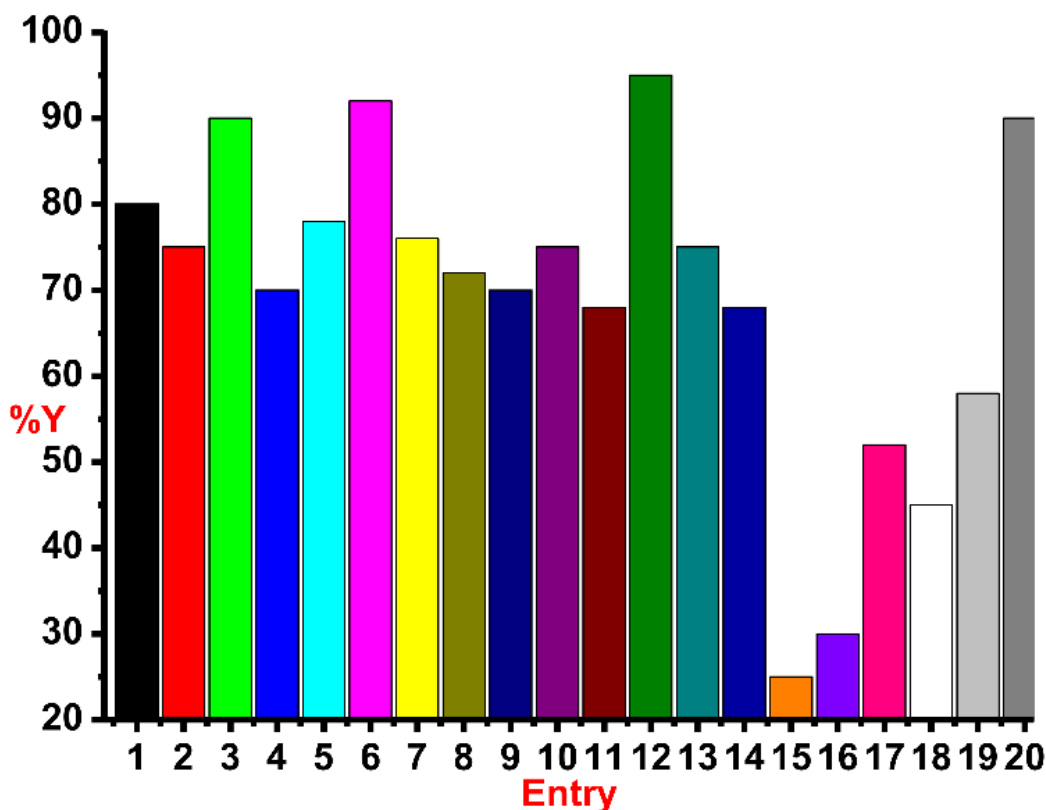


Figure 4.15: Screening of catalysts **11-24** in click catalysis (entries 1-14); Reaction conditions; phenyl acetylene (1.2 mmol), benzyl azide (1.0 mmol), catalyst (1 mol%) and neat condition at RT, E-entry, Entries: **15**; only CuCl, **16**; only CuI, **17**; IMes=S and CuCl, **18**; IMes.HCl and CuCl, **19**; PPh₃ and CuI, **20**; 0.5 mol% **22** for 4 h, %Y; %-Isolated yield by column chromatography

The catalytic reactions were carried out under neat conditions at room temperature (Scheme 4.7). Notably, the catalysts **11-16**, **18** and **20** (entries 1-6,8,10) gave very good conversion (70-92%) within 1 h [19]. Besides, linear copper(I) chalcogenones (**17**, **19** and **21**) gave moderate yield (68-76%, entries 7, 9 and 11). Moreover, the coordination polymers (**23** and **24**) (68-75%, entries 13-14) are found to be active like linear chalcogenones in this catalysis. Despite the fact that the phosphine based copper(I) iodide (**22**) was found to be much more efficient (95%, entry 12) among all the catalysts isolated herein. The catalysts **13**, **16** and **22** were found to be efficient in this catalysis (90-95%, entries 3, 6 and 12) among all the isolated catalysts **11-24** (Chart 4.4). Therefore the effect of ligand for this transformation has been investigated by carrying out the experiments with only copper(I) chloride (entry 15) or copper(I) iodide (entry 16) and noticed a poor yield. The *insitu* generated catalysts gave considerable yields (52-58%, entries 17 and 19). Besides, the IMes.HCl addition to CuCl is

also produced a decent yield (45%, entry 18). Therefore, the entries 15-19 employ the significance of the presence of ligand for this reaction and distinguishes the prominence of well-defined catalyst. However, the decrease in catalyst **22** quantity to 0.5 mol% led to the isolation of 90% yield after 4 h (entry 20). Thus the catalysts **13**, **16** and **22** seems to be the efficient catalysts.

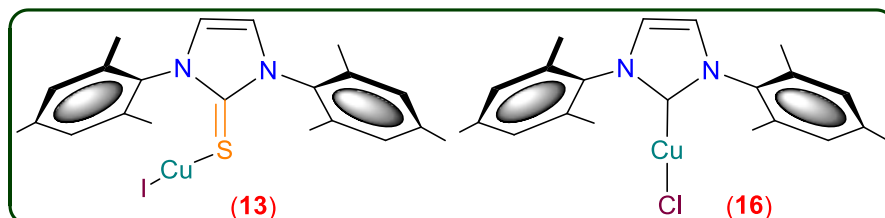


Chart 4.4: Catalysts used for the substrate scope in click catalysis

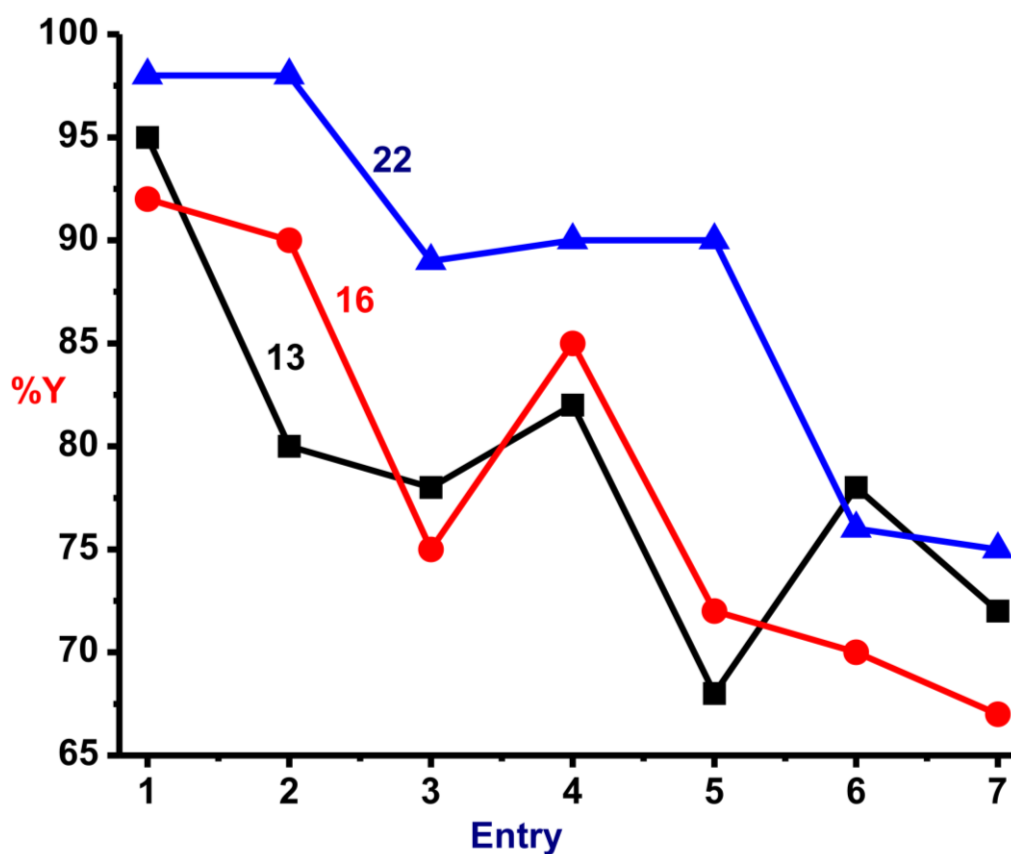
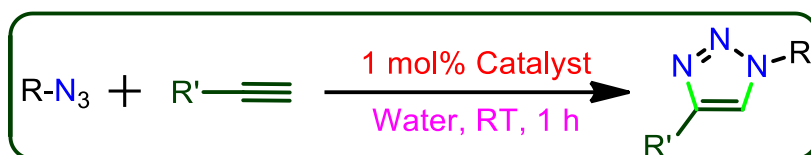
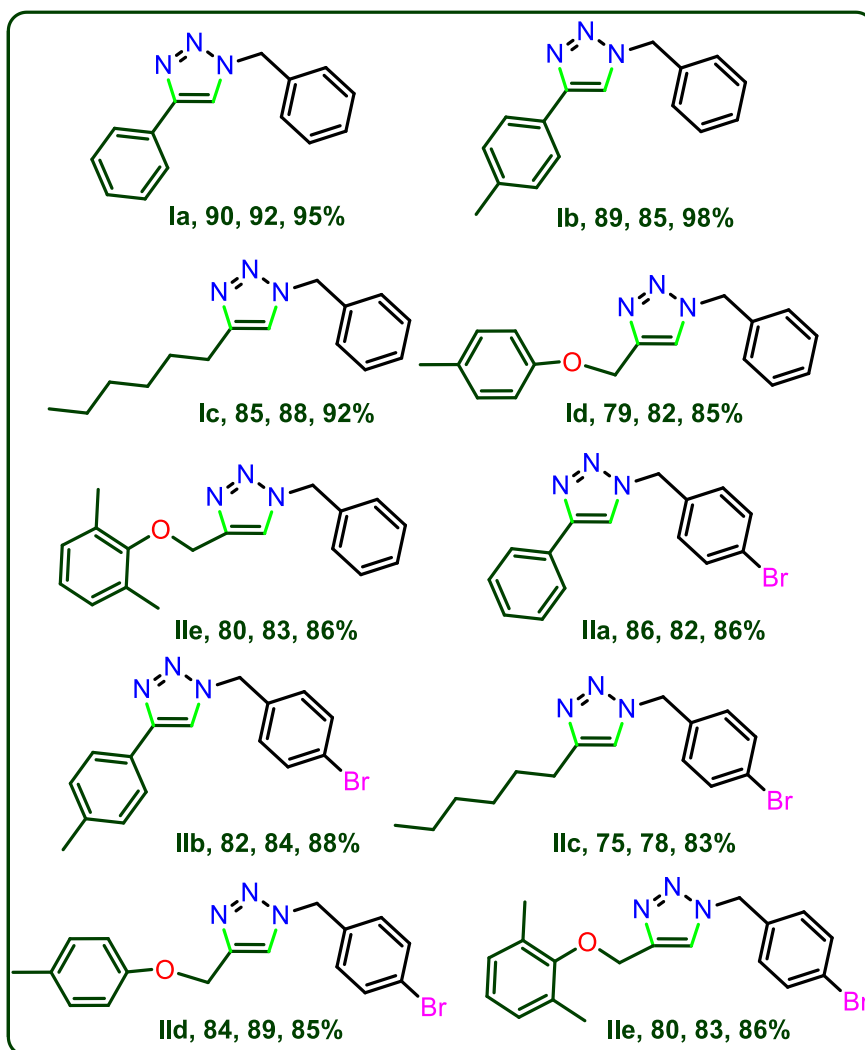


Figure 4.16: Solvent screening in various solvents using catalysts **13** (Black), **16** (Red) and **22** (Green); Reaction conditions: phenylacetylene (1.2 mmol), benzylazide (1.0 mmol), catalyst (1 mol%) and solvent at RT; Entries: 1; in Water, 2; in DMSO:Water, 3; in THF:Water, 4; in ^tBuOH:Water, 5; in ^tBuOH, 6; in DMSO and 7; in THF; %Y: %-Isolated yield by column chromatography

In order to investigate the effect of solvent in this reaction, the relatively better catalysts (**13**, **16** and **22**) were subjected to click catalysis in various polar solvents as described in figure 4.16. Virtually the identical out put was perceived for all three catalysts in different solvents. However, water was found to be a better choice (entry 1). Therefore, all three catalysts **13**, **16** and **22** were examined for the substrate scope in water (Scheme 4.8, Chart 4.5). Interestingly, the substantial discrepancies in reactivity have not been observed. The catalysts **13**, **16** and **22** were remarkably efficient.



Scheme 4.8: [3+2] cycloaddition of arylazides with terminal alkynes



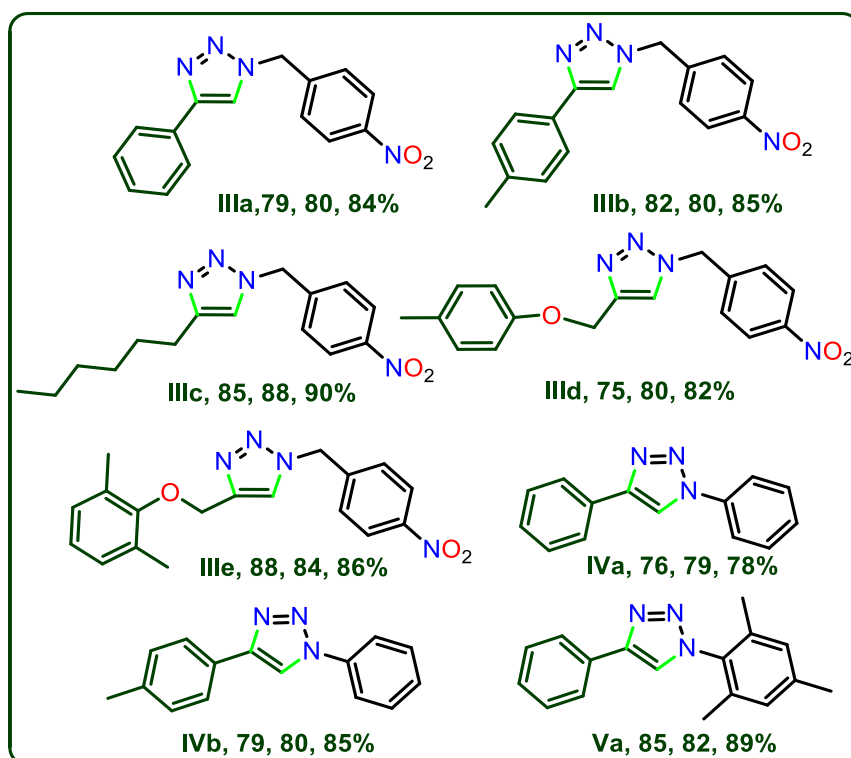


Chart 4.5: 1,2,3-triazoles isolated by click catalysis by **13**, **16** and **22** in water

The plausible mechanistic pathway through which the thione/selone supported copper(I) complex proceeds the click catalysis has been displayed in chart 4.6-4.7 [22].

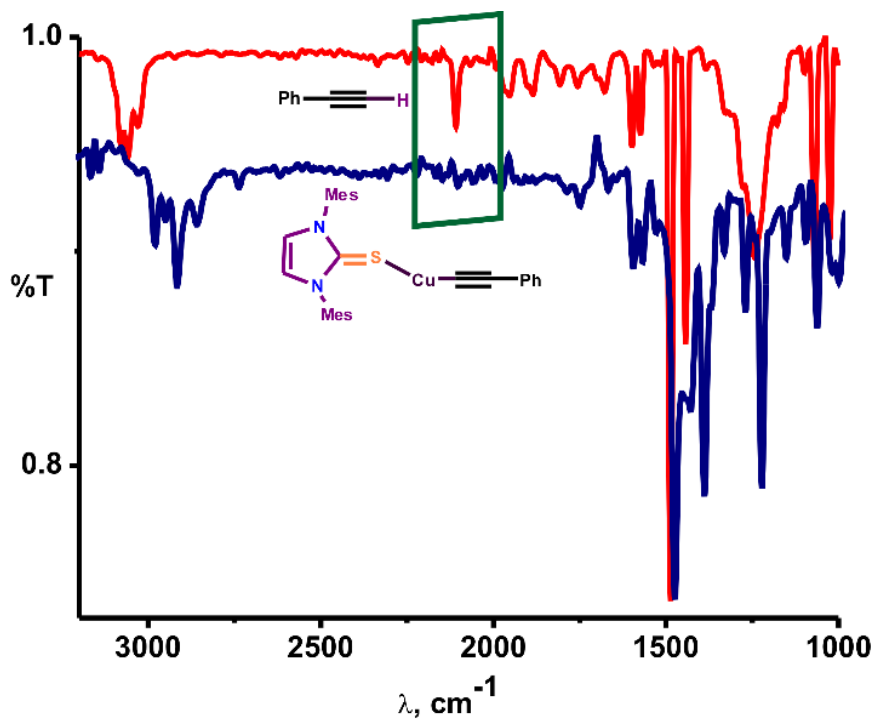


Figure 4.17: FT-IR spectral comparison of phenyl acetylene and its mixture with molecule

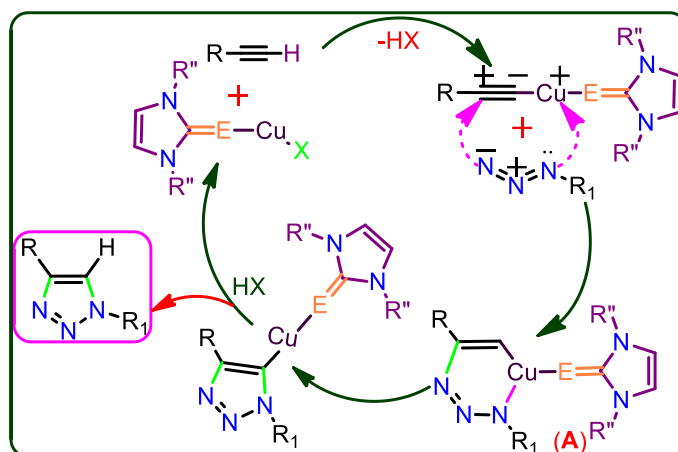


Chart 4.6: Plausible mechanism for Huisgen coupling reaction by catalyst **13**

The copper(I) catalyst is expected to form an intermediate **A** by coordinating with both terminal alkyne and azide (Chart 4.7). Followed by the successive reproduction of catalyst to yield the desired 1,2,3-triazoles.

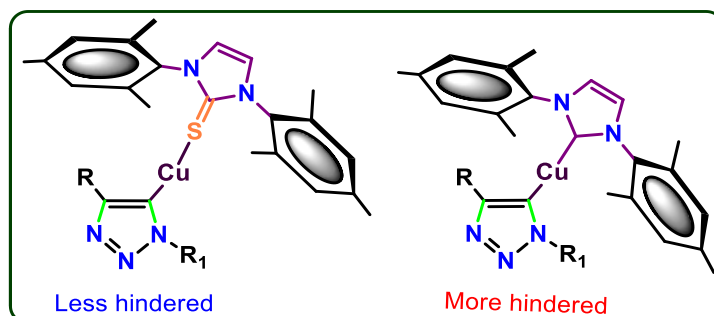


Chart 4.7: Expected steric hindrance at the metal centre in **13** and **16**

It is worth stating that, the steric hindrance in molecules **17-21** and **23-24** plays a major influence in constructing the intermediate **A**, which disfavors the product formation compared to catalysts **13** and **16**. The reasonably less steric hindrance exists at the metal centre in **13** due to the localization of metal centre away from NHC *via* thione, favours the formation of intermediate **A** in addition to the easy leaving iodine attached to the metal (Chart 4.7). Besides, the greater efficiency of **22** is anticipated by the presence of more number of electrophilic metal centers, while, **13** and **16** display relatively less activity because of the presence of weakly π -accepting ligands attached to the metal.

4.6. Copper catalysts mediated C–Si bond formation reactions

Alkynylsilane derivatives are the noticeable class of structural motifs in organic synthesis as Si-masked synthetic intermediates, particularly for C–C and C–X (X = hetero atom) bond formation reactions [23]. Cross-dehydrogenative coupling of terminal alkynes and hydrosilanes has been studied by using various metal salts such as $\text{H}_2\text{PtCl}_6/\text{I}_2$, CuCl/TMEDA (TMEDA = *N,N,N',N'*-tetraethylenediamine), LiAlH_4 , $\text{Zn}(\text{SO}_2\text{CF}_3)_2/\text{pyridine}$, MgO , and $\text{KNH}_2/\text{Al}_2\text{O}_3$ [24]. However, the metal complexes mediated cross-dehydrogenative coupling is limited, the only example known so far is $\text{M}(\eta^2\text{-Ph}_2\text{CNPh})(\text{hmpa})_3$ (M = Yb or Ca, hmpa = hexamethylphosphoramide) (Chart 4.8) [25].

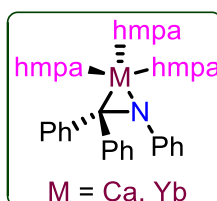
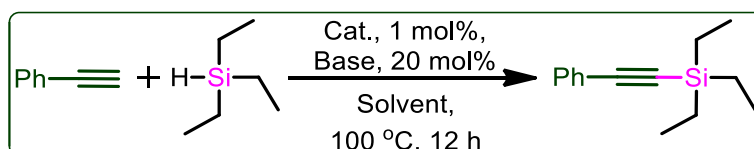


Chart 4.8: Catalysts used for cross-dehydrogenative coupling of alkynes

Initially, the dehydrogenative silylation was examined for suitable reaction conditions using phenyl acetylene and triethylsilane (1:1.2 equivalents) in acetonitrile at 100 °C for 12 h without base (entry 1) with 1 mol% catalyst **13** gave 65% of desired product. Interestingly, the addition of catalytic amounts (20 mol%) of organic base such as pyridine produced quantitative yield (entry 2). Nevertheless, the catalyst **16** and **22** also conceded the desired product in very good yield (entry 13, 14).



Scheme 4.9: Cross-dehydrogenative coupling of terminal alkynes

Consequently, catalyst **13** was utilized for this transformation to find out the suitable conditions. The effect of base was investigated by employing the reaction with K_2CO_3 (entry 4), KO^tBu (entry 5), NEt_3 (entry 6) and KOH (entry 7). However, none of them produces the quantitative yield (55-78% only). Then the solvent effect on this reaction was studied by using CH_3OH (entry 8), THF (entry 9), 1,4-dioxane (entry 10) and toluene (entry 11). The change in solvent does not favor the formation of desired product. Subsequently, the influence of temperature on the reaction rate was investigated (entry 12) by performing the reaction at room temperature. Even after extending the time for 24 h, the desired product formed is not

satisfactory. Similarly, the significance of catalyst in this transformation was reviewed by performing this experiment without catalyst. The yields are found to be inadequate (entry 3).

Table 4.5: Copper(I) mediated cross-dehydrogenative coupling reactions.^a

E	Solvent	Base	SMC (%)^b
1	CH ₃ CN	-	65
2	CH ₃ CN	Pyridine	98
3^c	CH ₃ CN	Pyridine	10
4	CH ₃ CN	K ₂ CO ₃	57
5	CH ₃ CN	KO ^t Bu	78
6	CH ₃ CN	NEt ₃	55
7	CH ₃ CN	KOH	68
8	CH ₃ OH	Pyridine	12
9	THF	Pyridine	19
10	1,4-dioxane	Pyridine	14
11	Toluene	Pyridine	30
12^d	CH ₃ CN	Pyridine	62
13^e	CH ₃ CN	Pyridine	95
14^f	CH ₃ CN	Pyridine	92

^aReaction conditions: Phenylacetylene (0.40 mmol), Triethylsilane (0.60 mmol), Catalyst (1 mol%), base (20 mol%), solvent (1.0 mL); SMC: Starting Material Conversion; ^bPercentage of conversions are based on GC (The given GC conversion values are the average of at least two independent measures); ^cwithout catalyst; ^dreaction at room temperature; ^ewith catalyst

16; ^fwith catalyst **22**

As presented in chart 4.9 phenyl acetylene and 1-octyne were treated with triethylsilane, dimethylphenylsilane and achieved over 90% yields (compounds VI-IX). Similarly the double dehydrogenative coupling was carried out using diphenylsilane to afford the silicon-tethered diyne building blocks (X-XI) with very good yield. It is worth mentioning that the dehydrogenative coupling of alkynes with triphenyl silane led to the recovery of starting materials that supports the unfavorable condition of steric bulk of silane in this transformation.

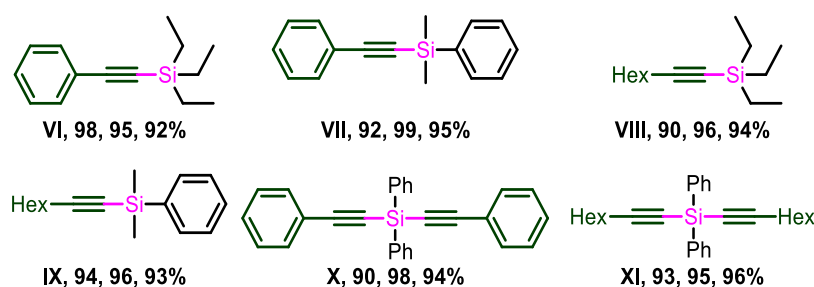


Chart 4.9: Alkynylsilanes isolated by **13**, **16** and **22**. Reaction conditions for X and XI; phenyl acetylene (0.80 mmol), diphenylsilane (0.40 mmol), catalyst (1 mol%), base (20 mol%) and solvent (1 mL)

4.7. Summary

In summary, copper(I) complexes supported by NHC (for **16**, **18** and **20**), NHC=E (for **11-15**, **17**, **19**, **21**, **23** and **24**) and PPh₃ (for **22**) were synthesized and structurally characterized. The molecules **11-15** were isolated as rare mononuclear NHC=E supported neutral copper(I) chalcogenones. The molecules **17**, **19** and **21** were isolated by ligand exchange reaction between [(IMes)CuCl] and IMes=Se (for **17** and **19**) and IPr=Se (for **21**) along with homoleptic copper(I)-NHC complexes **16**, **18** and **20**. The synthetic methodology of **16**, **18** and **20** represent the first synthetic strategy to isolate copper chalcogenones from copper carbene derivatives. Complexes **17-21** display a perfect linear geometry around copper(I) center. The molecules **23** and **24** were isolated from phosphine based copper(I) iodide complex **22**. These newly isolated molecules **11-24** were used as catalyst for [3+2] cycloaddition of azides with terminal alkynes. The catalysts **13**, **16** and **22** were relatively more active for cycloaddition reactions. Besides, cationic **13**, **16** and **22** were found to be efficient in C–Si bond formation reaction. Thus, (i) The ligand exchange experiment signifies the higher σ -donor abilities of NHC=E, (ii) PPh₃ based catalyst (**22**) is effective in click catalysis over NHC=E and NHC based catalysts, (iii) Less steric hindrance and more Lewis acidic metal centre facilitates the reaction, (iv) The efficiencies derived in this work are **22**>**13**>**16**>**11**=**12**=**14**=**15**>**18**=**20**=**17**=**19**=**21**=**23**=**24**, (v) σ -donor strength detected is in the following order; ImC>NHC>PPh₃. Nevertheless the investigations towards the comparison between NHC and NHC-analogous metal complexes in terms of stability, reactivity in organic transformations in order to reduce the reaction times and produce quantitative yields is in progress in our laboratory.

4.8. References

- [1] (a) S. V. C. Vummaleti, D. J. Nelson, A. Poater, A. G. –Suárez, D. B. Cordes, A. M. Z. Slawin, S. P. Nolan and L. Cavallo, *Chem. Sci.*, 2015, **6**, 1895–1904; (b) M. K. Barman, A. K. Sinha and S. Nembenna, *Green Chem.*, 2016, **18**, 2534-2541; (c) M. Melaimi, R. Jazzar, M. Soleilhavoup and G. Bertrand, *Angew. Chem. Int. Ed.*, 2017, **56**, 10046–10068; (d) D. J. Nelson, F. Nahra, S. R. Patrick, D. B. Cordes, A. M. Z. Slawin and S. P. Nolan, *Organometallics* 2014, **33**, 3640-3645.
- [2] (a) M. M. Kimani, C. A. Bayse, B. S. Stadelman and J. L. Brumaghim, *Inorg. Chem.*, 2013, **52**, 11685–11687; (b) E. E. Battin, M. T. Zimmerman, R. R. Ramoutar, C. E. Quarles and J. L. Brumaghim, *Metallomics*, 2011, **3**, 503–512.
- [3] J. Choi, N. Kang, H. Y. Yang, H. J. Kim and S. U. Son., *Chem. Mater.* 2010, **22**, 3586–3588.
- [4] (a) D. J. D. Wilson, S. A. Couchman and J. L. Dutton, *Inorg. Chem.* 2012, **51**, 7657-7668; (b) K. Verlinden, H. Buhl, W. Frank and C. Ganter, *Eur. J. Inorg. Chem.* 2015, **14**, 2416-2425; (c) D. J. Nelson, A. Collado, S. Manzini, S. Meiries, A. M. Z. Slawin, D. B. Cordes and S. P. Nolan, *Organometallics* 2014, **33**, 2048-2058; (d) A. Liske, K. Verlinden, H. Buhl, K. Schaper and C. Ganter, *Organometallics* 2013, **32**, 5269-5272.
- [5] (a) Y. Rong, A. A. -Harbi, B. Kriegel and G. Parkin, *Inorg. Chem.* 2013, **52**, 7172-7182; (b) V. Rani, H. B. Singh and R. J. Butcher, *Eur. J. Inorg. Chem.*, 2017, **31**, 3720-3728.
- [6] (a) C. A. Bayse, J. L. Brumaghim, *Biochalcogen Chemistry: The Biological Chemistry of Sulphur, Selenium and Tellurium*, ACS Symposium series 1152, American Chemical Society: Washington, DC, 2013, pp. 57-64; (b) M. M. Kimani, J. L. Brumaghim and D. VanDerveer, *Inorg. Chem.* 2010, **49**, 9200-9211; (c) M. M. Kimani, H. C. Wang and J. L. Brumaghim, *Dalton Trans.* 2012, **41**, 5248-5259; (d) M. M. Kimani, C. A. Bayse and J. L. Brumaghim, *Dalton Trans.* 2011, **40**, 3711-3723; (e) M. M. Kimani, D. Watts, L. A. Graham, D. Rabinovich, G. P. A. Yap and J. L. Brumaghim, *Dalton Trans.* 2015, **44**, 16313-16324; (f) B. S. Stadelman, M. M. Kimani, C. A. Bayse, C. D. McMillen and J. L. Brumaghim, *Dalton Trans.* 2016, **45**, 4697-4711.
- [7] (a) E. Alvarado, A. C. Badaj, T. G. Larocque and G. G. Lavoie, *Chem. Eur. J.*, 2012, **18**, 12112-12121; (b) J. Jin, H. –W. Shin, J. H. Park, J. H. Park, E. Kim, T. K. Ahn, D. H. Ryu and S. U. Son., *Organometallics* 2013, **32**, 3954-3959; (c) N. Ghavale, S. T. Manjare, H. B. Singh and R. J. Butcher., *Dalton Trans.*, 2015, **44**,

- 11893-11900; (d) K. Srinivas, C. N. Babu and G. Prabusankar., *Dalton Trans.*, 2015, **44**, 15636–15644; (e) H. R. Kim, H. G. Jung, K. Yoo, K. Jang, E. S. Lee, J. Yun and S. U. Son, *Chem. Commun.*, 2010, **46**, 758–760; (f) C. N. Babu, K. Srinivas and G. Prabusankar., *Dalton Trans.*, 2016, **45**, 6456-6465; (g) W. –G. Jia, Y. –B. Huang, Y. –J. Lin and G. –X. Jin., *Dalton Trans.*, 2008, 5612–5620; (h) Y. –B. Huang, W. –G. Jia and G. –X. Jin., *J. Organomet. Chem.*, 2009, **694**, 86–90; (i) A. K. Sharma, H. Joshi, R. Bhaskar and A. K. Singh., *Dalton Trans.* 2017, **46**, 2228-2237; (j) O. Prakash, K. N. Sharma, H. Joshi, P. L. Gupta and A. K. Singh., *Organometallics* 2014, **33**, 2535-2543; (k) K. Srinivas, P. Suresh, C. N. Babu, A. Sathyanarayana and G. Prabusankar., *RSC Adv.*, 2015, **5**, 15579–15590; (l) K. Srinivas, A. Sathyanarayana, C. N. Babu and G. Prabusankar., *Dalton Trans.*, 2016, **45**, 5196–5209; (m) L. –M. Zhang, H. –Y. Li, H. –X. Li, D. J. Young, Y. Wang and J. –P. Lang., *Inorg. Chem.* 2017, **56**, 11230-11243.
- [8] K. Srinivas and G. Prabusankar., *Dalton Trans.*, 2017, **46**, 16615-16622.
- [9] D. D. Perrin and W. L. F. Armarego, *Purification of laboratory chemicals*, Pergamon Press, London, 3rd edn, 1988.
- [10] O. V. Dolomanov, L. J. Bourhis, R. J. Gildea, J. A. K. Howard and H. Puschmann, *J. Appl. Crystallogr.*, 2009, **42**, 339–341.
- [11] (a) G. M. Sheldrick, *Acta Crystallogr. Sect. A: Found. Crystallogr.*, 1990, **46**, 467–473; (b) G. M. Sheldrick, *SHELXL-97, Program for Crystal Structure Refinement*, Universität Göttingen, Göttingen, 1997.
- [12] N. Parvin, S. Pal, S. Khan, S. Das, S. K. Pati and H. W. Roesky., *Inorg. Chem.*, 2017, **56**, 1706-1712.
- [13] H. Borrmann, I. Persson, M. Sandström and C. M. V. Stålhandske, *J. Chem. Soc., Perkin Trans. 1*, 2000, 393–402.
- [14] T. Steiner., *Angew. Chem. Int. Ed.* 2002, **41**, 48-76.
- [15] W. Xie, J. H. Yoon and S. Chang., *J. Am. Chem. Soc.* 2016, **138**, 12605-12614.
- [16] (a) M. R. L. Furst and C. S. J. Cazin., *Chem. Commun.*, 2010, **46**, 6924–6925; (b) N. M. Scott and S. P. Nolan., *Eur. J. Inorg. Chem.* 2005, 1815–1828; (c) G. A. Blake, J. P. Moerdyk and C. W. Bielawski., *Organometallics* 2012, **31**, 3373-3378.
- [17] (a) V. Charra, P. d. Frémont and P. Braunstein., *Coord. Chem. Rev.*, 2017, **293**, 48-79; (b) M. Slivarichova, R. C. d. Costa, J. Nunn, R. Ahmad, M. F. Haddow, H. A. Sparkes, T. Gray and G. R. Owen., *J. Organomet. Chem.*, 2017, **847**, 224-233.

- [18] (a) T. Nakamura, T. Terashima, K. Ogata and S. –i. Fukuzawa., *Org. Lett.*, 2011, **13**, 620-623; (b) S. D. –González, A. Correa, L. Cavallo and S. P. Nolan., *Chem. Eur. J.* 2006, **12**, 7558–7564.
- [19] S. D. –González, E. C. E. –Adán, J. B. –Buchholz, E. D. Stevens, A. M. Z. Slawin and S. P. Nolan., *Dalton Trans.*, 2010, **39**, 7595–7606.
- [20] (a) R. Berg, J. Straub, E. Schreiner, S. Mader, F. Rominger and B. F. Straub, *Adv. Synth. Catal.*, 2012, **354**, 3445-3450; (b) S. C. Sau, S. R. Roy, T. K. Sen, D. Mullangi and S. K. Mandal, *Adv. Syn. Catal.*, 2013, **355**, 2982-2991; (c) S. Hohloch, C. –Y. Su and B. Sarkar, *Eur. J. Inorg. Chem.*, 2011, 3067-3075; (d) F. Wang, H. Fu, Y. Jiang and Y. Zhao, *Green Chem.*, 2008, **10**, 452-456; (e) V. O. Rodionov, V. V. Fokin and M. G. Finn, *Angew. Chem. Int. Ed.*, 2005, **44**, 2210-2215; (f) S. I. Presolski, V. Hong, S.-H. Cho and M. G. Finn, *J. Am. Chem. Soc.*, 2010, **132**, 14570-14576; (g) S. –Q. Bai, L. L. Koh and T. S. A. Hor, *Inorg. Chem.*, 2009, **48**, 1207-1213.
- [21] (a) F. Lazreg and C. S. J. Cazin., *Organometallics* 2017, DOI:10.1021/acs.organomet.7b00506; (b) F. Lazreg, A. M. Z. Slawin, C. S. J. Cazin, *Organometallics* 2012, **31**, 7969–7975.
- [22] (a) C. W. Tornøe, C. Christensen and M. Meldal., *J. Org. Chem.* 2002, **67**, 3057-3064; (b) F. Himo, T. Lovell, R. Hilgraf, V. V. Rostovtsev, L. Noodleman, K. B. Sharpless and V. V. Fokin., *J. Am. Chem. Soc.* 2005, **127**, 210-216.
- [23] (a) Y. R. Leroux, H. Fei, J.-M. Noël, C. Roux, P. Hapiot, *J. Am. Chem. Soc.* 2010, **132**, 14039–14041; (b) R. Gleiter, D. B. Werz, *Chem. Rev.* 2010, **110**, 4447–4488; (c) J. P. Brand, D. F. González, S. Nicolai, J. Waser, *Chem. Commun.* 2011, **47**, 102–115; (d) B. M. Trost, M. T. Rudd, M. G. Costa, P. I. Lee, A. E. Pomerantz, *Org. Lett.* 2004, **6**, 4235–4238.
- [24] (a) M. G. Voronkov, N. I. Ushakova, I. I. Tsykhanskaya, V. B. Pukhnarevich, *J. Organomet. Chem.* 1984, **264**, 39; (b) H. Q. Liu, J. F. Harrod, *Can. J. Chem.* 1990, **68**, 1100; (c) M. Itoh, M. Kobayashi, J. Ishikawa, *Organometallics* 1997, **16**, 3068; (d) T. Tsuchimoto, M. Fujii, Y. Iketani, M. Sekine, *Adv. Synth. Catal.* 2012, **354**, 2959; (e) M. Itoh, M. Mitsuzuka, T. Utsumi, K. Iwata, K. Inoue, *J. Organomet. Chem.* 1994, **476**, c30; (f) T. Baba, A. Kato, H. Yuasa, F. Toriyama, H. Handa, Y. Ono, *Catal. Today* 1998, **44**, 271.
- [25] (a) K. Takaki, M. Kurioka, T. Kamata, K. Takehira, Y. Makioka, Y. Fujiwara, *J. Org. Chem.* 1998, **63**, 9265; (b) F. Buch, S. Harder, *Organometallics* 2007, **26**, 5132.

Chapter 5

Summary and Conclusion

ImC are air and moisture stable NHC analogues, which can act as an excellent two electron donors toward elements across the periodic table. However the applications of metal ImC complexes are limited. In particular, the first catalytic application of Cu-ImC was reported in 2010 by Son *et al.*, which is known as the only report known as of today. In particular the catalytic efficiency of Cu-ImC complexes are much superior than that of Cu-NHC catalysts. Indeed, this dissertation deals with the synthesis of different mono, bis ImC supported copper(I) complexes for carbon-boron, carbon-nitrogen and carbon-silicon bond formation reactions. Chapter one (Introduction) reviews the complete literature on ImC and their copper derivatives. Chapter two to four deals with the synthesis, characterization and application of newly prepared ImC and their copper derivatives. The final section of each chapter lists the references from the literature, which are indicated in the text (Chapters 1-4) by appropriate numbers appearing as square brackets. Lists of abbreviations, table, scheme, and figure captions appearing in this report are collected together in the beginning of the thesis chapters. The summary and conclusion are reported in chapter 5.

In chapter 2, the syntheses and structures of copper(I) chalcogenone complexes are described. The homoleptic mononuclear copper(I) complexes $[(IPr=E)_2Cu]ClO_4$, IPr=E, 1,3-bis(2,6-diisopropylphenyl)imidazoline-2-thione (**1**) and 1,3-bis(2,6-diisopropylphenyl)imidazoline-2-selone (**2**); $[(IMes=E)_2Cu]ClO_4$, IMes=E, 1,3-bis(2,4,6-trimethylphenyl)imidazole-2-thione (**3**) and 1,3-bis(2,4,6-trimethylphenyl)imidazole-2-selone (**4**); $[(IPr=E)_2Cu]BF_4$, E = S (**5**); E = Se (**6**) and $[(IMes=E)_2Cu]BF_4$, E = S (**7**); E = Se (**8**) are formed from the reduction of copper(II) to copper(I) with the corresponding imidazoline-2-chalcogenones (Chart 5.1). X-ray structure analyses of seven compounds (**1–3** and **5–8**) show that the copper(I) ion is in a perfect linear coordination, while **4** is in quasi-linear geometry. Molecules **2**, **4**, **6** and **8** are the first structurally characterized homoleptic copper(I) selone complexes. The optical and thermal properties of imidazoline-2-chalcogenones and their copper(I) derivatives are investigated.

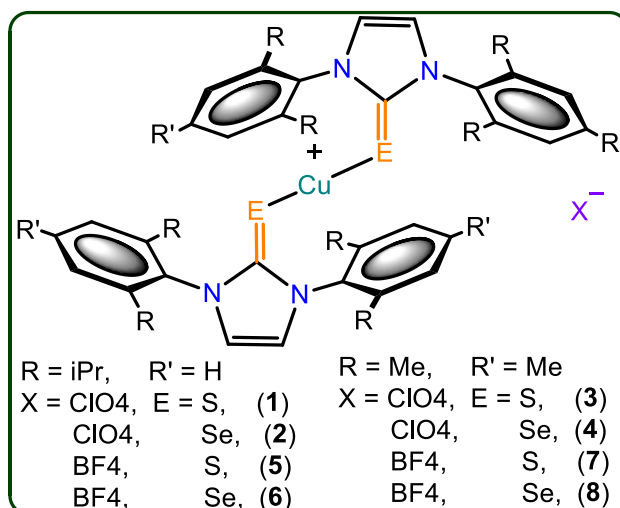
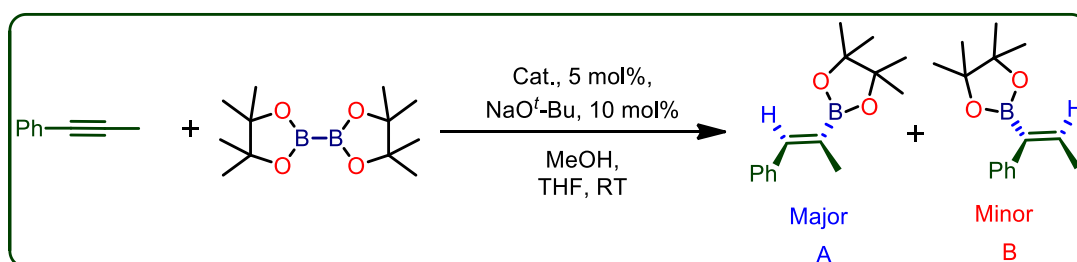


Chart 5.1: Catalysts (1-8) isolated in this chapter

These complexes are able to act as catalysts in regioselective borylation of numerous unsymmetrical alkynes, yielding synthetically useful vinylboronates (Scheme 5.1). Among catalysts 1-8, catalyst 4 is highly selective towards the regioselective boron addition of 1-phenyl-1-propyne.



Scheme 5.1: Regioselective borylation of 1-phenyl-1-propyne using 1-8

Among the isolated catalysts (1-8), the catalysts 4 showed better catalytic efficiency in terms of isolated yields and selectivity over NHC-Cu catalysts reported earlier (Chart 5.2).

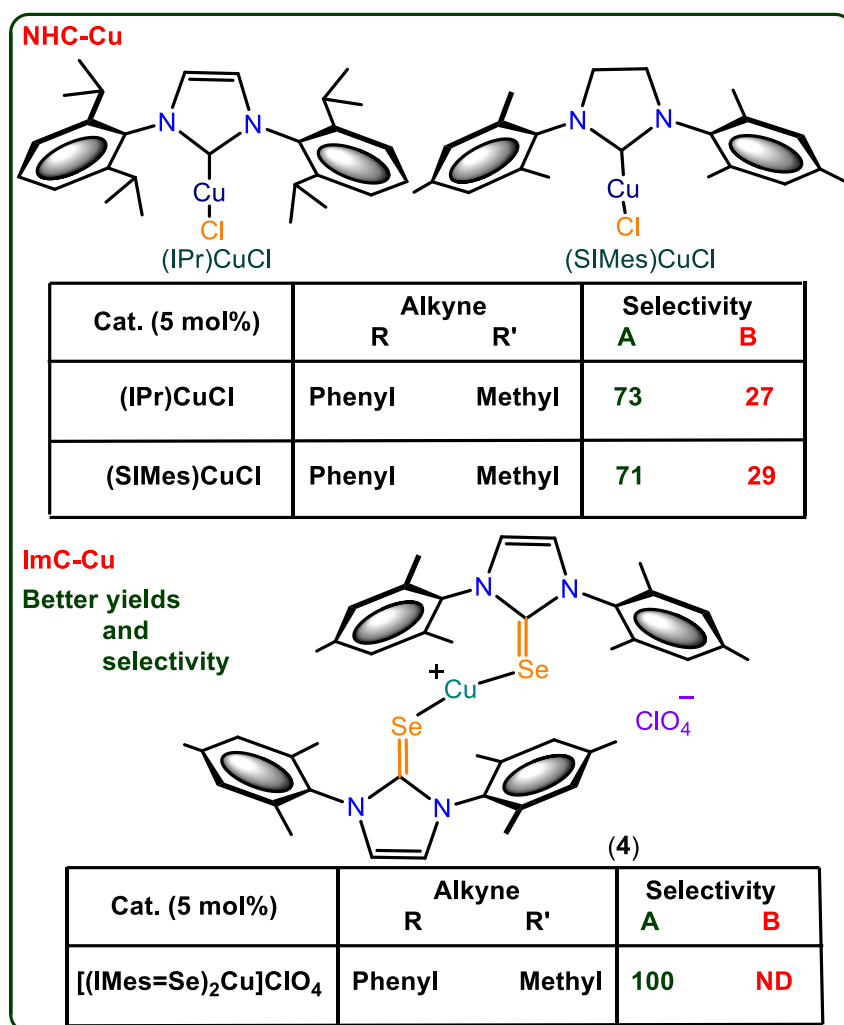


Chart 5.2: Comparison between NHC-Cu and ImSe-Cu in borylation of alkynes

In chapter 2, two mega size copper(I) cubic cages, [$\{\text{Cu}(\mathbf{Bptp})\}_8(\text{PF}_6^-)(\text{PF}_6^-)_7$ (**9**) and [$\{\text{Cu}(\mathbf{Bpsp})\}_8(\text{PF}_6^-)(\text{PF}_6^-)_7$ (**10**) supported by imidazole-2-chalcogenone ligands (\mathbf{Bptp} = 2,6-bis(1-isopropylimidazole-2-thione)pyridine or \mathbf{Bpsp} = 2,6-bis(1-isopropylimidazole-2-selone)pyridine) have been synthesized and characterized (Chart 5.3). The formation of ionic salts **9** and **10** were confirmed by FT-IR, multinuclear (^1H , ^{13}C , ^{31}P and ^{19}F) NMR, UV-vis, TGA, CHN analysis, BET, single crystal X-ray diffraction and powder X-ray diffraction techniques. To the best of our knowledge, these are the first examples of octanuclear copper(I) cluster in a perfect cubic architecture with copper-copper distances of 8.413 Å or 8.593 Å. Interestingly, these anion-centered Cu^I_8 cubic arrangements are not supported by cubic centered ions or face centered molecules. Formation of cationic cubic cages were accompanied by the association of twelve ligands (\mathbf{Bptp} or \mathbf{Bpsp}) with eight trigonal planar

[CuSe₃] vertex. The cationic charge of cubic cages were satisfied by eight PF₆⁻ counter anions, in which one of the PF₆⁻ anion occupies at the centre of Cu₈ cube without any interaction.

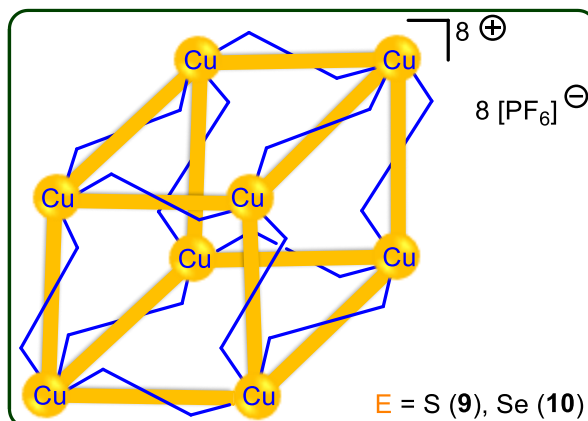
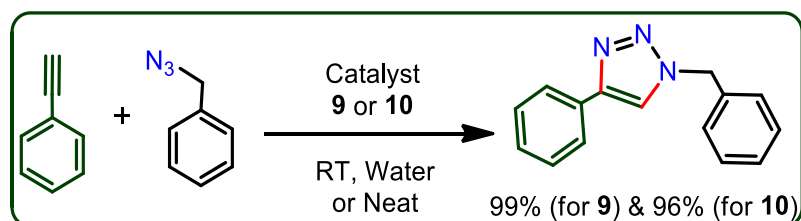


Chart 5.3: Molecular structure of **9** and **10**

The copper(I) cubic cages are found to be highly active catalysts in click chemistry (Scheme 5.2) as well as hydroamination reactions. The scope of the catalytic reactions have been investigated with thirty five different combinations in click reactions and six different combinations in hydroamination of alkynes.



Scheme 5.2: Catalysts **9** and **10** mediated one-pot synthesis of triazoles

The isolated catalysts (**9** and **10**) showed better catalytic efficiency in terms of reaction times with most NHC-Cu catalysts, however, these are as good as the best click catalysts [(IAd)CuX, X = Cl, Br and I] reported as of now (Chart 5.4).

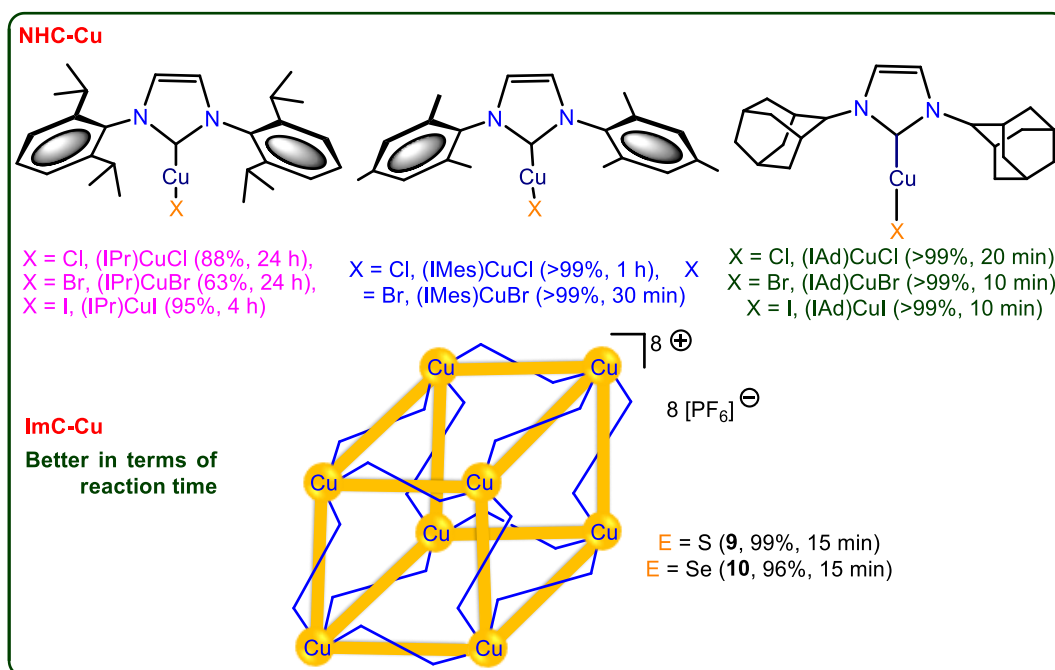


Chart 5.4: Comparison between NHC-Cu and ImC-Cu in click catalysis

In chapter 3, the syntheses and structures of ten new copper(I) chalcogenone complexes are described. The mononuclear copper(I) complexes (IMes=E)CuX [E = S, Se, IMes=E 1,3-bis(2,4,6-trimethylphenyl)imidazol-2-thione (**11-13**) and 1,3-bis(2,4,6-trimethylphenyl)imidazol-2-selone (**14-15**)] (Scheme 7.11), (NHC=E)₂CuX, [NHC=E; IMes=Se, X = CuCl₂ (**17**), NHC=E; IMes=Se, X = PF₆ (**19**) and NHC=E = IPr=Se, X = PF₆ (**21**) [IPr=Se, 1,3-bis(2,6-diisopropylphenyl)imidazoline-2-selone], and a polynuclear copper(I) complexes [(Ebis)CuI]_n, (**23**) [Ebis = 1,2-bis(3-methyl-4-imidazolin-2-selone)ethane], [(Ebpis)_{1.5}CuBF₄]_n (**24**) [Ebpis = 1,2-bis(3-isopropyl-4-imidazolin-2-selone)ethane] were isolated and characterized by FT-IR, multinuclear NMR.

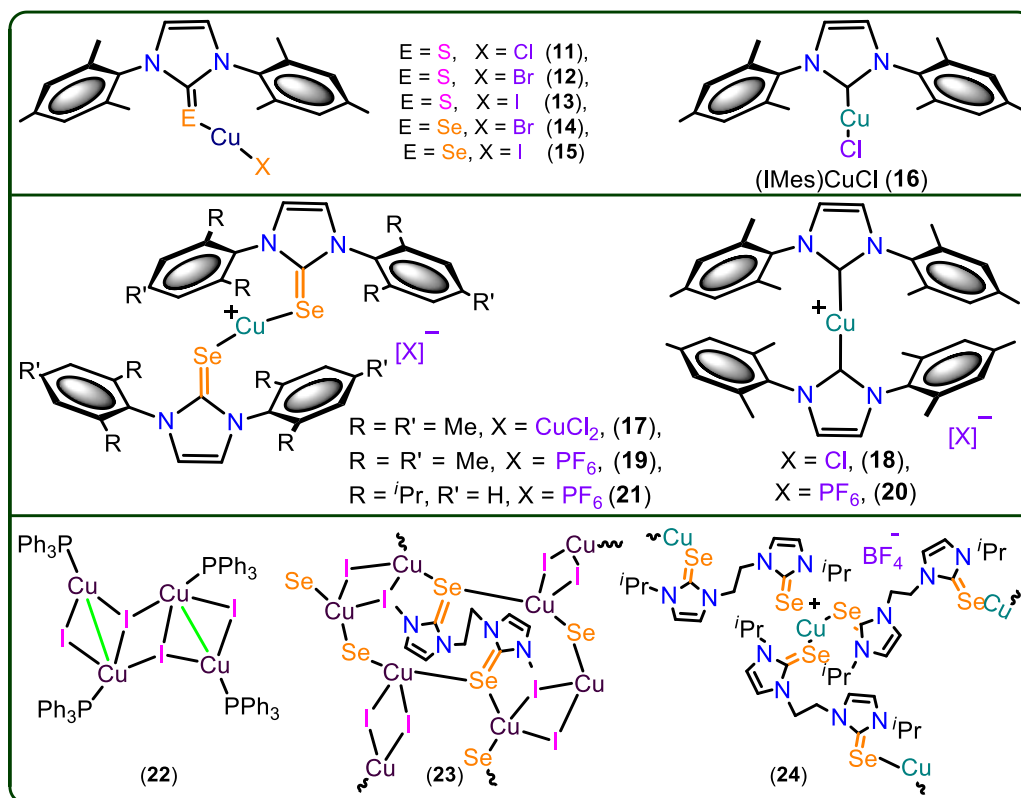
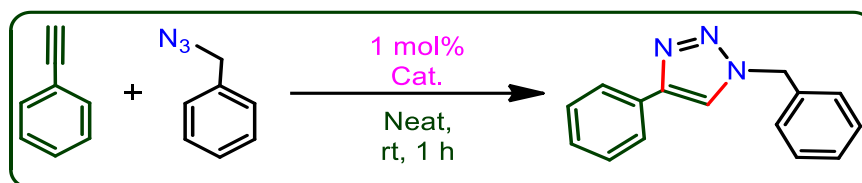


Chart 5.5: Catalysts (11-24) isolated in this chapter

Interestingly, the linear copper(I) complexes **17**, **19** (Chart 5.5) and **21** were also isolated from [(IMes)CuCl] (**16**) by ligand transfer method. Besides, the complexes **23** and **24** were synthesized from the isolated tetranuclear copper(I) complex, [(PPh₃)₄Cu₄I₄] (**22**). The single crystal X-ray structures of **11-15**, **17**, **19**, **21** and **23-24** depicts the existence of different coordination modes around copper(I) metal center. The copper center in **11-15** show *quasi*-linear coordination, **17**, **19**, **21** exhibit perfect linear coordination, **23** shows tetrahedral coordination, while **24** display a perfect trigonal planar coordination. The UV-vis absorption aspects of copper(I) derivatives have been investigated.

Moreover, all these complexes (**11-24**) were able to act as catalyst in [3+2] cycloaddition of azides with alkynes (Scheme 5.3) to yield 1,2,3-triazoles. Among catalysts **11-24**, catalysts **13**, **16** and **22** are exceedingly active towards the synthesis of 1,2,3-triazoles.



Scheme 5.3: Catalysts **11-24** mediated [3+2] cyclo addition reaction

The isolated catalysts (**11-24**) showed almost similar catalytic efficiency in terms of reaction times and yields with most NHC-Cu catalysts, however, the phosphine derived copper complex showed better activity among the isolated catalysts (Chart 5.6).

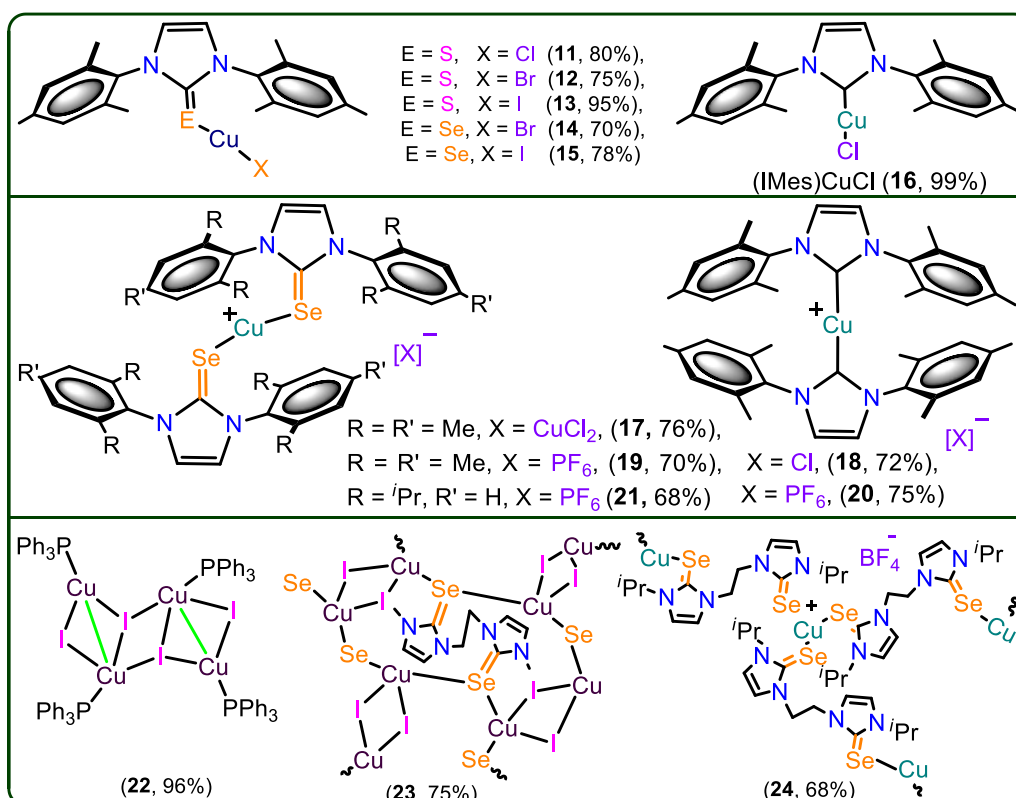


Chart 5.6: Comparison between Phosphine-Cu, NHC-Cu and ImC-Cu in click catalysis

List of Publications

- 1) **Katam Srinivas**, Paladugu Suresh, Chatla Naga Babu, Arruri Sathyanarayana and Ganesan Prabusankar, Heavier chalcogenone complexes of bismuth(III) trihalides: potential catalysts for acylative cleavage of cyclic ethers, *RSC Adv.*, **2015**, 5, 15579-15590.
- 2) **Katam Srinivas**, Chatla Naga Babu and Ganesan Prabusankar, Linear Cu(I) chalcogenones: synthesis and application in borylation of unsymmetrical alkynes, *Dalton Trans.*, **2015**, 44, 15636-15644.
- 3) **Katam Srinivas**, Chatla Naga Babu and Ganesan Prabusankar, Thermal, Optical and Structural Properties of Disulfide and Diselenide Salts with Weakly Associated Anions, *J. Mol. Struct.*, **2015**, 1086, 201-206.
- 4) **Katam Srinivas**, Arruri Sathyanarayana, Chatla Naga Babu and Ganesan Prabusankar, Bismuth(III)dichalcogenones as Highly Active Catalysts in Multiple C-C Bond Formation Reactions, *Dalton Trans.*, **2016**, 45, 5196-5209.
- 5) **Katam Srinivas** and Ganesan Prabusankar, Large Cu^{I}_8 Chalcogenone Cubic Cages with Non-interacting Counter Ion, *Dalton Trans.*, **2017**, 46, 16615-16622.
- 6) Chatla Naga Babu, **Katam Srinivas** and Ganesan Prabusankar, Facile access to zinc and cadmium selones: highly active catalysts for Barbier reactions in aqueous media, *Dalton Trans.*, **2016**, 45, 6456-6465.
- 7) Chatla Naga Babu, Paladugu Suresh, **Katam Srinivas**, Arruri Sathyanarayana and Ganesan Prabusankar, Catalytically Active Lead(II)-Azolium Coordination Assemblies with Diversified Lead(II) Coordination Geometries, *Dalton Trans.*, **2016**, 45, 8164-8173.
- 8) Ganesan Prabusankar, Arruri Sathyanarayana, Paladugu Suresh, Chatla Naga Babu, **Katam Srinivas** and Bhanu Prakasa Rao Metla, N-Heterocyclic Carbene Supported

Heavier Group 14 Elements: Recent Progress and Challenges, *Coord. Chem. Rev.*, **2014**, 269, 96-133.

- 9) Arruri Sathyanarayana, **Katam Srinivas**, Anindita Mandal, Saswati Gharami and Ganesan Prabusankar, Synthesis, Spectral and Structural Properties of Bis-imidazole Selones, *Journal of Chemical Sciences*, **2014**, 126, 1589-1595.
- 10) Moulali Vaddamanu, Ramesh Karupnaswamy, **Katam Srinivas** and Ganesan Prabusankar, Facile Access to Diselenide Containing Macrocyclic Ring from Diselone, *Chemistry Select*, **2016**, 1, 4668-4671.
- 11) Ganesan Prabusankar, Arruri Sathyanarayana, Ipsita Nath, **Katam Srinivas** and Paladugu Suresh, A Facile Access to Sterically Less Crowded to More Crowded Organo Triselones, *Chemistry Select*, **2017**, 3, 1294-1299. (Equal contributions).
- 12) Ramesh Karupnaswamy, Mathupandi Mannarsamy, Moulali Vaddamanu, **Katam Srinivas** and Ganesan Prabusankar, The upshots of altering N-substituents in bismuth(III) selone complexes, *Eur. J. Inorg. Chem.*, **2017**, *submitted* (Equal contributions).
- 13) **Katam Srinivas** and Ganesan Prabusankar, An unusual cleavage of aryloxy ring followed by 1,2-shift in OCO pincer ligand by bismuth(III), *to be submitted*.
- 14) **Katam Srinivas** and Ganesan Prabusankar, Copper(I) Chalcogenone: Can They be Better Catalyst than Copper(I) Carbene and Copper(I) Phosphine?, *to be submitted*.
- 15) **Katam Srinivas** and Ganesan Prabusankar, Zinc(II) Chalcogenone: Synthesis and structural characterization, *to be submitted*
- 16) **Katam Srinivas**, Nadeeshwar Muneeshwar and Ganesan Prabusankar, Super bulky selone supported bi nuclear Antimony(III) halide complexes: Discovery of an unusual coordination modes of selone, *to be submitted*.

List of Conferences Attended

- [1] Oral presentation in 41st International Conference on Coordination Chemistry (**ICCC-41**), 21-25th July 2014, **Singapore**.
- [2] Poster presentation in 17th CRSI National Symposium in Chemistry (**CRSI-17th**), 06-08th February 2015, CSIR-NCL, Pune, **India**.
- [3] Poster presentation in 10th Mid-year CRSI Symposium in Chemistry (**CRSI-10th**), 23-25th July 2015, National Institute of Technology, Trichy, **India**.
- [4] Poster presentation in Modern Trends in Inorganic Chemistry (**MTIC – XVI**), 03-05th December, 2015, Jadavpur University, Kolkata, **India**.
- [5] Oral presentation in 5th International Symposium on Functionalization and Applications of Soft/Hard Materials (**Soft/Hard 2016**), 22-23rd January 2016, Ritsumeikan University, **Japan**.
- [6] Poster presentation in Frontiers in Inorganic and Organometallics Conference, 14-15th April, 2016, IIT Indore, **India**.
- [7] Oral presentation in 6th International Symposium on Functionalization and Applications of Soft/Hard Materials (**Soft/Hard 2017**), 20-22nd January 2017, Ritsumeikan University, **Japan**.
- [8] Poster presentation in Modern Trends in Inorganic Chemistry (**MTIC – XVII**), 11-14th December, 2017, NCL Pune, Maharashtra, **India**.
- [9] Oral presentation in 2nd In House Symposium (**IHS-2018**) at Indian Institute of Technology Hyderabad, 10th March, 2018, **India**.

Bio-data

Dr. Katam Srinivas,

Research Scholar,

Dr. G. Prabusankar's Research Group, IIT Hyderabad,

E-Mail : cy13p0004@iith.ac.in; Phone : +91 95 53 54 76 88;

Fax : +91 40 23 01 60 32



Educational Qualifications

Ph.D

Jan-2013 – Mar-2018

Department of Chemistry

Indian Institute of Technology Hyderabad, India
(CGPA: 9.40)

M.Sc

Aug-2007 – Nov-2009

Organic Chemistry

Kakatiya University, Telangana, India

B.Sc

Jun-2003 – Apr-2006

Botany, Zoology and Chemistry

Osmania University, Telangana, India

Award and Fellowship

Nov-2016 to Jan-
2017

JASSO scholarship, Japan

Jul-2016

DST-DAAD Scholarship, Indo-German

Jan-2016 to Mar-
2016

Ritsumeikan University Scholarship, Japan

2015, 2016 and 2017

Excellence in Research Awards, IITH, India

Apr-2016

*Best Poster Award by Dalton Transactions,
at IIT Indore, India*

Jan-2015

CSIR-UGC Senior Research Fellowship, India

June 2012

*CSIR-UGC Junior Research Fellowship (All
India 87th Rank), India*

June 2011

Qualified CSIR-UGC lectureship, India

Teaching Experience

- 3Y 6M
1. Teaching experience in Sri Medha Junior college, Sri Sathya Sai Junior and Degree college, Telanagana, India
 2. Worked as a teaching assistant for M.Sc 2013-2015 batch in IIT Hyderabad.

Residential Address

Katam Srinivas s/o Sattaiah
Village: Yella Reddy Bavi,
Mondal: Devara Konda,
District: Nalgonda,
State: Telangana,
India
PIN: 508248

Present Address

Katam Srinivas c/o Dr.G.Prabusankar's
Research Group
Department of Chemistry,
Indian Institute of Technology Hyderabad,
Kandi, Sangareddy, Medak, Telangana,
India
PIN: 502285

Declaration

I hereby declare that the information given above is true and correct to the best of my knowledge and belief.



Katam Srinivas